# The relationship between the water regime and morphology of soils in the Weatherley catchment, northerly Eastern Cape

by

**Cornelius Wilhelm van Huyssteen**

(M.Sc. Agric. University of Stellenbosch)

Dissertation submitted in fulfilment of the requirements
for the Doctor of Philosophy in Soil Science degree
in the faculty of Natural and Agricultural Sciences,
Department of Soil, Crop and Climate Sciences,
University of the Free State,
Bloemfontein.

Promoter: Dr. P.A.L. le Roux
Co-promoter: Dr. M. Hensley

November 2003

# DECLARATION

I declare that the dissertation hereby submitted by me for the Doctor of Philosophy in Soil Science degree at the University of the Free State is my own independent work and has not previously been submitted by me at another university / faculty. I furthermore cede copyright of the dissertation in favour of the University of the Free State.

Signature: ..... Date: 23/4/2004

# ABSTRACT

The Weatherley catchment is situated close to Maclear in the northern Eastern Cape Province. Soil water contents have been measured regularly, as part of a long-term project, at 28 sites in the catchment for six years to quantify the soil water regime. For this study ten of these sites were selected, described and analysed in detail to characterize the soil properties. This data was used to determine the relationship between soil water regime and soil profile morphology.

A correlation was found to exist between mean annual duration of water saturation above 0.7 of porosity ($AD_{s>0.7}$, days $year^{-1}$) and other soil properties. $CEC_{soil}$ increases from 3.5 to 11.5 $cmol_c\ kg^{-1}$, base saturation increases from 25 to 44 %, and the underlying unspecified material with signs of wetness or G horizons occur closer to the soil's surface as mean $AD_{s>0.7}$ increases.

Orthic A horizons that occur in seeps are wetter, with mean $AD_{s>0.7}$ 212 – 365 days $year^{-1}$, than orthic A horizons that occur on ridges with mean $AD_{s>0.7}$ of < 25 days $year^{-1}$. The former have common and many Fe oxide mottles, whereas the latter lack clear mottling. $AD_{s>0.7}$ data shows that orthic A horizons overlying red apedal B, yellow-brown apedal B or neocutanic B horizons are well drained, while those overlying E, soft plinthic B and G horizons are wetter. It is proposed that orthic A horizons can be subdivided into wetness classes using the occurrence of mottles, as well as the nature of the underlying horizon.

The Longlands (P201 and P207) and Westleigh (P204) soils, characterized by the occurrence of a soft plinthic B horizon, have intermediate mean $AD_{s>0.7}$. They increase from 84 to 157 days $year^{-1}$ in orthic A horizons, to 231 days $year^{-1}$ in soft plinthic B horizons and 360 days $year^{-1}$ in the underlying unspecified material with signs of wetness. The chromatic soils, including Pinedene (P202), Tukulu (P203) and Bloemdal (P210) soil forms, defined as having yellow-brown apedal B, neocutanic B or red apedal B horizons as the second horizon in the profiles respectively have the driest water regime of the soils studied. The A and B1 horizons

have mean $AD_{s>0.7}$ < 40 days $year^{-1}$, the B2 horizons 88 days $year^{-1}$, and the underlying unspecified material with signs of wetness 130 to 350 days $year^{-1}$.

Pooling the data from all the profiles studied produces the following mean $AD_{s>0.7}$ for the different diagnostic horizons: G horizons = 324 ± 20 days $year^{-1}$; unspecified material with signs of wetness = 243 ± 40 days $year^{-1}$; E horizons = 163 ± 56 days $year^{-1}$; soft plinthic B horizons = 148 ± 45 days $year^{-1}$; orthic A horizons = 144 ± 40 days $year^{-1}$; and chromatic (red apedal B, yellow-brown apedal B and neocutanic B) horizons = 88 ± 51 days $year^{-1}$. There is an association between mean $AD_{s>0.7}$ and other soil properties. For example clay content, CEC, basic cations and pH are highest in G horizons and lowest in chromatic horizons. CBD extractable Fe and Mn are found to be roughly twice as much in soft plinthic B, chromatic B and unspecified material with signs of wetness horizons compared to orthic A, E or G horizons.

Digital soil horizon photographs were quantified and classified into diagnostic red, yellow-brown, grey and black colours, using the Red and Green values of RGB-notation in ArcView SpatialAnalyst. This methodology produced promising results, as proven by classification of photographed Munsell colour sheets. Colour classification of horizon photographs generally supports the field colour classification of these horizons using Munsell colour sheets. In general, the profiles described for this study are dominated by diagnostic grey and yellow-brown colours, with the exception of the Bloemdal (P210) which is diagnostic red.

# OPSOMMING

Die Weatherley opvanggebied is naby Maclear in die Noordelike Oos-Kaapprovinsie geleë. As deel van 'n langtermyn projek is grondwaterinhoud gereeld vir ses jaar by 28 lokaliteite in die opvangebied gemeet om die grondwaterregime te kwantifiseer. Vir hierdie studie is tien van hierdie lokaliteite is geselekteer, in detail beskryf en geanaliseer om die grondeienskappe te karakteriseer. Hierdie data is gebruik om die verwantskap tussen grondwaterregime en grondmorfologie te bepaal.

'n Korrelasie is tussen jaarlikse duur van waterversadiging bo 0.7 van porositeit ($AD_{s>0.7}$, dae $jaar^{-1}$) en ander grondeienskappe gevind. $KUK_{grond}$ neem toe van 3.4 na 11.5 $cmol_c$ $kg^{-1}$, basis versadiging neem toe van 25 % na 44 %, en die onderliggende ongespesifiseerde materiaal met tekens van natheid of G horisonte kom nader aan die grondoppervlak voor, soos $AD_{s>0.7}$ toeneem.

Ortiese A horisonte wat in vleie voorkom is natter (gemiddelde $AD_{s>0.7}$ 212 – 365 dae $jaar^{-1}$) as ortiese A horisonte wat op kruine (gemiddelde $AD_{s>0.7}$ < 25 dae $jaar^{-1}$) voorkom. Eersgenoemde het volop en baie Fe oksied vlekke, terwyl laasgenoemde geen duidelike vlekke het nie. $AD_{s>0.7}$ data dui daarop dat ortiese A horisonte wat bo rooi apedale B, geelbruin apedale B of neokutaniese B horisonte voorkom goed gedreineer is, terwyl ortiese A horisonte wat op E, sagte plintiese B en G horisonte voorkom relatief nat is. Daar word voorgestel dat ortiese A horisonte in natheidsklasse onderverdeel kan word deur die voorkoms van vlekke en die aard van die onderliggende materiaal te gebruik.

Die Longlands (P201 en P204) en Westleigh (P207) gronde, gekarakteriseer deur die voorkoms van sagte plintiese B horisonte, het intermediêre gemiddelde $AD_{s>0.7}$. Dit neem toe van 84 tot 157 dae $jaar^{-1}$ in ortiese A horisonte, na 231 dae $jaar^{-1}$ in sagte plintiese B horisonte en 360 dae $jaar^{-1}$ in die onderliggende ongespesifiseerde materiaal met tekens van natheid. Chromatiese gronde, wat die Pindene (P202), Tukulu (P203) en Bloemdal (P210) insluit en gedefinieer is deur die voorkoms van 'n

neokutaniese B, geelbruin apedale B of rooi apedale B horison as die tweede horison in die profile onderskeidelik, het die droogste water regime van gronde wat bestudeer is. Die A en B1 horisonte het gemiddelde $AD_{s>0.7} < 40$ dae jaar$^{-1}$, die B2 horisonte 88 dae jaar$^{-1}$ en die onderliggende materiaal met tekens van natheid 130 tot 350 dae jaar$^{-1}$.

Groepering van data van al die profiele lewer die volgende gemiddelde $AD_{s>0.7}$ vir die verskillende diagnostiese horisonte: G horisonte = 324 ± 20 dae jaar$^{-1}$; ongespesifiseerde materiaal met tekens van natheid = 243 ± 40 dae jaar$^{-1}$; E horisonte = 163 ± 56 dae jaar$^{-1}$; sagte plintiese B horisonte = 148 ± 45 dae jaar$^{-1}$; ortiese A horisonte = 144 ± 40 dae jaar$^{-1}$; en chromatiese (rooi apedale B, geelbruin apedale B en neokutaniese B) horisonte = 88 ± 51 dae jaar$^{-1}$. Daar is 'n verwantskap tussen gemiddelde $AD_{s>0.7}$ en ander grondeienskappe. Byvoorbeeld die klei inhoud, KUK, basiese katione en pH is hoogste in G horisonte en laagste in chromatiese horisonte. CBD ekstraheerbare Fe en Mn is ongeveer dubbeld in sagte plintiese B, chromatiese B en ongespesifiseerde materiaal met tekens van natheid as in ortiese A, E of G horisonte.

Digitale grond horison foto's is in diagnostiese rooi, geelbruin, grys en swart kleure geklassifiseer en gekwantifiseer, deur die Rooi en Groen waardes van RGB notasie in ArcView SpatialAnalyst te gebruik. Die metode lewer belowende resultate, soos bewys deur die klassifikasie van foto's van Munsell kleurvelle. Kleurklassifikasie van horison foto's bevestig oor die algemeen veld kleurklassifikasie met behulp van Munsell kleur velle. Profiele in hierdie studie word oor die algemeen gedomineer deur diagnostiese grys en geelbruin kleure, met die uitsondering van P210 (Bloemdal) wat diagnosties rooi is.

# ACKNOWLEDGEMENTS

I wish to thank the following persons and institutions for their assistance during the execution of this study:

- Dr. P.A.L. le Roux my promoter for valuable advice and assistance.

- Dr. Malcolm Hensley my co-promoter for his vision and faith.

- The Water Research Commission, represented by Dr S. Mkhize and Mr H. Maaren, for funding a project entitled "The relationship between soil water regime and soil profile morphology in the Weatherley catchment, an afforestation area in the North Eastern Cape" (K5/1317), on which this dissertation is based.

- The Water Research Commission Steering Committee (Dr S. Mkhize, Prof M.V. Fey, Prof C.C. du Preez, Prof A.T.P. Bennie, Dr F. Ellis, Dr M. Hensley, Dr P.A.L. le Roux, Dr S.A. Lorentz, Dr D.P. Turner, Mr D. Butt, Mr P.G. Gardiner, Mr U.A. Idowu and Mr. J.J.N. Lambrechts) for valuable inputs during the steering committee meetings.

- Mondi (Mr P.G. Gardiner) and North Eastern Cape Forests (Mr D. Butt) for permission to use the Weatherley catchment as research site and for important assistance rendered.

- My colleagues at the Department of Soil, Crop, and Climate Sciences (Prof C.C. du Preez, Prof A.T.P. Bennie, Dr P.A.L. le Roux, Dr M. Hensley, Me E. Kotze, Me R. van Heerden, Mr M. Strydom and Mr L. Ehlers), especially the analytical staff (Me Y. Dessels, Mr E. Moeti and Mr F. Joseph), who conducted most of the analyses.

- Dr P.A.L. le Roux, Dr M. Hensley, Me M. Smit, Mr W. Boshoff, Mr F. Joseph, Mr D. Scholtz, Mr A.Q. Weldeyohannes and Mr T.B. Zere for support and assistance during the field investigations.

- My wife, Adré, for valuable and much needed support.

# CONTENTS

## APPENDICES

# LIST OF FIGURES

# LIST OF TABLES

# SYMBOLS USED

| | |
|---|---|
| $\theta$ | volumetric soil water content (mm) |
| $AD_{s>0.7}$ | annual duration of s above 0.7 of porosity (days $year^{-1}$) |
| Bd | Bloemdal soil form (orthic A – red apedal B – unspecified material with signs of wetness) |
| $C_d$ | dry colour Chroma |
| d | day |
| D | deep percolation (−) and capillary rise (+) |
| $D_{s>0.7}$ | duration of s above 0.7 of porosity (days per event) |
| DUL | drained upper limit |
| E | evaporation |
| Eo | reference evaporation |
| ET | evapotranspiration |
| $F_{s>0.7}$ | frequency of water saturation above 0.7 of porosity (events per year) |
| f | porosity |
| fi Sat | field saturation |
| gh | G horizon |
| gs | E horizon |
| $H_d$ | dry colour Hue |
| I | irrigation |
| Ka | Katspruit soil form (orthic A – G) |
| Kd | Kroonstad soil form (orthic A – E – G) |
| LL | lower limit of plant available water (mm) |
| Lo | Longlands soil form (orthic A – E – soft plinthic B) |
| max | maximum |
| min | minimum |
| ne | neocutanic B horizon |
| NWM | neutron water meter |
| on | unspecified material with signs of wetness |
| ot | orthic A horizon |
| Pn | Pinedene soil form (orthic A – yellow-brown apedal B – unspecified material with signs of wetness) |
| P | precipitation |
| R | run-off (−) and run-on (+) |
| re | red apedal B horizon |
| ro | rock |
| s | degree of water saturation (volume of water per volume of pores) |

| | |
|---|---|
| s>0.7 | degree of water saturation above 0.7 of porosity |
| so | saprolite |
| SOC | soil organic carbon |
| sp | soft plinthic B horizon |
| std | standard deviation |
| T | transpiration |
| Tu | Tukulu soil form (orthic A – neocutanic B – unspecified material with signs of wetness) |
| ud | unconsolidated material without signs of wetness |
| $V_d$ | dry colour Value |
| $\Delta W$ | Change in soil water content (mm) |
| We | Westleigh soil form (orthic A – soft plinthic B) |
| ye | yellow-brown apedal B horizon |

# 1 INTRODUCTION

## 1.1 Problem statement

South Africa is a water poor country. Procedures for establishing the water yield of catchments are therefore important, and become increasingly so as the demand for water increases. Any expansion of knowledge in this regard is therefore desirable. This led to the establishment of an intensively measured catchment on the farm Weatherley in the Eastern Cape Province. Various Water Research Commission (WRC) funded, and other projects are conducted in this catchment (Flugel, 1993; Lorentz & Pretorius, 2001; Lorentz *et al.,* 2001; Van Huyssteen *et al.,* 2002; 2003a). The relationship between soil water regime and soil profile morphology has, however, up to now received very little attention. Soil water regime refers to the state and availability of water in soil (Van der Watt & Van Rooyen, 1995) and is used in this research to refer to the degree of wetness of a soil, with the critical parameter mean $AD_{s>0.7}$, defined as the mean annual duration of water saturation above 0.7 of porosity, expressed in days $year^{-1}$.

There is a close relationship between the water regime of a soil profile and its morphology, since water plays a primary role in soil genesis. The quantity and quality of water available during pedogenesis is reflected in the morphology of the profile. The hydrological characteristics of soil can either be determined quantitatively by regular measurements, or qualitatively by inference from the soil properties such as colour, exchangeable bases, occurrence of mottles and concretions. Soil colour is the most common morphological soil property used to predict the water regime of soil. The major soil classification systems of the world apply soil colours as distinguishing criteria at various levels. The South African system applies it at the highest level to distinguish between diagnostic horizons, and thus soil forms. The definitions for colour defined horizons (Soil Classification Working Group, 1991) were compiled to differentiate between horizons with differing hydrological characteristics. The hypothesis is that red

apedal B horizons are freely drained, yellow-brown apedal B horizons are well drained, and E horizons are poorly drained (Le Roux *et al.,* 1999). This conforms to the hypothesis that degree of wetness determines the quantity and type of iron oxide minerals present and hence the soil colour (Schwertmann, 1993).

In a paper titled "Hydrology and Soil Science", Amerman (1973) concludes that hydrologists need an improved understanding of the hydrology of soils, and that they are looking to soil scientists for assistance. This need has up to now received relatively little attention in South Africa. Schwertmann wrote in 1985 that: "Studies in which soil temperature and soil moisture regimes are measured and directly related to the pedogenic Fe oxides would thus be very desirable."

Improved understanding of the relationship between the water regimes of soil profiles and their morphology will improve soil classification. This will lead to improved understanding of landscape hydrology and improved definitions of hydrological response units (Flugel, 1993), and similarly ecotopes (MacVicar *et al.*, 1974). This will contribute to improved pedotransfer and performance of models such as ACRU (Schulze, 1995) and SWAMP (Bennie *et al.*, 1998).

An experiment was laid out in the Weatherley catchment, close to Maclear, to monitor and model total catchment hydrology. The study has been in operation since 1995 and other soil water relationships were studied thoroughly. The development of pedotransfer functions from these results, for application to other catchments, will be enhanced if the relationship between soil water regime and soil morphology is better understood. The relationship between soil properties and soil water regime has been studied in South Africa (Donkin & Fey, 1991; Van Huyssteen, 1995; Le Roux, 1996) and in other countries (Blavet *et al.,* 2000; 2002).

## 1.2 Hypothesis

Both the genesis of soil and its suitability for common land uses (agricultural, ecological and engineering purposes) depend to a large extent on the soil water regime. The soil water regime can either be determined by regular long term measurements of soil water content or by inference from soil properties such as soil colour, exchangeable bases, and the occurrence of mottles and concretions. Soil colour has always been regarded as the best tool to predict the water status of soil (Cutler, 1983). The major soil classification systems of the world apply soil colour as distinguishing criteria. For example Soil Taxonomy (Soil Survey Staff, 1975) rates soil colours with a chroma equal to or less than two as indicators of a significant time of water saturation in that horizon per year. The frequency and / or duration of a specific degree of water saturation are, however, not specified. On the other hand it has been stated that the importance of soil colour is somewhat over rated, since plant roots are colour blind and the value of colour interpretation is often questioned (Evans & Franzmeier, 1986; Cogger & Kennedy, 1992).

In the South African soil classification system the definitions for colour defined diagnostic horizons were compiled to differentiate, amongst other things, between horizons with differing water regimes (Soil Classification Working Group, 1991). Distinguishing definitions for colour ranges were established by long term experience of field observations (Lambrechts, 1994, personal communication). These colour definitions form the basis of definitions for the diagnostic red apedal B, yellow-brown apedal B, and E horizons. Colour is also applied to differentiate between the families of several soil forms. The differentiation between families with yellow and grey E horizons is an example. It is speculated that yellow E horizons are somewhat better drained than grey E horizons. This is in line with the hypothesis of Schwertmann (1993) that water saturation impacts on the quantity and type of Fe oxide minerals, and therefore soil colour.

The relationship between soil morphology and soil water regime is used to delineate wetlands (Land-Use and Wetland/Riparian Habitat Working Group,

2000), because soils in wetlands typically have morphology associated with long periods of water saturation. Soil water content data for the Weatherley catchment may contribute to quantify this relationship.

Improved knowledge of the relationship between soil water regimes and soil morphology will improve technology transfer between catchments. Soil morphological features could thus be used to interpret the hydrology of catchments under similar climatic and geological conditions.

Elucidation of the relationship between soil profile morphology and soil hydrology will contribute towards understanding hillslope hydrological processes.

## 1.3 Objectives

a) To characterize and quantify the soil water regime and soil profile morphology in the Weatherley catchment.

b) To quantify the relationship between soil water regime and soil profile morphology in the Weatherley catchment.

# 2 LITERATURE REVIEW

## 2.1 Introduction

This chapter reviews the literature on the relationship between soil colour and soil water regime, especially colour indexes. It also focuses on iron oxide minerals in soil as well as soil forming processes where excess soil water influences soil morphology.

## 2.2 Soil colour and water content

The main challenge, when attempting to use colour in mathematical equations, is to present colour differences in some numerical format. Various authors have proposed different colour indexes in an attempt to attain this goal.

Godlove (1951) proposed a colour difference equation, which accounts for the difference in Value and Chroma scales:

$$\Delta E = \sqrt{2C_1C_2[1 - \cos(3.6 \times \Delta H)] + (\Delta C)^2 + (4\Delta V)^2} \qquad (2.1)$$

Where $C_1$ and $C_2$ are the Chroma units of two colours, separated by $\Delta C$ chroma units, $\Delta H$ hue units and $\Delta V$ value units. Two sets of different colours can therefore have the same colour difference, due to the fact that the Munsell colour system comprises a three dimensional space (Figure 2.5).

Torrent *et al.* (1983) studied soils from Europe and Brazil. Samples were ground to pass a 50 $\mu$m sieve and the colour determined with a spectrophotometer. They employed the redness rating (RR) index developed by Torrent *et al.* (1980), and found a high correlation between the index and hematite content. They found that the relationship between redness rating and hematite content varied between the samples from Europe and Brazil. They therefore proposed that different correlations be used for different locations.

$$RR = \frac{(10 - H_r) \times C}{V} \quad (2.2)$$

Where:

| | | |
|---|---|---|
| Hr | = | numeric hue (with 2.5 units between hue sheets) |
| C | = | Chroma |
| V | = | Value |

The equations developed by Torrent *et al.* (1983) to give the relationship between hematite content and redness ratings are as follows:

European soils: $RR = -0.1 + \{2.6 \times \text{hematite content (\%)}\}$ (2.3)
$(R^2 = 0.81)$

Brazilian soils: $RR = 2.45 + \{8.2 \times \text{hematite content (\%)}\}$ (2.4)
$(R^2 = 0.76)$

Evans & Franzmeier (1988) studied soils formed from loess on north-central Indiana, with the aim of devising a numerical index to predict saturation, based on soil morphology. They developed two colour indexes. $C1_h$ is based on Chroma alone, while $C2_h$ is based on numeric Hue + chroma:

$$C1_h \text{ or } C2_h = \frac{(A_m \times C1_m) + \{(A_1 \times C1_1) + (A_2 \times C1_2) + \ldots + (A_n \times C1_n)\} + (A_t \times C1_t)}{1 + A_t} \quad (2.5)$$

Where:

| | | |
|---|---|---|
| $A_m$ | = | abundance of matrix with colour index $C_m$ |
| | = | $1 - (A_1 + A_2 + \ldots + A_n)$ |
| $A_1, A_2 \ldots A_n$ | = | abundance of different sized and coloured mottles with colour index $C1_1, C1_2 \ldots C1_n$ |
| $A_t$ | = | abundance of clay cutans with colour index $C_t$ |
| C1 | = | Chroma |
| C2 | = | numeric Hue + Chroma |

Evans & Franzmeier (1988) found correlation coefficients between −0.62 and −0.92 ($R^2$ = 0.38 to 0.85), depending on the depth of the soil horizon and the temperature during saturation. They defined saturation as the presence of a

water table, measured in 14-day intervals using piezometers. They found no marked difference in correlation coefficients between C1 and C2.

Mokma & Cremeens (1991) studied the relationship between soil colour patterns, depth and duration of water tables, and developed a horizon colour index ($CI_h$) based on matrix colour, size and colour of mottles and continuity and colour of clay films:

$$CI_h = C_m + \{(S_1 \times C_1) + (S_2 \times C_2) + ... + (S_2 \times C_2)\} + (C_{cf} \times CI_{cf}) \quad (2.6)$$

Where:

| | | |
|---|---|---|
| $C_m$ | = | colour index of the soil matrix |
| | = | numeric Hue + (8 – Chroma) |
| $S_1$, $S_2$...Sn | = | size of mottles with colour index $C_1$, $C_2$...$C_n$ |
| $C_{cf}$ | = | continuity of clay cutans with colour index $C_{cf}$ |

They found a good correlation ($R^2$ = 0.76) with duration of water saturation, when temperature is above 5 °C. The equation used to predict duration of water saturation (Sat) from the horizon colour index is given by:

$$Sat = -52.9 + 7.3\ CI_h \quad (2.7)$$
$$(R^2 = 0.76)$$

Blavet *et al.* (2000) found a significant relationship between the duration of waterlogging (%), mean angular hue ($R^2$ = 0.52) and mean redness rating ($R^2$ = 0.52) as defined by Torrent *et al.* (1980 and 1983). Blavet *et al.* (2000) also concluded that waterlogging is rare in materials redder than 10YR and is almost permanent in materials greener than 2.5Y. This suggests that colour limits could be defined, when constructing relationships between soil morphology and the duration of water saturation. Blavet *et al.* (2000) employed sigmoïdal functions to describe the relationship. These relationships were, unfortunately, not reported. The lack of correlation between chroma and duration of water saturation is related to the fact that chroma only measures the saturation of a colour. The low correlation between Munsell Value and duration of water saturation ($R^2$ = 0.12) is explained by the

fact that Value is masked by the presence of organic matter (Schulze *et al.*, 1993 as cited by Blavet *et al.* 2000).

The major soil classification systems of the world (Soil Survey Staff, 1975 and FAO, 1998b) also use low soil chroma (< 2) as an indicator of long term water saturation for part of the year.

In South Africa Henning & Von Harmse (1993) found that soil saturation can be detected by hydromorphic properties such as the presence of grey matric colours, mottles, and the presence of diagnostic and non-diagnostic soft plinthic and G horizons. MacVicar (1978) also stated that the formation of soft plinthic B horizons is the result of current profile hydromorphy and not translocation of pre-weathered material. He suggests that the presence of water tables in these soils is consistent with red-yellow-grey vertical profile morphology, and the red-yellow-grey catenas found over vast areas of the country. In his opinion these features support the contention that plinthic soils are a result of current pedogenesis.

Van Huyssteen (1995) studied red apedal B, yellow-brown apedal B, yellow E and grey E horizons for one year on three catenas in the Grabouw district. He found that duration of free water was 1.3 % in red apedal B, 18.8 % in yellow-brown apedal B, 42.2 % in yellow E and 54.4 % in grey E horizons. [Duration of free water was defined as the period that free water was measured in each horizon, expressed in days per year as a percentage.] Fine silt, silt, clay and CEC as well as Fe and Al oxides decreased from red apedal B to yellow-brown apedal B to yellow E to grey E horizons. Total Fe oxides correlated with duration of free water ($R^2$ = 0.41) while amorphous ($R^2$ = 0.37) and fine crystalline Fe ($R^2$ = 0.40) were mainly correlated with dry soil colour chroma. He stated that dry soil colour is a good indicator ($R^2$ = 0.59) of duration of free water and developed the following equation to predict duration of free water in red apedal B, yellow-brown apedal B, yellow E and grey E horizons:

$$\text{Duration of free water (\%)} = 2.35 \times \text{Hue}_{dry} + 5.79 \times \text{Value}_{dry} - 7.31 \times \text{Chroma}_{dry} - 27.89 \quad (2.8)$$

Van Huyssteen (1995) concluded that the present colour definitions for red apedal B, yellow-brown apedal B and E horizons (Soil Classification Working Group, 1991) distinguish satisfactorily between these horizons with respect to duration of free water.

Le Roux (1996) studied published data on plinthite soils to determine the variation in environments where these soils occur and to relate the environmental factors to the nature of these soils. He constructed a phase diagram using aridity index and a soil index defined as {(Si + Cl) : depth of occurrence}. The phase diagram indicated that plinthite soils are in harmony with their present environment. He concluded that the conditions during soil formation correlate well with the current environment. Either the climate has not changed in pedogenic terms or it is now again similar to the conditions of formation. These results therefore support the conclusions drawn by MacVicar (1978) in this regard.

## 2.3 Iron oxide mineralogy and soil water content

### 2.3.1 Origin

According to Fitzpatrick (1980), iron is found in most igneous rocks. It is found in several minerals, for example olivine (61 % FeO), biotite (22 % FeO), augite (20 % FeO) and hornblende (13 % FeO). Iron-bearing minerals include pyrite ($FeS_2$), pyrrhotite (FeS), magnetite ($Fe_3O_4$), chromite ($FeCr_2O_4$) and ilmenite ($FeTiO_3$).

In magmatic rocks divalent iron is bound by silicate. This iron is released from the silicate minerals through protolysis or oxidation:

$$\underset{\text{[Fe(II) silicate]}}{\text{Fe(II)–O–Si} + H_2O} \longrightarrow \underset{\text{[Fe(III) oxide]}}{\text{Fe(III)OH} + \text{–Si–OH} + e^-} \qquad (2.9)$$

This reaction is irreversible and can therefore be used to estimate the degree of weathering. This can easily be done by expressing the dithionite-soluble Fe as a fraction of the total Fe (Schwertmann, 1985).

The released iron has a strong tendency to hydrolyse and form the oxides hematite ($Fe_2O_3$) and goethite (FeOOH) where the soil pH is in excess of 3. Below this pH, iron is normally present in the reduced form. The formation of $Fe^{3+}$ oxides is due to the high affinity of $Fe^{3+}$ for the OH ligand and the ready polymerisation of $Fe^{3+}$ as hydrolysis proceeds. The $Fe^{3+}$ oxides consequently have high solubility constants ($K_{sp} = 10^{-39}$ to $10^{-44}$) and the dissolution of iron oxides by protolysis is therefore improbable, because the soil pH is seldom low enough to permit this reaction.

Iron can, however, easily be mobilised through a reductive reaction:

$$FeOOH + e^- + 3H^+ \longrightarrow Fe^{2+} + 2H_2O \qquad (2.10)$$

This reaction takes place whenever reducing conditions occur, caused by the reduction in $O_2$ content by microbial and / or root respiration, normally under conditions of water saturation. The ferrous iron ($Fe^{2+}$) produced by this reaction can be re-oxidised or transported. New mineral phases can be formed during oxidation. The type and properties of the neo-formed minerals depend on the pedo-environment. The ferrous iron can be transported over very short to long distances, giving rise to spatial redistribution as mottles, concretions in the form of horizons within the soil profile or in the landscape. The removal of iron ultimately results in a grey colour – a result of the remaining soil matrix commonly consisting of quartz and clay minerals. The grey colours are manifested as mottles, cutans or horizons.

### 2.3.2 Minerals

**Goethite** ($\alpha$–FeOOH) has a needle-like crystal structure. The crystal structure may vary considerably – to such an extent that it cannot be used for identification. The needle length varies from 50 to 100 nm, but may be as

small as 20 nm. The surface area varies between 60 000 and 200 000 $m^2\ kg^{-1}$ (Schwertmann *et al.,* 1985; Schwertmann & Taylor, 1989). A high rate of Al substitution for Fe is observed in tropical soils and saprolite. Lower substitution of Al is prevalent in weakly acid soils and in redoximorphic soils (Fitzpatrick & Schwertmann, 1982).

The important soil factors that determine the relationship between goethite and hematite are temperature, water activity, pH and organic matter (Schwertmann, 1985).

Goethite or hematite is formed from the dehydration of ferrihydrite ($5Fe_2O_3 \cdot 9H_2O$). Hematite is favoured as the temperature increases. Goethite does not dehydrate to form hematite. With a decrease in the relative humidity and therefore the soil water content, there is a drastic decrease in the transformation of iron oxides. Hematite was, however, still formed in preference to goethite (Torrent *et al.*, 1982). It therefore seems that hematite formation is influenced more by temperature fluctuation than by the soil water content (Schwertmann, 1985).

The goethite : (goethite + hematite) ratio is a handy tool to correlate soil colour with Fe mineralogy. If the ratio is close to one, goethite is dominant and if the ratio approaches zero, then hematite predominates (Schwertmann, 1985). From the above-mentioned it should be clear that pedo-environments that favour the preservation of carbon (i.e. cool and moist conditions) also favour the formation of goethite relative to hematite. It also seems that the organic matter inhibits the formation of ferrihydrite and therefore also hematite. The formation of goethite from ferrihydrite also seems to be favoured as the pH decreases from 8 to 4. In warmer climates, the dominance of temperature favours the preferential formation of hematite from ferrihydrite.

**Hematite** ($\alpha$–$Fe_2O_3$) gives soils a bright red colour (5YR and redder). Due to its high pigmenting power, it can mask the yellow colour of goethite that may occur in higher concentrations. There is a significant correlation between the

redness of a soil and its hematite content (Torrent *et al.*, 1983). An increase in crystal size leads to a purple colour (Torrent & Schwertmann, 1987). Hematite has a hexagonal crystal shape. The crystal size varies between 20 and 50 nm and the surface area varies between 50 000 and 120 000 $m^2$ $kg^{-1}$. Al substitution for Fe is only half of that observed in goethite. The substitution of Al gives hematite a lighter colour (Barrón & Torrent, 1984 as cited by Schwertmann & Taylor, 1989).

**Lepidocrocite** ($\gamma$–FeOOH) is a polymorph of goethite and has an orange colour. It is widespread in redoximorphic soil, where it occurs as mottles, bands, pipe stems and concretions. The crystals usually form elongated plates or laths with serrated ends. Where lepidocrocite is formed by rapid oxidation, as is the case in root channels or at the soil's surface, the crystals tend to be very poorly developed and only a few layers thick. Al substitution is not common in lepidocrocite. It may be that small amounts of Al lead to the formation of goethite, instead of lepidocrocite (Taylor & Schwertmann, 1978).

Lepidocrocite should not be stable in pedo-environments, because goethite is kinetically more stable. It forms in hydromorphic soils when $Fe^{2+}$ is oxidised and is usually better crystallised than goethite. This may, however, vary depending on the rate of oxidation. If lepidocrocite precipitates inside structure units, the rate of $Fe^{2+}$ and $O_2$ supply will be low, and the oxides will be well crystallised. Inside macro pores and root channels the rate of $Fe^{2+}$ and air supply will be faster and less crystalline oxides will form. Less crystalline lepidocrocite is more reddish in colour (Schwertmann, 1985).

Lepidocrocite is found in association with goethite, but not with hematite. This may be because goethite and lepidocrocite form as a result of competitive processes. Goethite is formed preferentially as the $CO_2$ concentration increases. Goethite would thus be found closer to macro pores and root channels, where the $CO_2$ concentration is higher, and lepidocrocite would be found some distance away. It has been shown in laboratory experiments (Taylor & Schwertmann, 1978 as cited by Schwertmann, 1985) that > 10

mole % Al completely suppresses the formation of lepidocrocite. This will influence the occurrence of lepidocrocite in strongly acid, hydromorphic soils (Blume, 1968 as cited by Schwertmann, 1985).

**Magnetite** ($Fe_3O_4$) occurs as black grains in soil and is inherited from the parent material. Magnetite converts to hematite during pedogenesis. Fine-grained magnetite can also easily oxidise to maghemite, which contains $Fe^{2+}$ and $Fe^{3+}$ (Schwertmann, 1985).

**Maghemite** ($\gamma$–$Fe_2O_3$) occurs in many soils of the tropics and subtropics. It has a reddish-brown colour. Substitution of Al for Fe is possible. Maghemite is similar in structure to magnetite and is a dimorph of hematite (Schwertmann, 1985).

**Ferrihydrite** ($5Fe_2O_3 \cdot 9H_2O$) is widespread and is characteristic of young Fe accumulations. It typically precipitates during the oxidation of Fe-containing water as well as in podzol horizons. The colour of ferrihydrite is redder than goethite, but less so than hematite. It forms spherical particles, 3 to 7 nm in diameter, with a surface area of 200 000 to 500 000 $m^2\ kg^{-1}$ (Table 2.1). It therefore possesses the ability to adsorb silicate, phosphate and organic molecules. Ferrihydrite is almost completely soluble in ammonium oxalate (Schwertmann, 1985).

Table 2.1 General characteristics of iron oxide minerals (Schwertmann, 1985)

| Mineral | Hematite | Goethite | Lepidocrocite | Ferrihydrite | Maghemite | Magnetite |
|---|---|---|---|---|---|---|
| Composition | $\alpha$–$Fe_2O_3$ | $\alpha$–FeOOH | $\gamma$–FeOOH | $5\ Fe_2O_3 \cdot 9H_2O$ | $\gamma$–$Fe_2O_3$ | $Fe_3O_4$ |
| Density ($kg\ m^{-3}$) | 5 260 | 4 260 | 4 090 | 3 960 | 4 870 | 5 180 |
| Colour | bright red | yellowish-brown | orange | redder than goethite | reddish-brown | black |
| | 5R – 2.5YR | 7.5YR – 2.5Y | 5YR – 7.5 YR | 5YR – 7.5 YR | | |
| Size (nm) | 10 to 20 | 50 to 100 | | 3 to 7 | | |
| Surface area ($X\ 10^3\ m^2\ kg^{-1}$) | 50 to 120 | 60 to 200 | | 200 to 500 | | |

### 2.3.3 Properties

a) Mineral surface structure

The Fe ions at the surface of an oxide complete its ligand shell by hydroxylation in the presence of water. This is followed by the adsorption of water molecules through hydrogen bonding (Figure 2.1). The amount of water that is bound in a monomolecular layer increases with increasing surface area, but generally ranges between 0.3 and 0.4 mg $m^{-2}$. This water seems to be tightly bound and can only be driven off at 200 °C (Schwertmann & Taylor, 1989).

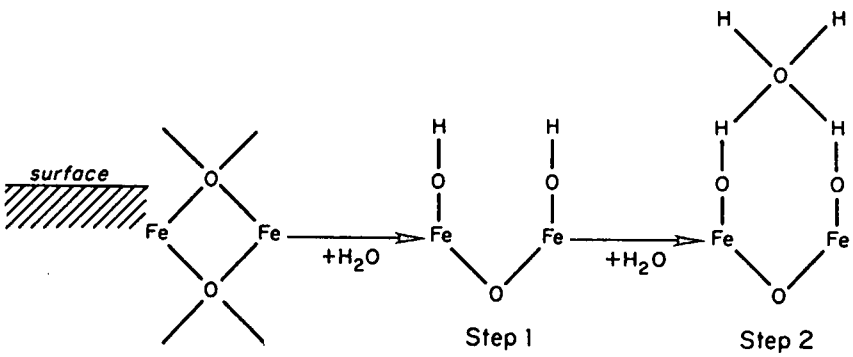


Figure 2.1 The reaction of surface Fe in oxides with water through two steps: hydroxylation (step 1) and hydration (step 2) (Schwertmann & Taylor, 1989).

b) Surface charge

A positive or negative charge can be created at the hydroxylated or hydrate surface by the adsorption of $H^+$ (Figure 2.2). The charge can therefore vary, depending on the soil pH. The pH at which the net surface charge equals zero is called the point of zero charge. The point of zero charge varies between 7 and 9, but is normally lower in soil (pH < 7) due to the adsorption of anions (Schwertmann & Taylor, 1989).

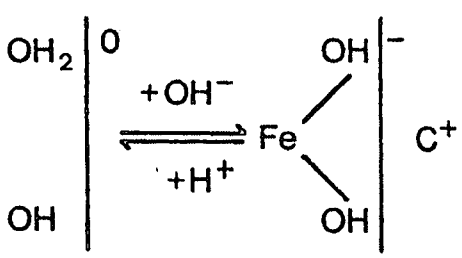


Figure 2.2 Adsorption and desorption of $H^+$ on Fe oxides, resulting in a pH dependent charge (Schwertmann & Taylor, 1989).

c) Ion adsorption

The positive or negative charge on Fe oxides are balanced by anions or cations, held in an outer diffuse double layer. Cations and anions can also chemically bind to the Fe oxide surface, thus increasing or decreasing the charge.

Heavy metals can be adsorbed by Fe oxides. The extent of adsorption is determined by the pH, due to its influence on the pH dependent charge. Heavy metals are adsorbed in the order Cu > Pb > Zn > Cd > Co > Ni > Mn (Schwertmann & Taylor, 1989).

Anions such as phosphate, silicate, molybdate, arsenate, selenate, sulfate and organic anions can also be adsorbed on Fe oxides. Borgaard (1983), for example, found that there is a correlation between adsorbed phosphate and the amount of oxalate extractable Fe. This can severely impact on P fertilization.

d) Adsorption of organic molecules

Humic acid and fulvic acid are found concentrated with Fe oxides in podzol horizons. The amount of fulvic and humic acid adsorbed on the surface of the Fe oxides increases as the pH decreases from 8 to 3. Simple organic acids and herbicides behave in a similar manner to humic and fulvic acids (Schwertmann & Taylor, 1989).

e) Aggregation and cementation

Finely divided Fe oxides can act as binding agents between individual soil particles, binding them into larger units. This results in aggregation or cementation (Schwertmann & Taylor, 1989).

Cementation is a process whereby Fe oxides fill the pores between the particles – through crystal growth – to form nodules and ferricretes. These are often quite large, although they may also be small. Cementation can

inhibit root and water movement, while at the same time immobilising nutrients.

Aggregation takes place when the positively charged Fe oxides form bridges between the negatively charged silicate clays. This process is pH dependent, because the positive charge on Fe oxides is pH dependent. It can therefore be expected that aggregation by Fe oxides will increase with an increase in Fe oxide content as well as a reduction in pH. The amount of Fe oxides required for aggregation is much lower than that required for cementation, although all intergrades are possible (Shadfan *et al.*, 1985). The lower the Fe oxide crystallinity and the higher the oxalate extractable fraction, the higher the aggregation effect. There also seem to be examples where Fe oxides do not affect aggregation (Borgaard, 1983; Deshpande *et al.*, 1964 and 1968; Schwertmann & Kämpf, 1985). The aggregation effect of Fe oxides therefore seems to vary with the amount and nature of Fe oxides as well as the nature of the pedo-environment during their formation.

### 2.3.4 Iron oxides and micro organisms

Although Fe oxides are highly insoluble, they can easily be mobilised through reduction by micro organisms. Reduction of Fe occurs whenever oxygen is deficient, and micro organisms use other electron acceptors during the oxidation of organic matter substrate. Reduction of $Fe^{3+}$ takes place when $O_2$ becomes deficient and the redox potential (Eh) has been lowered to approximately +100 mV (Bohn, McNeal & O'Connor, 1985).

The micro-organisms in the soil respire. This means that they use oxygen as final electron acceptor in a long range of chemical reactions in order to extract energy from the organic material they use as a food source. The use of oxygen as final electron acceptor ensures that the highest amount of energy can be released from the organic matter. Some micro organisms can use other electron acceptors in this process in the absence of oxygen, as is the case in soils saturated with water. These other elements are used in order of

decreasing redox potential. This ensures that the most energy is always released by the reaction. There are therefore three prerequisites for a decrease in the redox potential of the soil. The first is the presence of micro organisms, second is the presence of organic matter food substrate, and third a restricted oxygen supply. Data for this study suggests that organic matter is present throughout the profile, although it diminishes with depth (see for example Table 2 in Appendix A).

Various micro organism species, mainly anaerobic bacteria, can utilise Fe in this process (Ottow & Glathe, 1971; Schwertmann *et al.*, 1985). The $Fe^{2+}$ produced by this reaction is soluble and enters the soil solution. It can therefore be leached or it can move to a zone with a higher Eh, where it will be re-oxidised. The activity of $Fe^{2+}$ in the soil solution will therefore increase with a decrease in the Eh and pH. At a given Eh and pH the activity of $Fe^{2+}$ will increase with a decrease in the solubility of the $Fe^{3+}$ oxide (Schwertmann, 1985).

Typical reduction reactions (Bohn, McNeal & O'Connor, 1985) and their redox potentials in the soil are presented in Table 2.2. From these reactions it is clear that reduction will take place in the sequence: $NO_3^-$ – $MnO_2$ – FeOOH – $SO_4^{2-}$ – $H^+$, due to the decreasing redox potential and therefore energy supply, of each reaction.

Table 2.2 Typical reduction reactions and their redox potentials in the soil (Bohn, McNeal & O'Connor, 1985)

| Half reaction | Redox potential measured in soil (mV) |
|---|---|
| $O_2 + 4\,e^- + 4\,H^+ \rightarrow 2\,H_2O$ | 600 to 400 |
| $NO_3^- + 2\,e^- + 2\,H^+ \rightarrow NO_2^- + H_2O$ | 500 to 200 |
| $MnO_2 + 2\,e^- + 4\,H^+ \rightarrow Mn^{2+} + 2\,H_2O$ | 400 to 200 |
| $FeOOH + e^- + 3\,H^+ \rightarrow Fe^{2+} + 2\,H_2O$ | 300 to 100 |
| $SO_4^{2-} + 6\,e^- + 9\,H^+ \rightarrow HS^- + 4\,H_2O$ | 0 to −150 |
| $2\,H^+ + 2\,e^- \rightarrow H_2$ | −150 to −220 |
| $2\,CH_2O \rightarrow CO_2 + CH_4$ | −150 to −220 |

The products formed during anaerobic respiration are, however, not stable in soil and quickly oxidise in the presence of oxygen. Fe and Mn also play an important role in soil, because they act as colouring agents. Fe and Mn are immobile in their oxidised states. Reduction and redistribution or removal of these agents causes distinct colour patterns that can be associated with the water regime in soils, due to the above-mentioned relationships.

From the above one can expect that the redox potential will be lowest in soils with the longest duration of water saturation. This relation is clear from the redox potential data in Table 2.2.

There is an inverse relationship between redox potential (mV) and pH in soil. This is because $H^+$ is used in the reduction reactions during the oxidation of organic matter (Table 2.2). This causes a decrease in the $H^+$ concentration, resulting in an increased pH. It can be expected that horizons not saturated for long periods, have extracted soil water pH values closer to the measured soil pH. Soils with longer durations of saturation have higher pH values in the extracted soil water.

Ferrihydrite can be dissolved and reprecipitated within a few days, even under mildly reducing conditions. On the other hand coarse crystalline hematite will resist reduction even under long term reduced conditions (Schwertmann, 1985).

### 2.3.5 Determination

Iron oxides can be identified and quantified by their mineral-specific colour, differential dissolution and X-ray diffraction analysis (XRD).

Dithionite-citrate-bicarbonate (CBD) extracts practically all secondary Fe oxides ($Fe_d$) *i.e.* Fe not part of the clay lattice (Mehra & Jackson, 1960; McKeague et al., 1971). Acid ammonium oxalate extracts poorly crystalline and organic complexed Fe oxides ($Fe_o$). Pyrophosphate extracts organic complexed Fe oxides ($Fe_p$). The amorphous Fe oxide (mainly ferrihydrite)

content ($Fe_a$) can therefore be calculated as $Fe_o - Fe_p$. The crystalline Fe oxide content ($Fe_c$) can be calculated as $Fe_d - Fe_o$, while the ratio of oxalate ($Fe_o$) to dithionite ($Fe_d$) extractable iron quantifies the active iron fraction in the soil (Mehra & Jackson, 1960; Schwertmann, 1985, McKeague et al., 1971).

X-ray diffraction analysis is used for identification of the various crystalline phases (Brindley & Brown, 1980). Detection of Fe by these techniques is hampered by the low concentration of Fe. Concentration techniques can be used to overcome this. Particle size separation (Fe is usually found in the finer fractions), magnetic separation (Schulze & Dixon, 1979), and 5 M NaOH treatment which dissolves silicate clay minerals (Norrish & Taylor, 1961), can be used as concentration techniques.

## 2.4 Pedogenesis and water content

Iron plays a prominent role in four processes of soil formation. Brinkman (1979) proposes two processes (*cheluviation* and *ferrolysis*) for the genesis of a bleached horizon. In *ferrugination* and *gleying*, iron is responsible for the reddish and grey colouring of soils respectively (Buol, Hole & McCracken, 1973).

Cheluviation is the result of $Al^{3+}$ removal by chelating agents. This results in the dissolution of Al-rich minerals *e.g.* chlorites, and eventually montmorillonite. The removal of the weathering products ultimately results in a pure quartz matrix. Accumulation and liberation of $Al^{3+}$ from the chelates can cause the precipitation of an aluminium hydroxide, Al-interlayering in 2:1 clay minerals or synthesis of new clay minerals. Where these processes are dominant, soils will have a higher $CEC_{clay}$ in the A and E horizons than in the underlying B or C horizons. The clay fraction of the E horizon will also contain more montmorillonite and less chlorite, kaolinite and Fe oxides, compared to the lower horizons.

Ferrolysis relies on alternate reduced and oxidised conditions. During saturation, reduction takes place, consuming $H^+$ and releasing of $Fe^{2+}$. The dissolved $Fe^{2+}$ distorts the cation ratio and is adsorbed on the clay complex, releasing the exchangeable bases. Exchangeable bases, $Al^{3+}$ and $Fe^{2+}$ are leached, leading to Al-interlayering between the 2:1 clay minerals and ultimately the formation of 1:1 clays. Some Fe oxides may be trapped in the interlayer spaces during this process. This lowers the CEC and increases the Fe content of the clay fraction. During oxidation the $Fe^{2+}$ concentration in the soil solution decreases and exchangeable $Fe^{2+}$ is released to the outer soil solution where it is oxidised, with the associated release of $H^+$, leading to an acid environment and the formation of a $H^+$ saturated clay. This leads to clay decomposition, releasing Al and Mg that leads to the formation of Al and Mg saturated clays. The process is more rapid in smectite and vermiculite soils, than in chlorite and kaolinite soils. Horizons subjected to ferrolysis therefore have less smectite and vermiculite, more interlayered clays, a lower CEC and a higher Fe oxide content than the underlying horizons.

Ferrugination (Buol, Hole & McCracken, 1973) is the process of soil reddening in upland soils, resulting in dispersion and oxidation of Fe oxides throughout the profile. Gleying on the other hand is the reduction of Fe oxides, its segregation into mottles or concretions and / or its removal from the gleyed horizon.

Eluviation and leaching (Buol, Hole & McCracken, 1973) are analogous, in the sense that both refer to the removal of material (colloids and / or elements). Eluviation is the removal of suspended colloids while leaching refers to the removal of dissolved elements. Both processes require mobilisation and translocation of the material in question.

Illuviation and enrichment are analogous in a way similar to eluviation and leaching. Both require the interruption of translocation, resulting in immobilisation of the transported material in a horizon or solum. Illuviation

refers to the accumulation of clay minerals while enrichment refers to the accumulation of dissolvable elements.

The transformation of hematite to goethite is closely related to a change in the organic matter content of a soil, which is in turn determined by the climate (Schwertmann, 1971). Increased availability of organic mater results in increased reduction and / or complexing of Fe. Reprecipitation upon oxidation usually results in the formation of goethite. The hematite to goethite ratio therefore reflects the carbon regime of a soil, which in turn reflects the climate. Warm, dry conditions favouring the mineralisation of organic matter will therefore favour the formation and persistence of hematite. On the other hand, wet and cool conditions will favour the dissolution of hematite and the precipitation of goethite (Schwertmann, 1971).

Fey (1983) amended the theory of Schwertmann (1971) by proposing that the greater stability of goethite relative to hematite results in the preferential dissolution of the latter. This leads to the removal of the red colouring agent while the yellow goethite remains. The yellowing of soils will therefore be determined by the initial Fe content of the parent material, the extent of Al substitution, the availability of an organic substrate and the soil redox status. Fey (1983) concluded that "the intensity and duration of reducing conditions reflected by pedogenic yellowing will probably vary widely" and that "once it is possible to identify more quantitatively the soil conditions reflected by yellowing in its various forms, it should become possible to predict the extent to which chemical transformations such as denitrification and manganese reduction will manifest themselves as agronomic problems...".

McCarthy & Bremner (1992) supported the hypothesis of lower rates of reduction at lower levels of organic carbon deeper down in the soil. They frond that denitrification of nitrate is in subsoils is not due to a lack of denitrifying bacteria, but due to a lack of organic carbon. De Villiers (1965) found that lepidocrocite is active (hematite and goethite are absent) in yellow-

brown horizons where the organic mobilization of Fe is active, while hematite and goethite predominate in the deeper, red horizons.

In reduced soils Fe is mobilised through reduction, leading to an increase in exchangeable Fe, which replaces exchangeable bases on the exchange complex. This results in the mobilisation of Fe and exchangeable bases. For example, Tarekegne (2001) found that ammonium extractable nutrients increased with increasing severity of waterlogging and postulated that the damaging effects of waterlogging were not due to Mn, Fe, or Na toxicity, but rather decreased nutrient (P & Zn) uptake due to $O_2$ deficiency. The concentration of Mn and Fe greatly increased in the soil due to waterlogging.

Fiedler *et al.,* 2002 determined that redox conditions and an abundance of chelating agents are the main factors that lead to the mobilization of cations, Fe, Mn and clay. They found that redox conditions in the mid-catena zones led to the depletion of Fe and Mn, while accumulation of Fe, Mn and organic carbon took place lower down in the catena. They concluded that taxonomic soil type (Soil Survey Staff, 1975; FAO, 1998b) reflects pedogenic soil processes and soil material dynamics, but that these dynamics are not adequately represented for the low lying soils.

## 2.5 Colour models

The gift of sight and the perception of colour is probably an individual's greatest gift. We are able to distinguish different shapes and are able to associate different colours to that shape. This ability of man is also applied in soil classification, with nearly all diagnostic criteria reliant on visual soil properties. Colour of the soil is especially useful in this regard. The big challenge is, however, to be able to note soil colour in a standardised manner. With this in mind, the USDA adopted the Munsell color charts as a colour reference system (Soil Survey Staff, 1975). New technology, e.g. digital cameras, scanners and image processing software, however, opens new avenues to analyse images of soil profiles. The challenge now shifts to finding

correlations between the following different platforms: reality vs. captured image vs. computer analysis.

### 2.5.1 Munsell

During 1975 the Soil Survey Staff adopted the Munsell Soil Color Charts as standard soil colour referencing system (Soil Survey Staff, 1975). This was done in an attempt to standardise soil colour representation. Until then colour was noted in a freestyle manner.

The Munsell Soil Color Charts (Munsell Color Company, 1975) are extracts from the more comprehensive Munsell Book of Color (Munsell Color Company, 1980). The system takes the shape of a colour ball, where the central (vertical) axis denotes the "Value" (Figure 2.3). The Value ranges from zero at the bottom of the axis to ten at the top. Value denotes the darkness of a colour, where one is the darkest (absolute black) and nine is the lightest (absolute white). Absolute achromatic colours, where the chroma is zero, do therefore not have a hue and are designated as neutral. The letter "N" takes the place of the hue designation.

Looking from the top of the colour ball (Figure 2.4), the "Hue" forms radians from the central axis. The Hue is defined in terms of five major colours: red, yellow, green, blue and purple. Complementary colours (yellow-red, yellow-green, blue-green, purple-blue and red-purple) are arranged between these major colours. Each colour ranges from zero to ten. The zero value coincides with the ten value of the previous colour. The Hue's are arranged on a circular scale. This configuration gives rise to 100 Hue's, each separated by a 3.6 degree angle. Only the 2.5, 5, 7.5 and 10 hues are represented in the Munsell Soil Color charts. The separation between hue pages in the Munsell Soil Color Charts is therefore nine degrees (Melville & Atkinson, 1985).

Chroma ranges from zero for the neutral grey colours to about twenty (Figure 2.5). Chroma expresses the strength of a colour, or its departure from neutral at the same lightness. Not all chromas are found in soil and some are

therefore excluded from the Munsell Soil Color Charts. The chromas in the Munsell Soil Color Charts normally range from zero to eight.

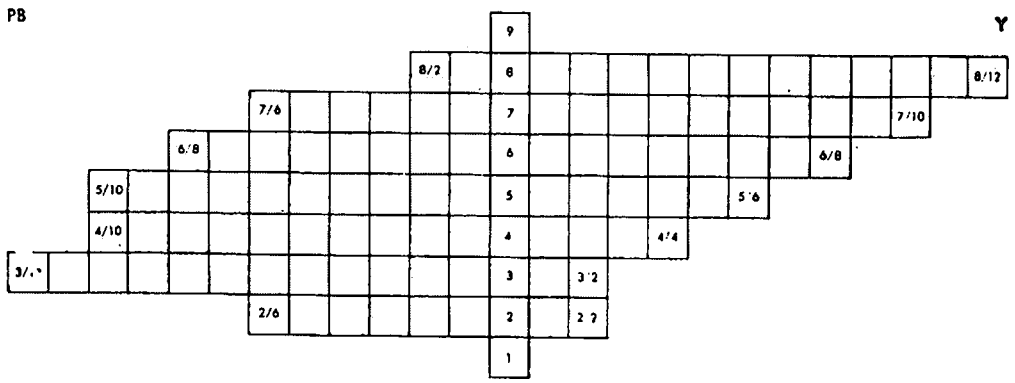


Figure 2.3 The partition of value and chroma along the 10Y – 10PB axis (Fujihara Industry Company, 1967). Note that the chromas differ at different values and hues.

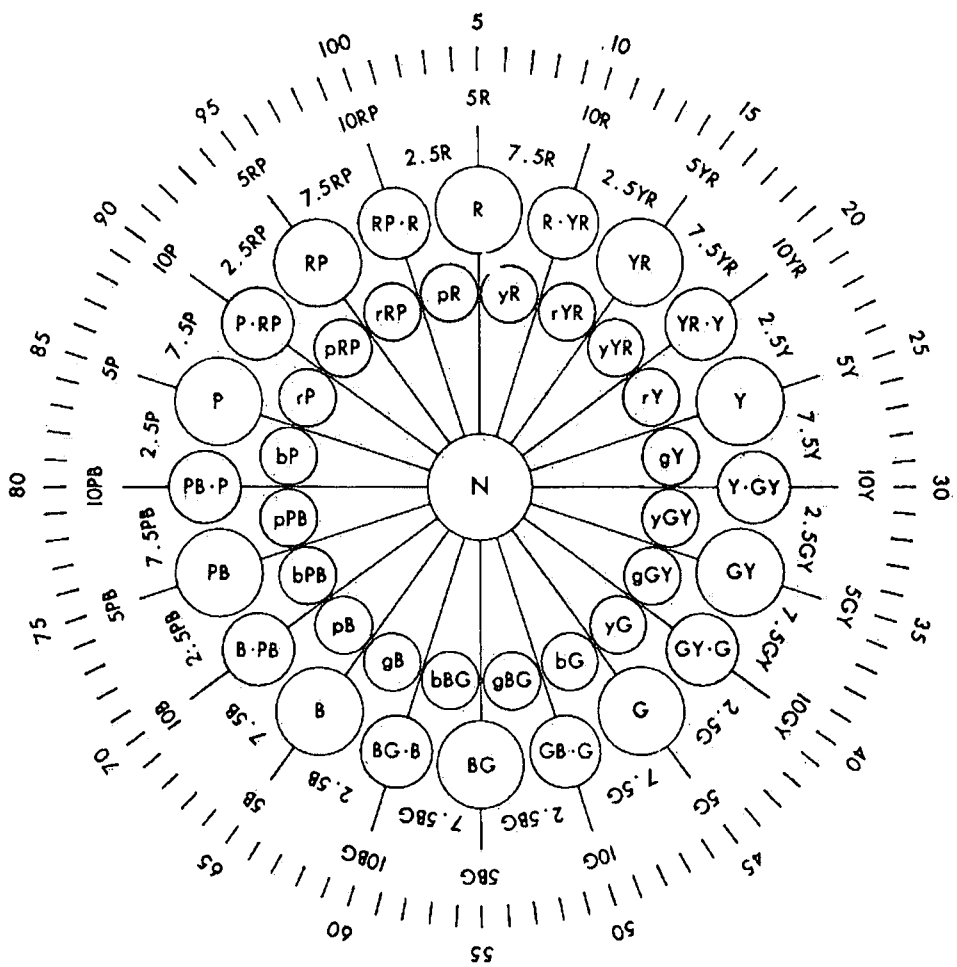


Figure 2.4 The division of Hues in the Munsell Color System (Fujihara Industry Company, 1967).

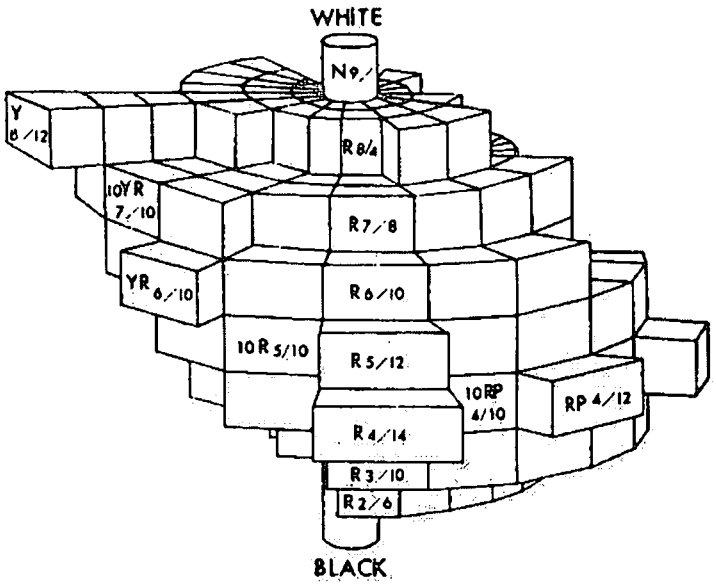


Figure 2.5 The Munsell color solid (Fujihara Industry Company, 1967). Note that colours further from the centre of the solid are further from one another.

The Munsell Color System is a decimal system i.e. there exist intermediaries between the different Hue's, values and chromas. These intermediaries are expressed as decimals e.g. 2.5YR3.2/4.8. The colours depicted in the Munsell Color System were selected to represent equal steps of visual colour perception (Melville & Atkinson, 1985). There are therefore discrete steps when the Munsell colour values are plotted against any other colour system (Figure 4.6).

Melville and Atkinson (1985) list the following main advantages of the Munsell Color System:

a) The system is not limited by present day colour production techniques, but can be expanded as production technology develops.
b) The colour chips are produced to very stringent tolerances.
c) Equal steps in visual perception and spacing exist between each of the colour co-ordinates.

"Few color systems are nearly as good in this respect; the Munsell system is the standard to which other systems are compared." (Billmeyer & Saltzman, 1981 as cited by Melville and Atkinson, 1985)

### 2.5.2 CIE

In 1931 the Commission Internationale de l'Eclairage (CIE), or the international commission on light, developed a system for specifying colour stimuli using tristimulus values for three imaginary primaries (Poynton, 1999). The CIE system works by weighting the spectral power distribution of an object in terms of three color matching functions. These functions are the sensitivities of a standard observer to light of different wavelengths. The weighting is performed over the visual spectrum, from around 360nm to 830nm in 1nm intervals. This process produces three CIE tri-stimulus values, XYZ, which describe the color. The main advantage of the CIE XYZ system is that it is completely device independent. The main disadvantage with CIE based colour spaces is the complexity of implementing them; in addition some are not user intuitive (Poynton, 1999). An example of the CIE colour space is given in Figure 2.6.

Conversion from RGB to CIE *XYZ* can be done with the following matrix (Poynton, 1999):

$$X = 0.412411 \times \text{Red} + 0.357585 \times \text{Green} + 0.180454 \times \text{Blue} \quad (2.11)$$

$$Y = 0.212649 \times \text{Red} + 0.715169 \times \text{Green} + 0.072182 \times \text{Blue} \quad (2.12)$$

$$Z = 0.019332 \times \text{Red} + 0.119195 \times \text{Green} + 0.950390 \times \text{Blue} \quad (2.13)$$

### 2.5.3 RGB

RGB (Red-Green-Blue) is an additive color system (Figure 2.7) based on trichromatic theory. RGB colour notation is commonly used in television cameras, computer graphics, *etc.* It is easy to implement, non linear, device dependent and unintuitive. Red, Green and Blue are also known as additive primary colours, because a color is produced by adding different quantities of the three components, red, green, and blue (Poynton, 1999). The values of RGB range from 0 to 255, which also define the colour space (Figure 2.8).

To convert between RGB and CMY, the following equations can be used, provided the RGB values are expressed as a fraction:

RGB to CMY

| | | | |
|---|---|---|---|
| Red | = 1−Cyan | (0 ≤ Cyan ≤ 1) | (2.14) |
| Green | = 1−Magenta | (0 ≤ Magenta ≤ 1) | (2.15) |
| Blue | = 1−Yellow | (0 ≤ Yellow ≤ 1) | (2.16) |

CMY to RGB

| | | | |
|---|---|---|---|
| Cyan | = 1−Red | (0 ≤ Red ≤ 1) | (2.17) |
| Magenta | = 1−Green | (0 ≤ Green ≤ 1) | (2.18) |
| Yellow | = 1−Blue | (0 ≤ Blue ≤ 1) | (2.19) |

The algorithm for conversion from RGB to Munsell colour notation is proprietary (Poynton, 1999). In this study a computer program, which allows for conversion between all the major colour notation systems, was used (Anon, 2003b). Look-up tables can also be used with equal success (Travis, 1991 as cited by Adderley *et al.*, 2002).

### 2.5.4 CMY

CMY (Cyan-Magenta-Yellow). CMY are known as subtractive colours (Figure 2.7), because the color is generated by subtracting different quantities of cyan, magenta and yellow from white. It is used in printing and photography. Printers often include a fourth (black) component to improve the colour range, to improve black colours, to save money and for speeding drying (because there is less ink to dry). CMY is fairly easy to implement but it is difficult to transfer properly from RGB – sometimes resulting in colour differences between those visible on screen and printed in documents. CMY is device dependent, non-linear and unintuitive (Poynton, 1999).

### 2.5.5 Application

Adderley, *at al.*, (2002) described a method for determining the colour of thin sections and converting it to Munsell color notation. They used a three-chip video camera to obtain HLS images (576 pixels x 760 pixels) through a polarizing microscope. CIE was calculated from the HLS images (Harrington,

1997 as cited by Adderley, *at al.,* 2002), which was then converted to Munsell color notation using look-up tables (Travis, 1991 as cited by Adderley, *at al.,* 2002).

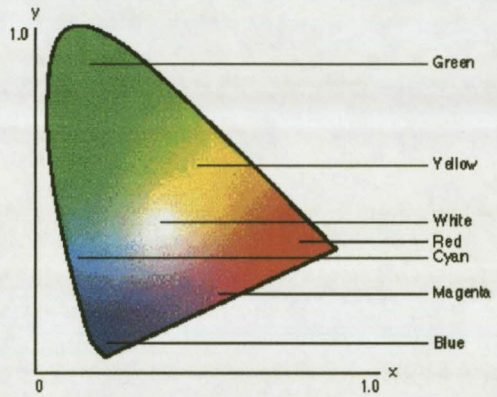


Figure 2.6 The CIE colour space (Anon., 2003a).

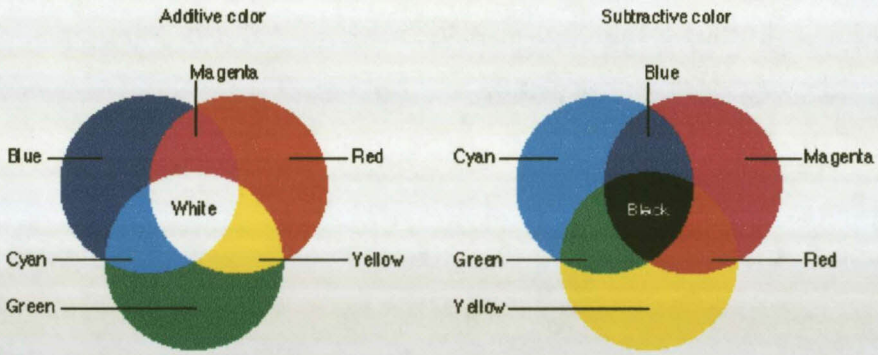


Figure 2.7 Examples of additive (RGB) and subtractive {CMY(K)} colour spaces (Anon., 2003a).

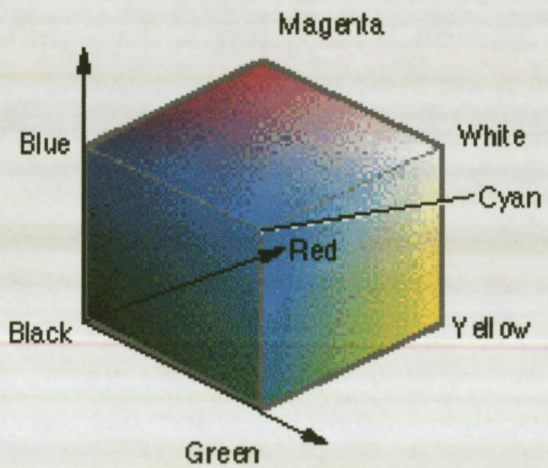


Figure 2.8 The RGB colour space (Anon., 2003a).

## 2.6 Summary

Due to their striking colour Fe oxides play an important role in soil morphology. They can be reduced, leached, eluviated, illuviated and oxidised. Fe oxides are therefore the main colouring agents responsible for the red and yellow colours in soil. Lack of Fe oxides on the other hand causes revelation of the grey soil matrix colours. It is mainly the redox status of a soil that determines the fate of Fe oxide, because it is not soluble or mobile in the oxidised state. The presence and distribution of Fe oxides can therefore be used to infer soil redox status.

# 3 GEOGRAPHY OF THE STUDY AREA

## 3.1 Introduction

The Weatherley study area is situated in one of the most picturesque areas of South Africa, on the foot slopes of the Drakensberg mountain range (Figure 3.1). The climate is cool and wet, with warm wet summers and cold dry winters. This region has only recently been deemed suitable for forestry and has been planted since 1989. Weatherley escaped this development and only received attention during 1995 when it was decided to utilise this catchment to monitor the impact of forestry on catchment water yield. Pitting in the Weatherley catchment was done during 9 to 18 April 2002. Partial planting of the catchment was done from 2 to 13 September 2002 (Figure 3.2).

## 3.2 Location

The study catchment is located in the north-eastern corner of the Eastern Cape Province. It occupies approximately 150 ha and constitutes most of the farm Weatherley. It is situated 4 km south-west of Maclear, on the road to Ugie (Figure 3.1). The study area is covered by the 1:50 000 sheet 3128AB Maclear (Chief Director of Surveys and Mapping, 1993).

## 3.3 Relief (macro / micro)

The study area is the upper-most catchment of one of the very small tributaries of the Mooi River (Figure 3.1). There is therefore no inflow of water into the catchment (Figure 3.3), which makes it highly attractive for hydrological studies. It drains in a north-easterly direction and is therefore closed on the eastern, southern and western slopes.

The eastern and southern slopes have prominent shelves at approximately 1 320 m above mean sea level. This is largely due to the resistance of Elliot sandstone against weathering.

The highest point in the catchment, at 1 352 m, occurs in the south western corner of the catchment. The stream runs in a north easterly direction and occurs at a height of between 1 254 and 1 286 m.

Moles and earthworms are very active in the catchment. This is probably due to the moist conditions that predominate in the soils. It leads to the formation of many surface mounds, to such an extent that walking becomes difficult. It is possible that macro faunal activity is associated with changing water regimes in the soil. Moles and earthworms will move to drier soil in summer when it rains and back to the wetter soils in the dry winter months.

## 3.4 Geology

Elliot sandstone and mudstone are found above approximately 1 300 m above mean sea level (Figure 3.4). This covers the upper slopes on the Eastern and Southern slopes. Below that sandstone and mudstone of the Molteno Formation predominates. There are two dolerite dykes in the catchment (Figure 3.4), both running roughly in a north-south direction, one in the south western corner and one in the north eastern corner. The former creates a natural sub catchment in the south western part of the catchment.

## 3.5 Climate

Two automatic weather stations were installed in the catchment on 1 January 1996 by the ARC-ISCW and were operated by NECF (BEEH, 2003). Data from these stations are not yet in a usable format. Annual mean rainfall is given in Table 3.1. A rain and mist gauge is also located at the eastern edge of the catchment (close to P201; Figure 3.3). A Bowen Ratio Apparatus, for the measurement of transpiration, was installed and operated by the CSIR-

Environmentek, from 13 July 2001 to 9 December 2001, just north of the upper-catchment weir.

The best climate data available is that recorded at Maclear, roughly 2.5 km from the Weatherley catchment (Table 3.2). The area has moderately high rainfall, which occurs mainly in summer. The mean annual aridity index $\left(\frac{\text{rainfall}}{\text{evaporation}}\right)$ is 0.50 and the value for the period December to March is 0.84.

The summer is hot, with mean maximum temperatures of 25 °C. Winters are cold and snow is common, especially on the surrounding higher lying areas. Mean winter minimum temperatures are 4 °C.

Table 3.1 Yearly rainfall, calculated from daily values, measured at Weatherley. Data is influenced by missing values (BEEH, 2003)

| Year | Rainfall (mm) |
|---|---|
| 1997 | 458.2 |
| 1998 | 1186.4 |
| 1999 | 1008.6 |
| 2000 | 1303.6 |
| 2001 | 924.8 |
| 2002 | 861.8 |
| Mean | 957.2 |

Table 3.2 Summarised climate data from a weather station roughly 2.5 km from the study area (Roberts *et al.* 1996)

| Month | Rainfall (mm) | Evaporation (A-pan) (mm) | Temperature (monthly means) (°C) | | |
|---|---|---|---|---|---|
| | | | Maximum | Minimum | Mean |
| January | 123 | 143 | 25 | 14 | 20 |
| February | 120 | 129 | 25 | 14 | 20 |
| March | 108 | 130 | 24 | 12 | 18 |
| April | 43 | 102 | 24 | 11 | 18 |
| May | 18 | 102 | 21 | 7 | 14 |
| June | 11 | 90 | 18 | 4 | 11 |
| July | 11 | 96 | 19 | 4 | 11 |
| August | 18 | 118 | 19 | 6 | 11 |
| September | 35 | 132 | 21 | 8 | 14 |
| October | 62 | 140 | 21 | 10 | 15 |
| November | 83 | 165 | 24 | 12 | 18 |
| December | 109 | 143 | 24 | 13 | 19 |
| Total | 741 | 1490 | | | |

## 3.6 Soils

Due to the high rainfall and the sandy lithology, the soils in the catchment are highly acidic. The soils also have a very low cation exchange capacity. A soil survey was done by Roberts *et al.* (1996), using Soil Classification – A Taxonomic System for South Africa (Soil Classification Working Group, 1991). The soils range from very wet (Katspruit soil form) to very dry (Hutton and Oakleaf forms). Most of the soils do, however, show clear signs of water saturation. These signs range from faint mottles to grey zones characterised by clay depletion, often referred to as silans or skeletans (Le Roux *et al.,* 2003; Soil Science Society of America, 2001). Strongly structured Sepane soils also occur on the northwest facing slopes in the southern part of the catchment (Figure 3.5).

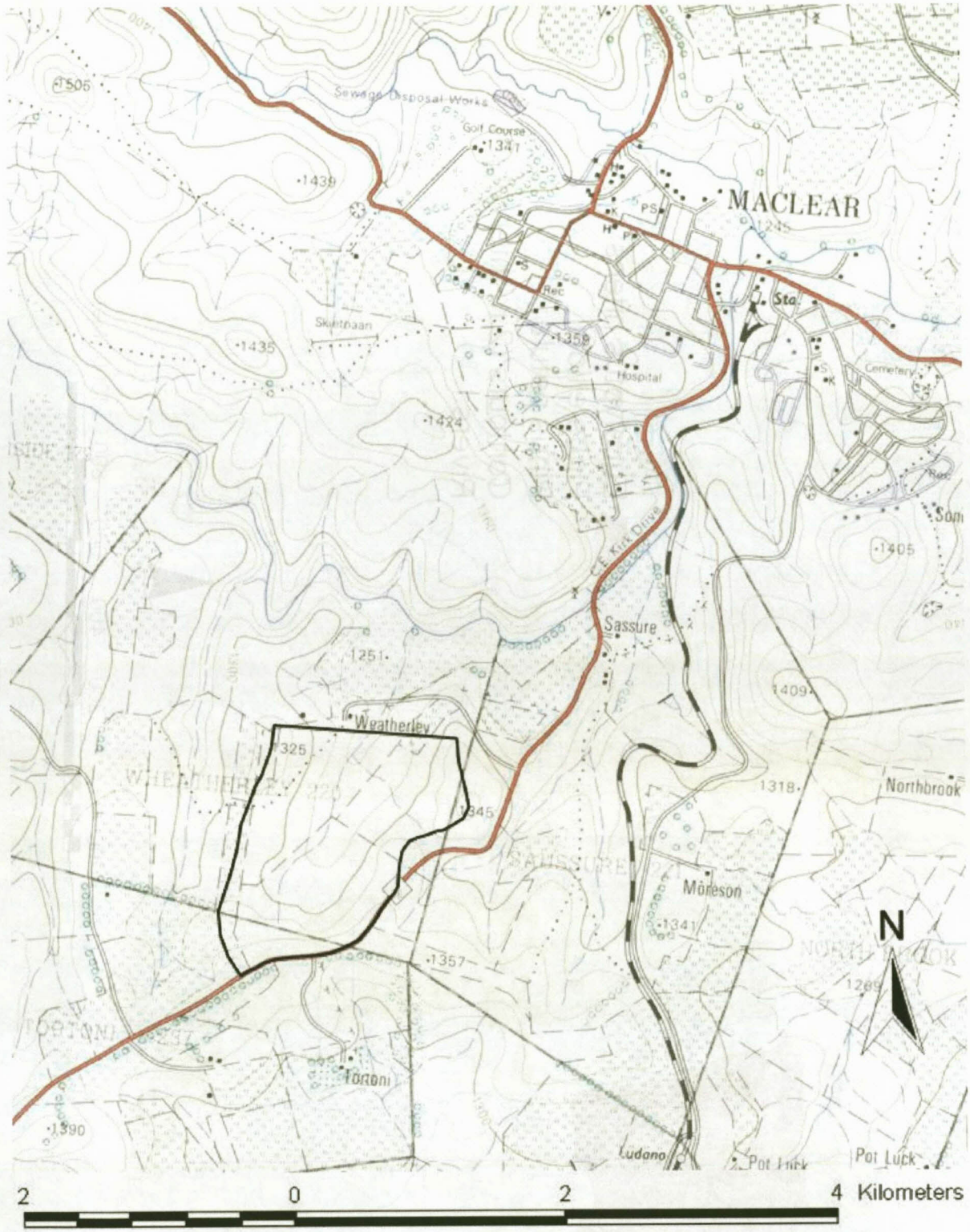


Figure 3.1 The location of the Weatherley catchment, 4 km south of Maclear on the road to Ugie (Chief Director of Surveys and Mapping, 1993).

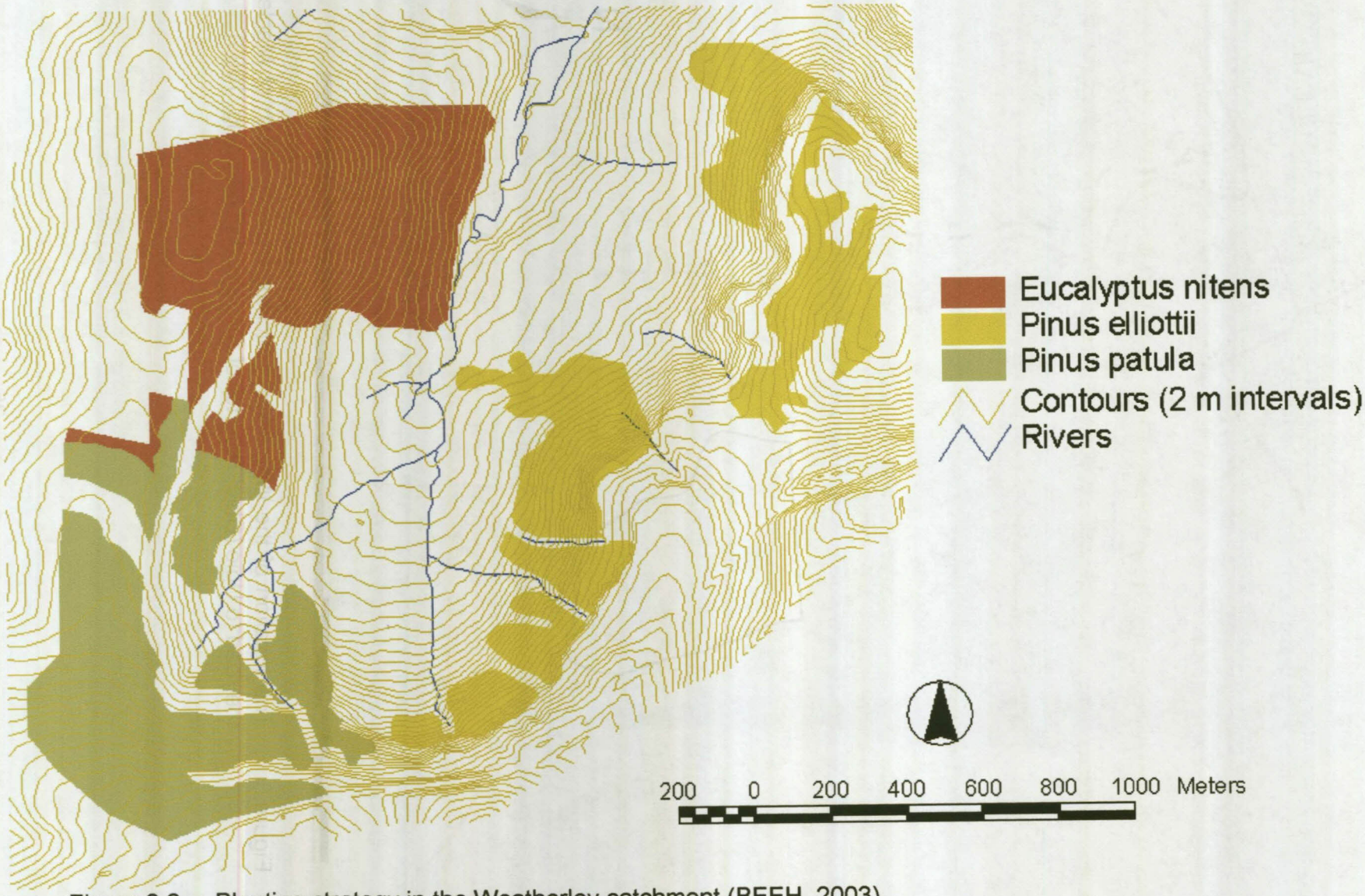


Figure 3.2 Planting strategy in the Weatherley catchment (BEEH, 2003).

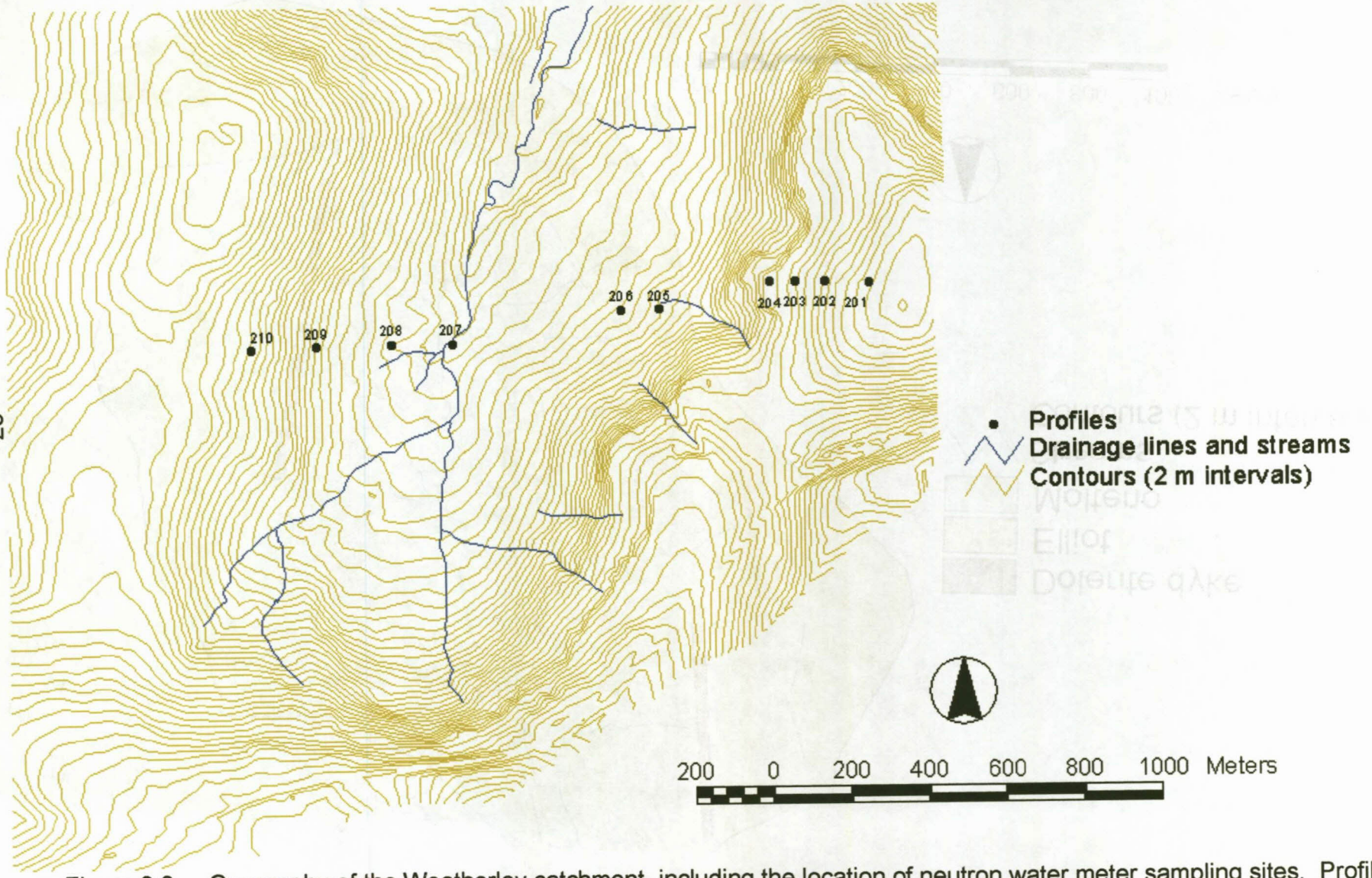


Figure 3.3 Geography of the Weatherley catchment, including the location of neutron water meter sampling sites. Profiles at measuring sites 201 to 210 were selected for this study.

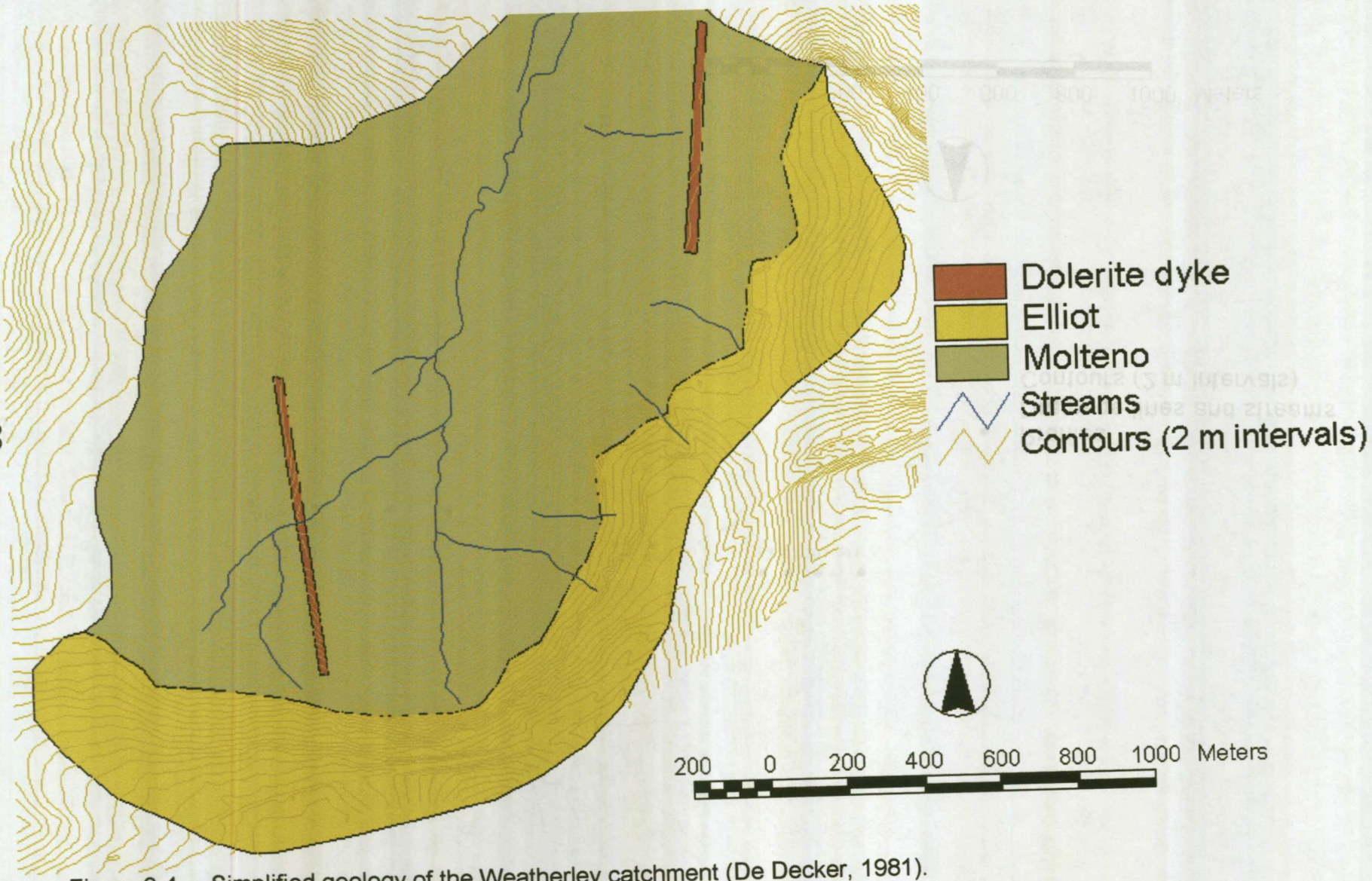


Figure 3.4 Simplified geology of the Weatherley catchment (De Decker, 1981).

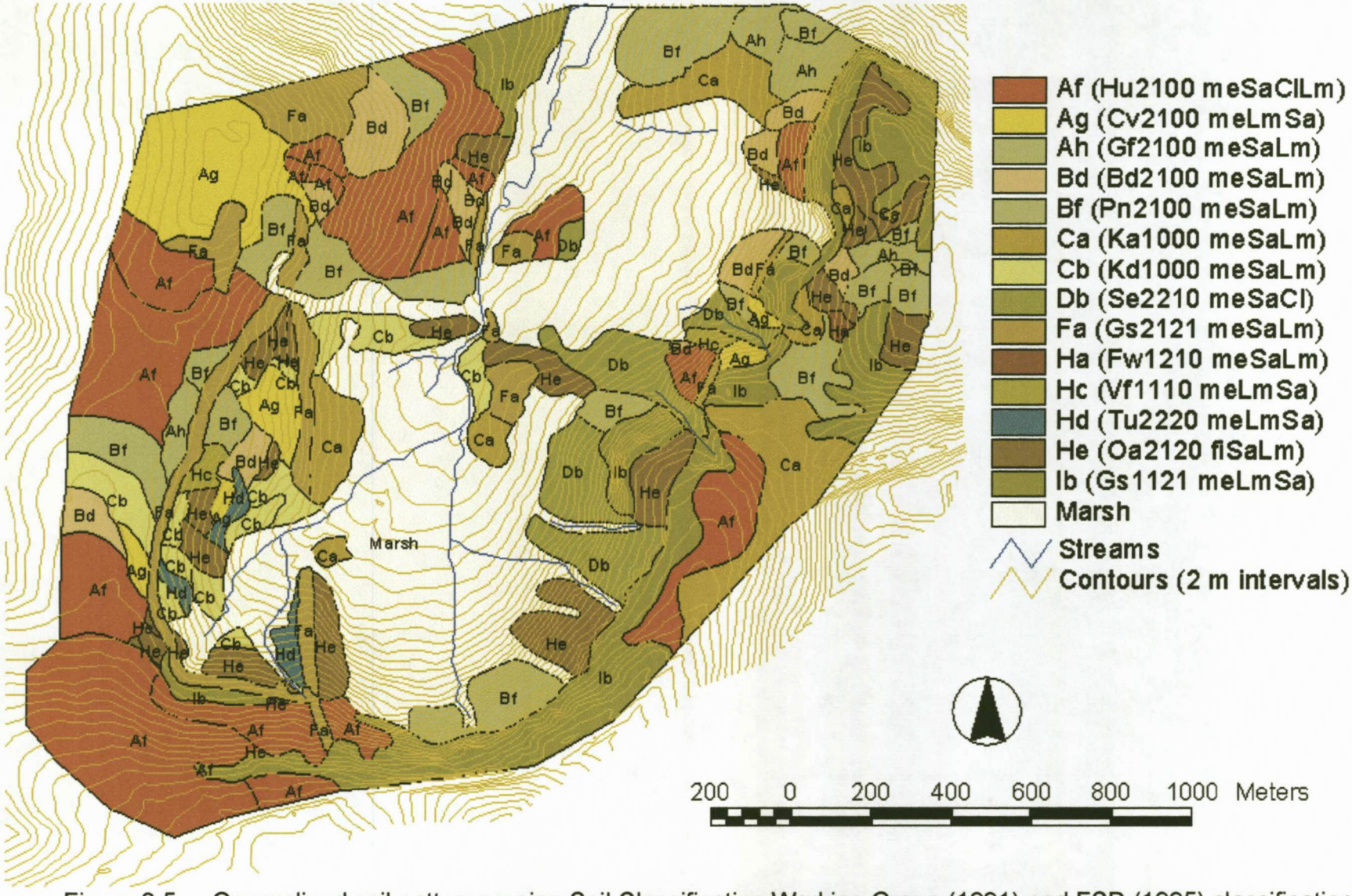


Figure 3.5 Generalised soil patterns, using Soil Classification Working Group (1991) and FSD (1995) classification, according to Roberts *et al.* (1996).

## 3.7 Hydrology

Runoff is measured at two crump weirs in the Weatherley catchment (Figure 3.3). Data for the lower weir is given in Figure 3.6. It is clear that runoff is concentrated in the first quarter of the year and that runoff normally occurs as peaks, presumably after large rain storms. A large variation in annual runoff is also clearly shown.

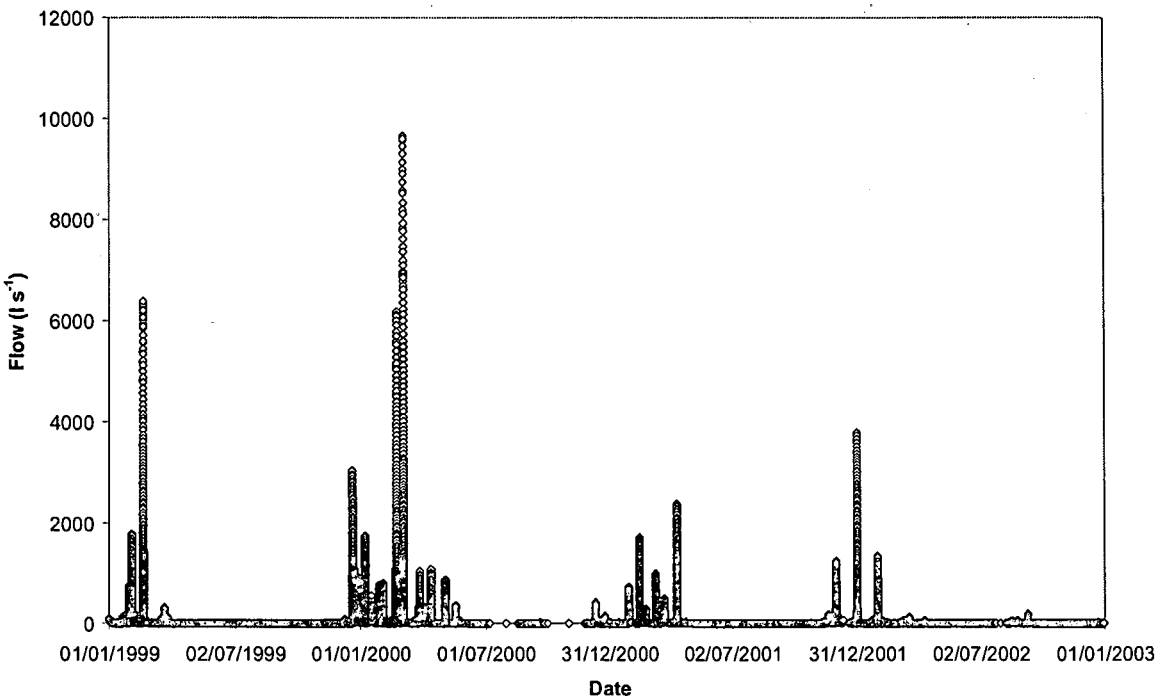


Figure 3.6 Hydrograph, showing runoff at the lower weir in the Weatherley catchment (BEEH, 2003).

## 3.8 Summary

The Weatherley catchment was selected mainly because a vast amount of work has been, and is continuously, being done at this site. It therefore offers the opportunity to build on previous research whilst at the same time creating the opportunity to make valuable contributions to future research. Lithology in the Weatherley catchment is mainly Elliot and Molteno sandstone, with two dolerite dykes bisecting it. The summers in are wet and hot, while the winters are cold and dry. The mean annual aridity index is 0.50. Soils in the Weatherley catchment are characterized by varying degrees of hydromorphy. This complicates the study, but also provides ample opportunity to study water saturation in these highly leached and sometimes permanently saturated soils.

# 4 METHODOLOGY

## 4.1 Introduction

The aim of data accumulation during this study was to measure those soil properties that would shed more light on the processes that influence soil morphology. In this regard, soil water content formed the backbone of the data accumulation phase. Bulk density, through its influence on volumetric water content and degree of saturation was further deemed to be very important. Soil profiles were described, classified, photographed and analysed to illustrate soil morphology and the soil chemical and physical environment as well as possible.

## 4.2 Selection of the study site

Defining the relationship between soil profile morphology and soil water regime is generally difficult due to the lack of sufficient quantitative and qualitative soil water data. This is not the case at Weatherley. The available information includes the following:

a) Detailed hydrological measurements over six years at 28 strategic sites and continuous tensiometer readings at selected sites.
b) Bulk density, hydraulic conductivity and matric suction curves for important horizons at selected sites.
c) Detailed soil survey data (28 modal profiles, with 427 soil auger observations by Roberts *et al.*, 1996).
d) Data from two automatic weather stations (BEEH, 2003).
e) Hydrological data from two Crump weirs, sited to allow for detailed process-based hydrological modelling (BEEH, 2003).
f) Runoff measurements from two runoff plots, situated on western and eastern side of the catchment (BEEH, 2003).

g) Evapotranspiration (ETo) measurements from a Bowen Ratio apparatus, located to measure integrated evaporation within the catchment (BEEH, 2003).
h) Four WRC project reports (Lorentz, 2001; Lorentz *et al.*, 2001; Van Huyssteen *et al.,* 2002; Van Huyssteen *et al.,* 2003a).
i) Two M.Sc. (Hydrology) theses (Esprey, 1997; Hickson, 2000).
j) Various conference papers (Lorentz & Esprey, 1998; Lorentz & Hickson, 2001; Le Roux *et al.,* 2003; Van Huyssteen *et al.,* 2003b; Van Huyssteen *et al.,* 2003c).

The Weatherley catchment was chosen for this study because of the vast amount of data that has been collected for the catchment. It further provided the opportunity to work across established research boundaries.

## 4.3 Field measurements

Neutron water meter measuring sites were selected by a hydrologist to elucidate hillside water movement. At that time there was no thought that these measuring sites would be used to relate soil profile morphology with soil hydrology. Because of all the measurements available now, the results can, however, also be used beneficially for the latter purpose. This is true in spite of some profiles being located in sites which are transitional or non-representative from a pedological point of view *e.g.* P204 (Longlands) and P207 (Westleigh; Figure 3.3).

Only ten profiles, sited at ten sites selected from the available 28 neutron water meter sites, were used due to the vast amount of data available in the Weatherley catchment. The ten profiles were selected to form a catena of soils, representing the western and eastern aspects of the catchment and also form the main catena from a hydrological point of view. The ten profiles (Figure 3.3) were sited so as to occur close to current neutron water meter access tubes and tensiometer nests, while keeping a distance of 2 m between the in-field instrumentation and the profile pits.

Initial pedological field measurements were done during the last two weeks of June 2001. During this period soil profiles were dug, profiles were described, and soil samples and bulk density samples were taken.

A profile pit was dug at each monitoring site and the soil profile morphology described in detail, using the methods proposed by Turner (1991). Additional features were noted and included in the descriptions. Special attention was given to colour variations and the occurrence of mottles.

The three dominant dry and wet matrix colours were described, using new Munsell Soil Color Charts (Munsell Color Company, 1975). An estimate of the occurrence (area percentage) of each colour was also made. The colour, size, shape, occurrence, boundary and cause of mottles were also described. Colours were described by a number of people, to eliminate personal bias.

Representative soil samples were taken per diagnostic horizon at 100 mm intervals throughout the solum. Intervals were varied to accommodate morphological variation and were increased to 200 or 300 mm in the lower part of the solum. Soil samples were air dried and crushed with a rubber pestle in a ceramic mortar. Samples were sieved through a 2 mm sieve to remove the gravel. The soil and gravel were weighed and stored.

Digital photographs of each profile and individual horizons were taken. These photographs were analysed, using GIS techniques, to quantitatively determine soil matrix colour and the colour, size, shape and quantity of mottles. Photographs were taken in direct sunlight.

The lithology of the parent material was described for each soil profile. Special attention was given to soil profiles with more than one parent material. Samples of the rock and saprolite were taken for analysis.

Bulk density was measured, using the core method (Blake & Hartge, 1986). Cores used had a larger than normal volume (933 000 $mm^3$) to increase sampling volume and decrease the risk of sample variation due to spatial variation. Bulk density data reported here are results obtained from core measurements taken during June 2001 and July 2003, as well as gamma probe measurements taken in 1997 (Hensley, personal communication), June 2001 and July 2003. Measurements reported by Esprey (1997) are also included. Undisturbed core samples (644 000 $mm^3$) were also taken.

Soil water contents were measured using a neutron water meter. Three CPN instruments (2022, 3411 and 8550) were used during the course of this study. The instruments were calibrated against each other, using standard high density plastic tubes (Reginato & Nakayama, 1987). Data is stored in a Microsoft Access database. This data was extracted and the volumetric soil water contents calculated. Volumetric soil water contents and degree of water saturation were calculated from the neutron water measurements. Calculations are described in section 4.4. Although neutron water meter (NWM) measurements were started on 9 November 1995, only data for nine measurements are available up to the end of 1996. Fairly regular measurements were taken during the ensuing years. Measuring depths were kept at standard 300 mm intervals. Although every effort was made to do regular measurements, the mean duration between measurements was 8.7 days, while the median duration between measurements is 7.0 days. Measurements were made 249 times at the relevant access tubes between 1 January 1997 and 10 January 2003.

## 4.4 Calculation of degree of water saturation

The degree of water saturation (Hillel, 1980) was calculated as:

$$s = \frac{V_w}{V_f} \tag{4.1}$$

Where: s = degree of saturation (as a fraction)

$V_w$ = water content ($mm^3$)

$V_f$ = total pore volume ($mm^3$)

The degree of saturation measures the volume of water relative to the total pore volume. It ranges from zero in dry soil to unity (one) when all soil pores are filled with water. Complete saturation is seldom reached, because some air is almost always trapped by the water in wet soil (Hillel, 1980). In soil with a small pore volume a small amount of water will lead to saturation, while in a soil with a larger pore volume, more water will be required to reach saturation.

The total porosity (f) was calculated as follows:

$$f = 1 - \frac{\rho_d}{\rho_s} \qquad (4.2)$$

Where: $\rho_d$ = bulk density ($kg\ m^{-3}$)

$\rho_s$ = particle density ($kg\ m^{-3}$)

Due to the relatively large duration between measurements (8.7 days mean), an effort was made to calculate intermediate values. This can be done in a number of ways. The first attempt was done by making a linear regression between two measurements. The relative contribution of a rainfall event was then calculated to estimate the increase in saturation:

$$s_{n+1} = \left(\frac{P_{n+1}}{\Delta P} + \frac{\Delta s}{1}\right) + s_n \qquad (4.3)$$

Where: $s_{n+1}$ = degree of saturation on day n+1 (day of rain event)

$P_{n+1}$ = rainfall on day n+1 (mm)

$\Delta P$ = total rainfall between measurements (mm)

$\Delta s$ = difference in degree of saturation between measurements

$s_n$ = degree of saturation on the date of first measurement

The proposed method was tested on the A horizon of profile 201. The calculation yielded disappointing results (Table 4.1). There was no significant

difference in the total duration of s above 0.5 of porosity. This method was therefore abandoned.

Table 4.1 The relationship between duration of s calculated from measured and calculated degrees of saturation for the A horizon of profile 201 over a period of 1 106 days

| Saturation limit | Duration of s | | | |
|---|---|---|---|---|
| | Measured | | Calculated | |
| | Days | % | Days | % |
| 0.5 | 533 | 48.2 | 529 | 47.8 |
| 0.4 | 746 | 67.5 | 741 | 67.0 |
| 0.3 | 951 | 86.0 | 950 | 85.9 |
| 0.2 | 1049 | 94.8 | 1049 | 94.8 |
| 0.1 | 1106 | 100.0 | 1106 | 100.0 |

The duration of s can be determined in two ways. Firstly by measuring the time intervals that s exceeds say 0.7 on a graph on which degree of water saturation is plotted against time, e.g. Figure 3 in Appendix A. The base line of the peaks > 0.7 is measured to obtain an estimate of the period in days. Secondly it may be calculated using the following equation:

$$AD_{s>0.7} = \sum_{s_n > 0.7}^{year} DOY_n - DOY_{n-1} \qquad (4.4)$$

Where:

$AD_{s>0.7}$ = duration of s above 0.7 of porosity (days $year^{-1}$)
$DOY_n$ = date of measurement
$DOY_{n-1}$ = date of previous measurement
s = degree of saturation
year = calendar year

An experiment was done to determine the relevance of results provided by the calculation and measurement methods. The results for profile 201 are given in Table 4.2 and shows satisfactory agreement between the two methods. It was therefore concluded that the calculation method can be used with reasonable confidence to determine duration of s above a certain fraction.

Duration of s was calculated by adding the duration of s > 0.7 events. A s > 0.7 event is defined as a measurement where s is in excess of 0.7 and s for the previous measurement is less than 0.7. This is based on the assumption that in the long-term, a particular measurement is representative of the soil water regime for the period between half way from the previous measurement that had s < 0.7, to half way towards the following measurement which also had s < 0.7. For two consecutive measurements with s > 0.7 the entire period would be included when using equation 4.4.

Table 4.2 The duration of s > 0.7 for profile 201, given by calculation and measurement methods

| Measuring depth (mm) | Duration of s > 0.7 ($D_{s>0.7}$) (% of time) | | |
|---|---|---|---|
| | Calculated | Measured | Difference |
| 150 | 1.77 | 1.91 | 0.14 |
| 450 | 3.39 | 5.26 | 1.87 |
| 750 | 27.00 | 27.27 | 0.27 |

Mean duration of s > 0.7 events was calculated as the fraction of mean yearly duration and frequency of saturation events:

$$F_{s>0.7} = \sum_{s>0.7}^{year} Date_n \qquad (4.5)$$

$$D_{s>0.7} = \frac{AD_{s>0.7}}{F_{s>0.7}} \qquad (4.6)$$

Where:

$F_{s>0.7}$ = frequency (events year$^{-1}$)

$D_{s>0.7}$ = mean duration of s > 0.7 events (days event$^{-1}$)

The term "annual duration of water saturation above 0.7 of porosity" ($AD_{s>0.7}$) is defined here to be very specific for the following reasons: Firstly, the redox system that was studied is a complex one. Soil water content, soil water $O_2$ content, soil Fe content and carbon content are but a few factors that determine the redox conditions in a soil. Secondly, these factors are further influenced by landscape position, climate parent material and living organisms.

The choice of 70 % of porosity as a lower threshold for the onset of significant reduction is therefore a first approximation. It is further likely that this value will be different for different horizons and soil profiles, due to the complex nature of the system, as specified above. The unit used for $AD_{s>0.7}$ in this study is days per year. It draws from the fact that duration of water saturation was calculated on an annual (calendar year) basis and that by expressing it as a fraction invites the reader to apply it on a monthly or weekly basis, which would be erroneous.

The time resolution for calculations can only be weekly, or a minimum of 7 days, because NWM measurements were done weekly. This is important to remember, as the calculation of means over the six years often resulted in durations less than 7 days, including fractions. It could therefore imply greater detail than is permitted by the data.

## 4.5 Laboratory measurements

All chemical analyses were done according to standard methods described by The Non-Affiliated Soil Analysis Work Committee (1990). Soil samples were analysed for particle size distribution (7 fractions), pH ($H_2O$ and KCl), exchangeable cations, cation exchange capacity (CEC), organic carbon, nitrogen, as well as dithionite-citrate-bicarbonate, pyrophosphate and oxalate extractable Fe and Mn.

The results of pyrophosphate and oxalate extraction of Fe and Mn yielded disappointing results, to such an extent that no attempt was made at interpretation thereof. It is also supported the findings of Loeppert & Inskeep (1996). They stated that: "... the pyrophosphate extract contained following high-speed sentrifugion includes microcrystalline iron oxide particles ..." and that "the pyrophosphate extractable Fe cannot be designated as organically bound Fe".

Due to the very low clay content in some of the horizons, the $CEC_{clay}$ was calculated by subtracting the $CEC_{organic\ matter}$ from the $CEC_{soil}$. This was then divided by the clay content to yield the $CEC_{clay}$. The organic matter content was calculated as 1.74 * organic carbon content and the $CEC_{organic\ matter}$ was taken as 200 $cmol_c\ kg^{-1}$ organic matter (Brady & Weil, 1996).

## 4.6 The soil water balance

To quantify the drainage water or "spare water" ("spare" since it is water over and above that available for ET), which becomes available for low flow, the soil water balance equation (Jury & Gardner, 1991) can be applied. The soil water balance equation was adapted for the situation at Weatherley and in particular to allow for run-on and capillary rise:

$$\Delta W = P \pm R \pm D - ET \quad (4.7)$$

Where:

| | | |
|---|---|---|
| $\Delta W$ | = | Change in soil water content (mm) |
| P | = | Precipitation |
| R | = | Run-off (−) and run-on (+) |
| D | = | Deep percolation (−), capillary rise (+) and lateral drainage (±) |
| ET | = | Evapotranspiration |

The change in soil water content can also be written as:

$$\Delta W = \theta_n - \theta_{n-1} \quad (4.8)$$

Where:

| | | |
|---|---|---|
| $\theta_n$ | = | Soil water content on day n |
| $\theta_{n-1}$ | = | Soil water content on day n−1 |

Therefore:

$$\theta_n - \theta_{n-1} = P \pm R \pm D - ET \quad (4.9)$$

Reasonable estimates can be made of ET, using the FAO Penman-Monteith equation (FAO, 1998a), including correlation with Bowen Ratio measurements (BEEH, 2003). It is therefore possible to estimate deep percolation or capillary

rise (± D), except ± D using equation 4.10, because data for all other factors are available.

$$\pm D = \theta_n - \theta_{n-1} - R + ET \pm R \qquad (4.10)$$

Although redox conditions, and resulting redox morphology, sets in at a soil water content approaching saturation, the volume of water involved can differ between soil horizons. This is due to the differences in bulk densities and therefore pore volumes. To make a reliable estimate of the volume of water where redox conditions set in, it is therefore necessary to have reliable bulk density values for each horizon. As Θ approaches saturation, the macro pores become increasingly more filled and the "spare water" or water that will be released for stream flow water, can be estimated. To do this, the volume of each soil horizon is needed. This can be calculated from a detailed soil map.

## 4.7 Digital photographs

Digital colour photographs were taken of each profile and master horizon, with a Sony MVC-FD83 digital camera. Photographs were cropped to remove shaded areas, the measuring tape, grass and other foreign matter from the photo. This photographic "sample" of each horizon was used in further calculations.

An attempt was made to classify the digital photograph into diagnostic red, yellow and grey colours (Soil Classification Working Group, 1991). Analyses of colour photographs were done using ArcView's SpatialAnalyst extension (ESRI, 2000). Digital photographs, however, use RGB notation (Poynton, 1999), while soil colour definitions are in Munsell colour notation (Soil Classification Working Group, 1991). The transformation between Munsell and RGB is discussed in section 2.5.3.

Calculated RGB values did, however, not correspond to the actual RGB values of a photographed Munsell hue sheet. There does, however, exist a

good correlation ($R^2$ = 0.99) between calculated and observed RGB values for the 7.5YR Munsell hue sheet (Figure 4.1).

Red = 0.9238x − 37.24 $R^2$ = 0.986 (4.11)

Green = 0.9975x − 38.96 $R^2$ = 0.985 (4.12)

Blue = 0.9841x − 35.74 $R^2$ = 0.987 (4.13)

Bartlett's test (Snedecor & Cochran, 1989) was done to determine the difference between the regression lines of Red, Green and Blue, determined by calculation and photography. The values are significantly higher than 3.12 – indicating that the lines differ at the 95 % confidence level (Table 4.3). The slopes and the Y-intercept also differ for the three equations.

Table 4.3 Bartlett's test results, indicating the difference in regression lines of calculated *vs.* photographed Red, Green and Blue

| | Red | Green | Blue |
|---|---|---|---|
| Bartlett | 24.68 | 20.61 | 3.22 |
| Line | 15.88 | 39.68 | 6.30 |
| Slope | 13.18 | 17.12 | 7.51 |

Lighting influences the colour of the object (Melville & Atkinson, 1985), but for all three colours this correlation seemed to be independent of lighting source when indirect indoor sunlight, direct sunlight, shaded sunlight and neon light were tested (Figure 4.2, Figure 4.3 and Figure 4.4). It is therefore proposed that analyses of digital photographs can be compared, irrespective of the lighting conditions. It is, however, imperative to correct the Munsell colour co-ordinates for instrument deviations from the calculated values, using the above equations.

There exists an exponential relationship between scanned and calculated RGB values for the 7.5YR hue sheet (Figure 4.5). It is not certain why this is, but it should be clear that there would be different results between the analyses of digital photographs and scanned optical photographs. This relationship was not studied in more detail, because all photographs in this study were made with a digital camera.

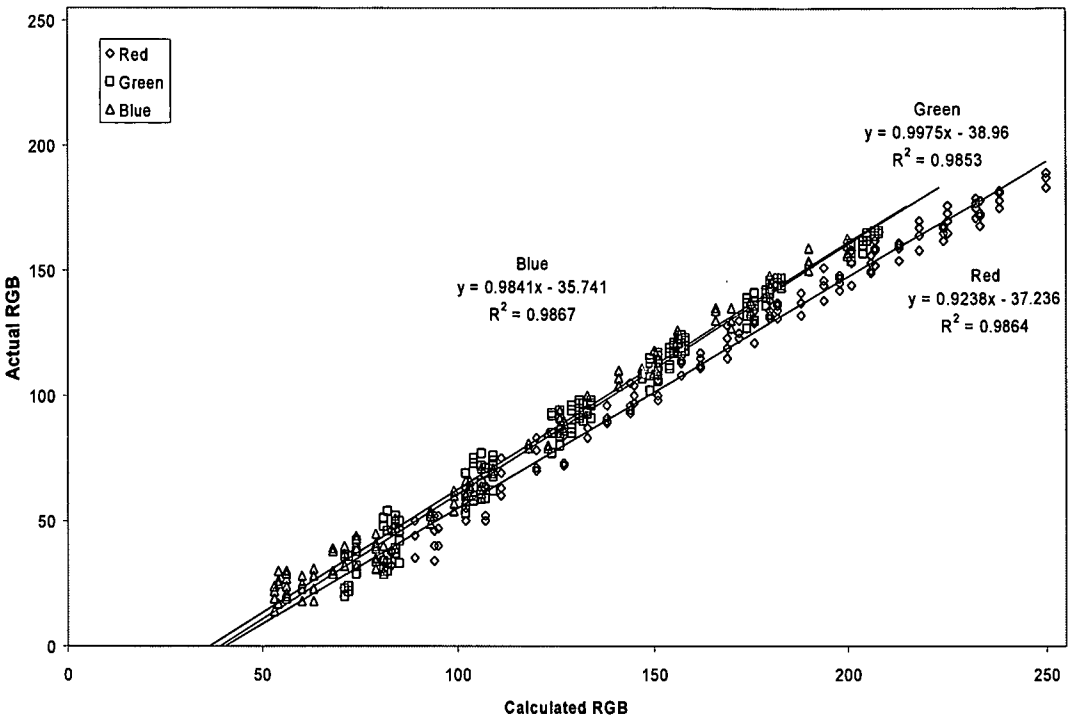


Figure 4.1 The relationship between calculated and photographed Red, Green and Blue values of the 7.5YR Munsell hue.

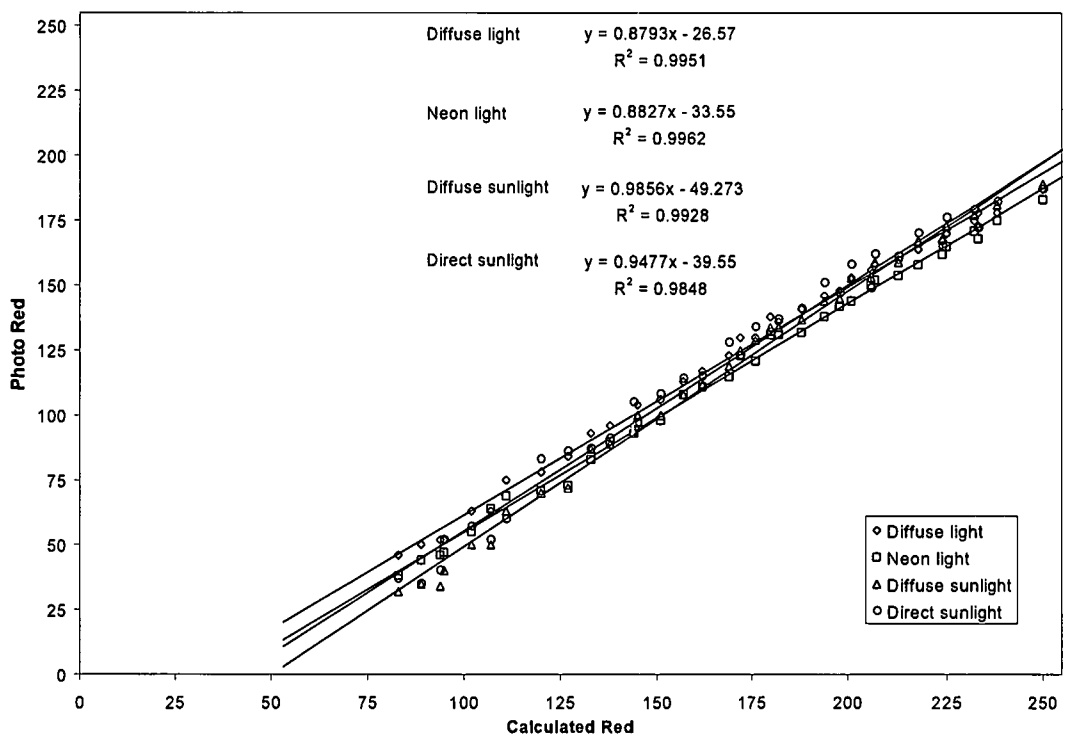


Figure 4.2 The relationship between calculated and photographed Red values of the 7.5YR Munsell hue, in different light sources.

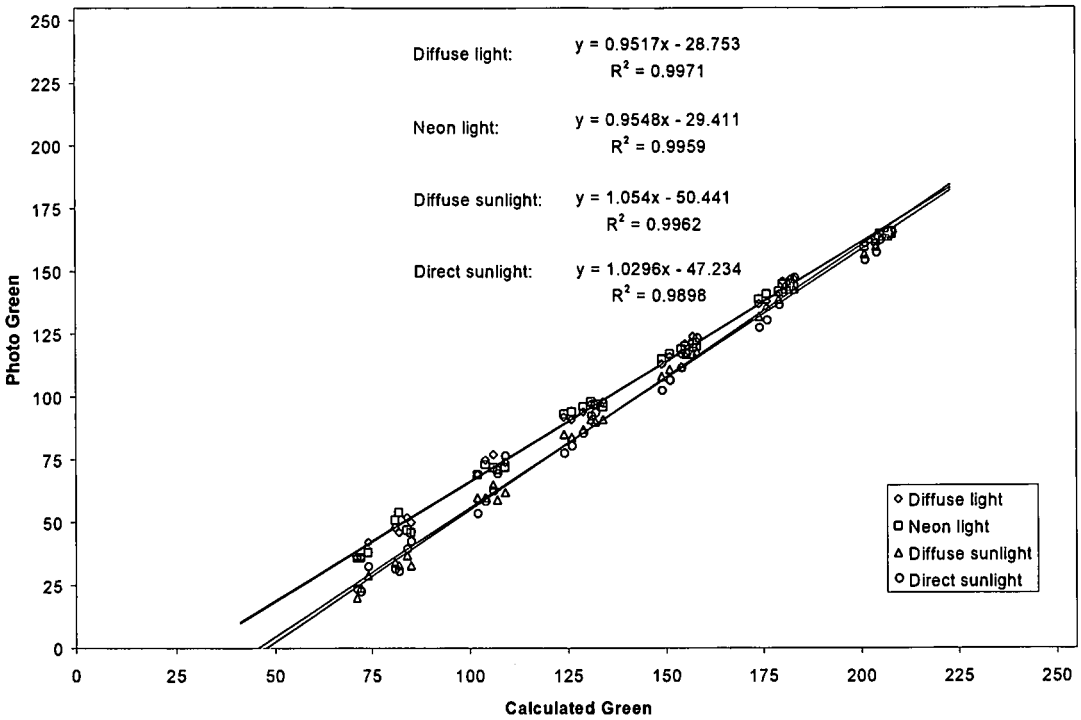


Figure 4.3 The relationship between calculated and photographed Green values of the 7.5YR Munsell hue, in different light sources.

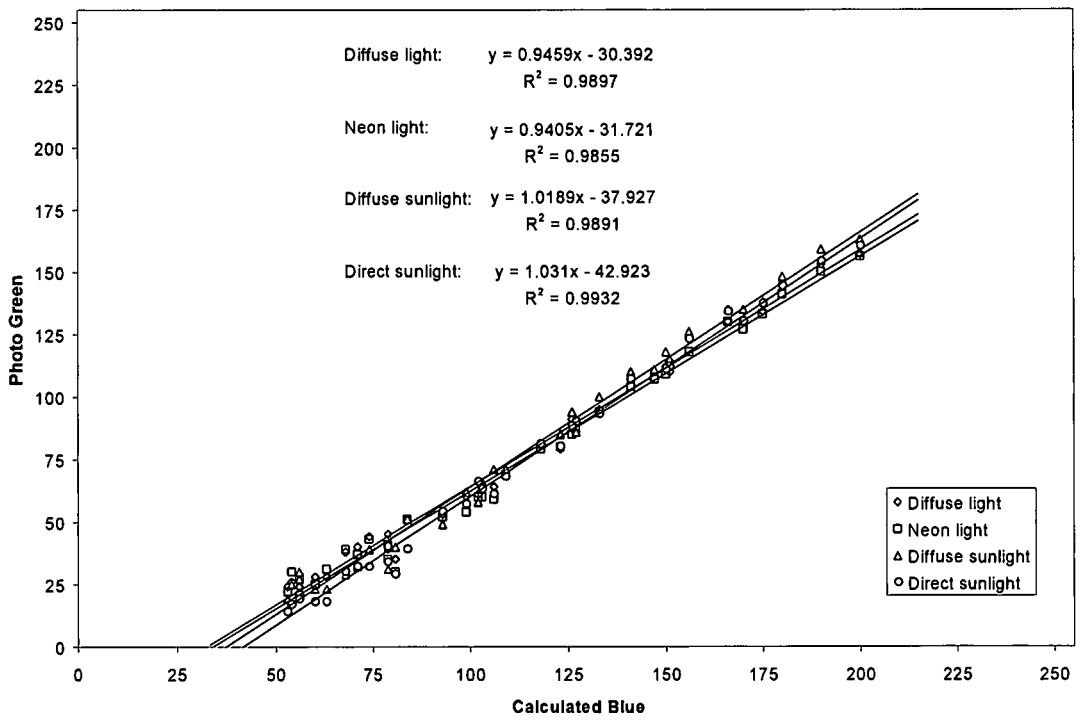


Figure 4.4 The relationship between calculated and photographed Blue values of the 7.5YR Munsell hue, in different light sources.

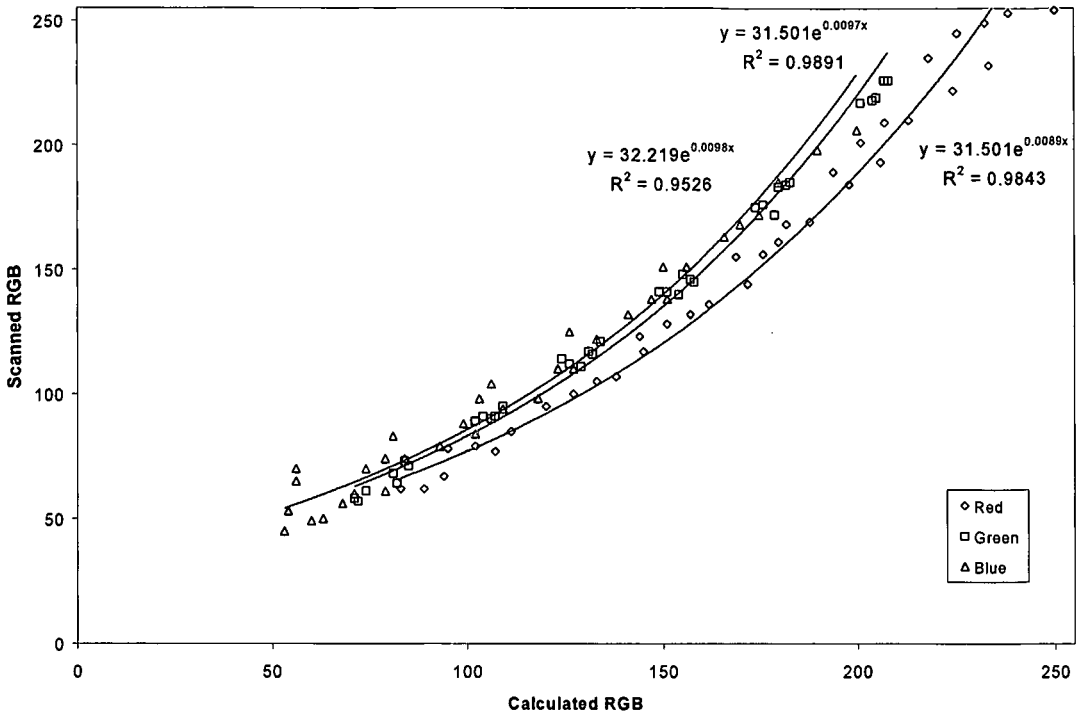


Figure 4.5 The relationship between calculated and scanned Red, Green and Blue values of the 7.5YR Munsell hue.

## 4.8 Interpretation of digital photographs

The biggest challenge in interpreting digital photographs is the difference in colour notation systems. As discussed previously, digital photographs are in RGB notation. This results in three values that need to be evaluated to determine the eventual colour. Furthermore, there exists an overlapping relationship between RGB and the diagnostic colour definitions of the Soil Classification Working Group (1991).

The distribution of diagnostic red, yellow-brown and grey colour classes as defined for red the apedal B, yellow-brown apedal B and E horizons (Soil Classification Working Group, 1991), plotted against Red and Green (RGB notation) are given in Figure 4.6, Figure 4.7 and Figure 4.8. Only Red and Green gave a meaningful differentiation between the diagnostic red, yellow-brown and grey classes. Two empirical lines were drawn to differentiate between grey and yellow and between yellow and red (Figure 4.6). The equations are listed below.

Between grey and yellow: Green = 0.88 * Red − 5 (4.14)

Between yellow and red: Green = 0.79 * Red − 11 (4.15)

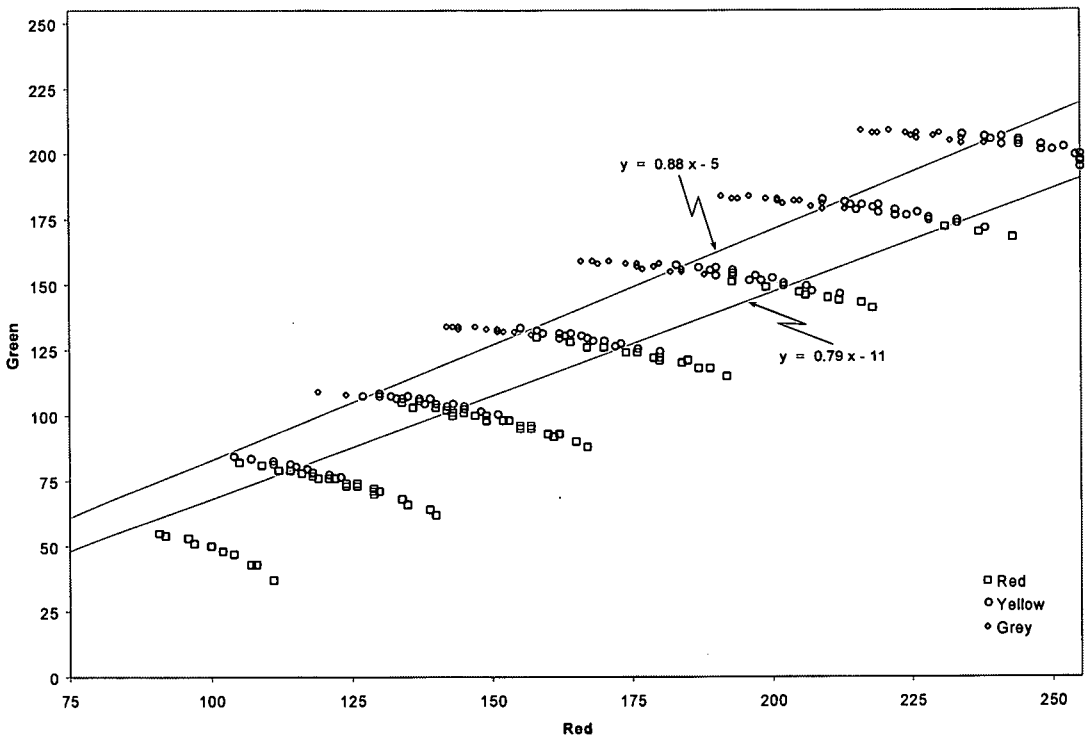


Figure 4.6 The distribution of diagnostic red, yellow-brown and grey colour classes (Soil Classification Working Group, 1991), when plotted against Red and Green (RGB notation). The two lines are used to differentiate between the grey and yellow-brown and between yellow-brown and red colour classes.

Because there is not a 1:1 relationship between calculated RGB and photo RGB values (section 4.7), equations 4.16 and 4.17 can now be derived by substitution of equations 4.11 and 4.12 into equations 4.14 and 4.15:

Photo Green = 0.95 * Photo Red − 3.7 (4.16)

And

Photo Green = 0.85 * Photo Red − 9.7 (4.17)

Black was calculated as those cells which had Red and Green values less than 75. These included shaded areas as well as manganese mottles and concretions. This is unfortunate, but unavoidable at this stage. Black was eliminated to remove the effect of shadows on the photograph.

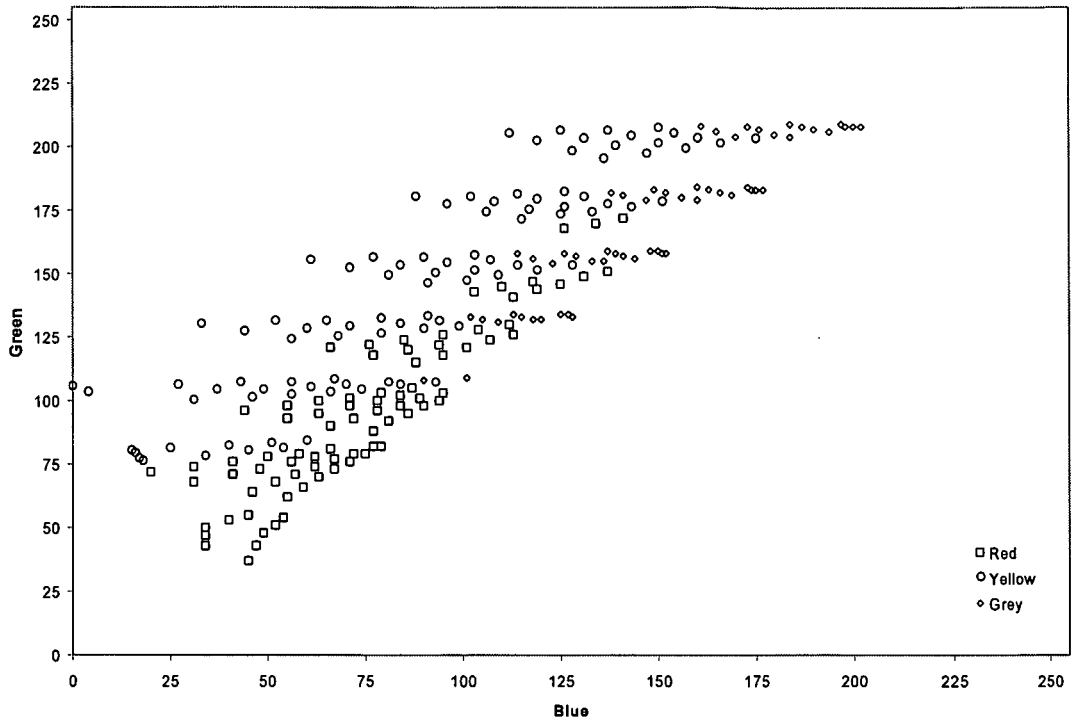


Figure 4.7 The distribution of diagnostic red, yellow-brown and grey colour classes (Soil Classification Working Group, 1991) plotted against Blue and Green (RGB notation).

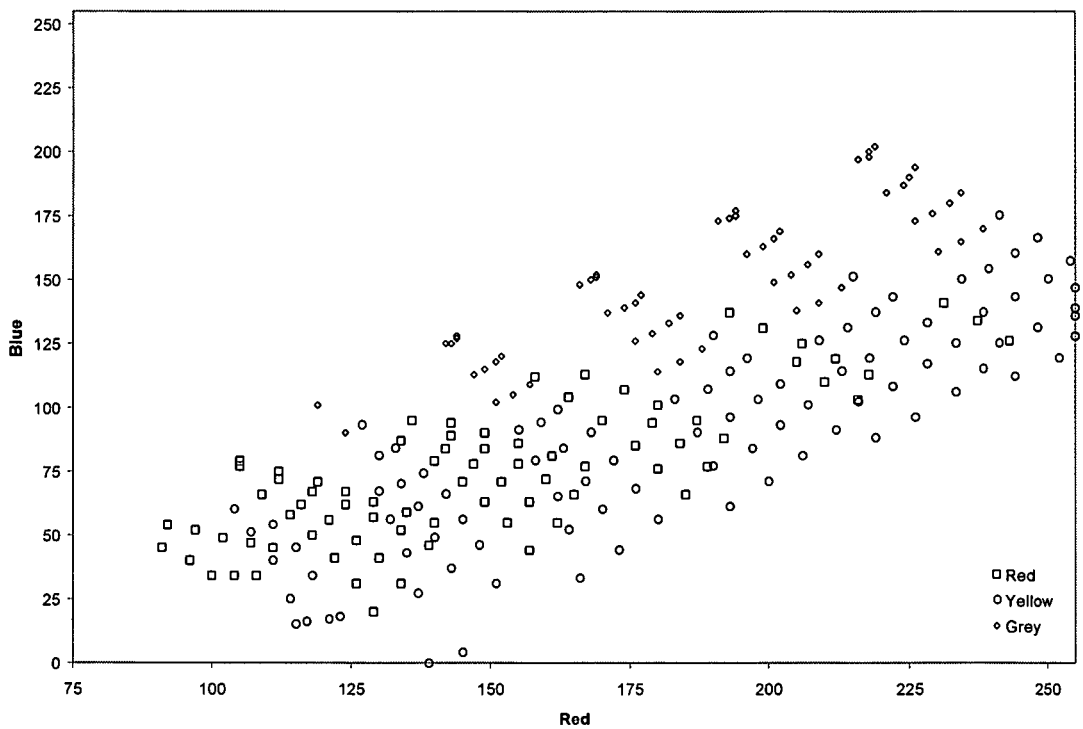


Figure 4.8 The distribution of diagnostic red, yellow-brown and grey colour classes (Soil Classification Working Group, 1991) plotted against Red and Blue (RGB notation).

Using equations 4.16 and 4.17 to classify RGB colours into diagnostic red, yellow-brown and grey classes resulted in an 18.7% (44 out of 235) miscalculation of the Munsell chips defined by the Soil Classification Working Group (1991). There was, however, little change in the amount classified into the diagnostic red, yellow-brown or grey classes (Table 4.4). Results are presented in Appendix B. It presents the RGB variation within each diagnostic red, yellow and grey zone by means of descriptive statistics. Photographs taken in the dry state were used in the calculations.

Table 4.4 Number of Munsell chips defined as diagnostic red, yellow-brown and grey class (Soil Classification Working Group, 1991) by calculation from RGB-values

| | Defined | Calculated |
|---|---|---|
| Red | 82 | 81 |
| Yellow | 95 | 97 |
| Grey | 58 | 57 |
| Total | 235 | 235 |

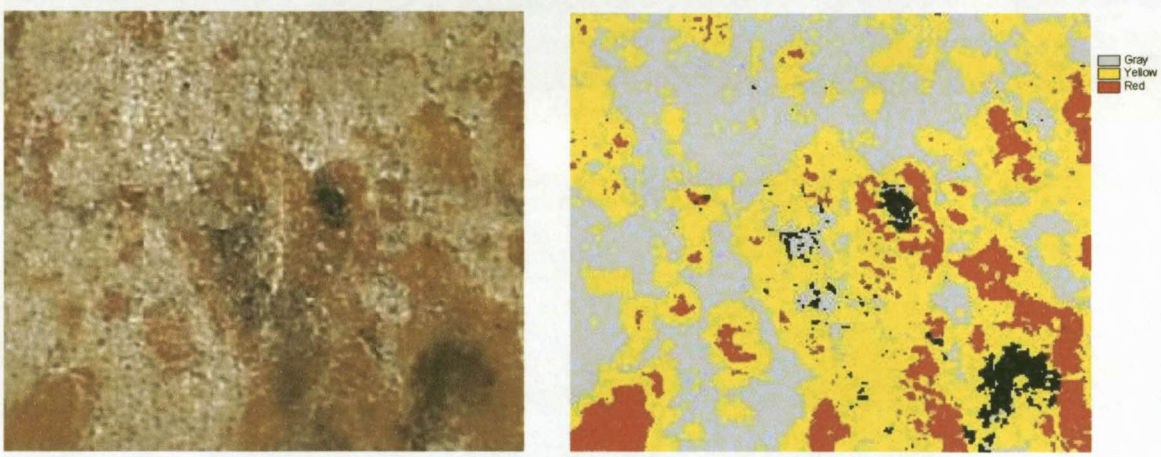


Figure 4.9 Result (right) of the application of equations 4.16 and 4.17 to classify a digital photograph (left) of a soft plinthic B horizon, using ArcView SpatialAnalyst (ESRI, 2000).

## 4.9 Summary

The study site was selected because of the availability of a large amount of relevant data. Methods used were kept standard, except for the development of the photograph interpretation procedure.

These initial results show promise for the use of digital photographs to be used as a versatile, reproducible, objective, quantitative, reliable and unintuitive tool for the analysis and interpretation of soil colour. The technology to do this is not yet refined and requires substantial user input. It does, however, enable users to objectively analyse and interpret soil colour features. The following equations can be used to differentiate between diagnostic grey, yellow-brown and red:

Photo Green = 0.95 * Photo Red − 3.7 (4.18)

Photo Green = 0.85 * Photo Red − 9.7 (4.19)

Initial results indicate a 19 % misclassification. Camera and lighting differences as well as the relationship between colour notation systems should receive further investigation. Results of this technique, applied for each horizon, tested against published techniques and correlation with soil water regime are discussed in chapter 6.

# 5 PROFILE CHARACTERIZATION

## 5.1 Introduction

The aim of this chapter is to describe the morphological, chemical and physical characteristics of the selected ten soil profiles. Colour quantifications and correlations are discussed in chapter 6; profile hydrological properties are described in chapter 7, while diagnostic horizon hydrological properties are described in chapter 8. The profile descriptions and analytical data for each profile are presented in Appendix A.

## 5.2 P201 (Longlands 2000)

The profile is situated in an upper midslope position, with a slope of 4 % (Figure 3.3). It has a coarse sandy loam texture throughout the profile. The clay content increases from 9 – 12 – 13 – 11 % from the A to the E, B and C horizons. The profile description and analytical data for this profile are given in Appendix A, Tables 1 and 2. The profile can be classified as Albic Hypodistric Arenosol (ferric) (FAO, 1998b) or Aeric Endoaquents (Soil Survey Staff, 1999).

### 5.2.1 Morphology

The brown (10YR4/4) orthic A horizon (0–430 mm) overlies slightly lighter, redder dull orange (7.5YR6/4) E (430–730 mm) and soft plinthic B horizons (730–980 mm) on saprolite. The E horizon colour borders the colour boundary to the yellow brown apedal B horizon. The colours of the underlying unspecified material with signs of wetness (weathering Elliott sandstone) vary from light yellow orange, (10YR8/4) to light brownish grey (7.5YR 7/2) to brown (10YR4/8).

Mottles in the A horizon are mainly of biologic origin – earthworm casts and / or filled earthworm and root channels (Table 5.1). There are common oxidised iron mottles in the E, as well as many grey bleached mottles. Both indicate an

alternating reducing and oxidising environment, causing reduction and relocation of iron. Some of this Fe might be leached downwards, to the soft plinthic B horizon, where it leads to the formation of many prominent Fe oxide mottles, occurring in association with Mn oxide mottles. The occurrence of both Mn and Fe oxide mottles is normally an indication of a less severe reducing environment, than the case where only Fe oxide mottles are present, because $Mn^{4+}$ is normally reduced and leached before $Fe^{2+}$ (Table 2.2).

Table 5.1 Mottle distribution in P201 (Longlands 2000)

| Horizon | Depth (mm) | Occurrence | Size | Contrast | Colour dry | Colour Wet | Cause |
|---|---|---|---|---|---|---|---|
| ot | 430 | few | fine | Faint | 10YR4/2 | 10YR3/2 | biological |
| gs | 730 | common | fine | Distinct | 2.5YR4/8 | 10R4/8 | oxidized iron |
| | | many | fine | Distinct | 10YR4/4 | 10YR3/3 | bleached |
| sp | 1 000 | few | fine | Distinct | 2.5YR3/0 | 2.5YR2.5/0 | manganese |
| | | many | fine | Prominent | 2.5YR4/8 | 10R4/8 | oxidized iron |
| on | 1 210 | none | | | | | |

### 5.2.2 Chemical properties

This profile has the lowest $CEC_{soil}$ of all ten profiles. $CEC_{soil}$ decreases from 5 $cmol_c\ kg^{-1}$ in the orthic A to 3 $cmol_c\ kg^{-1}$ in the E (Figure 5.1). It increases slightly to the transition with the soft plinthic B and then decreases further lower down in the soft plinthic B. The decrease in $CEC_{soil}$ seems to be linked with the decrease in organic matter from the surface of the soil downwards, because the clay content stays virtually constant and the $CEC_{clay}$ varies with depth. The sum of bases (S) decreases in the same order as $CEC_{soil}$. The low values for $CEC_{soil}$ and sum of bases are consistent with the required removal of colloidal material, supporting the classification of the E horizon.

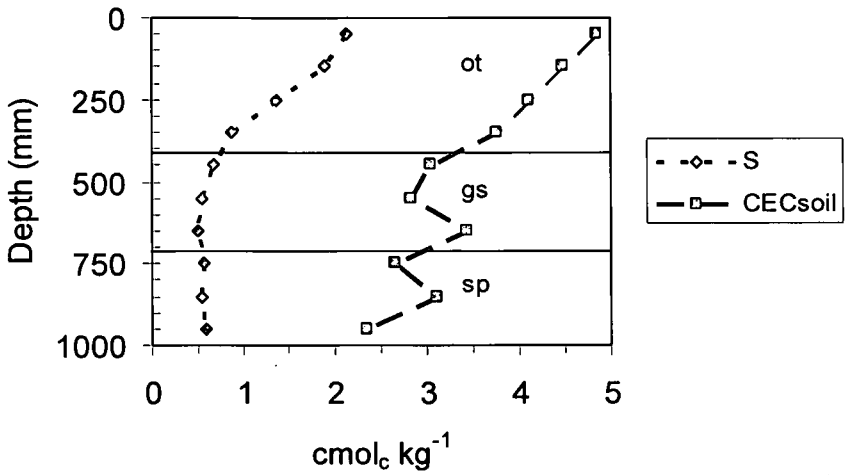


Figure 5.1 $CEC_{soil}$ and S values for P201 (Longlands 2000).

The $CEC_{clay}$ for P201 (Longlands) is very low (Figure 5.2), ranging from 7.0 to 23.9 $cmol_c\ kg^{-1}$. This is indicative of mainly kaolinite, fine mica and / or chlorite (Brady & Weil, 1996). This soil is expected to have very little swelling and shrinkage, as is evident from the apedal massive structure.

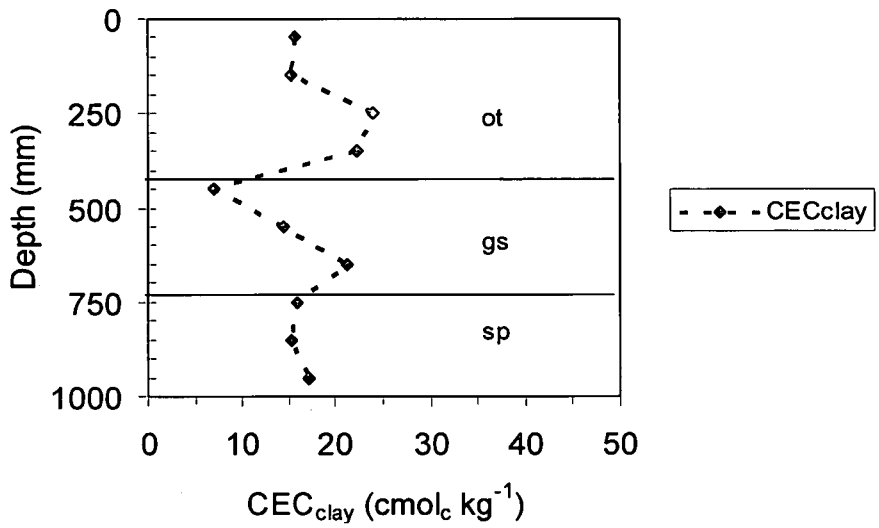


Figure 5.2 $CEC_{clay}$ for P201 (Longlands 2000).

$pH_{Water}$ and $pH_{KCl}$ are somewhat constant throughout the profile, decreasing slightly from 4.73 and 4.54 in the topsoil to 4.14 and 4.52 in the bottom of the profile (Figure 5.3). $pH_{Water}$ and $pH_{KCl}$ differ only slightly from one another, indicating very little reserve acidity (Brady & Weil, 1996) in this profile.

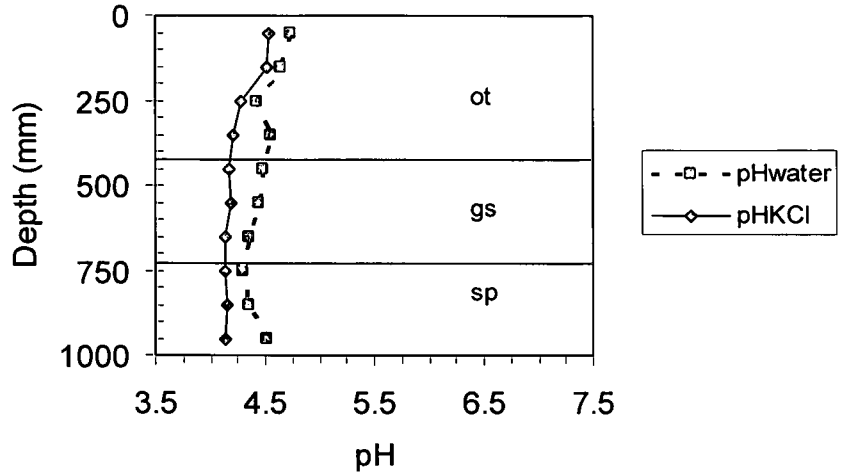


Figure 5.3 $pH_{Water}$ and $pH_{KCl}$ for P201 (Longlands 2000).

Percentage base saturation (BS) decreases from 44 in the topsoil to 15 in the E and then increases to 25 in the lower soft plinthic B horizon (Figure 5.4). The decrease is associated with a continuous decrease in sum of bases (S) with depth in the profile (Figure 5.1).

Organic carbon content (OC) decreases with depth (Figure 5.4). It decreases systematically from 1.0 % in the upper to 0.4 % in the lower A horizon. The sharp increase in the upper E and soft plinthic B horizon may be due to sampling error as roots and root channels exist in all horizons.

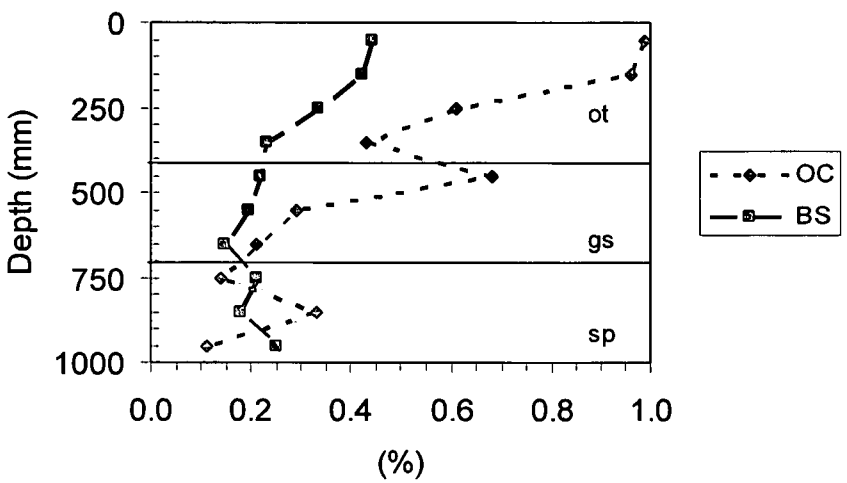


Figure 5.4 Distribution of organic carbon (OC, as a percentage) and base saturation (BS, as a fraction) in P201 (Longlands).

Total Fe content (CBD extractable Fe) is fairly constant at 4 510 to 6 875 mg $kg^{-1}$ throughout the profile (Figure 5.5). The peak occurs in the lower part

of the E horizon, just above the soft plinthic B. It therefore seems that maximum Fe accumulation in the soil matrix (excluding concretions >2 mm), is not in the soft plinthic B, but rather just above it (Figure 5.6).

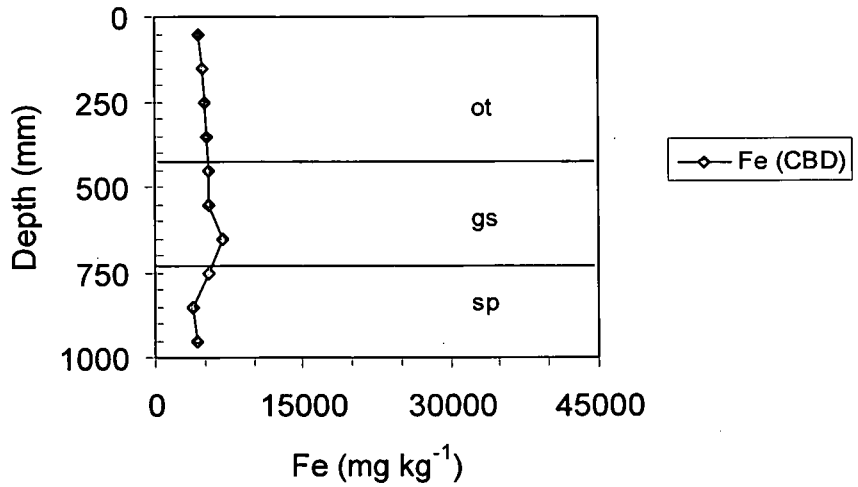


Figure 5.5 CBD extractable Fe for P201 (Longlands 2000).

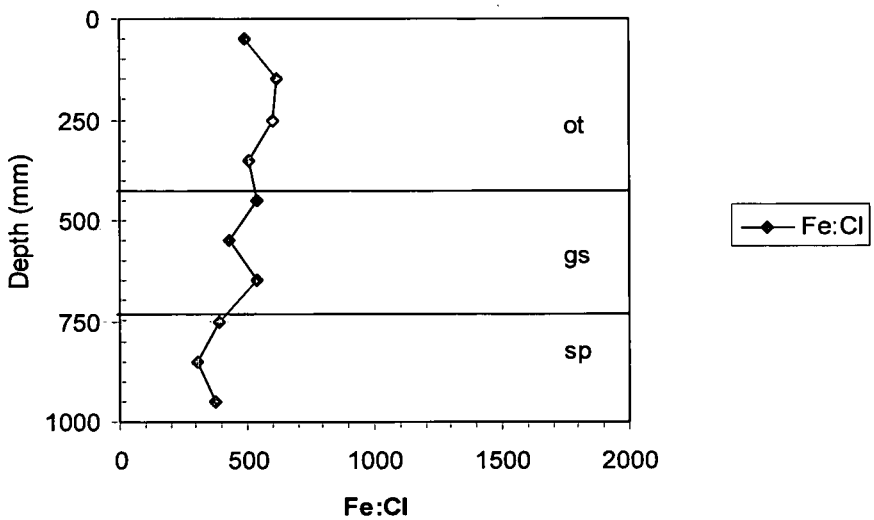


Figure 5.6 The CBD extractable Fe to clay ratio for P201 (Longlands 2000).

As in the case of Fe, the distribution of Mn also stays fairly constant throughout the profile (Figure 5.7). It ranges from 8.0 to 31.5 mg $kg^{-1}$. Unlike Fe it is lowest in the E and has a marked accumulation in the orthic A and soft plinthic B horizon (Figure 5.8).

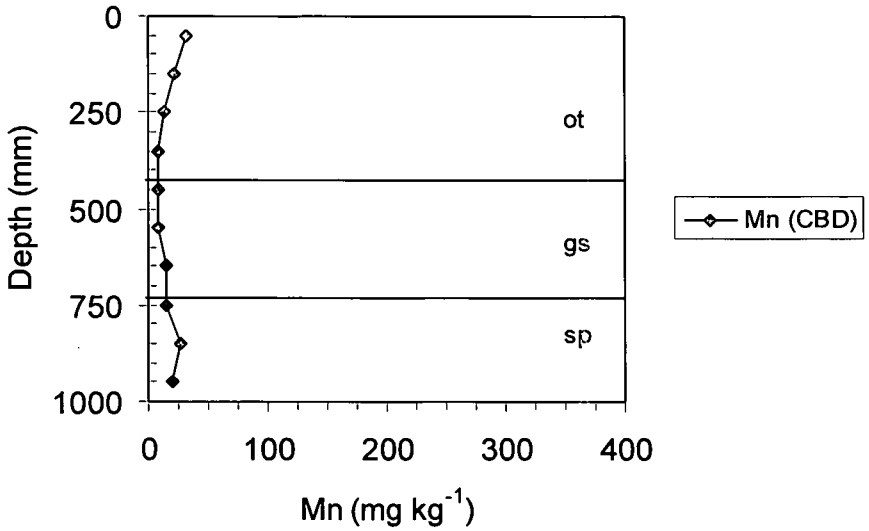


Figure 5.7 CBD extractable Mn for P201 (Longlands 2000).

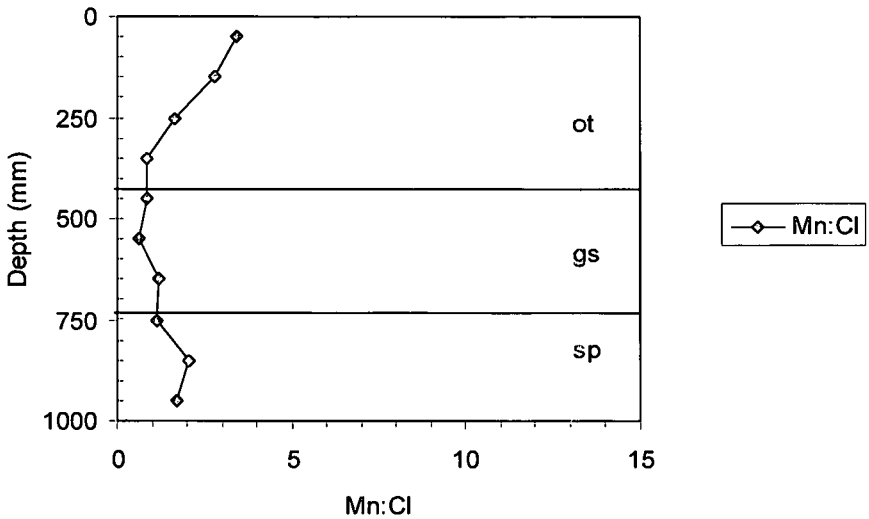


Figure 5.8 The CBD extractable Mn to clay ratio for P201 (Longlands 2000).

### 5.2.3 Physical properties

There is a systematic increase in clay content from 7 to 14 %, with depth throughout the profile (Figure 5.9). A slight decrease occurs at 100 to 300 mm in the A horizon. If a uniform parent material is assumed more clay removal has taken place from the A than from the E, or luviation played an important role in the genesis of the profile. This hypothesis supports the borderline colour of the E horizon as being a borderline E / yellow-brown apedal B horizon. There is a marked decrease in silt content at the boundary between the A and the E horizon. This probably indicates a lithological discontinuity, as the sand content increases correspondingly.

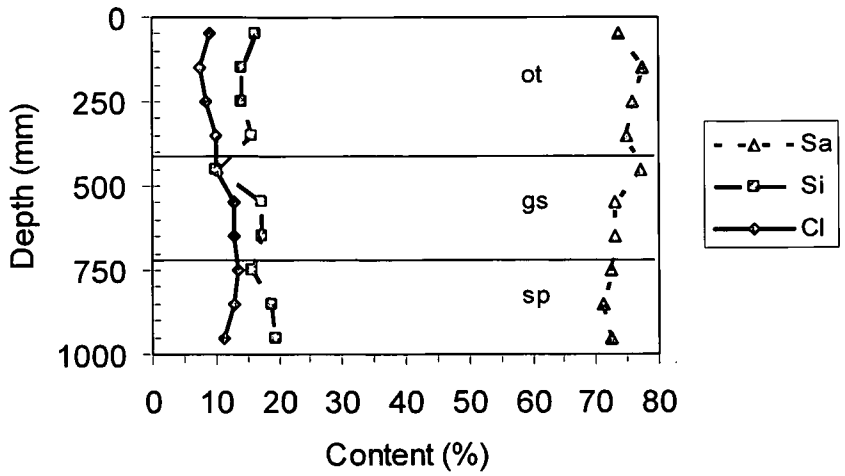


Figure 5.9 Particle size distribution of the fine earth fraction of P201 (Longlands 2000).

Bulk density increases from 1.53 Mg $m^{-3}$ in the topsoil to 1.84 Mg $m^{-3}$ at 1 050 mm (Table 5.2). There is therefore a decrease in the porosity that could lead to poor aeration and an increased possibility for anaerobic conditions and reduction to occur. The high bulk density may also restrict root development.

Table 5.2 Bulk density and porosity for P201 (Longlands 2000)

| Depth (mm) | Bulk density (Mg $m^{-3}$) | Porosity (%) |
|---|---|---|
| 150 | 1.53 | 42.3 |
| 450 | 1.57 | 40.8 |
| 750 | 1.65 | 37.7 |
| 1050 | 1.84 | 30.6 |

### 5.2.4 Genesis

The profile is situated 74 m from the crest of the upper shelf. As such it is expected to receive some water through lateral movement, from the higher lying soils, saturating the subsoil for prolonged periods (section 7.2). The topographical position will have promoted the genesis of the borderline E / yellow-brown apedal B character of the second horizon. The underlying Elliot sandstone is probably the main parent material of the profile. This is supported by a somewhat constant medium sand to coarse sand ratio close to 1.5. The particle size distribution of the soil is expected to vary as lenses of coarser material in the exposed parent material indicate variable sedimentation conditions as well as lithological discontinuities. The white quartz sandstone is low in clay, Fe, Mn and basic cations. Weathering and

pedogenesis is expected to have produced the profile which has been described. At 1.0 % the organic carbon content is higher than the mean for the topsoils studied. This is probably due to good plant growth in the well drained environment, coupled with an adequate supply of basic cations.

Clay, $pH_{Water}$, $pH_{KCl}$, Fe and Mn does not vary significantly with depth, pointing to a young profile. The lower $CEC_{clay}$ in the E horizon is, however, evidence of ferrolysis in the horizon, due to periodic water saturation. The increase in the occurrence and prominence of mottles and segregation of Fe and Mn as concretions with depth indicate a substantial increase in wetness. It is speculated that during wet periods more stagnant conditions prevail in the soft plinthite, while leaching dominates in the E horizon. The increase in redness from the A to the E horizon can be explained by the lower organic carbon content in the E horizon, inhibiting the reduction and subsequent removal of Fe.

## 5.3 P202 (Pinedene 1100)

The profile is situated in an upper midslope position, with a slope of 4 % (Figure 3.3). It has a medium sandy loam texture in the A and B horizons, with a fine sandy loam texture in the two C horizons. The clay content increases systematically (10 – 16 – 20 – 25 %) down the profile. The profile description and analytical data for this profile are given in Appendix A, Tables 3 and 4. The profile can be classified as Gleyic Orthi-distric Cambisol (FAO, 1998b) or Oxyaquic Hapludalts (Soil Survey Staff, 1999).

### 5.3.1 Morphology

The orthic A horizon (0–400 mm) has a dull yellowish brown (10YR4/3) colour. The yellow-brown apedal B horizon (400–820 mm) is brighter and lighter (bright brown, 7.5YR5/6) in colour. The unspecified material with signs of wetness is grey like the A horizon but pale (light grey, 10YR8/2 in the C1 (820–90 mm) and a pinkish white (2.5YR8/2) colour in the C2 (990–1500 mm). The colour therefore becomes paler (value increases) with depth.

The orthic A horizon of profile 202 does not have any mottles (Table 5.3). There are, however few reddish brown and orange Fe oxide mottles in the bright brown yellow-brown apedal B horizon. Grey matrix colour as well as common faint reddish brown and bright brown Fe oxide mottles in the C1 horizon lead to the classification of unspecified material with signs of wetness. The C2 horizon has few reddish brown and many bright yellowish brown Fe oxide mottles. It is also classified as unspecified material with signs of wetness. No concretions were observed in the profile.

Table 5.3 Description of mottles in P202 (Pinedene 1100)

| Horizon | Depth (mm) | Occurrence | Size | Contrast | Colour dry | Colour wet | Cause |
|---|---|---|---|---|---|---|---|
| ot | 400 | None | | | | | |
| ye | 820 | Few | Med | Faint | 7.5Y6/4 | 7.5YR6/8 | Oxidized iron |
| | | Few | Fine | Faint | 7.5YR6/8 | 7.5YR4/4 | Oxidized iron |
| on | 990 | Common | Med | Faint | 5YR4/6 | 5YR4/6 | Oxidized iron |
| | | Common | Med | Faint | 7.5YR5/6 | 7.5YR5/8 | Oxidized iron |
| on | 1500 | Few | Fine | Prominent | 2.5YR4/6 | 2.5YR4/4 | Oxidized iron |
| | | Many | Fine | Prominent | 10YR6/8 | 10YR5/8 | Oxidized iron |

### 5.3.2 Chemical properties

$CEC_{soil}$ of the orthic A is lower than that of P201 (Longlands 2000). It increases from 10 $cmol_c\ kg^{-1}$ in the lower unspecified material with sighs of wetness. This increase is linked with a slight increase in clay content to the C horizon. Sum of bases is higher than in P201 (Longlands). There is a slight decrease in sum of bases from the A to the B horizon (Figure 5.10).

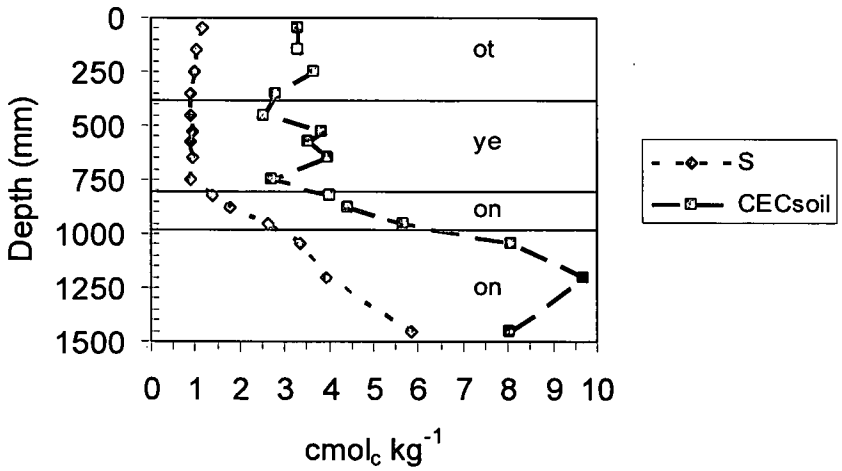


Figure 5.10 $CEC_{soil}$ and S values for P202 (Pinedene 1100).

The $CEC_{clay}$ increases with depth from 7.1 $cmol_c\ kg^{-1}$ in the topsoil to 35.8 $cmol_c\ kg^{-1}$ in the subsoil (Figure 5.11). The increase in $CEC_{clay}$ is linked with a marked decrease in the organic carbon content coupled with an increase in the clay content. It might therefore be an artefact of the calculation used to calculate $CEC_{clay}$. The $CEC_{clay}$ distribution points to advanced weathering in the orthic A and yellow-brown apedal B horizons, where kaolinite predominates, and less chemical weathering in the gleyed deep subsoil.

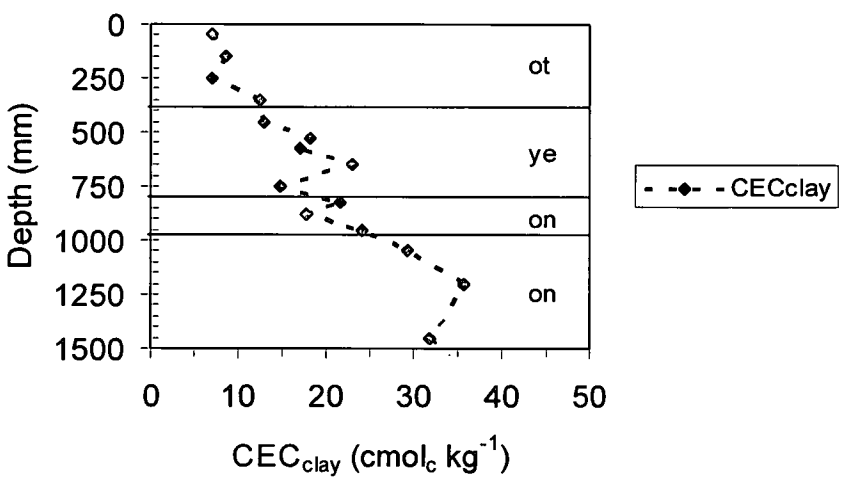


Figure 5.11 $CEC_{clay}$ for P202 (Pinedene 1100).

$pH_{Water}$ and $pH_{KCl}$ are constant throughout the profile. $pH_{Water}$ ranges between 4.44 and 4.67, while $pH_{KCl}$ ranges between 4.00 and 4.25 (Figure 5.12). The difference between $pH_{Water}$ and $pH_{KCl}$ (almost half a unit) indicates more residual acidity in this profile, than was the case with P201 (Longlands 2000).

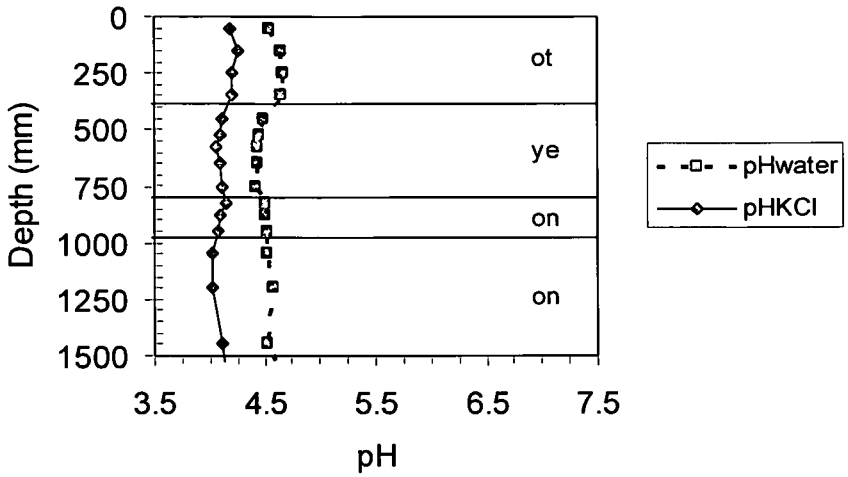


Figure 5.12 $pH_{Water}$ and $pH_{KCl}$ for P202 (Pinedene 1100).

Base saturation increases from 35 % in the A horizon to 74 % in the lower unspecified material with sighs of wetness (Figure 5.13). This is associated with an increase in basic cation concentration that more or less follows the increase in $CEC_{soil}$ and a small increase in the clay content.

Organic carbon content decreases rapidly from 0.7 % in the upper A horizon to 0.4 % in the lower A horizon (Figure 5.13). It then decreases gradually to 0.1 % in the unspecified material with signs of wetness.

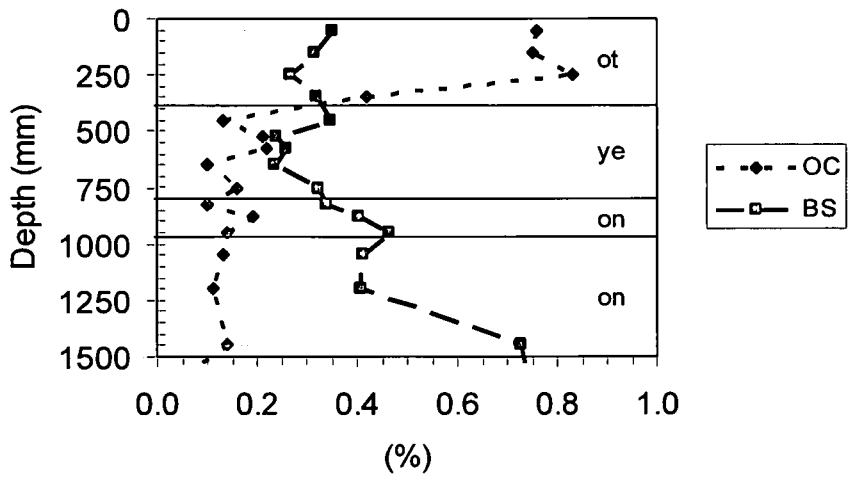


Figure 5.13 Distribution of organic carbon (OC, as a percentage) and base saturation (BS, as a fraction) in P202 (Pinedene 1100).

Total Fe content increases from 4 372 mg $kg^{-1}$ in the A horizon to 7 045 mg $kg^{-1}$ in the B horizon (Figure 5.14). It then increases sharply to 15 600 mg $kg^{-1}$ in the upper unspecified material with signs of wetness, before

dropping to 6 347 mg $kg^{-1}$ in the lower half. It is therefore an indication of active Fe accumulation in the upper unspecified material with signs of wetness (Figure 5.15).

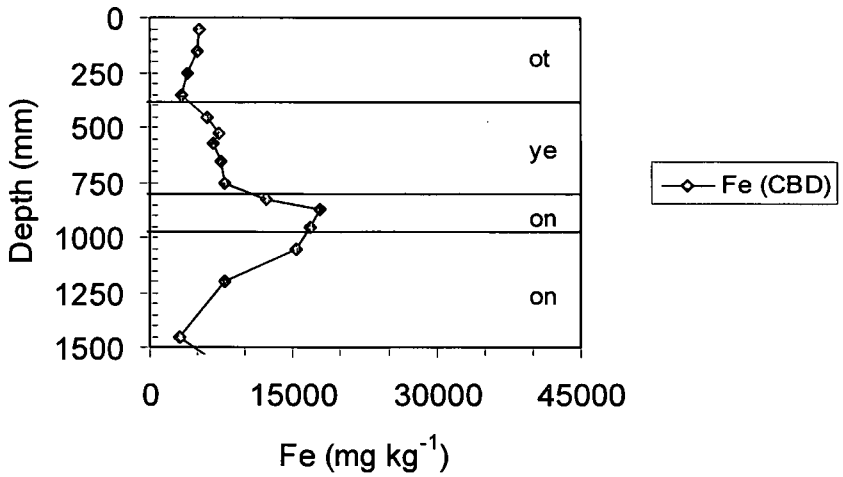


Figure 5.14 CBD extractable Fe for P202 (Pinedene 1100).

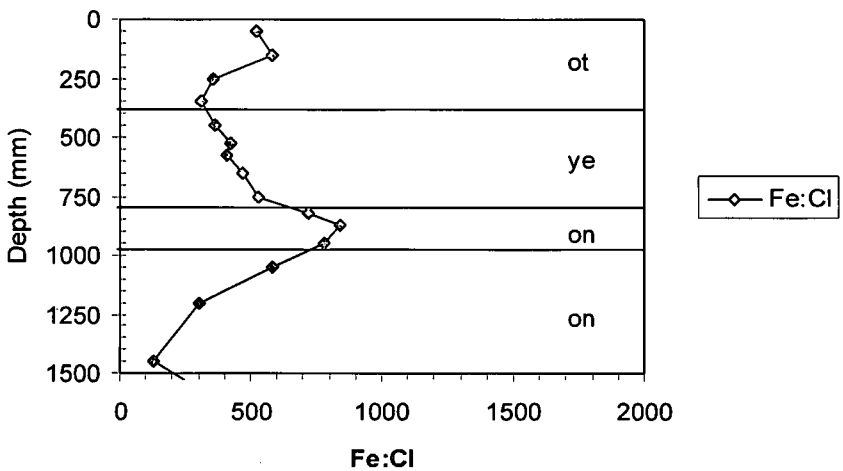


Figure 5.15 The CBD extractable Fe to clay ratio for P202 (Pinedene 1100).

Total Mn content is also highest in the upper part of the unspecified material with signs of wetness (Figure 5.16). It therefore supports the hypothesis that Fe and Mn accumulation is active at this depth. The Mn peak occurs in the upper unspecified material with signs of wetness, 100 mm higher up in the profile than the peak of Fe accumulation (Figure 5.17).

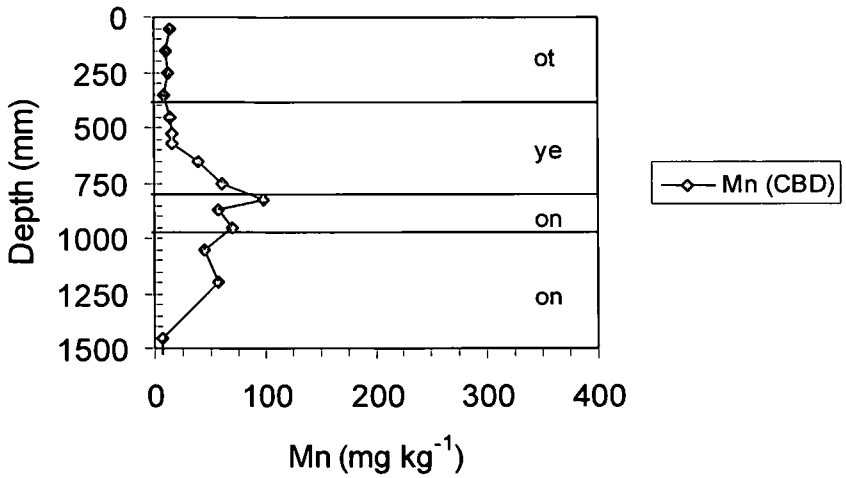


Figure 5.16 CBD extractable Mn for P202 (Pinedene 1100).

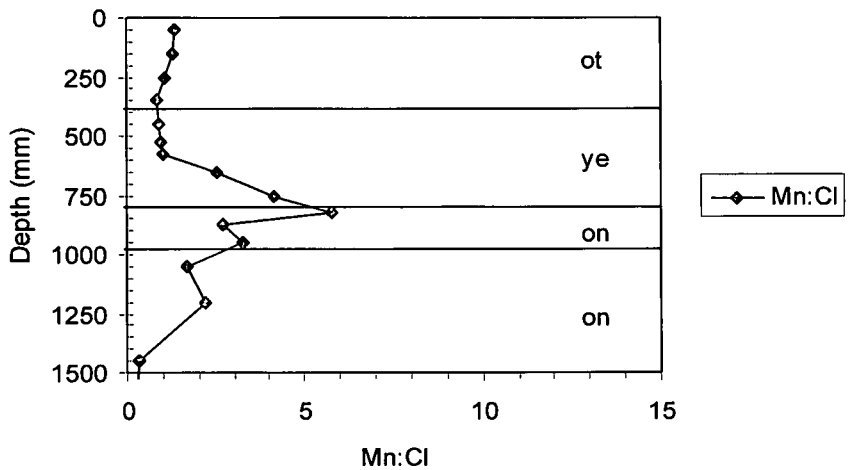


Figure 5.17 The CBD extractable Mn to clay ratio for P202 (Pinedene 1100).

### 5.3.3 Physical properties

Clay content (Figure 5.18) in the A (10 %) is much less than in the B horizon (16 %). The B horizon qualifies as a luvic B. The clay content increases further from the B to the C1 (20 %) and C2 (25 %) horizons. There is also a marked increase in silt content from the B to the C1 horizon. The increase in clay and silt content probably results in decreased hydraulic conductivity, promoting reducing conditions.

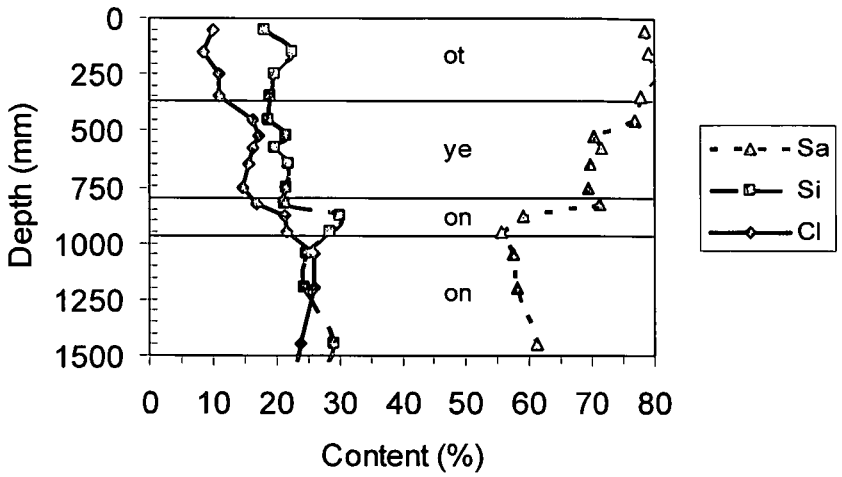


Figure 5.18 Texture of the fine earth in P202 (Pinedene 1100).

The bulk density is almost similar at 150 and 450 mm (1.68 and 1.61 Mg $m^{-3}$ respectively). It then increases to around 1.72 Mg $m^{-3}$ between 750 and 1 350 mm (Table 5.4). The bulk density below 450 mm is sufficient to impede root growth. This will impact on the growth of *Pinus patula*, if planted here, which is particularly sensitive to high bulk density. Aeration will be impeded and therefore the possibility for reduction will be increased.

Table 5.4 Bulk density and porosity for P202 (Pinedene 1100)

| Depth (mm) | Bulk density (Mg $m^{-3}$) | Porosity (%) |
|---|---|---|
| 150 | 1.68 | 36.6 |
| 450 | 1.61 | 39.2 |
| 750 | 1.72 | 35.1 |
| 1050 | 1.71 | 35.5 |
| 1350 | 1.72 | 35.1 |

### 5.3.4 Genesis

The profile occurs 160 m from the crest, on the upper Elliott shelf. It therefore receives considerable amounts of water through lateral drainage keeping the C horizon saturated for most of the year (section 7.3). This is evident from the mottling and grey colours in the C1 and C2 horizons. The profile has properties typical of a binary profile, having both sandstone and mudstone as parent materials. This is supported by the medium sand : coarse sand ratio that varies from 2.5 in the upper 550 mm to 1.5 in the 550 – 900 mm layer and 0.5 deeper than 900 mm. The organic carbon content is roughly 0.8 % in the topsoil, decreasing abruptly to 0.2 % in the deeper soil.

This profile is characterized by a steady increase in clay content with depth and a sharp increase in $CEC_{soil}$ and $CEC_{clay}$ from a depth of 750 mm. This may be inherited from the differing parent materials or indicates luviation of clay from the A to the B. The pH is stable throughout the profile, while Fe and Mn sharply increase at about 750 to 1 000 mm. The small difference between $pH_{Water}$ and $pH_{KCl}$ might be due to the youthful nature of this profile. It seems that basic cations, Fe and Mn have been leached from the A and B horizons. Some of these could have accumulated in the C1 and C2 horizons, while the rest could have been leached lateraly or verticaly. Accumulation of clay and cations in the C horizons can be partially due to the high bulk density of these horizons. Luviation of clay could also have taken place in conjunction with the cations. This would have resulted in the overall pale colour of this profile. The Mn peak occurs slightly higher in the profile than that of Fe. This is due to the fact that Mn reduced first, followed by Fe, when the Eh drops and indicates capillary action from a reduced water table (Table 2.2). This might be the first signs of soft plinthic B horizon formation.

## 5.4 P203 (Tukulu 2100)

The profile is situated in an upper midslope position, with a slope of 8 % (Figure 3.3). It has a coarse sandy loam texture, except for the B horizon which has a medium sandy loam texture. The clay content increases (10 – 13 – 14 – 28 %) down the profile. The profile description and analytical data for this profile are given in Appendix A, Tables 5 and 6. The profile can be classified as Gleyic Hyperdistric Arenosol (FAO, 1998b) or Oxyaquic Udorthents (Soil Survey Staff, 1999).

### 5.4.1 Morphology

The orthic A (0–380 mm) has a dull yellowish brown (10YR5/3) colour. The neocutanic B horizon and the upper unspecified material with signs of wetness (C1) have a dull orange (7.5YR7/4) colour. The lower unspecified material with signs of wetness (C2) has a light grey (7.5YR8/2) colour.

There are no mottles in the A horizon (Table 5.5). Common, coarse, prominent, bright brown and dull orange Fe oxide mottles occur in the neocutanic B horizon. The many, medium, distinct orange and bright reddish brown Fe oxide mottles and grey matrix colour in the C1 resulted in its classification as unspecified material with signs of wetness. The C2 also has many prominent bright brown and yellowish brown Fe oxide mottles. No concretions were observed in the profile.

Table 5.5 Description of mottles in P203 (Tukulu 2100)

| Horizon | Depth (mm) | Occurrence | Size | Contrast | Colour dry | Colour Wet | Cause |
|---|---|---|---|---|---|---|---|
| ot | 380 | None | | | | | |
| ne | 960 | Common | Coarse | Prominent | 2.5YR5/8 | 2.5YR4/8 | Oxidized iron |
| | | Common | Coarse | Prominent | 5YR7/4 | 5YR6/4 | Oxidized iron |
| on | 1300 | Few | Med | Distinct | 5YR6/8 | 5YR5/8 | Oxidized iron |
| | | Many | Med | Distinct | 5YR5/8 | 5YR4/6 | Oxidized iron |
| on | 1500 | Many | Fine | Prominent | 2.5YR5/8 | 2.5YR4/6 | Oxidized iron |
| | | Many | Fine | Prominent | 10YR5/6 | 7.5YR6/8 | Oxidized iron |

### 5.4.2 Chemical properties

$CEC_{soil}$ decreases down the A (from 3.7 to 2.6 $cmol_c\ kg^{-1}$), but then increases to a mean of 5.7 $cmol_c\ kg^{-1}$ in the B horizon (Figure 5.19). The decrease of $CEC_{soil}$ in the A seems to be linked to the decrease of organic matter in the A horizon, because there is actually an increase in clay from the upper to the lower A horizon. $CEC_{soil}$ increases slightly from 5.7 $cmol_c\ kg^{-1}$ in the B to 5.9 $cmol_c\ kg^{-1}$ in the C1 and C2 horizons. This increase is linked with an increase in clay content from the 12.1 % in the B to 13.8 % in the C1 and 27.8 % in the C2 horizon.

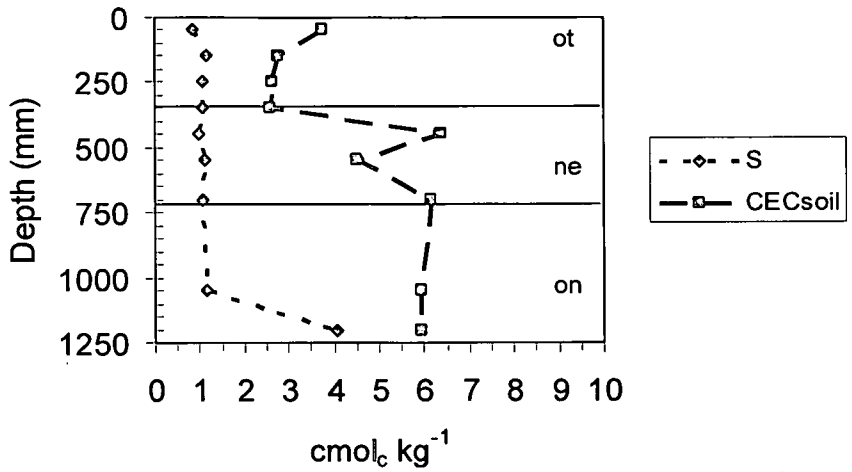


Figure 5.19 $CEC_{soil}$ and S values for P203 (Tukulu 2100).

$CEC_{clay}$ decreases with depth from 72.3 cmol$_c$ kg$^{-1}$ in the topsoil to 20.8 cmol$_c$ kg$^{-1}$ in the subsoil (Figure 5.20). The high $CEC_{clay}$ in the first sample is possibly due to an under-estimation of the organic carbon content in this sample. The $CEC_{clay}$ of 16.9 and 15.4 cmol$_c$ kg$^{-1}$ in the next two samples is much more in line with the values found in the topsoil of the previous two profiles. This profile was classified as Tukulu 2100, where the neocutanic B horizon signifies a lack of pedogenesis (Le Roux *et al.,* 1999). This seems to be supported by the relatively high $CEC_{clay}$ in the neocutanic B horizon, typical of fine mica and chlorite (Brady & Weil, 1996). The $CEC_{clay}$ drops to even further in the unspecified material with signs of wetness, possibly indicating that clay minerals have not yet been released from the parent material.

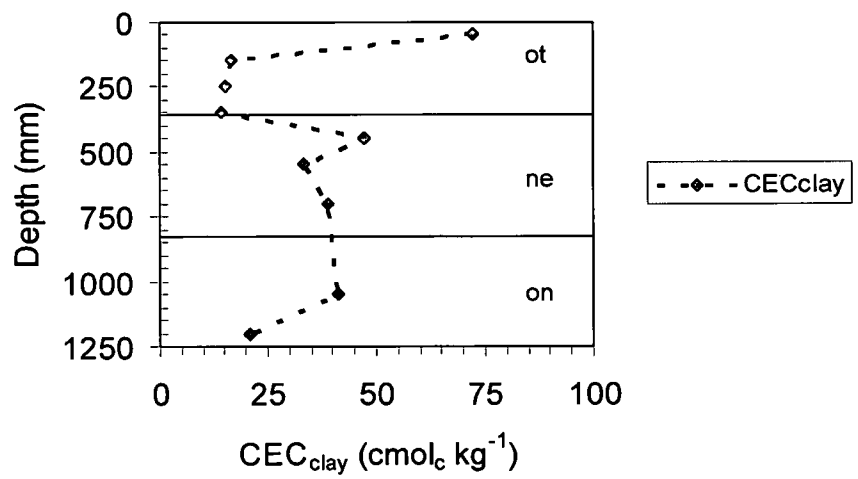


Figure 5.20 $CEC_{clay}$ for P203 (Tukulu 2100).

$pH_{Water}$ increases slightly from 4.25 in the topsoil to 4.82 in the subsoil, while $pH_{KCl}$ increases from 4.06 to 4.17 (Figure 5.21). The increase in pH as well as the increased difference between $pH_{Water}$ and $pH_{KCl}$ is most probably linked to the increase in base saturation down the profile. The mean pH in this profile is similar to that in the previous two profiles.

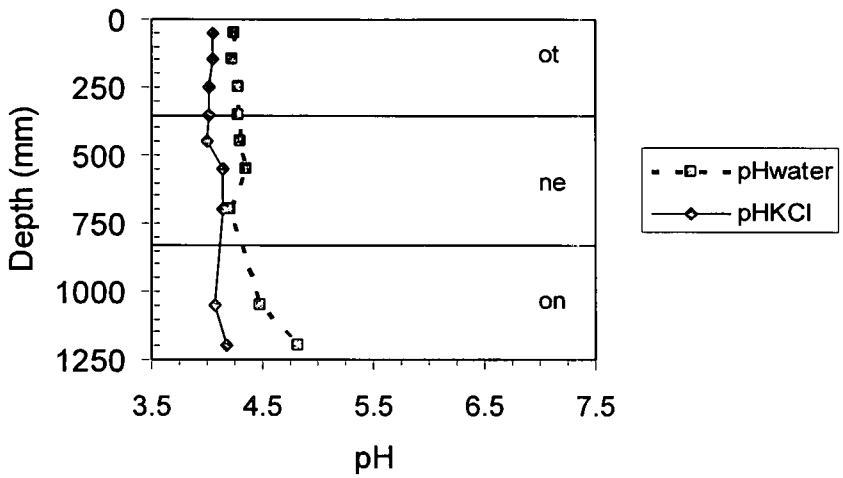


Figure 5.21 $pH_{Water}$ and $pH_{KCl}$ for P203 (Tukulu 2100).

Base saturation increases from 23 % in the upper A horizon to 41 % in the lower A horizon (Figure 5.22). It then decreases to 19 % in the B horizon and increases to 69 % in the lower unspecified material with signs of wetness. This pattern is determined by the $CEC_{soil}$ distribution in the profile, rather than the sum of basic cations which is constant at approximately 1.0 $cmol_c\ kg^{-1}$ in the profile, only increasing to 4.1 in the lower unspecified material with signs of wetness (Figure 5.18).

Organic carbon decreases from 0.31 % at the soil surface to 0.04 % deeper than 1 200 mm (Figure 5.22). This profile has the lowest topsoil organic carbon content of all ten profiles. This might be linked to the sandy nature of these soils (< 10 %), resulting in less vigorous plant growth adding less organic matter to the soil as well as faster mineralization of soil organic matter.

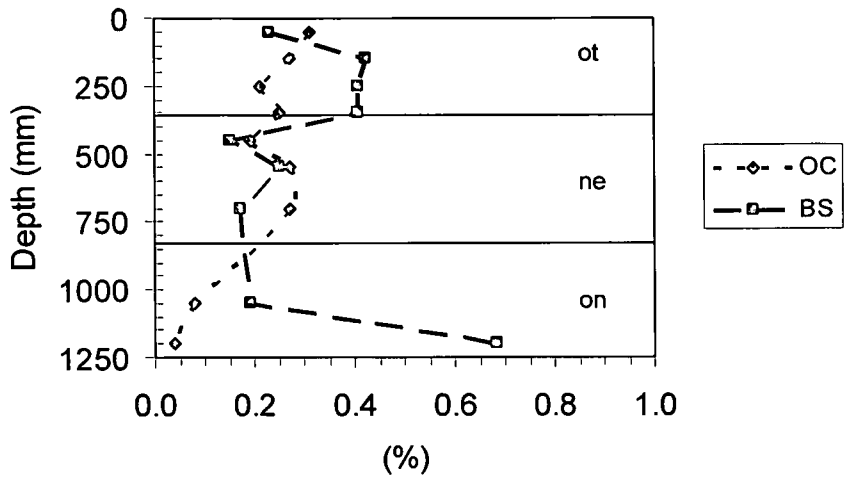


Figure 5.22 Distribution of organic carbon (OC, as a percentage) and base saturation (BS, as a fraction) in P203 (Tukulu 2100).

Total Fe content increases from 4 839 mg $kg^{-1}$ in the topsoil to 8 100 mg $kg^{-1}$ in the subsoil (Figure 5.23). There is a slight accumulation of Fe in the middle of the neocutanic B horizon, indicating some plinthitisation in the horizon (Figure 5.24).

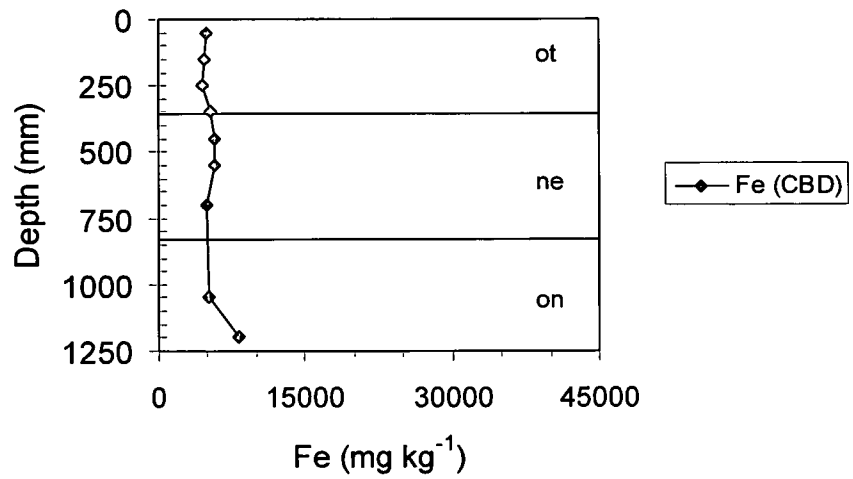


Figure 5.23 CBD extractable Fe for P203 (Tukulu 2100).

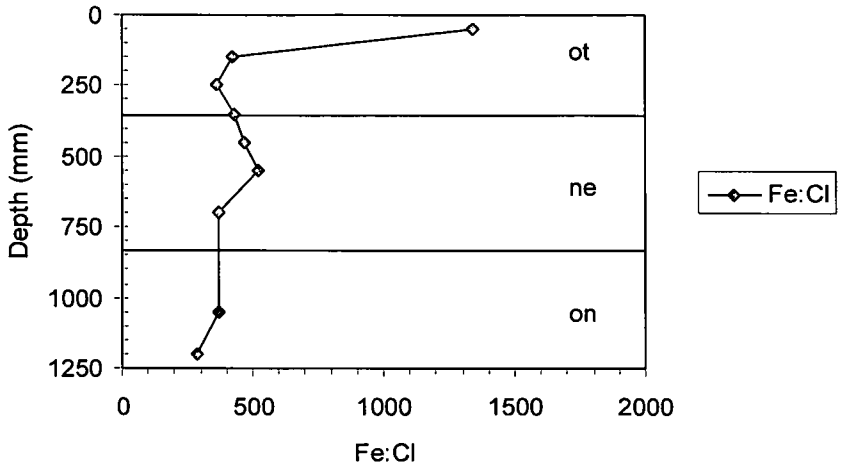


Figure 5.24 The CBD extractable Fe to clay ratio for P203 (Tukulu 2100).

The total Mn distribution (Figure 5.25) is similar to that of Fe. It decreases from 18.3 mg $kg^{-1}$ in the topsoil to 14.7 mg $kg^{-1}$ in the neocutanic B and then increases to 36.5 mg $kg^{-1}$ in the unspecified material with signs of wetness. The slightly higher Mn content in the unspecified material with signs of wetness might support the classification of this horizon, pointing to the accumulation of Mn under slightly reducing conditions (Figure 5.26).

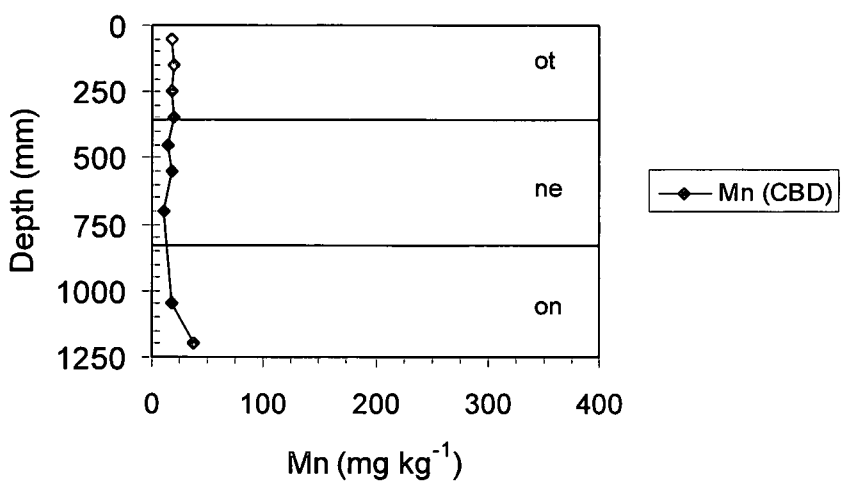


Figure 5.25 CBD extractable Mn for P203 (Tukulu 2100).

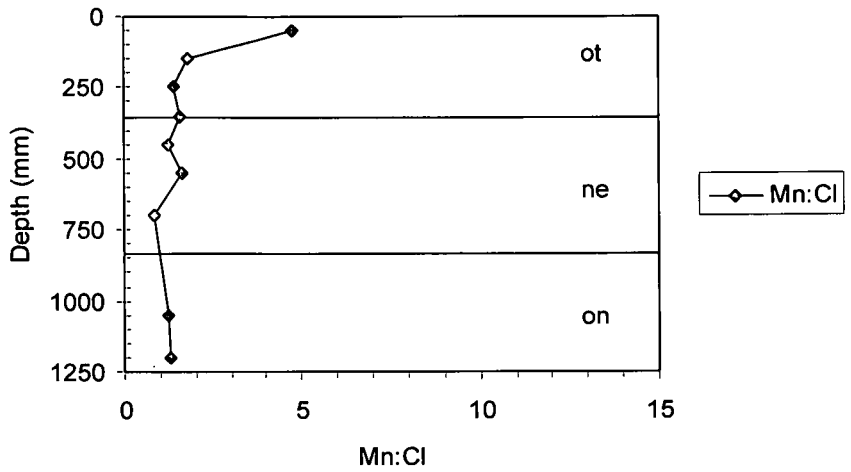

Figure 5.26 The CBD extractable Mn to clay ratio for P203 (Tukulu 2100).

### 5.4.3 Physical properties

The clay content stays fairly constant (± 11 %) throughout the A and B horizon, except for the very low (3.7 %) clay contents over the first 100 mm (Figure 5.27). This is probably due to the desert pavement-like feature observed on the surface of the first four profiles, situated on the upper Elliott sandstone shelf. The clay content then sharply increases to the C, which has 28 % clay. There is a marked decrease in silt content at 350 mm, corresponding with an increase in the sand (primarily medium and coarse sand) content. This might indicate a lithologic discontinuity.

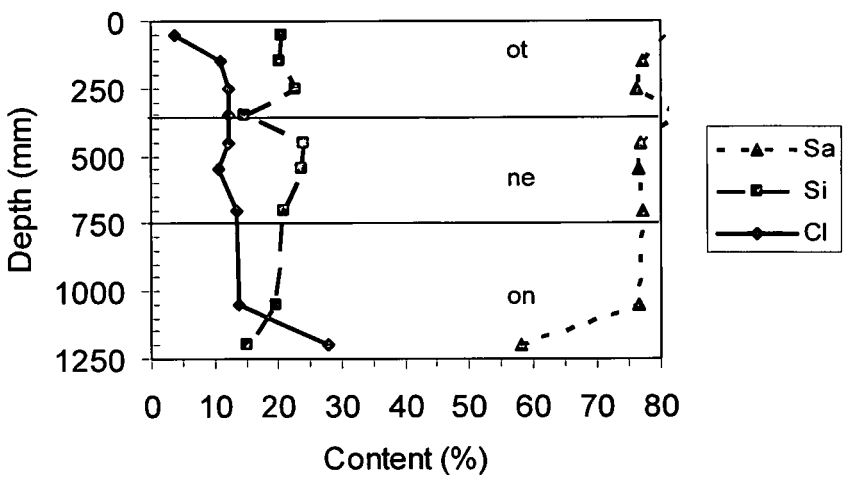

Figure 5.27 Texture of the fine earth in P203 (Tukulu 2100).

Bulk density in profile 203 (Table 5.6) is somewhat lower at 750 mm (1.62 Mg $m^{-3}$) than at 150 mm (1.65 Mg $m^{-3}$) or 450 mm (1.74 Mg $m^{-3}$). The higher bulk density of 1.74 Mg $m^{-3}$ at 450 mm coincides with a higher silt content as

well as a higher CEC and lower base saturation. The higher silt content may be responsible for the higher bulk density.

Table 5.6 Bulk density and porosity for P203 (Tukulu 2100)

| Depth (mm) | Bulk density (Mg $m^{-3}$) | Porosity (%) |
|---|---|---|
| 150 | 1.65 | 37.7 |
| 450 | 1.74 | 34.3 |
| 750 | 1.62 | 38.9 |
| 1050 | 1.75 | 34.0 |
| 1350 | 1.77 | 33.2 |

### 5.4.4 Genesis

The profile is the third in the toposequence studied, occurring 216 m from the crest on the upper Elliott shelf. It is positioned at the break of a smaller shelf. As is the case with the previous two profiles, this profile would therefore receive a considerable amount of water through lateral drainage (see section 7.4). Parent material is expected to be Elliott sandstone, partly transported during weathering of the shelf. The profile is typical of a young profile, showing marked non-uniformity in colour, especially in the B horizon. The medium sand : coarse sand ratio varies between 1.3 and 2.0 in the upper 1 200 mm, indicating a somewhat uniform parent material. Organic carbon content is very low (< 0.3 %) throughout the profile.

The clay content is somewhat uniform at 11 % throughout the profile, only increasing to almost 30 % at 1 200 mm. Base saturation decreases from 40 % in the A to 20 % in the B and then increases to 60 % at 1 200 mm. There is no horizon formation in terms of pH, Fe or Mn. The low Fe and Mn concentrations support the hypothesis of less weathering, youthfulness and therefore the occurrence of neocutanic B horizons. Some redistribution of basic cations has, however, taken place. Mottles in the subsoil indicate significant periods of saturation, possibly due to lateral water accumulation from the upper soils.

## 5.5 P204 (Longlands 2000)

The profile is situated in a footslope position, with a slope of 2 % (Figure 3.3). The orthic A horizon has a loamy medium sand texture, and the rest of the profile a fine sandy loam texture, except for the G horizon which is a coarse sandy loam. The clay content increases (8 – 10 – 14 – 30 %) down the profile. The profile description and analytical data for this profile are given in Appendix A, Tables 7 and 8. The profile can be classified as Stagnic Hyperdistric Gleysol (ferric) (FAO, 1998b) or Aeric Albaqualts (Soil Survey Staff, 1999).

### 5.5.1 Morphology

A greyish brown (7.5YR6/2) orthic A horizon (0–140 mm) overlies an orange (7.5YR7/5) E (140–300 mm) on a light grey (10YR8/2) soft plinthic B (300–470 mm) on a light grey (10YR8/2) G horizon (470–1 000 mm).

Few fine prominent bright reddish orange Fe oxide mottles are present in the A horizon, many distinct bright reddish orange Fe oxide mottles in the E, reddish brown and brown Fe oxide mottles in the soft plinthic B and many prominent reddish brown mottles in the G horizon (Table 5.7). No concretions were observed in the profile.

Table 5.7 Description of mottles in P204 (Longlands 2000)

| Horizon | Depth (mm) | Occurrence | Size | Contrast | Colour dry | Colour wet | Cause |
|---|---|---|---|---|---|---|---|
| ot | 140 | Few | Fine | Prominent | 5YR5/8 | 2.5YR4/8 | Oxidized iron |
| gs | 300 | Many | Med | Distinct | 5YR5/8 | 2.5YR4/8 | Oxidized iron |
| sp | 470 | Common | Coarse | Prominent | 2.5YR4/8 | 2.5YR4/8 | Oxidized iron |
| | | Common | Coarse | Prominent | 10YR4/8 | 7.5YR8/3 | |
| on | 1000 | Many | Fine | Prominent | 2.5YR4/8 | 2.5YR4/8 | Geogenic iron |

### 5.5.2 Chemical properties

This profile has a much higher $CEC_{soil}$ soil than the previous three. CEC increases throughout the profile, from 7.7 $cmol_c\ kg^{-1}$ in the topsoil to 22.7 $cmol_c\ kg^{-1}$ in the subsoil (Figure 5.28). There is a slight decrease in the E and the upper unspecified material with signs of wetness. This could be indicative of clay degradation due to Fe loss from the E horizon. The increase in $CEC_{soil}$ is correlated with an increase in the clay content of the soil.

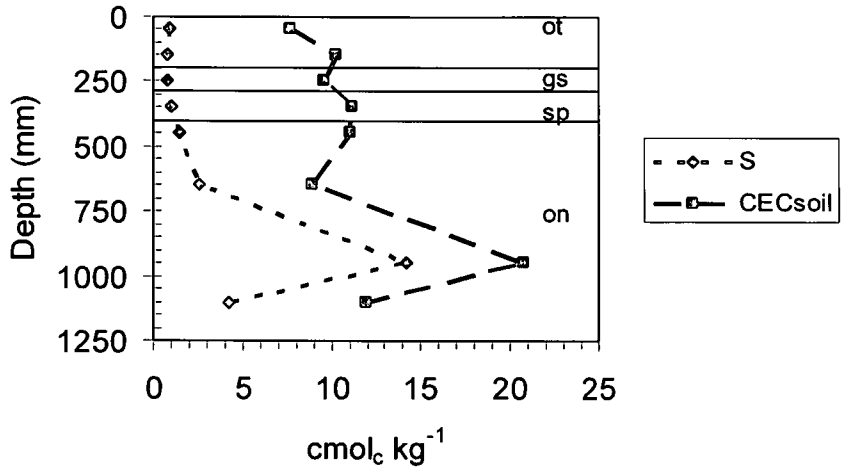


Figure 5.28 $CEC_{soil}$ and S values for P204 (Longlands 2000).

$CEC_{clay}$ decreases from 106.5 $cmol_c\ kg^{-1}$ in the topsoil to 39.3 $cmol_c\ kg^{-1}$ in the subsoil (Figure 5.29). The high $CEC_{clay}$ in the orthic A, E and soft plinthic B horizons is most probably due to montmorillonite, while the lower $CEC_{clay}$ in the subsoil could be indicative of less montmorillonite.

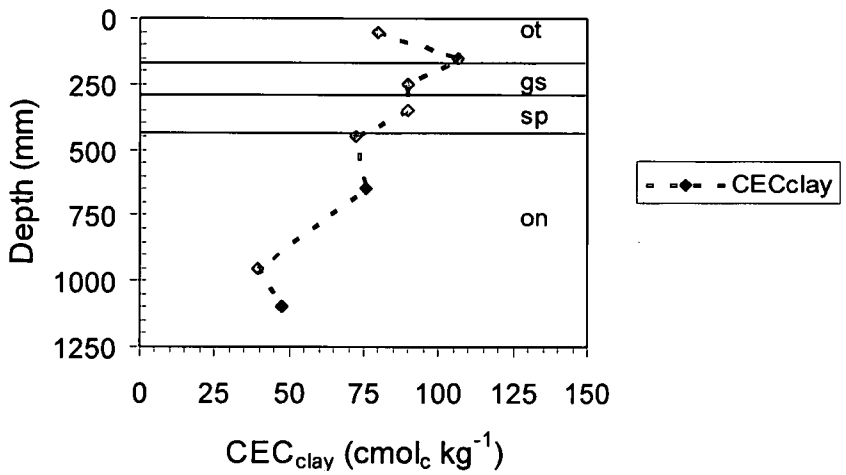


Figure 5.29 $CEC_{clay}$ for P204 (Longlands 2000).

$pH_{Water}$ is almost one unit higher in this profile than in the previous three profiles. It increases from 4.96 in the topsoil to 6.06 in the upper E horizon and then decreases to 5.45 in the subsoil (Figure 5.30). A somewhat constant $pH_{KCl}$, varying between 4.36 and 4.44, characterizes this profile.

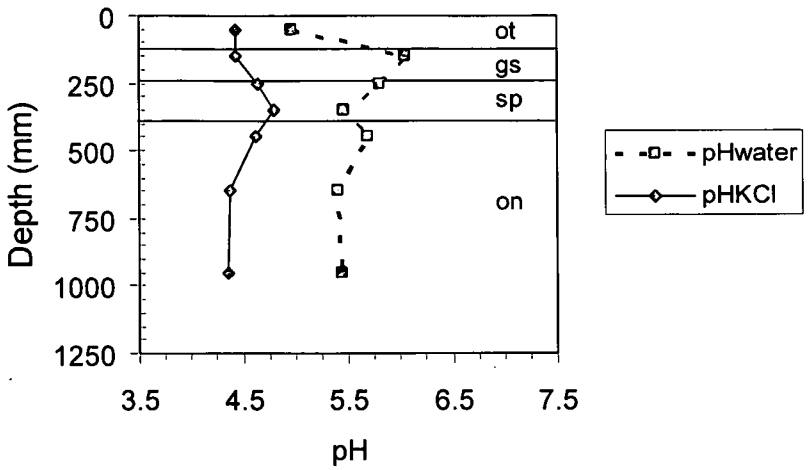


Figure 5.30 $pH_{Water}$ and $pH_{KCl}$ for P204 (Longlands 2000).

Base saturation increases with the CEC, but is lower in the E and soft plinthic B horizons than in the A (Figure 5.31). This supports the classification of the E horizon.

Organic carbon decreases from 0.05 % in the topsoil to 0.03 % in the lower soft plinthic B horizon (Figure 5.31). It then increases slightly to 0.09 % in the G horizon, possibly linked with the accumulation of clay in this horizon.

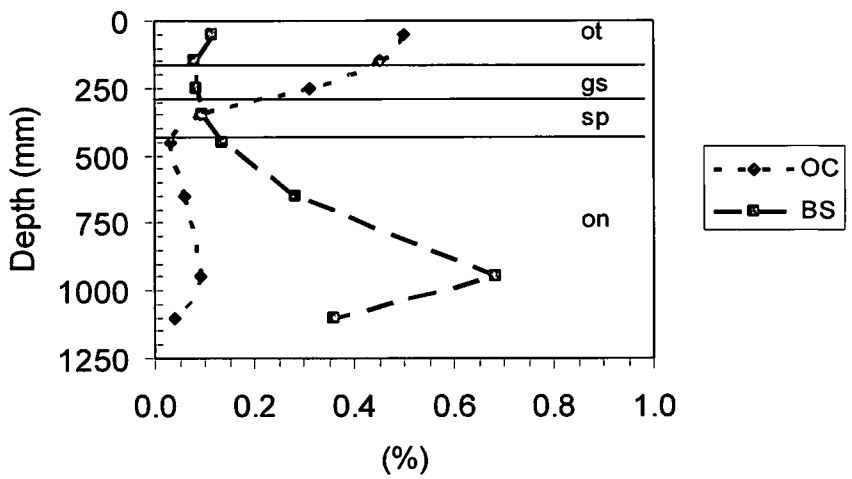


Figure 5.31 Distribution of organic carbon (OC, as a percentage) and base saturation (BS, as a fraction) in P204 (Longlands 2000).

Total Fe content increases from 3 360 mg $kg^{-1}$ in the A horizon to 7 145 mg $kg^{-1}$ in the E, 12 600 mg $kg^{-1}$ in the soft plinthic B and then decreases to 3 363 mg $kg^{-1}$ in the underlying non-diagnostic unspecified material with signs of wetness (Figure 5.32). The high total Fe content and Fe : clay ratio in the

soft plinthic B is a clear indication of Fe accumulation in this horizon (Figure 5.33).

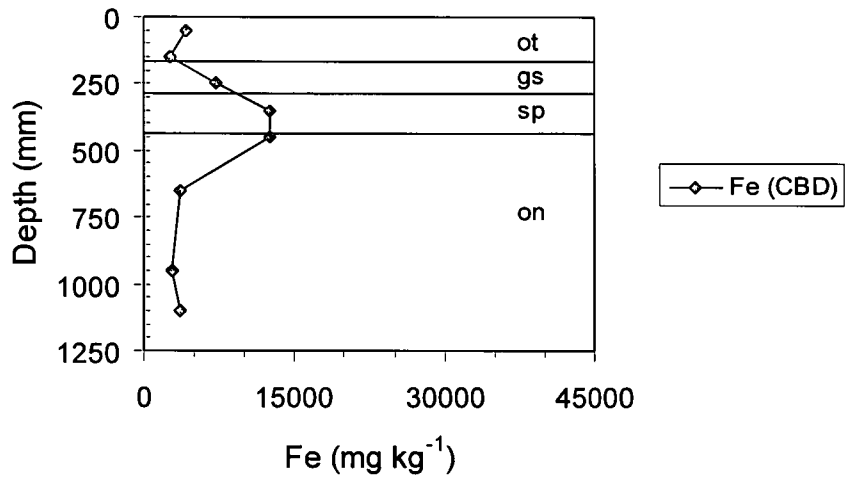


Figure 5.32 CBD extractable Fe for P204 (Longlands 2000).

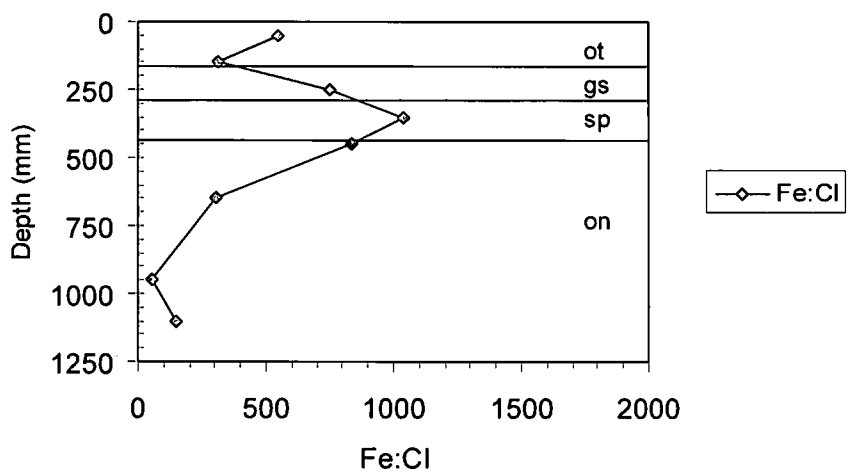


Figure 5.33 The CBD extractable Fe to clay ratio for P204 (Longlands 2000).

The total Mn content increases from 6.8 mg $kg^{-1}$ in the A horizon to 54.5 mg $kg^{-1}$ in the E horizon, decreases to 12.8 mg $kg^{-1}$ in the soft plinthic and then increases to 17.8 mg $kg^{-1}$ in the underlying non-diagnostic unspecified material with signs of wetness (Figure 5.34). The distribution of total Mn in the profile seems to contradict that of total Fe, with the Mn peak occurring in the E, while the Fe peak occurs in the soft plinthic B horizon. This might be due to the difference in the redox potentials of these two elements (Table 2.2) and inpicating possible upward movement of Fe and Mn due to capillary rise. Due to its low concentration, the distribution of Mn is furthermore influenced by the CEC, while the distribution of Fe is not, due to its larger concentration. The

Mn would therefore accumulate in an environment that is less reduced (E horizon), while it is removed from the more reduced environment in the soft plinthic B (Figure 5.35).

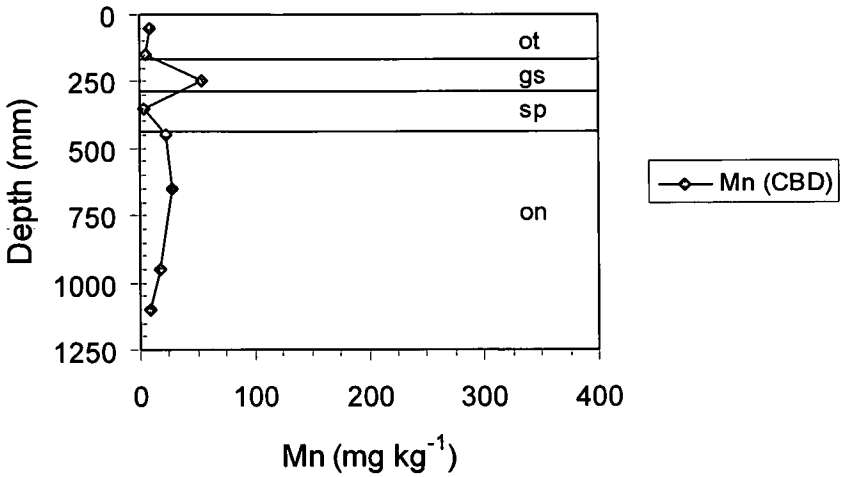


Figure 5.34 CBD extractable Mn for P204 (Longlands 2000).

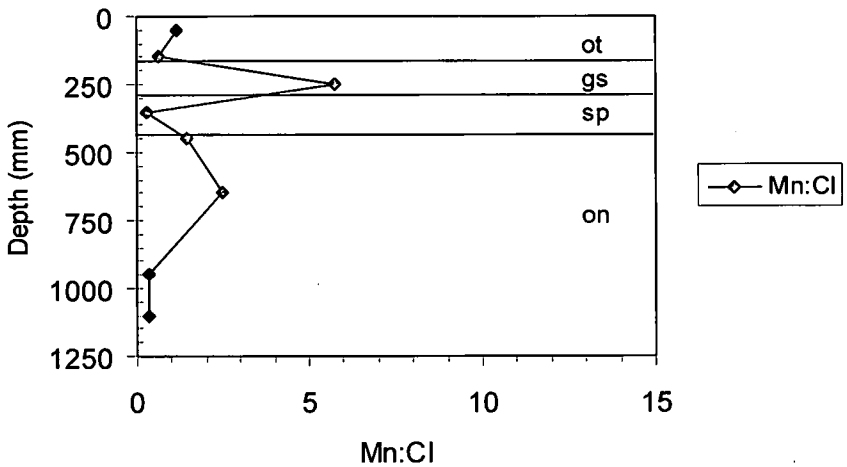


Figure 5.35 The CBD extractable Mn to clay ratio for P204 (Longlands 2000).

### 5.5.3 Physical properties

The clay content increases steadily from the A (8 %), through the E (10 %) to the soft plinthic B (14 %) horizon (Figure 5.36). This indicates eluviation of clay from the A and E horizons to the soft plinthic B horizon, and therefore supports the classification of an E horizon. The sharp decrease in clay from the soft plinthic B to the upper part of the C horizon is probably due to ferrolysis, which leads to clay degradation. This is supported by the observed silans in the upper C horizon. From there, the clay content rises sharply to 52 % at a depth of 500 to 1 100 mm, and then decreases to 25 % below

1 100 mm. The sharp increase in clay content could be due to eluviation from the upper horizons and upslope profiles, while the decrease is probably due to lack of weathering.

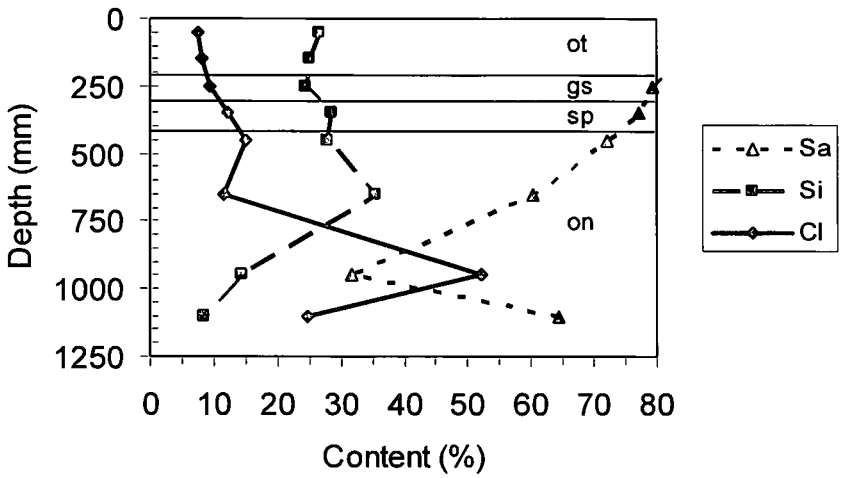


Figure 5.36 Texture of the fine earth in P204 (Longlands 2000).

Bulk density in profile 204 is extremely high, with only the topsoil having a density (1.60 Mg $m^{-3}$) conducive to root growth (Table 5.8). The bulk density increases to 1.82 Mg $m^{-3}$ at 1 050 mm. The increased density is most probably due to the unweathered nature of the subsoil.

Table 5.8 Bulk density and porosity for P204 (Longlands 2000)

| Depth (mm) | Bulk density (Mg $m^{-3}$) | Porosity (%) |
|---|---|---|
| 150 | 1.60 | 39.6 |
| 450 | 1.74 | 34.3 |
| 750 | 1.82 | 31.3 |
| 1050 | 1.82 | 31.3 |

### 5.5.4 Genesis

The profile is the last in the toposequence occurring on the upper Elliott shelf in a linear concave topographical locality, 263 m from the crest. It therefore receives a considerable volume of water and basic cations through lateral drainage. The increased water volume is evident in the presence of common and many mottles in the B and G horizons. The profile is typical binary, with the clay content constant in the A, E and B horizons and then increasing sharply into the G horizon. The binary nature is supported by the medium sand : coarse sand ratio that is higher than 2.0 in the upper 1 100 mm and

lower than 1.0 below 1 100 mm. The organic carbon is very low, decreasing from 0.50 % at 50 mm to 0.09 % at 350 mm.

The base saturation content is very low, and increases to 68 % only in the G horizon. pH is fairly uniform throughout the profile, with the exception of $pH_{Water}$ that increases in the soft plinthic B and $pH_{KCl}$ that increases in the E horizon. There is a clear increase of Fe in the soft plinthic B, while Mn is highest in the E horizon. This indicates plinthitisation in the soft plinthic B and a possible initiation thereof in the E horizon. Mn accumulation in the E horizon can be due to capillary rise, followed by the oxidation of Mn.

The higher $CEC_{clay}$ in this profile could be the result of its position in the landscape, at the bottom of the upper catena. The profile would therefore receive cations and anions leached from the upper soils and would accumulate here. The abundance of cations will favour the formation of montmorillonite clays. The accumulation of cations is also evident from the base saturation, reaching almost 70 % in the G horizon.

The high clay content and bulk density lead to a reduction in hydraulic conductivity. This coupled with the position at the lower end of the catena lead to increased saturation and the formation of mottles in the subsoil. The presence of common and many mottles in the soft plinthic B and G horizons is indicative of prolonged durations of water saturation. This is demonstrated in section 7.5.

## 5.6 P205 (Kroonstad 2000)

The profile is situated in a lower midslope position, with a slope of 7 % (Figure 3.3). It has a coarse sandy loam texture throughout the profile. The clay content decreases from the A to the E horizon and then increases to the G (13 – 11 – 11 – 28 %). The profile description and analytical data for this profile are given in Appendix A, Tables 9 and 10. The profile can be classified

as Gleyic Albic Planosol (hyperdistric) (FAO, 1998b) or Aeric Albaqualts (Soil Survey Staff, 1999).

### 5.6.1 Morphology

A dark greyish yellow (2.5Y5/2) orthic A horizon (0–220 mm) overlies a yellowish grey (2.5Y6/1) E1 (220–460 mm), on a greyish yellow brown (10YR6/2) E2 (460–660 mm) on a light grey (2.5Y7/1) G horizon (660–1 400 mm).

There are no mottles in the A horizon, indicating a dry water regime. The E1 and E2 horizons have common greyish red humus, and many bright yellowish brown Fe oxide mottles (Table 5.9). The G horizon is characterized by common reddish brown and bright yellowish brown Fe oxide mottles. No concretions were observed in the profile.

Table 5.9 Description of mottles in P205 (Kroonstad 2000)

| Horizon | Depth (mm) | Occurrence | Size | Contrast | Colour dry | Colour wet | Cause |
|---|---|---|---|---|---|---|---|
| ot | 220 | None | | | | | |
| gs | 460 | Common | Med | Distinct | 2.5Y4/2 | 2.5Y3/2 | Humus |
| | | Many | Med | Distinct | 10YR6/6 | 10YR4/6 | Oxidized iron |
| gs | 660 | Common | Med | Prominent | 2.5Y4/2 | 2.5Y3/2 | Humus |
| | | Common | Med | Distinct | 10YR6/8 | 7.5YR5/8 | Oxidized iron |
| gh | 1400 | Common | Fine | Prominent | 2.5YR4/8 | 10R4/8 | Oxidized iron |
| | | Common | Med | Prominent | 10YR6/8 | 7.5YR4/8 | Oxidized iron |

### 5.6.2 Chemical properties

$CEC_{soil}$ increases from 10.5 $cmol_c\ kg^{-1}$ in the A to 17.6 $cmol_c\ kg^{-1}$ in the G horizon (Figure 5.37). This is associated with a decrease in organic matter content and an increase in the clay content from the A to the G horizon.

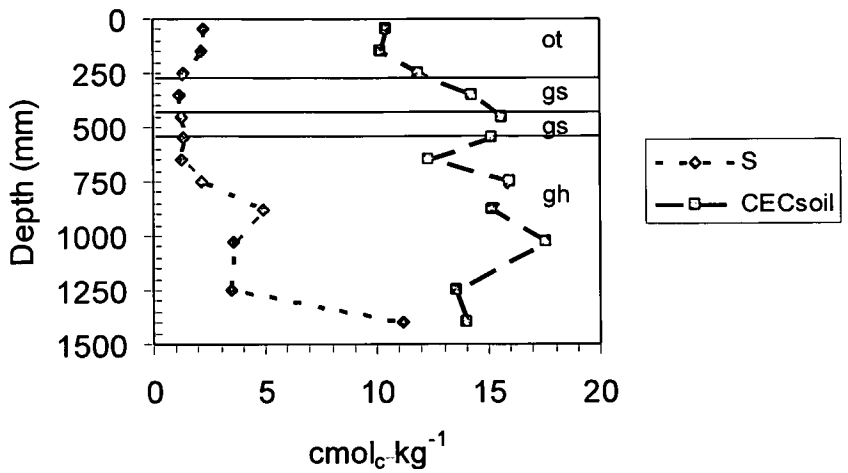


Figure 5.37 $CEC_{soil}$ and S values for P205 (Kroonstad 2000).

$CEC_{clay}$ increases from 82.2 $cmol_c\ kg^{-1}$ in the topsoil to 132.4 $cmol_c\ kg^{-1}$ in the E1 and then decreases to 40.7 $cmol_c\ kg^{-1}$ in the G horizon (Figure 5.38). The high $CEC_{clay}$ in the E and relatively low $CEC_{clay}$ in the G horizons are similar to that observed in profile 204. It is therefore proposed that these two profiles developed in similar cumulative environments, resulting in the formation of high CEC clays *e.g.* montmorillonite.

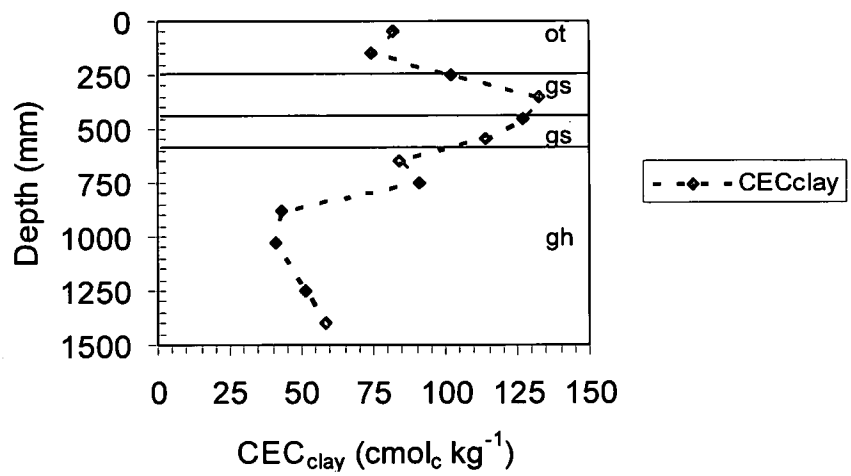


Figure 5.38 $CEC_{clay}$ for P205 (Kroonstad 2000).

$pH_{Water}$ increases from 5.38 in the topsoil to 5.97 in the subsoil (Figure 5.39). $pH_{KCl}$ stays somewhat constant at 4.20 to 4.57 throughout the profile. The $pH_{KCl}$ – value of 5.82 at a depth of 875 mm is most probably due to experimental error. The large difference between $pH_{Water}$ and $pH_{KCl}$ indicates a large residual acidity in this profile. As in the case of profile 204.

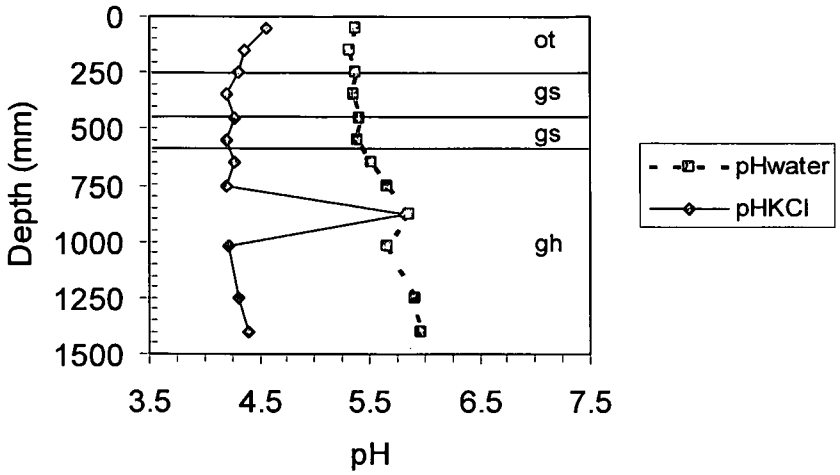


Figure 5.39 $pH_{Water}$ and $pH_{KCl}$ for P205 (Kroonstad 2000).

Base saturation decreases from 0.2 % in the A to 0.1 % in the E1 and E2, increasing to 0.3 % in the G horizon (Figure 5.40). The decrease in base saturation from the A to the E supports the classification of the E, whiles the increase in base saturation to the G supports its classification.

Organic carbon decreases from 0.8 % in the A to 0.5 % in the upper E1, which then increases to 0.8 % the lower E1 horizon (Figure 5.40). Organic carbon decreases further to a mean of 0.2 % in the G horizon.

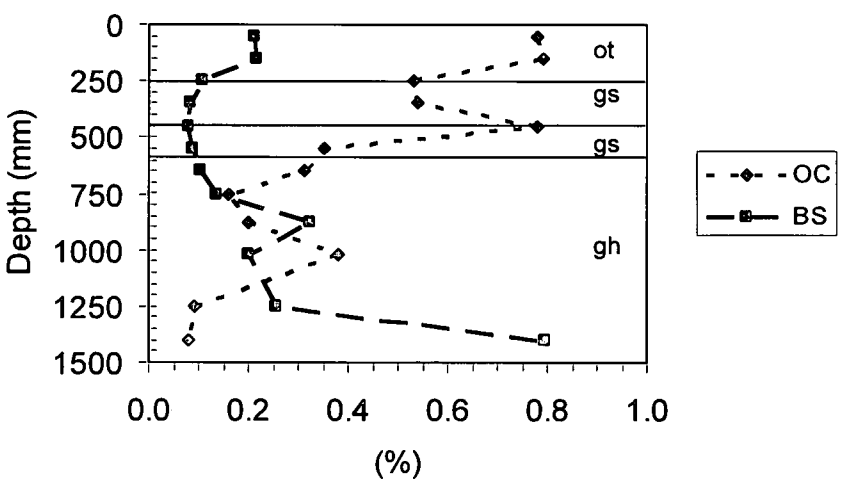


Figure 5.40 Distribution of organic carbon (OC, as a percentage) and base saturation (BS, as a fraction) in P205 (Kroonstad 2000).

Total Fe content is fairly constant at 4 500 to 5 000 mg $kg^{-1}$ throughout the profile (Figure 5.41). It is higher in the E1 horizon, with a maximum of 5 625 mg $kg^{-1}$ and lower in the E2 horizon, with a minimum of 3 865 mg $kg^{-1}$. The

Fe content is variable in the G horizon, with a mean of 4 793 mg $kg^{-1}$. It therefore seems that some Fe accumulation has taken place in the E1 horizon, while it has been depleted from the E2 and from zones in the G horizon (Figure 5.42).

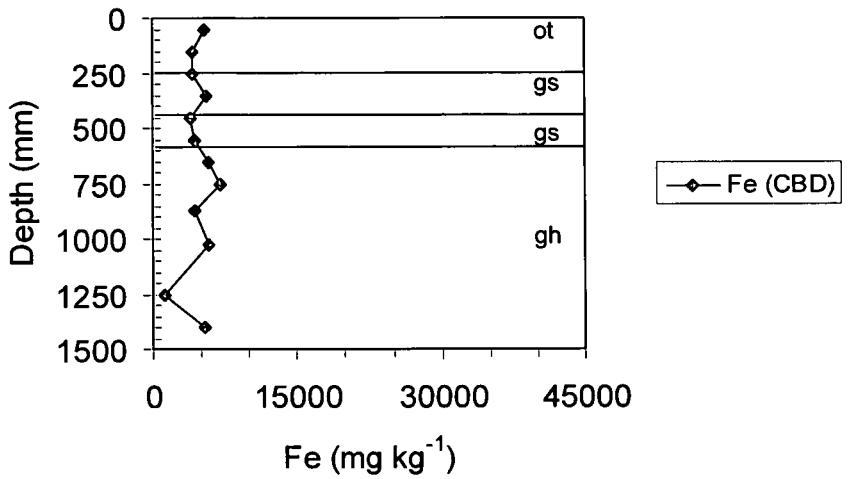


Figure 5.41 CBD extractable Fe for P205 (Kroonstad 2000).

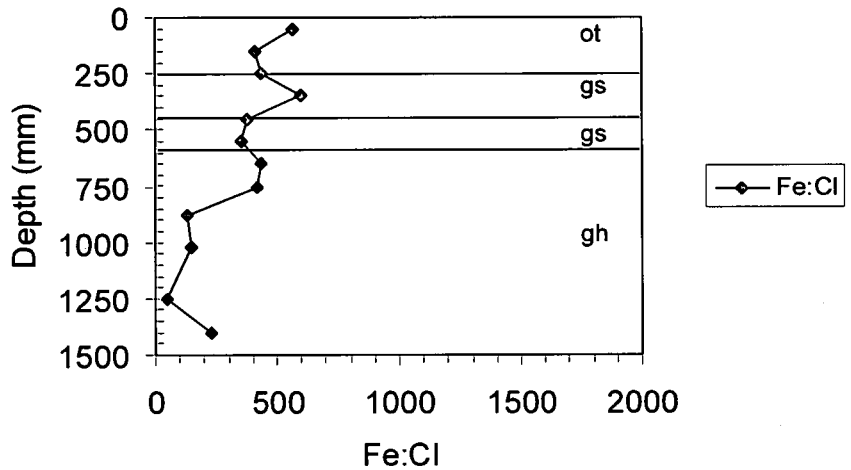


Figure 5.42 The CBD extractable Fe to clay ratio for P205 (Kroonstad 2000).

Maximum total Mn accumulation has taken place at the top (69.0 mg $kg^{-1}$) and lower half (75.0 mg $kg^{-1}$) of the G horizon (Figure 5.43). This accumulation of Mn above that of Fe is similar to that in P204. The A (4.5 – 5.0 mg $kg^{-1}$) and E1 (3.5 – 4.0 mg $kg^{-1}$) horizons seem to have undergone depletion of Mn. There is also a slight accumulation (11.0 – 46.0 mg $kg^{-1}$) of Mn in the E2 and upper G horizon (Figure 5.44).

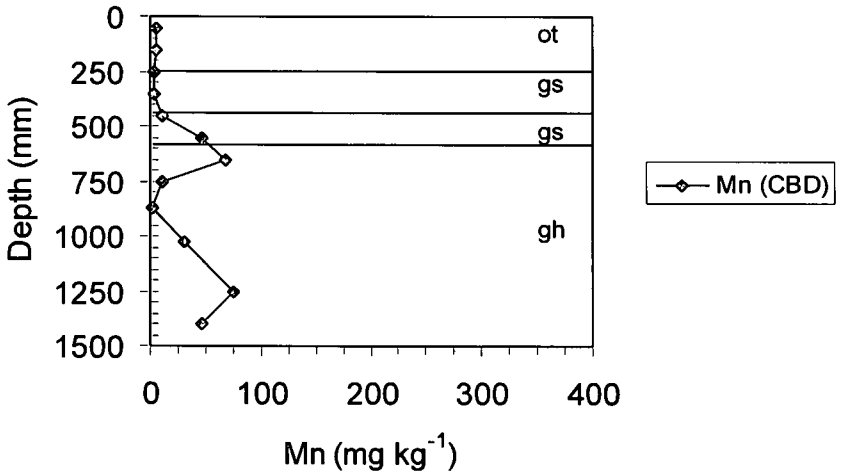


Figure 5.43 CBD extractable Mn for P205 (Kroonstad 2000).

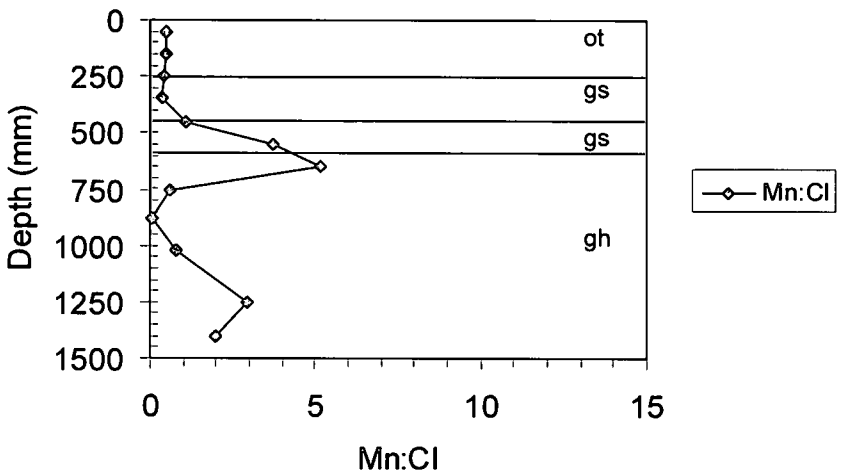


Figure 5.44 The CBD extractable Mn to clay ratio for P205 (Kroonstad 2000).

### 5.6.3 Physical properties

The texture pattern in this profile is remarkably similar to the previous profile. Clay content (Figure 5.45) is fairly stable throughout the A (10 %), E1 (10 %) and E2 (13 %) horizons, but then sharply increases in the G horizon (28 %). The texture pattern supports the classification of the E and G horizons, given the removal of clay in the E and the accumulation thereof in the G.

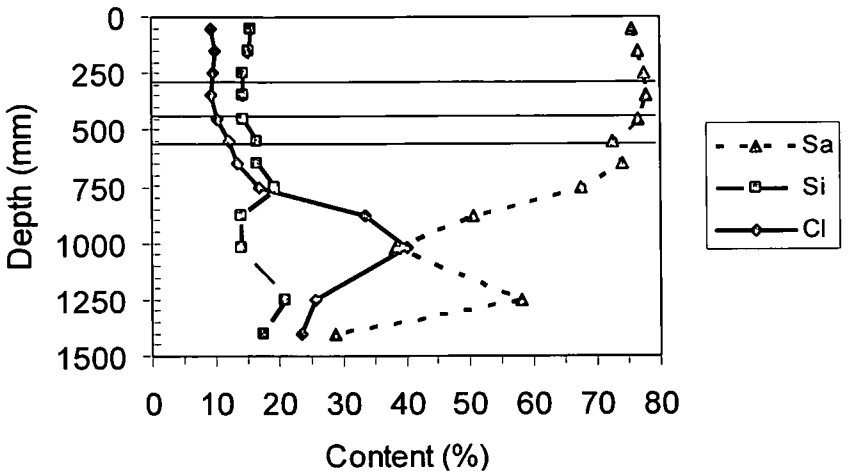


Figure 5.45 Texture of the fine earth in P205 (Kroonstad 2000).

Bulk density increases from 1.66 Mg $m^{-3}$ at 150 mm to 1.79 Mg $m^{-3}$ at 1 050 mm (Table 5.10). The bulk density throughout the profile is very high and will seriously impact on root growth. It will also cause reduction to set in at lower water contents, due to the low pore volume.

Table 5.10 Bulk density and porosity for P205 (Kroonstad 2000)

| Depth (mm) | Bulk density (Mg $m^{-3}$) | Porosity (%) |
|---|---|---|
| 150 | 1.66 | 37.4 |
| 450 | 1.69 | 36.2 |
| 750 | 1.72 | 35.1 |
| 1050 | 1.79 | 32.5 |
| 1350 | 1.73 | 34.7 |

### 5.6.4 Genesis

The profile is situated just below the upper Elliott shelf. The location of this profile in the landscape dictates that it could have originally been situated in a midslope water course – similar to the position where profile 206 is currently situated. Erosion could have moved the water course, resulting in a drier soil water regime (section 7.6). The parent material is expected to be Molteno sandstone, although transportation and accumulation could have taken place. The medium sand : coarse sand ratio varies between 1.7 and 2.0, increasing in the subsoil. It therefore points to a single parent material, different from the first four profiles. The organic carbon content is variable, but decreases with depth, from 0.8 % in the topsoil to 0.08 % in the subsoil.

The profile is characterized by an increasing clay content, as well as decreasing $CEC_{clay}$ and base saturation. Fe content is variable, but decreases with depth. Mn content increases with depth. The profile is remarkably similar to profile 204, both having increasing base saturation and decreasing $CEC_{clay}$ with depth. The main difference seems to be the lack of Fe redistribution, which would have led to the formation of a soft plinthic B horizon, in this profile relative to profile 204. There is, however, marked Mn redistribution in the G horizon of this profile. This might be the initial phases of soft plinthic B horizon formation. The pale colours in the A, E1 and E2 horizons are consistent with Fe and Mn removal. The removal of Mn in the first two horizons points to reducing and leaching conditions in that locality. The accumulation of Mn in the upper G horizon is probably an indication that there is less reduction and / or leaching here due to the impervious nature of this horizon. The increase of Mn in the lower half of the G horizon is either due to absolute accumulation, or due to Mn removal in the upper part of the horizon (700 – 950 mm). The removed Mn could have been moved upwards by capillary rise to the upper G, or it could have leached to the lower G horizon. The hypothesis for removal of Mn is plausible if the occurrence of silans in the upper G horizon is taken into account.

## 5.7 P206 (Kroonstad 1000)

The profile is situated in a lower footslope position, with a slope of 3 % (Figure 3.3). The orthic A and E horizons have a loamy texture, while the G horizon has a clay loam texture. The clay content decreases from the A to the E and then increases to the G horizon (21 – 17 – 38 %). The profile description and analytical data for this profile are given in Appendix A (Tables 11 and 12). The profile can be classified as Mollic Gleyic Planosol (albic, endo-eutric) (FAO, 1998b) or Typic Argialbolls (Soil Survey Staff, 1999).

### 5.7.1 Morphology

A brownish grey (10YR5/1) orthic A horizon (0–550 mm) overlies a brownish grey (10YR5/1) E (550–800 mm) on a brownish grey (10YR6/1) G horizon (800–1100 mm).

Few distinct bright brown Fe oxide mottles in the A, few prominent black Mn oxide mottles as well as common bright brown Fe oxide mottles in the E and many prominent bright brown Fe oxide mottles in the G horizon are an indication that this profile is saturated for long periods (Table 5.11). No concretions were observed in the profile. Pores in the A are rusty, while those in the E and G horizons are bleached.

Table 5.11 Description of mottles in P206 (Kroonstad 1000)

| Horizon | Depth (mm) | Occurrence | Size | Contrast | Colour dry | Colour wet | Cause |
|---|---|---|---|---|---|---|---|
| ot | 550 | Few | Fine | Distinct | 7.5YR5/8 | 10YR4/6 | Oxidized iron |
| gs | 800 | Few | Fine | Prominent | 10YR2/1 | 10YR2/1 | Manganese |
| | | Common | Fine | Prominent | 7.5YR5/8 | 10YR4/6 | Oxidized iron |
| gh | 1100 | Many | Med | Prominent | 7.5YR5/8 | 10YR5/8 | Oxidized iron |

### 5.7.2 Chemical properties

$CEC_{soil}$ soil decreases sharply from 31.0 $cmol_c\ kg^{-1}$ in the topsoil to a low of 6.4 $cmol_c\ kg^{-1}$ in the lower E2 (Figure 5.46). It then increases to 12.8 $cmol_c\ kg^{-1}$ in the G. The decrease in $CEC_{soil}$ follows a decrease in organic matter content from the A to the E, while the increase in $CEC_{soil}$ in the G horizon is associated with an increase in clay content.

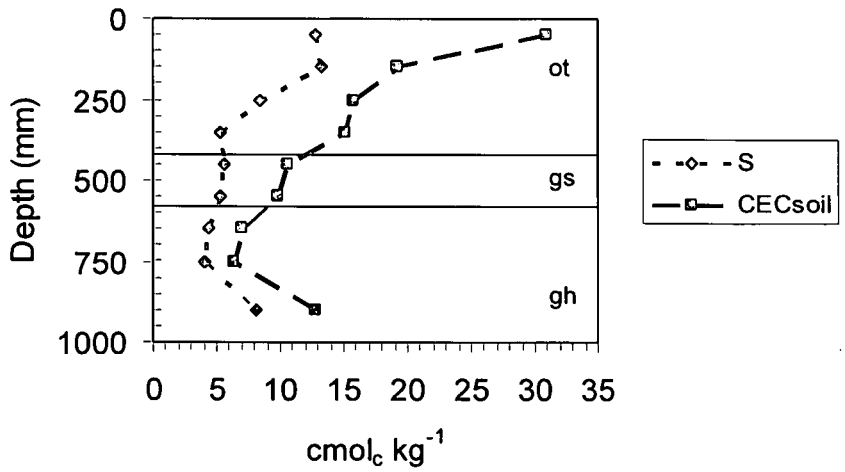


Figure 5.46 $CEC_{soil}$ and S values for P206 (Kroonstad 1000).

$CEC_{clay}$ decreases throughout the profile, from 68.3 in the topsoil to 32.2 in the lower part of the G horizon (Figure 5.47). This pattern is similar to that observed for profiles 204 and 205, where there is a decrease in $CEC_{clay}$ throughout the profile. They differ in the sense that the mean $CEC_{clay}$ is 40 cmol$_c$ kg$^{-1}$ lower in this profile and that there is a decrease in $CEC_{clay}$ in the E, relative to the increase in $CEC_{clay}$ observed in profile 205.

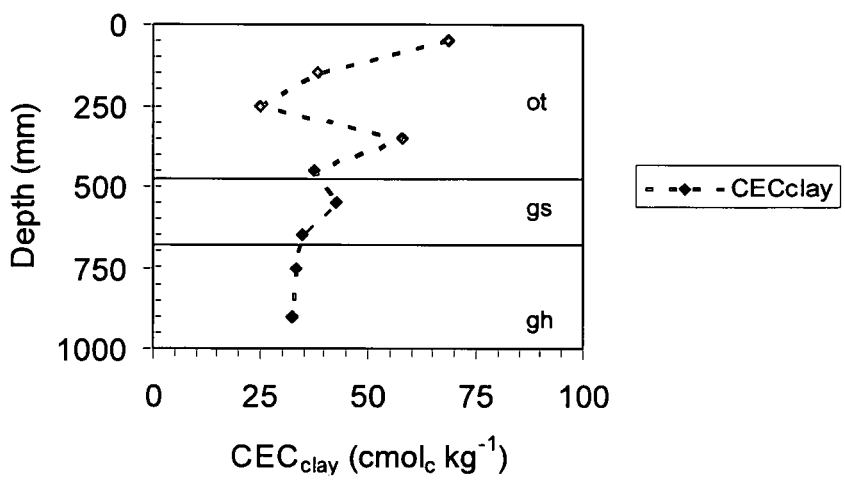


Figure 5.47 $CEC_{clay}$ for P206 (Kroonstad 1000).

$pH_{Water}$ is constant at 5.70 to 6.23 throughout the profile (Figure 5.48). $pH_{KCl}$ decreases from 5.66 in the topsoil to 4.28 in the subsoil. The high $pH_{Water}$ in relation to the previous profiles can be an indication of a cumulative pedological environment. This is supported by the base saturation which is in excess of 50 %. The widening difference between $pH_{Water}$ and $pH_{KCl}$ indicates increasing residual acidity with depth.

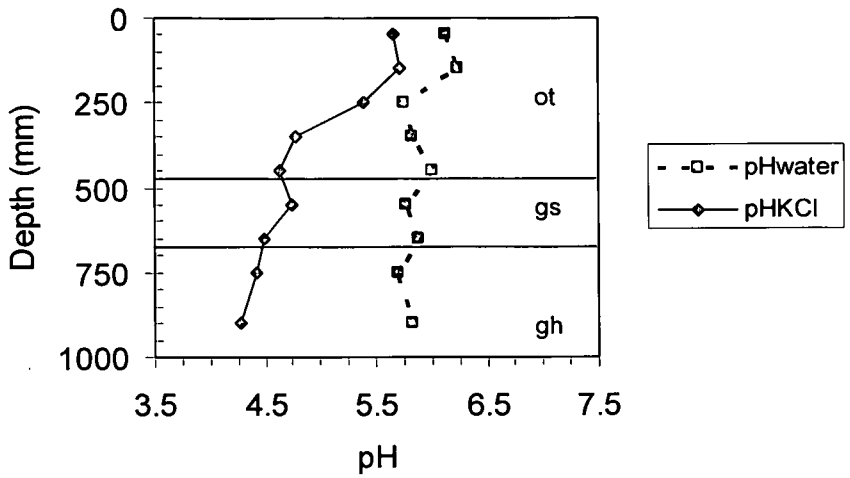


Figure 5.48 $pH_{Water}$ and $pH_{KCl}$ for P206 (Kroonstad 1000).

Base saturation is practically constant throughout the profile, ranging between 50 % in the A and 64 % in the E and G horizons (Figure 5.49). This profile does not have the clear decrease in base saturation associated with the E horizon, which can be observed in P201 (Longlands), P204 (Longlands) and P205 (Kroonstad).

Organic carbon decreases from 4.4 % in the topsoil to 0.18 in the lower E2 and 0.16 % in the G horizon (Figure 5.49). Of all profiles studied, this profile has the highest organic carbon content in its topsoil, largely due to its occurrence in a seep that inhibits mineralization of organic matter.

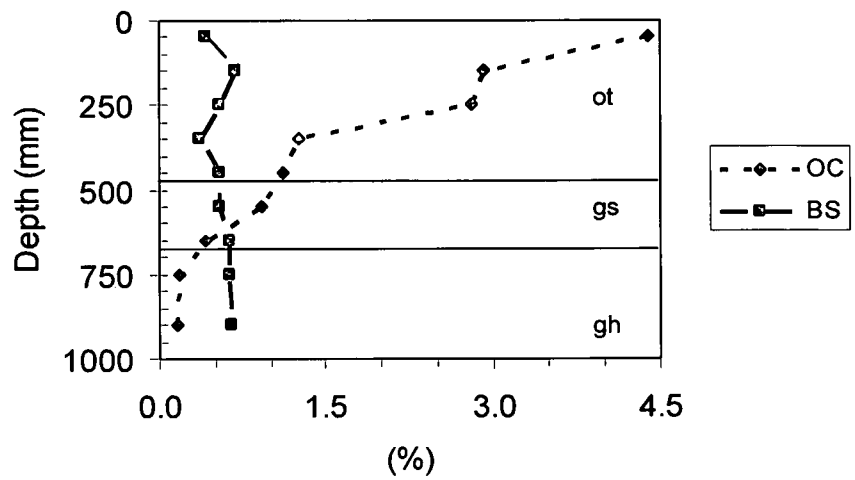


Figure 5.49 Distribution of organic carbon (OC, as a percentage) and base saturation (BS, as a fraction) in P206 (Kroonstad 1000).

Total Fe content decreases down the profile, from 7 975 mg $kg^{-1}$ in the topsoil to 1 240 mg $kg^{-1}$ in the lower G horizon (Figure 5.50). The total Fe content decreases markedly from a depth of 300 to 700 mm, pointing to an absolute removal of Fe from the profile (Figure 5.51). This might point to erroneous demarcation of the E horizon. As was stated previously, the high organic matter content in A and E horizon partially masked the presence of the E horizon.

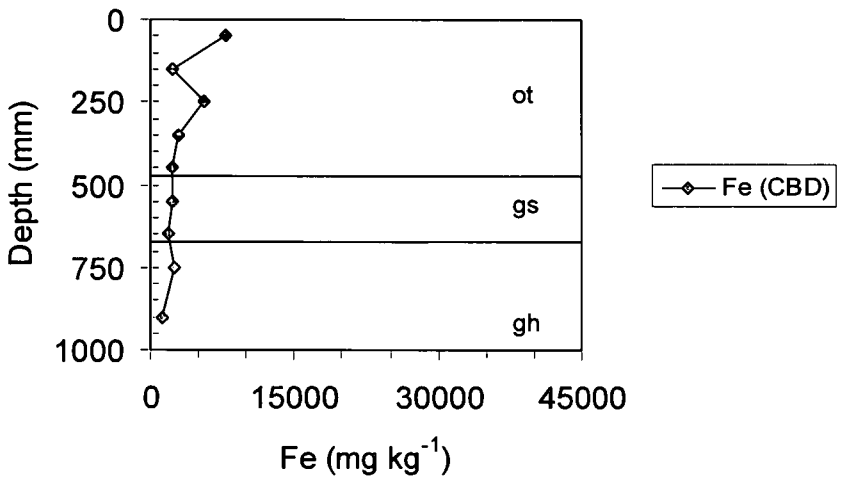


Figure 5.50 CBD extractable Fe for P206 (Kroonstad 1000).

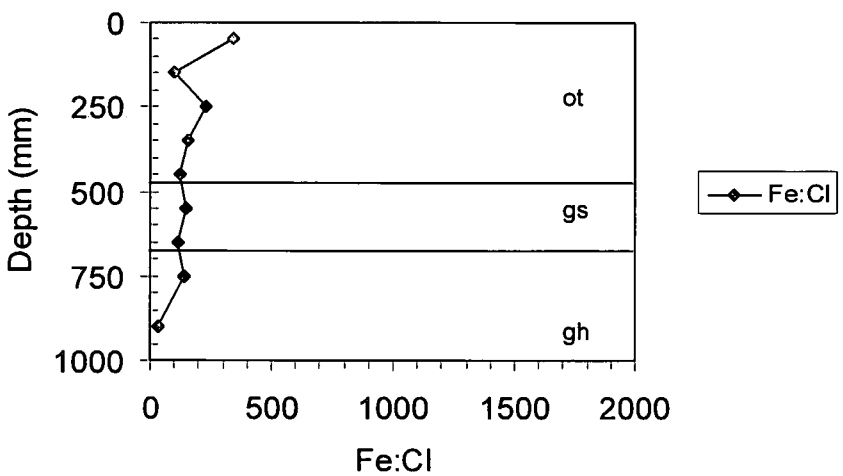


Figure 5.51 The CBD extractable Fe to clay ratio for P206 (Kroonstad 1000).

Total Mn content is fairly low in the A and E horizons (Figure 5.52). It decreases from a maximum of 41.0 mg $kg^{-1}$ in the topsoil to 4.0 mg $kg^{-1}$ in the lower E and then increases to 147.0 mg $kg^{-1}$ in the lower G horizon (Figure 5.53).

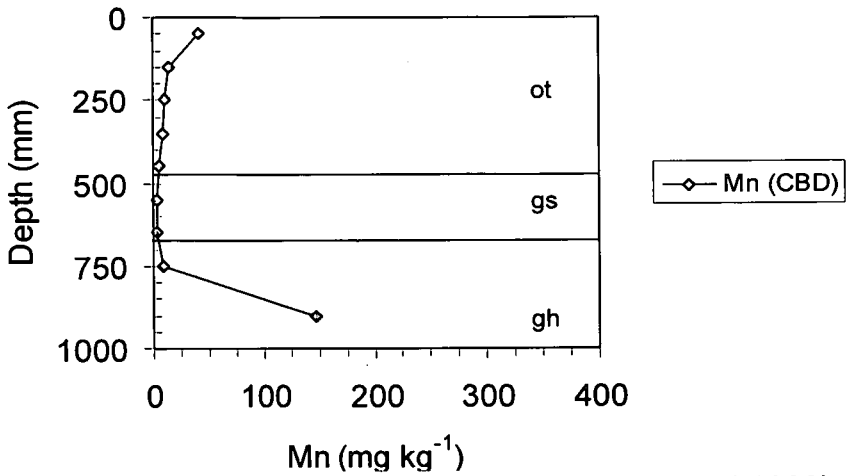


Figure 5.52 CBD extractable Mn for P206 (Kroonstad 1000).

The Mn is mainly associated with the cation exchange complex, except in the lower part of the G horizons where there seems to be an absolute accumulation (Figure 5.53).

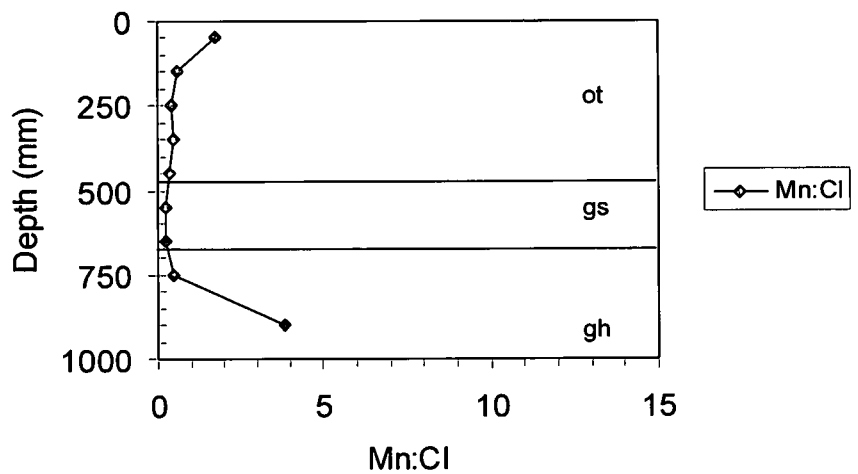


Figure 5.53 The CBD extractable Mn to clay ratio for P206 (Kroonstad 1000).

### 5.7.3 Physical properties

The clay content decreases from 22 % in the A horizon to 17 % in the E, and increases to 38 % in the G horizon (Figure 5.54). The sharp decrease in clay content at 300 mm might indicate that the lower boundary of the A horizon should be at this depth, or at least that the 300 – 500 mm horizon is a transition between the orthic A and the E horizon (the grey colour could be masked by the presence of large amounts of organic matter). The increase in clay content from the E to the G is consistent with the classification.

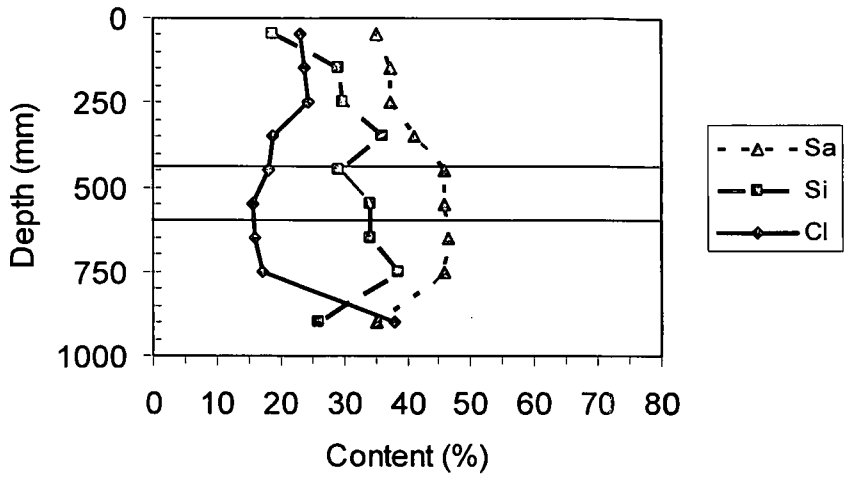


Figure 5.54 Texture of the fine earth in P206 (Kroonstad 1000).

The bulk density is very low (0.99 Mg $m^{-3}$) at 150 mm (Table 5.12). It then increases to 1.76 Mg $m^{-3}$ at 450 mm and 1.70 Mg $m^{-3}$ at 1 050 mm. The low bulk density at 150 mm is due to the extremely high organic matter content in the topsoil, while the high bulk density in the subsoil is typical of these G horizons.

Table 5.12 Bulk density and porosity for P206 (Kroonstad 1000)

| Depth (mm) | Bulk density (Mg $m^{-3}$) | Porosity (%) |
|---|---|---|
| 150 | 0.99 | 62.6 |
| 450 | 1.76 | 33.6 |
| 750 | 1.66 | 37.4 |
| 1050 | 1.70 | 35.8 |

### 5.7.4 Genesis

Profile 206 is situated in a midslope water course, with a spring just above the profile, resulting in a vast supply of water from the phreatic water table. The presence of a water table in the dry season and rusty root channels and pores in the topsoil are indicative of this (section 7.7). The profile is expected to have Molteno sandstone as parent material. The medium sand : coarse sand ratio, ranging between 0.8 and 1.0, supports this. The profile is characterized by a very high organic carbon content in the A horizon (4.4 %) that decreases steadily down the profile. The accumulation of organic matter is explained by the long periods of water saturation that excludes oxygen and thus prevents mineralization of organic matter, leading to its accumulation.

The clay content is fairly constant throughout the A and E horizons, but increases markedly in the G horizon. The base saturation is constant, increasing from 40 to 65 % through the profile. The high base saturation percentage is due to the setting of the profile in a site of accumulation. $pH_{Water}$ is constant, while $pH_{KCl}$ decreases down the profile. Total Fe decreases down the profile, while Mn decreases down the profile, before increasing sharply at 900 mm. The organic carbon in the A horizon masks the grey colour of the soil matrix. This resulted in the presence of an E horizon being overlooked in the lower A horizon. The bleached colour of the A and E horizons is the result of removal of Fe. Mn in the A and E horizons is mainly associated with the clay complex. The accumulation of Mn in the G horizon is probably due to leaching from the overlying horizons as well as release from primary minerals, coupled with very slow leaching from the horizon.

## 5.8 P207 (Westleigh 1000)

The profile is situated in a valley bottom position, with a slope of 3 % (Figure 3.3). The orthic A as well as the B1 and B2 soft plinthic B horizons have a silty loam texture, while the underlying unspecified material with signs of wetness has a clay texture. The clay content increases from the A to the B1, decreases to the B2 and then sharply increases to the unspecified material with signs of wetness (23 – 24 – 19 – 46 %). The profile description and analytical data for this profile are given in Appendix A, Tables 13 and 14. The profile can be classified as Gleyic-stagnic Albeluvisol (ferric, hyperdistric) (FAO, 1998b) or Aeric Albaqualts (Soil Survey Staff, 1999).

### 5.8.1 Morphology

A greyish yellow brown (10YR6/2) orthic A horizon (0–300 mm) overlies a dull yellow orange (10YR6/3) soft plinthic B1 (300–560 mm) on a light grey (10YR8/1) soft plinthic B2 (560–670 mm) on a light grey (10YR8/2) unspecified material with signs of wetness (670–1 300 mm).

Mottles increase in prominence and become slightly paler down the profile (Table 5.13). Common fine distinct yellowish brown mottles in the A increase to many medium distinct yellowish brown mottles in the B1. The occurrence of mottles then decreases to common prominent yellowish brown Fe oxide mottles in the B2, but increase to many prominent bright yellowish brown Fe oxide mottles in the unspecified material with signs of wetness. The B2 horizon is characterized by many round gravel sized (2 – 6 mm) Fe and Mn concretions. The A and B1 horizons have many rusty pores and the B2 horizon and unspecified material with signs of wetness have few bleached pores.

Table 5.13 Description of mottles in P207 (Westleigh 1000)

| Horizon | Depth (mm) | Occurrence | Size | Contrast | Colour dry | Colour wet | Cause |
|---|---|---|---|---|---|---|---|
| ot | 300 | Common | Fine | Distinct | 10YR5/7 | 10YR4/6 | Oxidized iron |
| sp | 560 | Many | Med | Distinct | 10YR5/7 | 10YR4/6 | Oxidized iron |
| sp | 670 | Common | Med | Prominent | 10YR5/6 | 10YR4/6 | Oxidized iron |
| on | 1300 | Many | Fine | Prominent | 10YR6/8 | 10YR4/6 | Oxidized iron |

### 5.8.2 Chemical properties

$CEC_{soil}$ decreases from 10.4 $cmol_c\ kg^{-1}$ in the topsoil to 6.7 $cmol_c\ kg^{-1}$ at the lower boundary of the second soft plinthic B horizon (Figure 5.55). It then increases to 14.7 $cmol_c\ kg^{-1}$ in the underlying unspecified material with signs of wetness. The decrease in $CEC_{soil}$ is correlated with the decrease in organic carbon, while the increase is correlated with an increase in clay content.

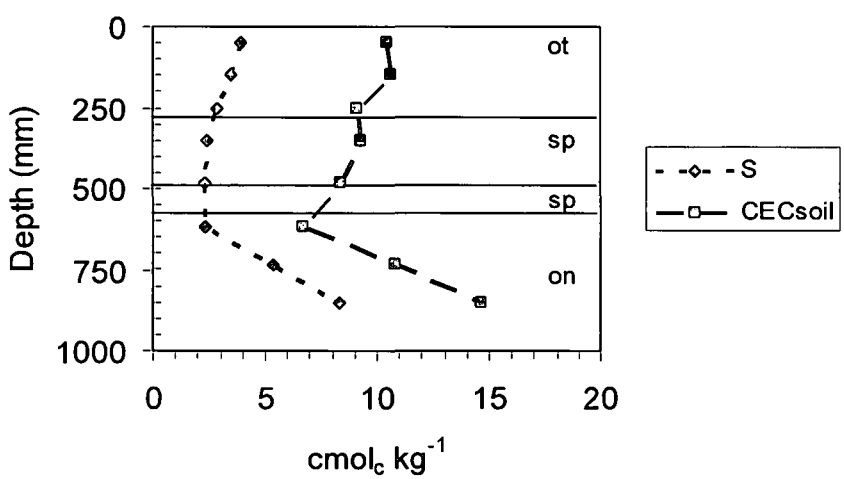


Figure 5.55 $CEC_{soil}$ and S values for P207 (Westleigh 1000).

$CEC_{clay}$ is relatively low in this profile, increasing from 23.5 $cmol_c\ kg^{-1}$ in the topsoil to 31.0 $cmol_c\ kg^{-1}$ in the lower part of the second soft plinthic B horizon. It then decreases slightly to 25.7 $cmol_c\ kg^{-1}$ in the unspecified material with signs of wetness (Figure 5.56). The $CEC_{clay}$ in this profile is similar to that in profile 201 and 202, the latter which is characterized by limited pedogenesis. The $CEC_{clay}$ is an indication of a mixture of kaolinite, fine mica and chlorite. The base saturation is high, in the region of 30 to 60 %. It therefore indicates a cumulative environment.

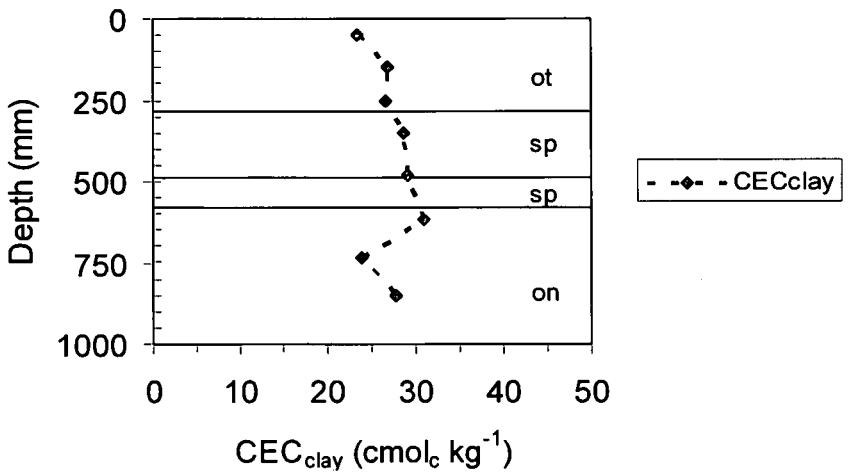


Figure 5.56 $CEC_{clay}$ for P207 (Westleigh 1000).

$pH_{Water}$ increases with depth, from 5.35 in the topsoil to 6.36 in the subsoil (Figure 5.57). $pH_{KCl}$ stays constant at 4.07 to 4.46 throughout the profile. The pH pattern is similar to that of profile 205 (Kroonstad 2000).

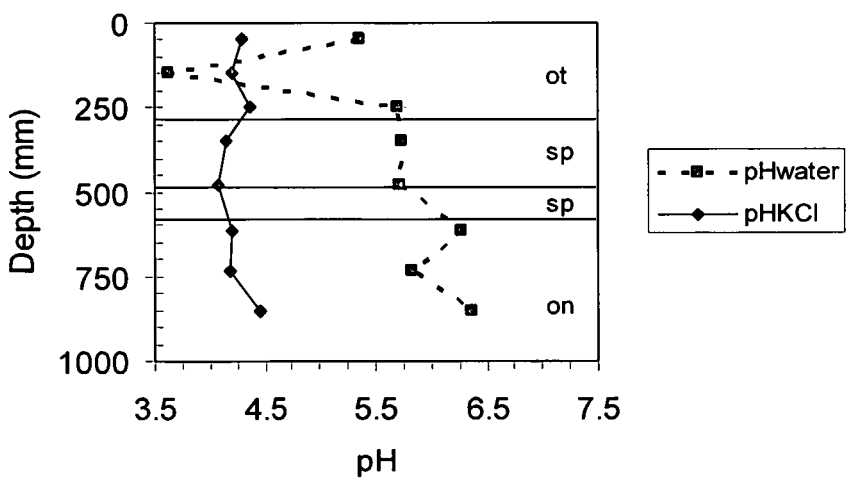


Figure 5.57 $pH_{Water}$ and $pH_{KCl}$ for P207 (Westleigh 1000).

Base saturation decreases slightly from 38 % in the topsoil to 26 % in the soft plinthic B and then increases to 57 % in the unspecified material with signs of wetness (Figure 5.58). The decrease in base saturation is linked with an absolute decrease in basic cations, in the same order as $CEC_{soil}$. The decrease in basic cations indicates significant leaching from the soft plinthic B and accumulation in the unspecified material with signs of wetness.

Organic carbon decreases from 1.6 % in the topsoil to 0.2 % in the unspecified material with signs of wetness (Figure 5.58). The organic carbon content does not seem to be influenced by diagnostic horizons.

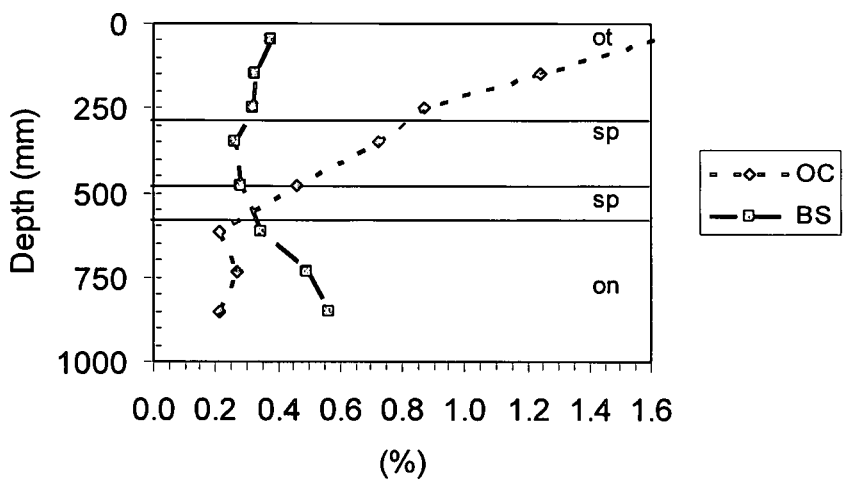


Figure 5.58 Distribution of organic carbon (OC, as a percentage) and base saturation (BS, as a fraction) in P207 (Westleigh 1000).

Total Fe content is fairly constant in the first three horizons, decreasing from a maximum of 8 200 mg $kg^{-1}$ in the topsoil to a minimum of 6 825 mg $kg^{-1}$ in the B1 before increasing to 7 980 mg $kg^{-1}$ in the B2 (Figure 5.59). The B1 was described as having many Fe oxide mottles. It would appear from the analyses as if removal of Fe has taken place from this horizon (Figure 5.60). This would be a motivation for the classification of this horizon as an E horizon. The slight increased Fe content in the B2 horizon was expected, as it has common Fe oxide mottles.

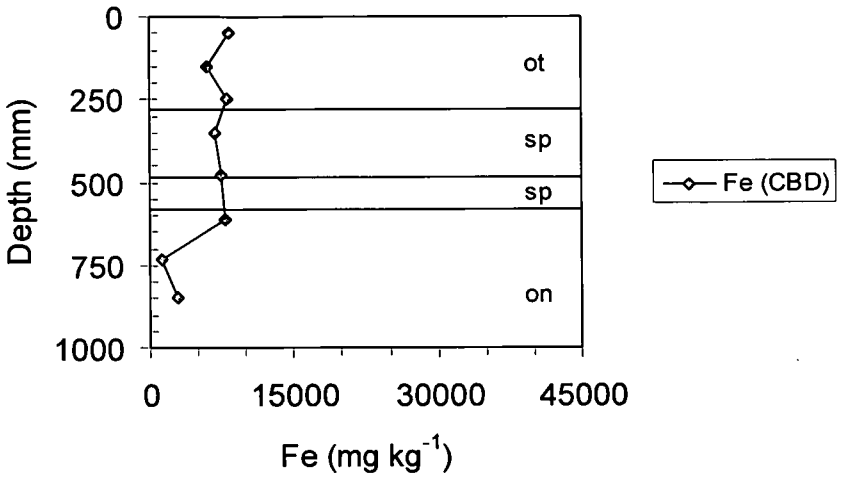


Figure 5.59 CBD extractable Fe for P207 (Westleigh 1000).

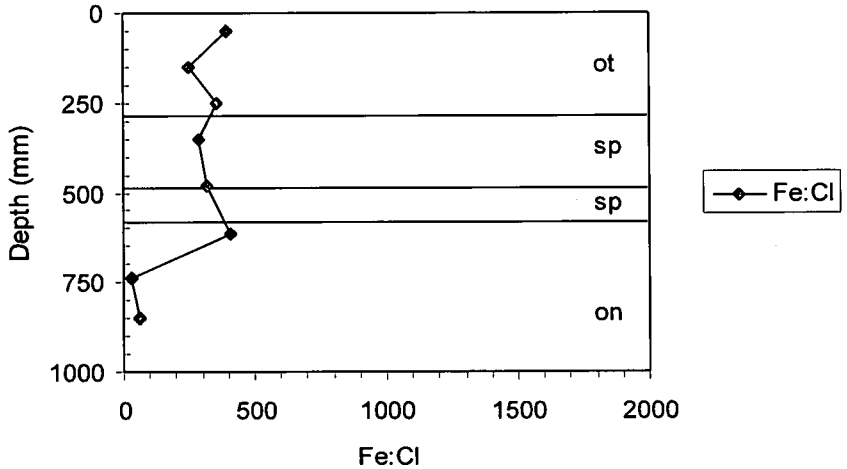


Figure 5.60 The CBD extractable Fe to clay ratio for P207 (Westleigh 1000).

Total Mn content decreases from 103.0 mg $kg^{-1}$ in the topsoil to a minimum of 50.0 mg $kg^{-1}$ in the B1, and then increases to 183.5 mg $kg^{-1}$ in the B2 and 229.0 mg $kg^{-1}$ in the C horizon (Figure 5.61). This distribution indicates reduction and removal of Mn from the B1 and accumulation in the B2 and C horizons (Figure 5.62).

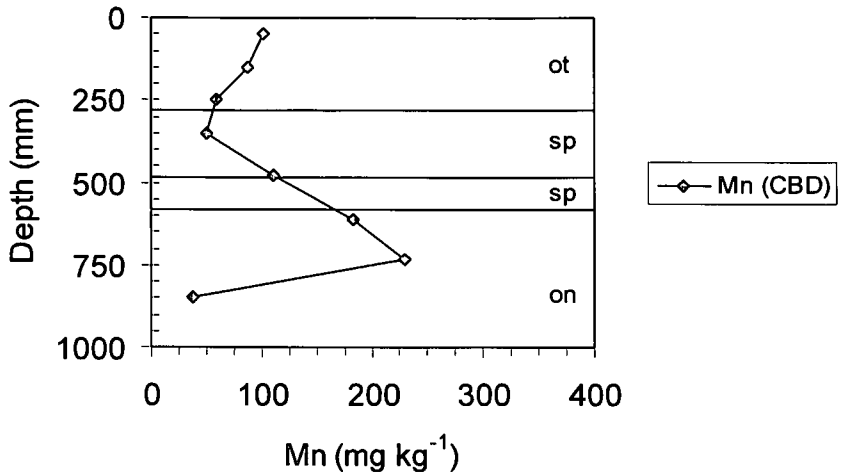


Figure 5.61 CBD extractable Mn for P207 (Westleigh 1000).

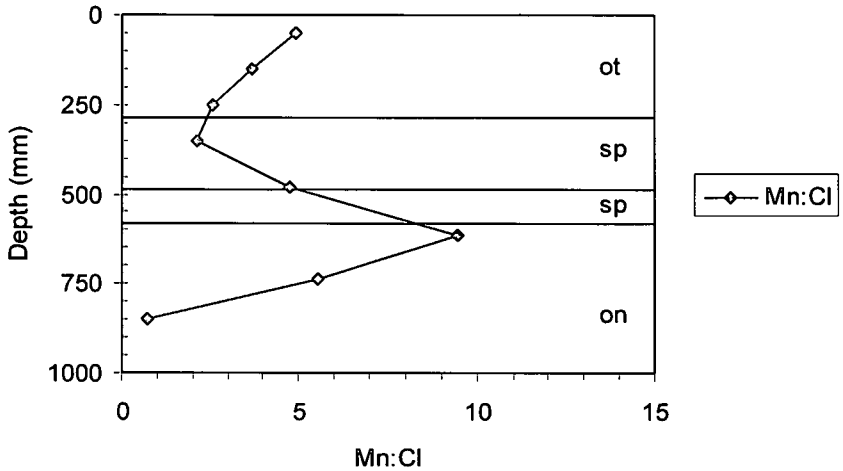


Figure 5.62 The CBD extractable Mn to clay ratio for P207 (Westleigh 1000).

### 5.8.3 Physical properties

Clay content is fairly stable from the A to the B1, but then drops sharply to the B2 (Figure 5.63). The clay content then sharply increases in the C horizon. The low clay content in the B2 might indicate that it should somewhat be classified as an E horizon.

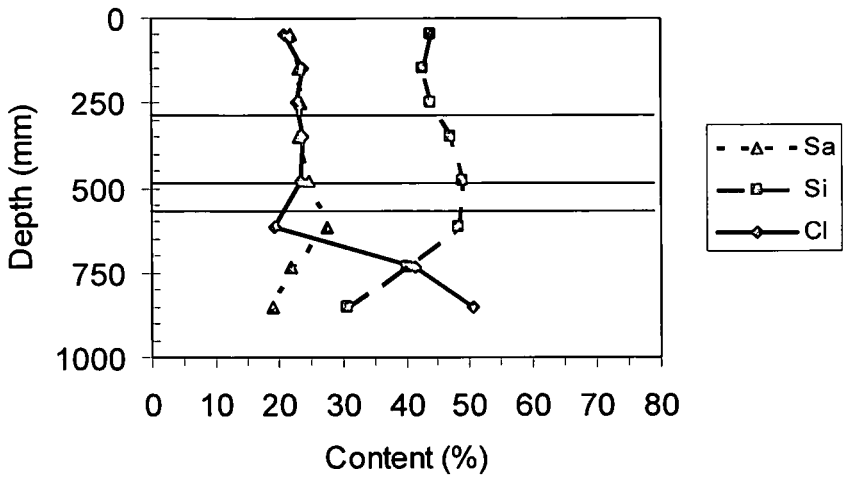


Figure 5.63 Texture of the fine earth in P207 (Westleigh 1000).

The bulk density is 1.58 Mg $m^{-3}$ at 150 mm and increases to 1.68 Mg $m^{-3}$ at 750 mm (Table 5.14). The increase in bulk density in the subsoil is typical of these soils.

Table 5.14 Bulk density and porosity for P207 (Westleigh 1000)

| Depth (mm) | Bulk density (Mg $m^{-3}$) | Porosity (%) |
|---|---|---|
| 150 | 1.58 | 40.4 |
| 450 | 1.63 | 38.5 |
| 750 | 1.68 | 36.6 |

### 5.8.4 Genesis

This profile occurs on the flood plain 12 m from the stream. It is therefore subject to seasonal flooding and is expected to have a variable parent material. Because the measuring site was selected primarily for hydrological purposes, it is located in a transitional position from a pedological point of view. The medium sand : coarse sand ratio varies between 1.0 and 0.4, indicating a variable parent material. Organic carbon content is fairly high in the topsoil (1.6 %) and decreases constantly throughout the profile.

The initial requirement for the classification of an E horizon is a Munsell colour value which is one unit higher than the overlying horizon. The second horizon in this profile has the same colour value as the overlying horizon for the dry colour and has a colour value one unit higher than the overlying horizon in the wet state. It therefore fits the definition only in the wet state. The further fits

the E horizon definition in terms of dry colour, mottles, consistency and structure. There is no clear evidence for the removal of Fe oxides, clay or organic material from the second horizon. The horizon therefore does not comply with the definition for the removal of colloidal material. Instead the third horizon, classified as soft plinthic B has the lowest clay and organic carbon content. Although typical of a transition from an E to a soft plinthic B horizon, the second horizon satisfies all requirements for a soft plinthic B horizon (*viz.* more than 10 % mottles, grey colours under it, loose consistency and position in the profile). The profile was therefore classified as Westleigh and not Longlands.

The profile has a fairly stable clay content in the A, B1 and B2 horizons, but increases sharply to the C horizon. $pH_{Water}$ increases with depth, while $pH_{KCl}$ decreases slightly. Fe seems to be concentrated in the A, B1 and B2 horizons, while Mn seems to be removed from the B1 and concentrated in the C horizon. The accumulation of Fe in the B1 and B2 horizons supports the classification of soft plinthic B horizons. The grey colour in the A and B1 horizons indicates removal of Fe and Mn. In the case of Fe, this is not supported by the analyses. Mn does, however, show marked depletion from the B1 horizon.

## 5.9 P208 (Kroonstad 1000)

The profile is situated in a lower footslope position, with a slope of 1 % (Figure 3.3). The orthic A horizon has a silty loam texture, while the rest of the profile has a loam texture. The clay content increases down the profile (13 – 17 – 25 – 25 %). The profile description and analytical data for this profile is given in Appendix A, Tables 15 and 16. The profile can be classified as Albic Planosol (epidistric) (FAO, 1998b) or Aeric Albaqualts (Soil Survey Staff, 1999).

### 5.9.1 Morphology

A brownish grey (10YR6/1) orthic A horizon (0–350 mm) overlies a greyish yellow brown (10YR6/2) E (350–530 mm) on a light grey (10YR7/1) G1 (530–800 mm) on a greyish yellow brown (10YR6/2) G2 horizon (800–1 400 mm).

Common distinct yellowish brown and bright yellowish brown Fe oxide mottles are present in the A, G1 and G2 horizons (Table 5.15). The occurrence of mottles increases to many in the E horizon, but are of the same colour and contrast. The occurrence of mottles in this profile is indicative of long $AD_{s>0.7}$, but also removal of Fe from the E horizon. No concretions were observed. There are common distinct Fe oxide mottles and many bleached pores in the A horizon. The E horizon has many bleached pores. The G1 horizon has many bleached pores, while the G2 has common normal pores.

Table 5.15 Description of mottles in P208 (Kroonstad 1000)

| Horizon | Depth (mm) | Occurrence | Size | Contrast | Colour dry | Colour wet | Cause |
|---|---|---|---|---|---|---|---|
| ot | 350 | Common | Fine | Distinct | 10YR5/8 | 10YR4/6 | Oxidized iron |
| gs | 530 | Many | Med | Distinct | 10YR5/8 | 10YR4/6 | Oxidized iron |
| gh | 800 | Common | Med | Distinct | 10YR6/6 | 10YR4/6 | Oxidized iron |
| gh | 1700 | Many | Med | Distinct | 10YR5/8 | 10YR5/6 | Oxidized iron |
| | | Common | Med | Distinct | 10YR4/3 | 10YR4/2 | Humus |

### 5.9.2 Chemical properties

$CEC_{soil}$ decreases from 10.1 $cmol_c\ kg^{-1}$ in the topsoil to 4.9 $cmol_c\ kg^{-1}$ in the E and then increases to 11.3 $cmol_c\ kg^{-1}$ in the G horizon (Figure 5.64). As was the case with P207 (Westleigh), the decrease in $CEC_{soil}$ is associated with a decrease in organic carbon, while the increase is associated with an increase in the clay content.

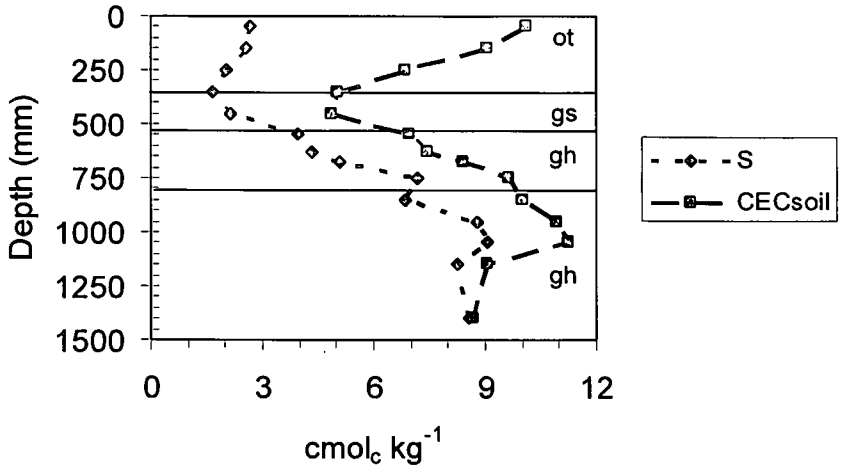


Figure 5.64 $CEC_{soil}$ and S values for P208 (Kroonstad 1000).

$CEC_{clay}$ is moderately high (53.5 $cmol_c\ kg^{-1}$) in the topsoil, decreases to 25.8 $cmol_c\ kg^{-1}$ in the E and then gradually increases to an mean of 37.3 $cmol_c\ kg^{-1}$ in the G horizon (Figure 5.65). The $CEC_{clay}$ is indicative of kaolinite, fine mica and chlorite clay minerals (Brady & Weil, 1996). The lower $CEC_{clay}$ in the E horizon is similar to that observed in the E horizon of profile 206.

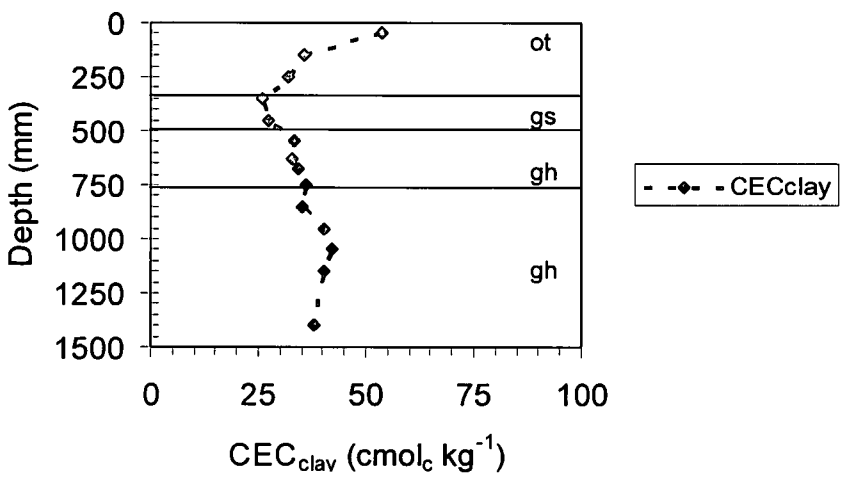


Figure 5.65 $CEC_{clay}$ for P208 (Kroonstad 1000).

$pH_{Water}$ and $pH_{KCl}$ increases with depth throughout the profile (Figure 5.66). $pH_{Water}$ increases from 5.17 in the A horizon to 7.13 in the lower G horizon, while $pH_{KCl}$ increases from 4.05 to 5.43. The increasing pH, as well as the difference between $pH_{Water}$ and $pH_{KCl}$ is similar to that observed in profiles 204, 205 and 207.

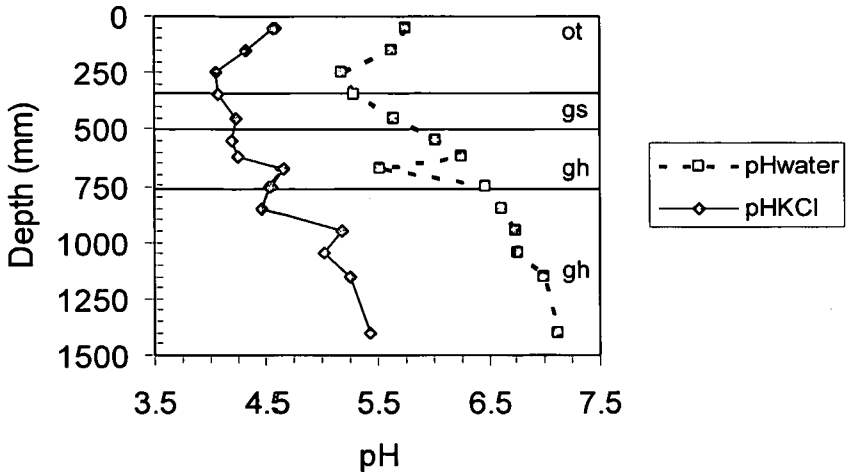


Figure 5.66 $pH_{Water}$ and $pH_{KCl}$ for P208 (Kroonstad 1000).

Base saturation increases from 27 % in the topsoil to 98 % in the G horizon (Figure 5.67). The increase is associated with sum of bases that follows the same pattern as the $CEC_{soil}$ and is probably due to basic cation accumulation as a result of lateral water movement.

Organic carbon quickly decreases from 1.1 % in the topsoil to 0.2 % in the upper G horizon and then gradually decreases to 0.02 % at 1 500 mm (Figure 5.67).

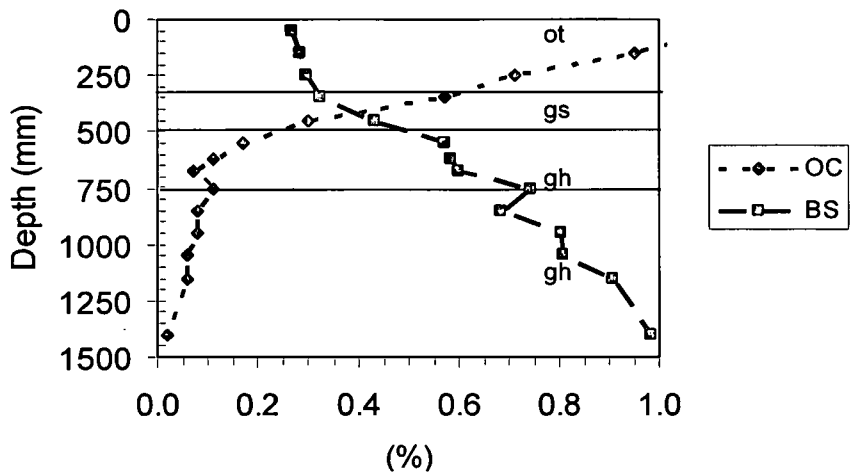


Figure 5.67 Distribution of organic carbon (OC, as a percentage) and base saturation (BS, as a fraction) in P208 (Kroonstad 1000).

Total Fe content decreases from 2 955 mg $kg^{-1}$ in the topsoil to 1 820 mg $kg^{-1}$ in the E, and then increases to 7 555 mg $kg^{-1}$ in the G1 and 7 840 mg $kg^{-1}$ in the G2 (Figure 5.68). It has a minimum of 1 335 mg $kg^{-1}$ in the upper part of

the G2. The low Fe content in the E horizon indicates reduction and leaching of Fe from this horizon, while the relatively higher Fe content in the G horizon might be due to Fe accumulation in this horizon (Figure 5.69). The lower Fe content in the upper G horizon indicates selective removal of Fe here, as evidenced by the silans. The G horizon of profile 205 has a similar reduction in Fe content within the G horizon.

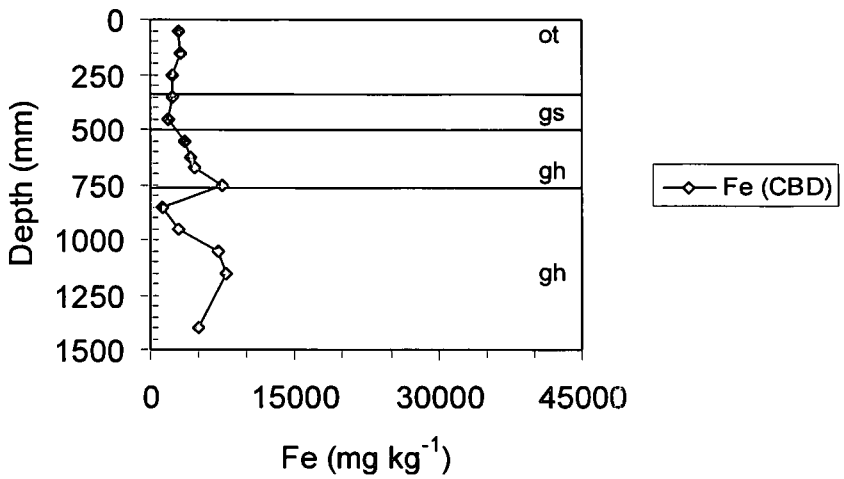


Figure 5.68 CBD extractable Fe for P208 (Kroonstad 1000).

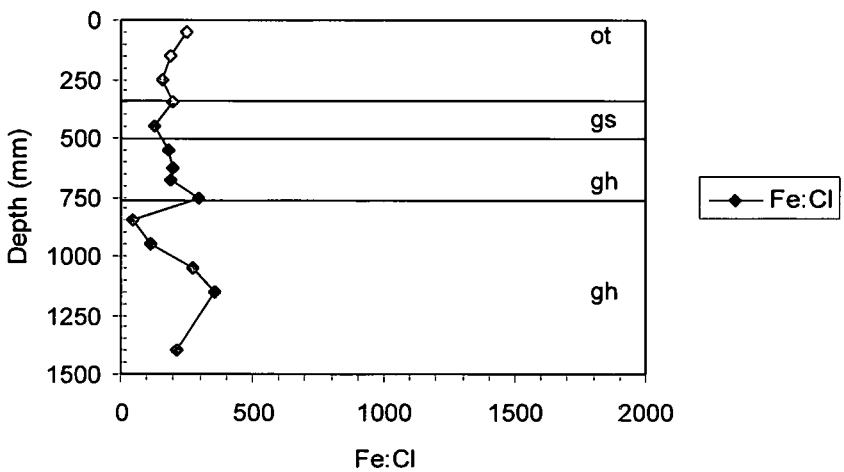


Figure 5.69 The CBD extractable Fe to clay ratio for P208 (Kroonstad 1000).

Total Mn increases from 1.5 mg $kg^{-1}$ in the topsoil to 8.0 mg $kg^{-1}$ in the E, 109.0 mg $kg^{-1}$ in the G1 and 359.5 mg $kg^{-1}$ in the G2 (Figure 5.70). The slight increase in Mn content in the E horizon contradicts the theory of reduction and removal of Fe from this horizon (Figure 5.71). Mn shows peaks at 800 – 900 mm, at 1 000 mm – 1 100 mm, and a low point 900 – 1 000 mm. This is

similar to that observed for the Fe contents, but occurring 100 mm lower in the profile.

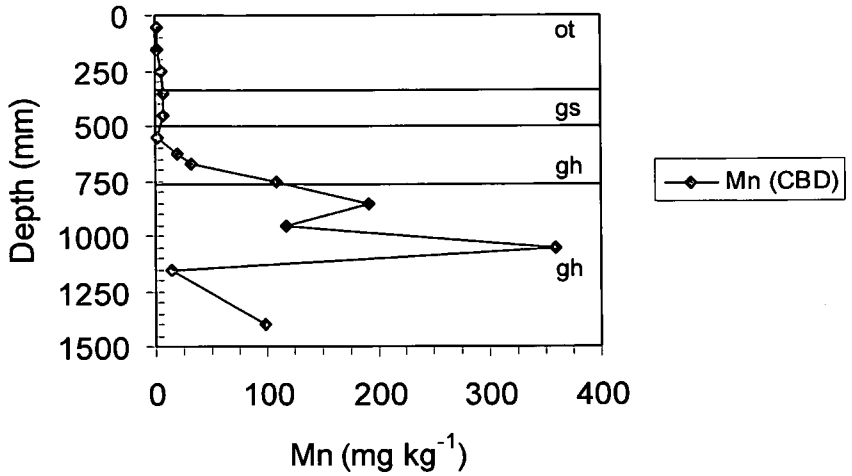


Figure 5.70 CBD extractable Mn for P208 (Kroonstad 1000).

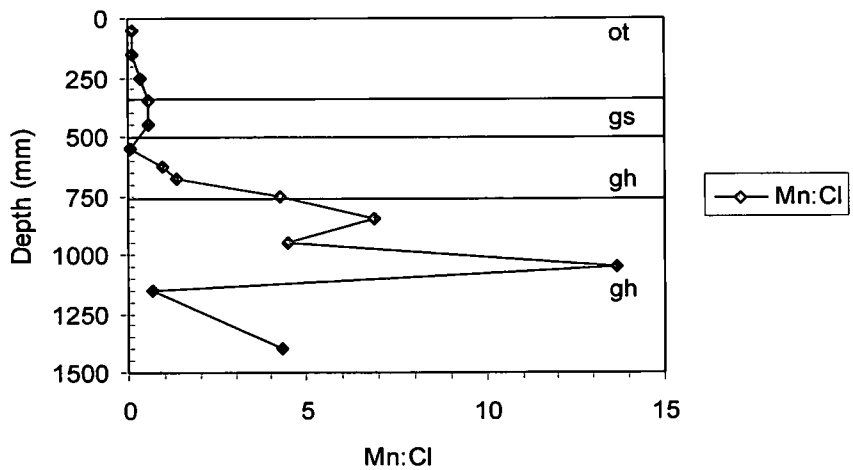


Figure 5.71 The CBD extractable Mn to clay ratio for P208 (Kroonstad 1000).

### 5.9.3 Physical properties

Clay content increases throughout the profile, but decreases slightly at 350 mm, supporting the classification of an E horizon (Figure 5.72). The increase in clay content from the E to the G horizon also supports the classification of the latter. The silt content in this profile is somewhat different from that in the other profiles, indicating a possible difference in parent material, and possibly due to the dolerite dyke upslope from the profile (Figure 3.4).

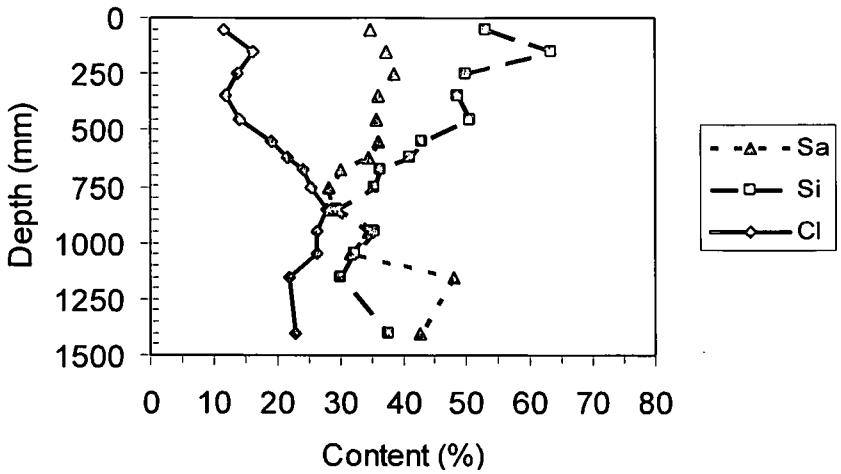


Figure 5.72 Texture of the fine earth in P208 (Kroonstad 1000).

Bulk density increases from 1.44 Mg $m^{-3}$ at 150 mm to 1.76 Mg $m^{-3}$ at 750 mm (Table 5.16). The bulk density in the topsoil is lower than in most other profiles. This is probably due to the relatively high organic matter content of the horizon.

Table 5.16 Bulk density and porosity for P208 (Kroonstad 1000)

| Depth (mm) | Bulk density (Mg $m^{-3}$) | Porosity (%) |
|---|---|---|
| 150 | 1.44 | 45.7 |
| 450 | 1.62 | 38.9 |
| 750 | 1.76 | 33.6 |
| 1050 | 1.75 | 34.0 |
| 1350 | 1.74 | 34.3 |

### 5.9.4 Genesis

This profile occurs on the western side of the catchment. As such it seems that the profile developed in a cumulative environment, which would lead to increased base and water saturation. The parent material is probably mixed Molteno sandstone and mudstone as well as some dolerite – occurring just above P209 (Katspruit). The medium sand : coarse sand ratio varies between 0.7 and 1.8, supporting a parent material of mixed origin. The organic carbon content decreases from 1.2 % in the topsoil to 0.02 % at 1 400 mm. It indicates that this profile is wetter, leading to the increased accumulation of organic matter.

Clay content steadily increases throughout the profile, except in the E and lower G horizons where it decreases. $CEC_{clay}$ decreases from the A to the E horizon, and then increases to the middle of the G2 horizon. Base saturation increases steadily from 40 % in the A to almost 100 % in the lower G2 horizon. $pH_{Water}$ and $pH_{KCl}$ increases down the profile. Fe decreases in the E and then increases into the G, while Mn is low in the topsoil and in the top of the G horizon. The E horizon has undergone clear degradation of clay and removal of clay and Fe, supporting its classification. The lowest Mn content seems to be just below the E horizon. Removal of Fe from the E horizon has also resulted in ferrolysis, causing clay degradation and a decrease in the $CEC_{clay}$. The classification of the G horizon is supported by the accumulation of clay and basic cations. The profile has a pale colour throughout, pointing to prolonged periods of water saturation (section 7.9).

## 5.10 P209 (Katspruit 1000)

The profile is situated in an upper midslope position, with a slope of 8 % (Figure 3.3). The orthic A horizon has a loam texture, while the rest of the profile has a clay loam texture. The clay content increases down the profile (16 – 36 – 36 %). The profile description and analytical data for this profile is given in Appendix A, Tables 17 and 18. The profile can be classified as Stagnic Orthi-eutric Gleysol (FAO, 1998b) or Aeric Endoaquults (Soil Survey Staff, 1999).

### 5.10.1 Morphology

A greyish yellow brown (10YR5/2) orthic A horizon (0–450 mm) overlies a brownish grey (10YR6/1) G horizon (450–1 100 mm) on brownish grey (10YR6/1) saprolite (1 100–1 400 mm).

Many distinct and prominent Fe oxide mottles are present throughout the profile (Table 5.17). Their colour differs from brown in the A to bright yellowish brown in the G and bright brown in the saprolite. No concretions were

observed in the profile. The A horizon has many bleached and rusty pores, while the G horizon has bleached and rusty pores.

Table 5.17 Description of mottles in P209 (Katspruit 1000)

| Horizon | Depth (mm) | Occurrence | Size | Contrast | Colour dry | Colour wet | Cause |
|---|---|---|---|---|---|---|---|
| ot | 450 | Many | Fine | Distinct | 7.5YR4/6 | 7.5YR3/4 | Oxidized iron |
| gh | 1100 | Many | Fine | Prominent | 10YR6/8 | 7.5YR5/8 | Oxidized iron |
| so | 1400 | Many | Fine | Distinct | 7.5YR5/8 | 7.5YR4/6 | Oxidized iron |

### 5.10.2 Chemical properties

$CEC_{soil}$ decreases gradually from 9.4 $cmol_c\ kg^{-1}$ in the topsoil to 5.7 $cmol_c\ kg^{-1}$ in the upper G horizon (Figure 5.73). It then increases to 13.1 $cmol_c\ kg^{-1}$ in the lower G horizon. The decrease in $CEC_{soil}$ is linked with a decrease in organic carbon, while the increase is probably due to a clay increase.

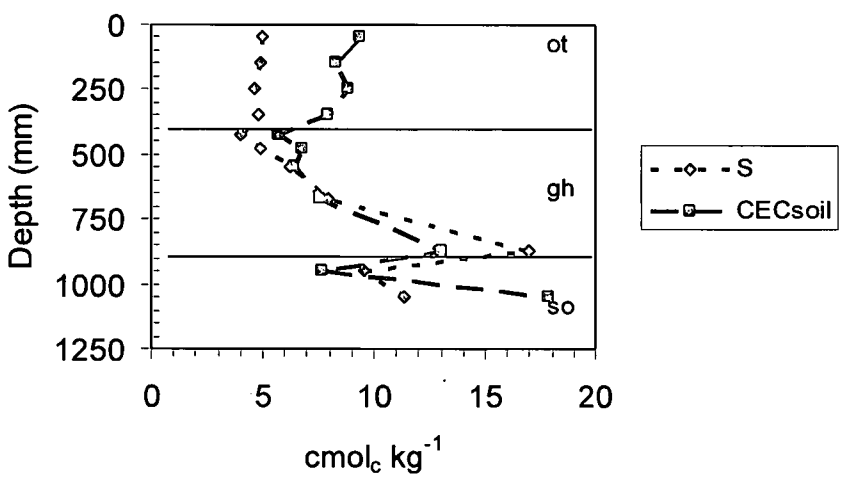


Figure 5.73 $CEC_{soil}$ and S values for P209 (Katspruit 1000).

$CEC_{clay}$ increases in the A horizon from 27.2 $cmol_c\ kg^{-1}$ at 50 mm to 40.7 $cmol_c\ kg^{-1}$ at 350 mm (Figure 5.74). It then decreases to a mean of 24.9 $cmol_c\ kg^{-1}$ in the G horizon.

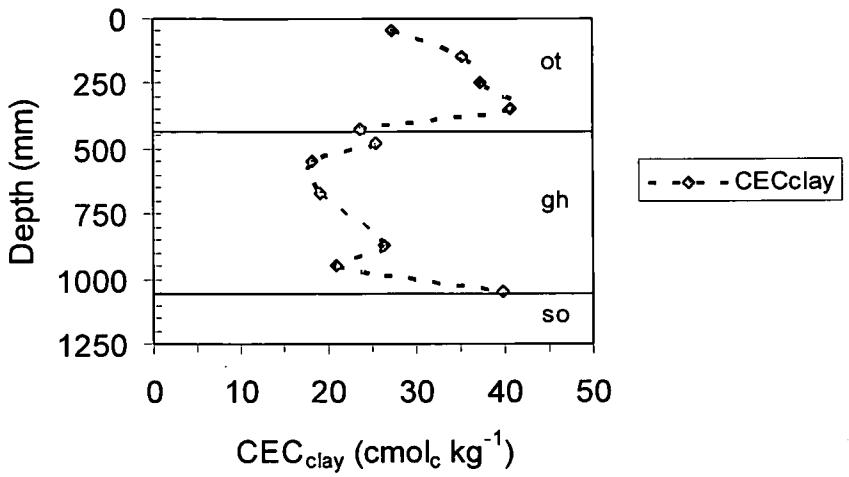


Figure 5.74 $CEC_{clay}$ for P209 (Katspruit 1000).

$pH_{Water}$ and $pH_{KCl}$ increase with depth (Figure 5.75). $pH_{Water}$ increases from 5.60 in the topsoil to 6.64 in the subsoil, while $pH_{KCl}$ increases from 4.71 to 5.35. The distribution is similar, although with slightly larger values than that observed in profiles 204, 205, 207 and 208.

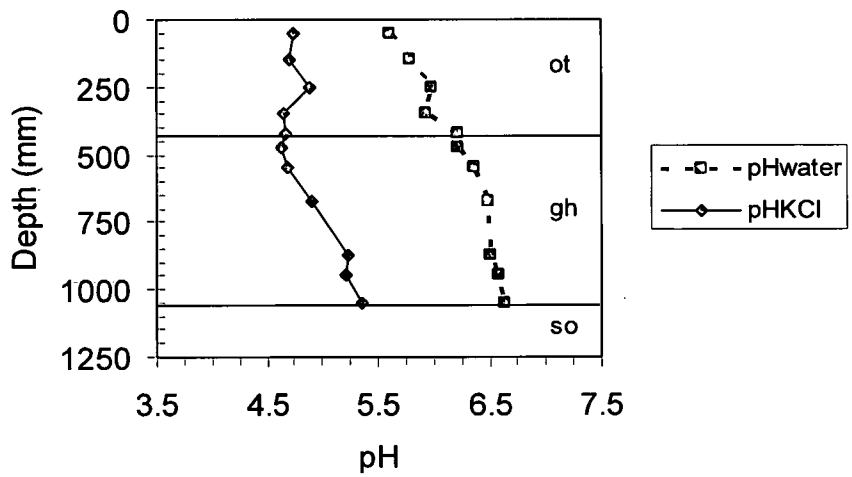


Figure 5.75 $pH_{Water}$ and $pH_{KCl}$ for P209 (Katspruit 1000).

Base saturation increases from 57 % in the topsoil to over 100 % in the G horizon (Figure 5.76). This is associated with a similar increase in sum of bases that more or less follows the $CEC_{soil}$ distribution.

Organic carbon decreases sharply from 1.4 % in the topsoil to 0.6 in the lower A horizon (Figure 5.76). It then decreases more gradually to 0.1 % in the lower G horizon.

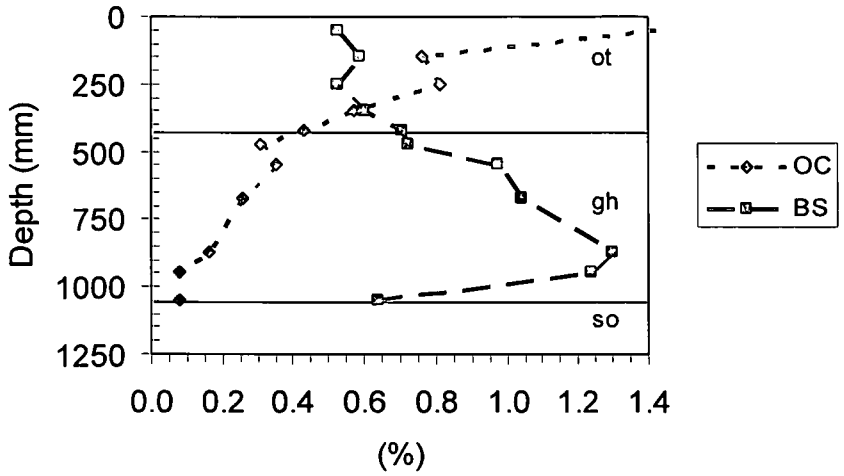


Figure 5.76 Distribution of organic carbon (OC, as a percentage) and base saturation (BS, as a fraction) in P209 (Katspruit 1000).

Total Fe content increases from 5 255 mg $kg^{-1}$ at the surface to 7 180 mg $kg^{-1}$ in the lower A horizon, and then decreases to 390 mg $kg^{-1}$ in the lower G horizon (Figure 5.77). The peak at 500 mm is most probably due to accumulation of Fe in the upper part of the G horizon. The accumulation of Fe is also evidenced by the occurrence of many fine prominent Fe oxide mottles in the G horizon (Table 5.17). The distribution of Fe in the profile points to some Fe accumulation in the lower part of the A horizon, a large accumulation in the upper G horizon and almost a depletion of Fe in the lower G horizon. This is supported by the Fe : Cl ratio (Figure 5.78).

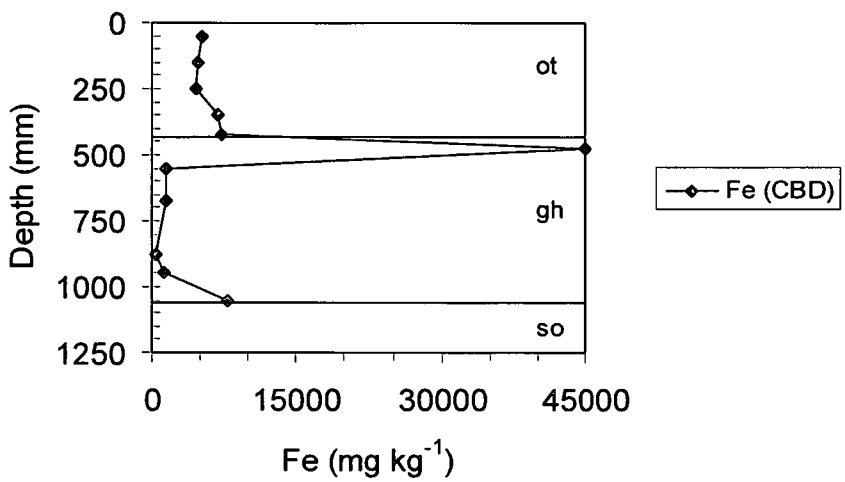


Figure 5.77 CBD extractable Fe for P209 (Katspruit 1000).

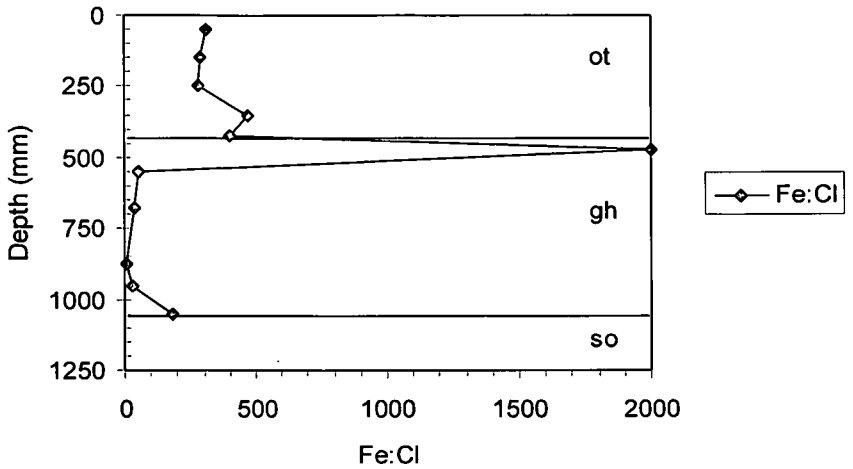


Figure 5.78 The CBD extractable Fe to clay ratio for P209 (Katspruit 1000).

Total Mn contents decrease from 82.0 mg $kg^{-1}$ at the soil surface to a low of 8.0 in the lower A horizon, it has a peak of 26.0 mg $kg^{-1}$ on the boundary with the G horizon and two peaks of 47.5 mg $kg^{-1}$ and 95.5 mg $kg^{-1}$ in the G horizon (Figure 5.79). The decrease in Mn in the lower A horizon might be the first indication of E horizon development. It is contrary to the higher Fe content in the lower A horizon, but probably due to the difference in redox potential between Fe and Mn. The peaks and dips of Mn in the G horizon are most probably due to the presence of silans (Figure 5.80). It can also be explained by heterogeneous redox conditions that resulted in the segregation on Mn into mottles.

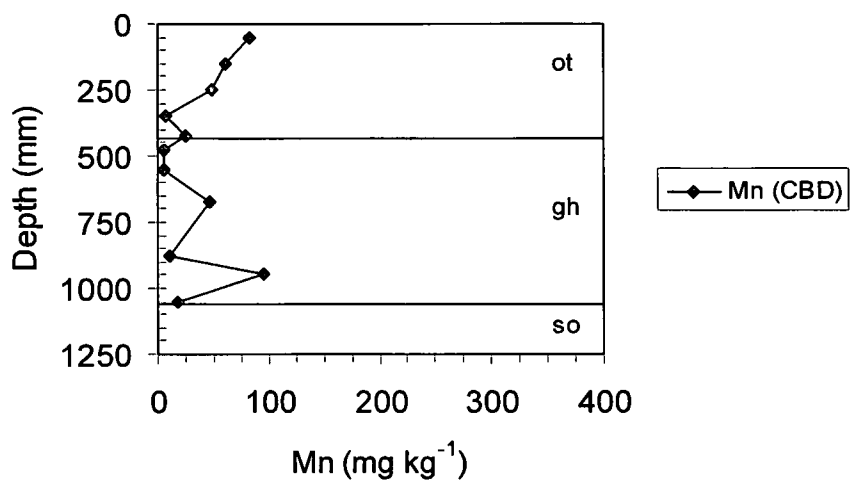


Figure 5.79 CBD extractable Mn for P209 (Katspruit 1000).

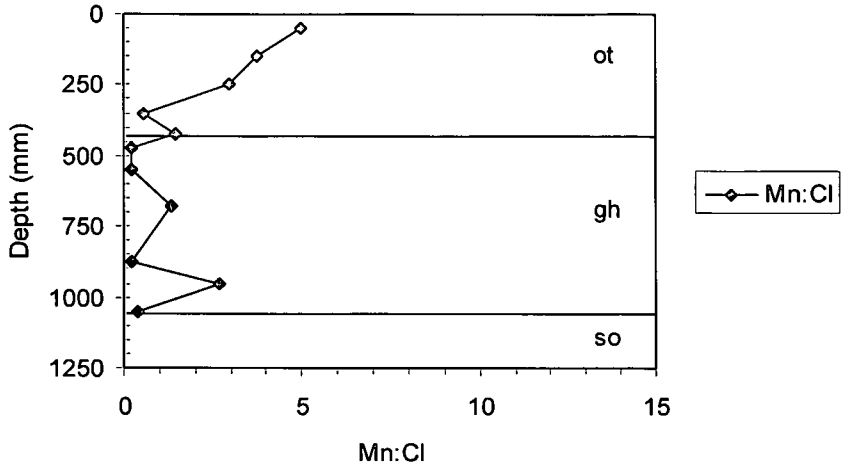


Figure 5.80 The CBD extractable Mn to clay ratio for P209 (Katspruit 1000).

### 5.10.3 Physical properties

The clay content steadily increases from 16 % in the A to 48 % at 900 mm in the G horizon (Figure 5.81). There is a slight decrease (1 %) in clay content at 300 – 400 mm, possibly indicating the presence of an E horizon. The high silt content, similar to that of P208 (Kroonstad), also possibly indicates a different parent material. It should be remembered that P208 (Kroonstad) and P209 (Katspruit) are located just below a dolerite dyke (Figure 3.4).

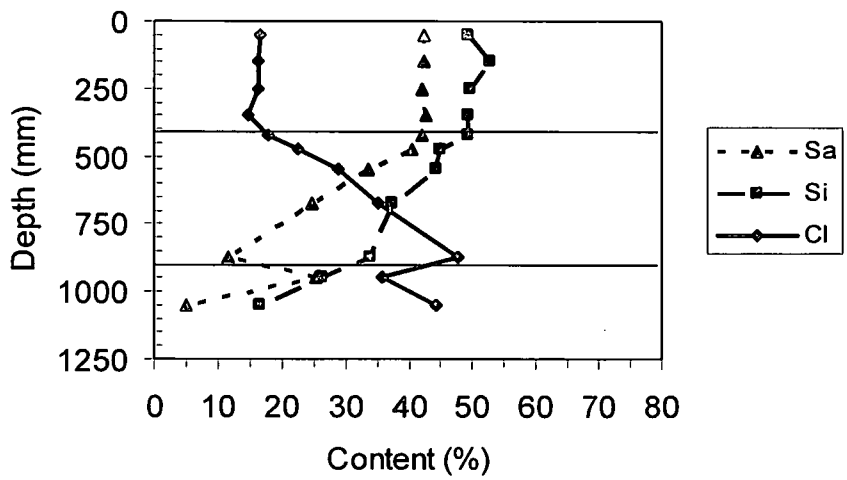


Figure 5.81 Texture of the fine earth in P209 (Katspruit 1000).

Bulk density increases steadily from 1.45 Mg $m^{-3}$ at 300 mm to 1.73 Mg $m^{-3}$ at 1 350 mm (Table 5.18). This results in the porosity decreasing accordingly and will lead to a reduction in the saturated hydraulic conductivity. Saturation can therefore be expected to occur at lower water contents in the subsoil than in the topsoil.

Table 5.18 Bulk density and porosity for P209 (Katspruit 1000)

| Depth (mm) | Bulk density ($Mg\ m^{-3}$) | Porosity (%) |
|---|---|---|
| 150 | 1.45 | 45.3 |
| 450 | 1.65 | 37.7 |
| 750 | 1.64 | 38.1 |
| 1050 | 1.73 | 34.7 |
| 1350 | 1.73 | 34.7 |

### 5.10.4 Genesis

The profile occurs just below a dolerite outcrop. The profile therefore developed in a cumulative environment, where water and basic cations have accumulated. It is hypothesised that the profile has developed from Molteno sandstone with some influence from the dolerite. The medium sand : coarse sand ratio varies between 0.4 and 1.0, supporting the mixed parent material hypothesis. Organic carbon contents decreases from 1.4 % in the topsoil to 0.1 % in the subsoil. The high organic carbon content points to a wet environment where organic carbon can accumulate.

$CEC_{soil}$ also increases, base saturation, $pH_{Water}$ and $pH_{KCl}$ increases down the profile. The high base saturation might also be due to the contribution of basic cations from the dolerite dyke. The Fe and Mn content are variable, but both decrease down the profile. The profile is somewhat similar to the previous one, P208 (Kroonstad), except for the G horizon that is more yellow in this case. It is therefore expected that genesis of these two profiles should be similar. The classification of the G horizon is supported by the high $CEC_{clay}$ and base saturation, indicative of accumulation of basic cations in the horizon. Periodic saturation with water has led to the redistribution of Fe and Mn, but not sufficiently to lead to the formation of a soft plinthic B horizon.

## 5.11 P210 (Bloemdal 1100)

The profile is situated in an upper midslope position, with a slope of 5 % (Figure 3.3). It has Molteno sandstone as parent material, and is situated above the dolerite dyke. It The A1 horizon has a clay loam texture, the A2, B1

and B2 horizons have a loam texture and the C1 horizon a coarse sandy loam texture. The clay content is fairly stable throughout the profile (19 – 17 – 24 – 18 – 17 – 20 %), but increases sharply at 780 mm. The profile description and analytical data for this profile are given in Appendix A, Tables 19 and 20. The profile can be classified as Hyper-distric Regosol (FAO, 1998b) or Oxyaquic Hapludalfs Soil Survey Staff, 1999).

### 5.11.1 Morphology

A greyish yellow brown (10YR4/2) orthic A1 horizon (0–260 mm) overlies a dull yellowish brown (10YR4/3) A2 (260–530 mm) on a brown (7.5YR4/6) red apedal B1 (530–800 mm) on an orange (7.5YR6/6) red apedal B2 (810–1 200 mm) on dull orange (7.5YR6/4) unspecified material with signs of wetness (1 200–1580 mm).

This profile is characterized by a lack of Fe oxide mottles (Table 5.19). There are no mottles in the A1 and A2, humus mottles in the B1 and B2 and no mottles in the C1 or C2. There are, however, many distinct greyish brown humus mottles in the two red apedal B horizons. No concretions were observed and pores are normally coated throughout the profile.

Table 5.19 Description of mottles in P210 (Bloemdal 1100)

| Horizon | Depth (mm) | Occurrence | Size | Contrast | Colour dry | Colour wet | Cause |
|---|---|---|---|---|---|---|---|
| ot | 260 | None | | | | | |
| ot | 530 | None | | | | | |
| re | 810 | Many | Med | Distinct | 7.5YR4/2 | 7.5YR3/2 | Humus |
| re | 1200 | Many | Fine | Distinct | 7.5YR4/2 | 7.5YR3/2 | Humus |
| on | 1580 | None | | | | | |

### 5.11.2 Chemical properties

$CEC_{soil}$ decreases from 6.6 $cmol_c\ kg^{-1}$ in the topsoil to 4.5 $cmol_c\ kg^{-1}$ in the lower part of the red apedal B horizon (Figure 5.82). It then decreases rapidly to 2.8 $cmol_c\ kg^{-1}$ at 1 500 mm in the lower unspecified material with signs of wetness. The decrease in $CEC_{soil}$ must be linked with a decrease in organic carbon content, because there is no decrease in clay content.

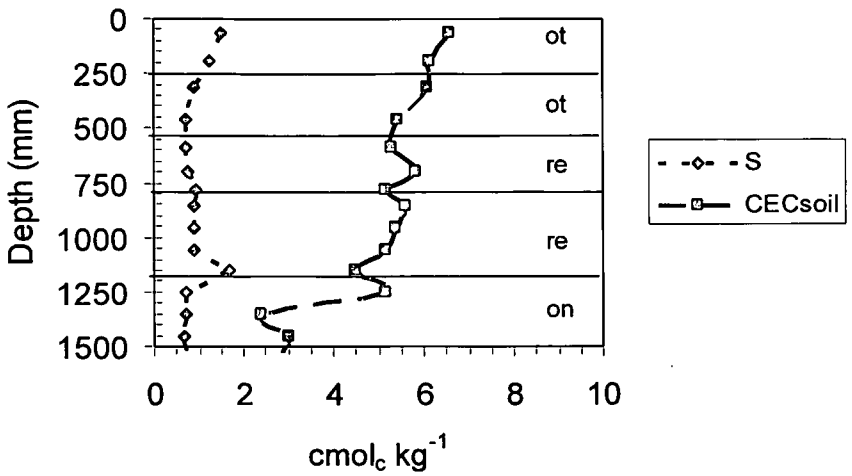


Figure 5.82 $CEC_{soil}$ and S values for P210 (Bloemdal 1100).

$CEC_{clay}$ is highly variable in profile 210. It ranges from 11.1 $cmol_c\ kg^{-1}$ to 38.6 $cmol_c\ kg^{-1}$ (Figure 5.83). The variable $CEC_{clay}$ is probably an artefact of the procedure used – the organic carbon and clay content is also variable. The $CEC_{clay}$ is, however, low and indicates the presence of kaolinite, fine mica and chlorite clays (Brady & Weil, 1996).

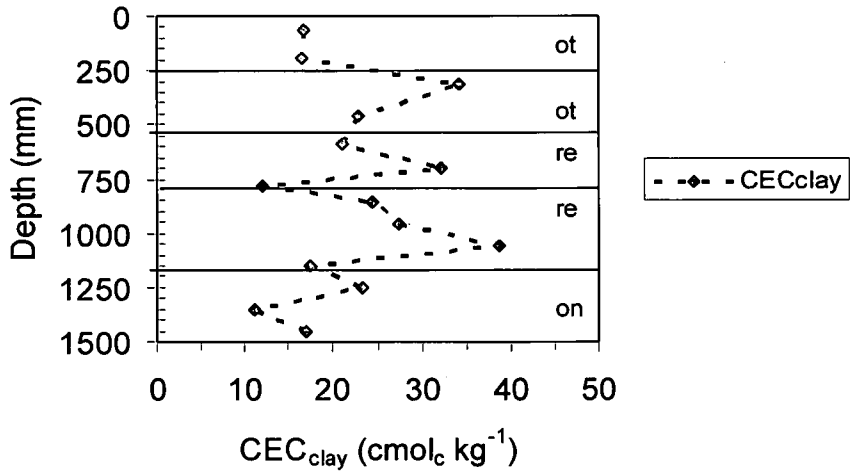


Figure 5.83 $CEC_{clay}$ for P210 (Bloemdal 1100).

The $pH_{Water}$ is somewhat constant throughout the profile, ranging from 5.09 to 5.60 (Figure 5.84). The $pH_{KCl}$ decreases sharply from 5.10 in the topsoil to 3.85 at the top of the red apedal B horizon (590 mm). It then stays constant with increasing depth. Although the distribution pattern differs the magnitude is remarkably similar to that in profiles 204 to 209, excluding 206.

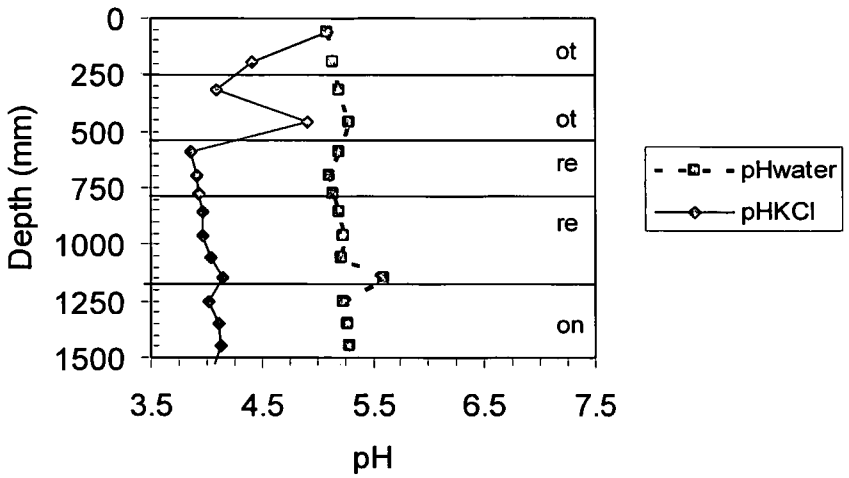


Figure 5.84 $pH_{Water}$ and $pH_{KCl}$ for P210 (Bloemdal 1100).

Base saturation is somewhat constant at 15 to 25 % throughout the profile and is associated with a narrow range in basic cation content of 1.0 to 1.5 $cmol_c\ kg^{-1}$ throughout the profile, and a decreasing $CEC_{soil}$ (Figure 5.85).

Organic carbon decreases sharply from 1.0 % in the topsoil to 0.4 % in the lower A horizon (Figure 5.85). It then decreases gradually to 0.1 % in the lower red apedal B horizon.

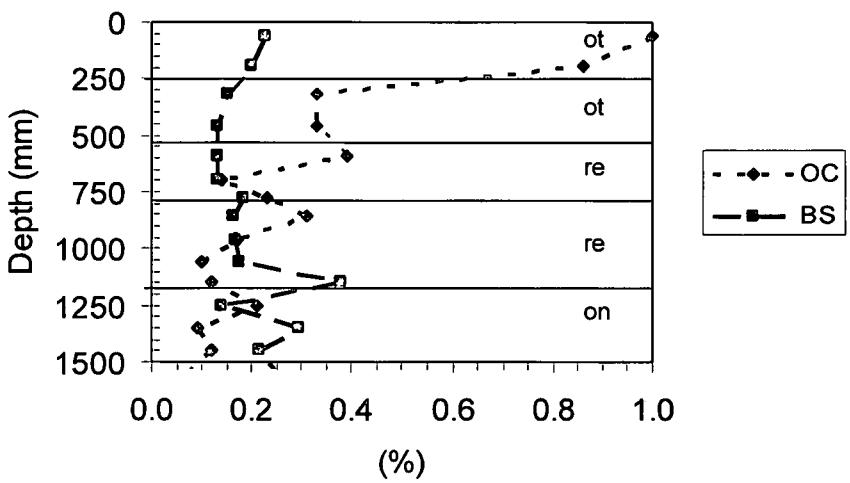


Figure 5.85 Distribution of organic carbon (OC, as a percentage) and base saturation (BS, as a fraction) in P210 (Bloemdal 1100).

Total Fe contents in this profile do not show clear horizonation, ranging between 3 860 mg $kg^{-1}$ and 13 950 mg $kg^{-1}$ (Figure 5.86). The peak occurs in the lower part of the B2 horizon, while the lowest point occurs at a depth of 200 – 300 mm in the A1 horizon. The the lack of Fe horizonation can be

expected from these soils, because no removal and / or accumulation of Fe are evident from the morphology. The lack of Fe horizonation might also be due to even removal or accumulation of Fe in the profile. The decreasing organic carbon content and increasing water saturation probably resulted in this profile not being exposed to sufficiently reduced conditions that could have led to the formation of a soft plinthic or E horizon. The peak at 1 010 – 1 100 mm might be the first indications of Fe localisation and accumulation (plinthite formation) due to a fluctuating water table on the unspecified material with signs of wetness (Figure 5.87).

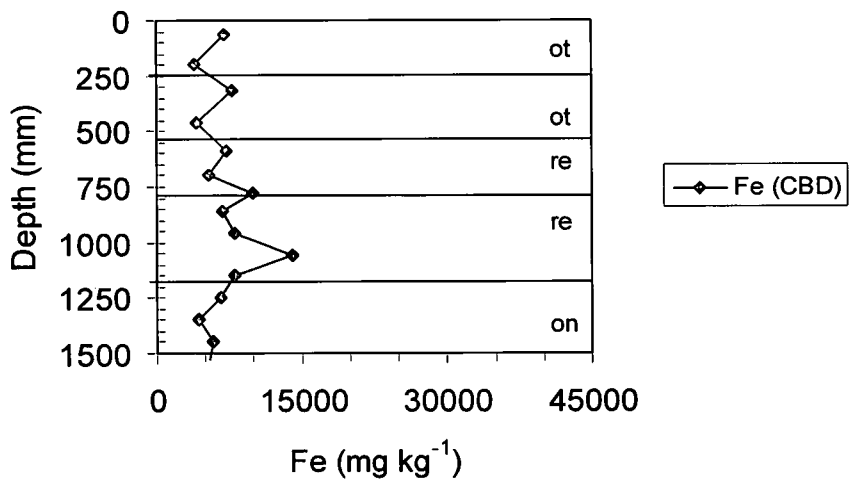


Figure 5.86 CBD extractable Fe for P210 (Bloemdal 1100).

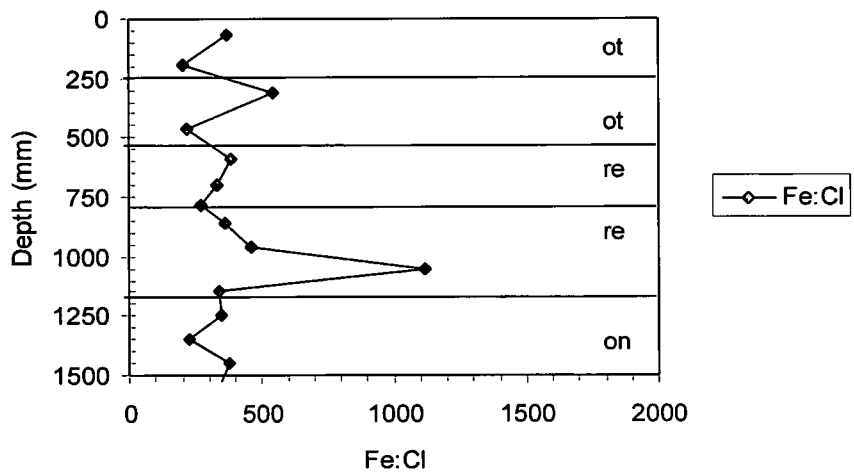


Figure 5.87 The CBD extractable Fe to clay ratio for P210 (Bloemdal 1100).

Total Mn contents increase from 11.5 mg $kg^{-1}$ in the topsoil to 118.0 mg $kg^{-1}$ in the lower part of the B2 horizon, and then decrease to 72.5 mg $kg^{-1}$ in the C horizon (Figure 5.88). The increased Mn contents in the B1 and B2 horizons

might be due to reduction and leaching at soil surface followed by oxidation lower down in the profile, as well as the initial stages of plinthitisation (Figure 5.89).

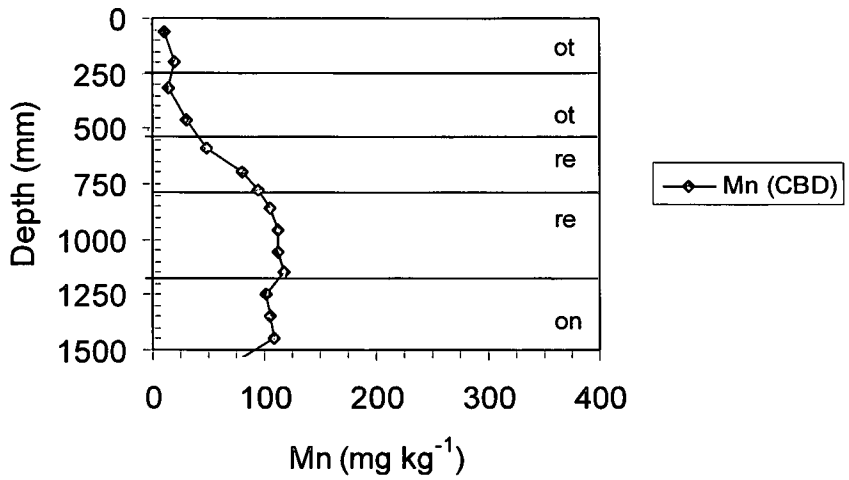


Figure 5.88 CBD extractable Mn for P210 (Bloemdal 1100).

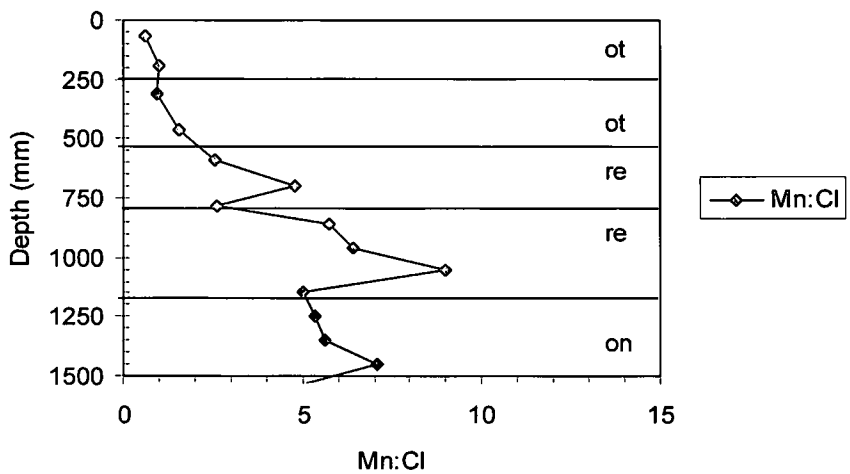


Figure 5.89 The CBD extractable Mn to clay ratio for P210 (Bloemdal 1100).

### 5.11.3 Physical properties

Clay content is somewhat uniform throughout the profile, ranging from 19 % in the A to 24 % in the B and 17 % in the C1 (Figure 5.90). The increase in clay content at 750 mm might be due to clay illuviation at this depth. The decreasing clay content in the C1 and C2 horizons are due to the slower rate of weathering at this depth. Silt and sand patterns indicate a different parent material to that in the other profiles.

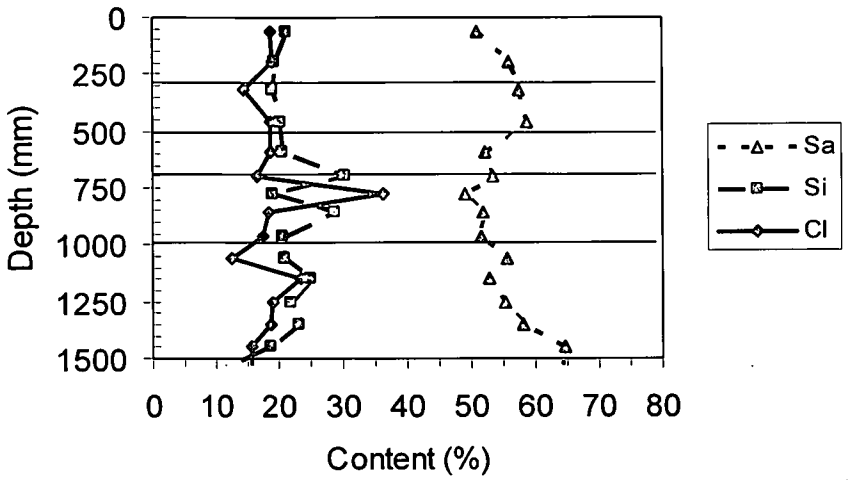

Figure 5.90 Texture of the fine earth in P210 (Bloemdal 1100).

Bulk density increases down the profile, from 1.39 Mg $m^{-3}$ in the A horizon to 1.82 Mg $m^{-3}$ at 1 350 mm (Table 5.20). This results in a corresponding decrease in the porosity and will therefore lead to a reduction of the saturated hydraulic conductivity. It is also expected that saturation will set in earlier in the lower parts of the profile, due to the diminished porosity.

Table 5.20 Bulk density and porosity for P210 (Bloemdal 1100)

| Depth (mm) | Bulk density (Mg $m^{-3}$) | Porosity (%) |
|---|---|---|
| 150 | 1.39 | 47.5 |
| 450 | 1.62 | 38.9 |
| 750 | 1.72 | 35.1 |
| 1050 | 1.70 | 35.8 |
| 1350 | 1.82 | 31.3 |

### 5.11.4 Genesis

The profile is the first in the western toposequence, and is situated above the dolerite dyke. It will therefore not be influenced by the dolerite parent material. Contribution of water through lateral drainage is also expected to be limited. It is, however, not clear if the parent material is Elliott or Molteno sandstone. Due to the altitude, it is probably mostly derived from Molteno sandstone, but Elliott sandstone could have had an influence on the soil's properties. The medium sand : coarse sand ratio varies between 0.3 and 0.9, a range similar to that observed in P209 (Katspruit), where dolerite had a marked impact. The organic carbon content decreases from 1.0 % in the topsoil to 0.1 % in the

subsoil. There is thus a marked accumulation of organic matter, probably due to the higher base saturation.

The clay content and base saturation decreases slightly down the profile while the $CEC_{soil}$ decreases. The $CEC_{clay}$ is highly variable, but decreases slightly down the profile. The total Fe content is variable, while the Mn content seems to increase with depth. The clay and Fe content indicate a profile that has undergone weathering and pedogenesis, not leading to clear horizonation. There are, however, signs of Fe accumulation just above the unspecified material with signs of wetness, although it is not evident in the morphology. This can be the first stage in the development of a soft plinthic B horizon. The profile is uniformly red in colour, although the topsoil is much darker. This is probably due to the higher organic carbon content in the topsoil. Only humus mottles were described in the profile, which suggests homogeneous redox conditions and a lack of water saturation (section 7.11). This is also evident from the lack of clay, Fe and / or Mn redistribution. The pale red colour of the profile in the dry state is probably a result of homogeneous leaching of Fe and Mn from the profile.

## 5.12 Summary

P201 (Longlands), P202 (Pinedene), P203 (Tukulu) and P204 (Longlands) are situated on the upper Elliot sandstone shelf. The profiles are therefore typically sandy. Profile morphology indicates that soil wetness increases from P201 to P204, with the exception of P203 that is slightly drier. The occurrence of Fe and Mn mottles as well as rusty root channels in the orthic A horizons increase accordingly. Soils become more clayey and base saturation tends to increase. The unspecified material with signs of wetness occurs closer to the soil's surface, possibly indicating increased erosion closer to the edge of the Elliott shelf.

P205, P206 and P208 were classified as Kroonstad soil forms, while P209 was classified as a Katspruit soil form. These profiles are similar in the sense

that they develop in cumulative environments. $CEC_{soil}$, $CEC_{clay}$, base saturation and pH are therefore higher than the other profiles.

P207 (Westleigh) is somewhat of an outlier, since it developed close to the stream and is therefore characterized by a highly variable parent material. It occupies a transitional position between the Westleigh and Longlands forms. It seems that the profile has undergone localization and accumulation of Fe to form a soft plinthic B horizon, rather than an E horizon as the second horizon in the profile.

P210 (Bloemdal) seems to freely drained and have the driest water regime in terms of its morphology. It is sandy in nature, lacks an impervious layer in the subsoil and is therefore well drained. The profile has a characteristic red colour, which is pale in the dry state. Clay content, $CEC_{clay}$ and Fe do not show clear horizonation with depth. There are, however, signs of Fe accumulation above the unspecified material with signs of wetness, possibly indicating plinthisation.

# 6 QUANTIFICATION OF SOIL COLOUR

## 6.1 Introduction

The results of digital photographs classification are presented in Appendix B, Table 1. This table presents the RGB variation within each diagnostic red, yellow and grey zone by means of descriptive statistics. These results can be summarised to calculate the occurrence of each diagnostic colour, using the amount of cells classified into each colour (Table 6.1). Erroneous colour classification (section 4.7 & 4.8) may influence the results. All colours refer to the dry state, because only photographs taken in the dry state were used in the calculations. Yellow and grey E horizons can therefore not be differentiated.

## 6.2 Incidence of diagnostic colours

The digital colour classification of most of the orthic A horizons as diagnostic grey is in line with the Munsell notations determined during the field descriptions (Table 6.2). The grey colour in A horizons may form during varying periods of wetness (section 8.2). Diagnostic grey dominates in E, G and unspecified materials with signs of wetness. The grey count can increase, decrease or remain constant down the profile. Yellow-brown colours dominate in some orthic A horizons, the yellow-brown apedal B horizons, the upper soft plinthic B of P207 (Westleigh), neocutanic B horizons and unspecified materials with signs of wetness under neocutanic B horizons, while red colours only dominate in the red apedal B horizons and the G horizon of P204 (Longlands) (Table 6.1).

Table 6.1 The occurrence of diagnostic red, yellow and grey colours (Soil Classification Working Group, 1991) as well as black determined from digital photographs taken per diagnostic horizon

| Profile | Form | Depth (mm) | Horizon | Grey | Yellow | Red | Black |
|---|---|---|---|---|---|---|---|
| | | | | | % | | |
| P201 | Lo | 430 | ot | 3.0 | 96.9 | 0.0 | 0.1 |
| | | 730 | gs | 0.0 | 98.6 | 1.3 | 0.1 |
| | | 1000 | sp | 78.5 | 19.4 | 0.5 | 1.6 |
| | | 1210 | on | 90.9 | 8.1 | 0.1 | 0.9 |
| P202 | Pn | 400 | ot | 91.0 | 3.5 | 0.0 | 5.4 |
| | | 820 | ye | 28.6 | 67.4 | 0.1 | 3.9 |
| | | 990 | on | 64.2 | 27.2 | 0.1 | 8.5 |
| | | 1500 | on | 74.7 | 17.3 | 1.0 | 7.0 |
| P203 | Tu | 380 | ot | 88.6 | 4.5 | 0.0 | 6.9 |
| | | 960 | ne | 8.2 | 83.1 | 6.0 | 2.7 |
| | | 1300 | on | 9.2 | 81.9 | 4.2 | 4.7 |
| P204 | Lo | 140 | ot | 92.4 | 6.5 | 0.0 | 1.1 |
| | | 300 | gs | 63.5 | 35.7 | 0.2 | 0.6 |
| | | 470 | sp | 9.6 | 62.6 | 27.0 | 0.8 |
| | | 1000 | on | 9.9 | 44.3 | 45.1 | 0.6 |
| P205 | Kd | 220 | ot | 10.6 | 87.0 | 0.1 | 2.3 |
| | | 460 | gs | 98.9 | 0.4 | 0.0 | 0.7 |
| | | 660 | gs | 91.7 | 8.1 | 0.1 | 0.1 |
| | | 1400 | gh | 5.1 | 52.5 | 41.8 | 0.6 |
| P206 | Kd | 550 | ot | 90.3 | 0.1 | 0.0 | 9.6 |
| | | 800 | gs | 99.2 | 0.2 | 0.0 | 0.6 |
| | | 1100 | gh | 98.0 | 1.7 | 0.0 | 0.3 |
| P207 | We | 300 | ot | 94.6 | 3.6 | 0.0 | 1.8 |
| | | 560 | sp | 27.1 | 71.8 | 0.0 | 1.1 |
| | | 670 | sp | 70.4 | 26.9 | 0.1 | 2.6 |
| | | 1300 | on | 66.0 | 31.1 | 0.1 | 2.8 |
| P208 | Kd | 350 | ot | 92.9 | 0.6 | 0.0 | 6.5 |
| | | 530 | gs | 98.7 | 0.1 | 0.0 | 1.2 |
| | | 800 | gh | 89.4 | 10.3 | 0.0 | 0.2 |
| | | 1700 | gh | 96.3 | 2.9 | 0.0 | 0.8 |
| P209 | Ka | 450 | ot | 55.4 | 40.3 | 0.0 | 4.3 |
| | | 1100 | gh | 54.6 | 38.0 | 5.5 | 2.0 |
| | | 1400 | so | 98.4 | 1.1 | 0.0 | 0.5 |
| P210 | Bd | 260 | ot | 65.3 | 32.3 | 0.0 | 2.3 |
| | | 530 | ot | 68.7 | 28.8 | 0.0 | 2.5 |
| | | 810 | re | 0.2 | 67.6 | 31.6 | 0.6 |
| | | 1200 | re | 0.0 | 36.4 | 62.2 | 1.4 |
| | | 1580 | on | 0.0 | 44.3 | 54.8 | 0.9 |

Table 6.2 Results of Munsell colour calculation from RGB values determined from digital photographs

| Profile | Form | Depth (mm) | Horizon | Calculated from photo | | | Dry Munsell colour (field) | Calculated from RGB | | |
|---|---|---|---|---|---|---|---|---|---|---|
| | | | | R | G | B | | Hue | Value | Chroma |
| P201 | Lo | 430 | ot | 133 | 118 | 97 | 10YR4/4 | 0.68Y | 7.26 | 1.33 |
| | | 730 | gs | 153 | 126 | 84 | 7.5YR6/4 | 1.45Y | 7.49 | 2.6 |
| | | 1000 | sp | 133 | 125 | 121 | 7.5YR6/4 | 3.05YR | 7.43 | 0.49 |
| | | 1210 | on | 138 | 136 | 141 | 7.5YR7/2 | 3.63P | 7.68 | 0.61 |
| P202 | Pn | 400 | ot | 120 | 121 | 120 | 10YR4/3 | 1.29G | 7.29 | 0.05 |
| | | 820 | ye | 62 | 62 | 48 | 7.5YR5/6 | 0.52GY | 5.43 | 1.13 |
| | | 960 | on | 134 | 127 | 119 | 10YR8/2 | 9.17YR | 7.47 | 0.51 |
| | | 1500 | on | 132 | 127 | 114 | 2.5Y8/2 | 3.75Y | 7.45 | 0.64 |
| P203 | Tu | 380 | ot | 123 | 119 | 117 | 10YR5/3 | 2.76YR | 7.26 | 0.25 |
| | | 960 | ne | 40 | 42 | 27 | 7.5YR7/4 | 2.07GY | 4.54 | 1.77 |
| | | 1300 | on | 140 | 120 | 93 | 7.5YR7/4 | 0.44Y | 7.33 | 1.74 |
| P204 | Lo | 140 | ot | 127 | 122 | 111 | 7.5YR6/2 | 2.99Y | 7.33 | 0.57 |
| | | 300 | gs | 136 | 126 | 107 | 7.5YR7/5 | 2.21Y | 7.44 | 1.02 |
| | | 470 | sp | 154 | 126 | 97 | 10YR8/2 | 8.76YR | 7.52 | 2.06 |
| | | 1000 | on | 159 | 126 | 112 | 10YR8/2 | 2.31YR | 7.57 | 1.99 |
| P205 | Kd | 220 | ot | 134 | 119 | 99 | 2.5Y5/2 | 0.38Y | 7.29 | 1.28 |
| | | 460 | gs | 122 | 120 | 112 | 2.5Y6/1 | 5.77Y | 7.26 | 0.38 |
| | | 660 | gs | 136 | 129 | 112 | 10YR6/2 | 3.46Y | 7.5 | 0.84 |
| | | 1400 | gh | 163 | 129 | 99 | 2.5Y7/1 | 7.75YR | 7.62 | 2.29 |
| P206 | Kd | 550 | ot | 110 | 115 | 120 | 10YR5/1 | 2.36PB | 7.12 | 0.71 |
| | | 800 | gs | 142 | 141 | 139 | 10YR5/1 | 1.23Y | 7.78 | 0.09 |
| | | 1100 | gh | 157 | 153 | 132 | 10YR6/1 | 6.64Y | 8.04 | 0.83 |
| P207 | We | 300 | ot | 128 | 124 | 119 | 10YR6/2 | 9.75YR | 7.38 | 0.31 |
| | | 560 | sp | 138 | 126 | 103 | 10YR6/3 | 2.25Y | 7.44 | 1.25 |
| | | 670 | sp | 142 | 132 | 116 | 10YR8/1 | 1.21Y | 7.59 | 0.88 |
| | | 1300 | on | 137 | 128 | 106 | 10YR8/2 | 3.54Y | 7.48 | 1.11 |
| P208 | Kd | 350 | ot | 111 | 114 | 116 | 10YR6/1 | 0.52PB | 7.1 | 0.33 |
| | | 530 | gs | 133 | 133 | 136 | 10YR6/2 | 9.53PB | 7.6 | 0.36 |
| | | 800 | gh | 136 | 131 | 124 | 10YR7/1 | 0.27Y | 7.56 | 0.4 |
| | | 1700 | gh | 131 | 131 | 128 | 10YR6/2 | 0.37GY | 7.54 | 0.12 |
| P209 | Kd | 450 | ot | 119 | 111 | 100 | 10YR5/2 | 0.67Y | 7.06 | 0.71 |
| | | 1100 | gh | 139 | 127 | 110 | 10YR6/1 | 0.56Y | 7.48 | 1.01 |
| | | 1400 | so | 157 | 158 | 146 | 10YR6/1 | 2.28GY | 8.14 | 0.42 |
| P210 | Bd | 260 | ot | 120 | 114 | 111 | 10YR4/2 | 3.10YR | 7.14 | 0.38 |
| | | 530 | ot | 120 | 113 | 106 | 10YR4/3 | 8.56YR | 7.11 | 0.52 |
| | | 810 | re | 151 | 121 | 98 | 7.5YR4/6 | 6.74YR | 7.41 | 1.99 |
| | | 1200 | re | 153 | 117 | 84 | 7.5YR6/6 | 8.29YR | 7.33 | 2.64 |
| | | 1580 | on | 165 | 128 | 87 | 10YR6/4 | 9.43YR | 7.59 | 2.85 |

The digital classified colour of the diagnostic horizons in P201 (Longlands 2000) is totally dominated by a single diagnostic colour, contrary to other profiles. The orthic A and E horizons are dominantly yellow (96.9 % and 98.6 % respectively) and change abruptly to dominantly grey in the soft plinthic B (78.5 %) and saprolite (90.9 %) horizons. This correlates with Munsell

determined brown (10YR4/4) colour in the orthic A, a red dull orange (7.5YR6/4) colour E and a red dull orange (7.5YR6/4) colour soft plinthic B horizons. (Table 6.2). There are very few red colours (1.3 %) in the E, some yellow (19.4 %) and very few black (1.6 %) in the soft plinthic B horizon and some yellow in the saprolite (8.1 %). Yellow, red and black colours due to mottling are expected in the E, soft plinthic B and underlying saprolite horizons.

The E horizon, classified as diagnostic grey in the dry state during field investigations, may have classified as yellow during calculation due to two reasons. Firstly the observed dry Munsell colour (7.5YR6/4), is a colour definition boundary value. Secondly, the mathematical description of diagnostic grey, yellow-brown and red can be improved to allow for more accurate colour classification. The combination of colours in the saprolite is expected, given the typical pale Elliott sandstone and the redistribution of Fe and Mn in the weathered localities.

In profile P202 (Pinedene 1100), the orthic A horizon and both layers of the unspecified material with signs of wetness are dominated by a digitally determined diagnostic grey colour (91.0 %, 64.2 % and 74.7 % respectively) and the yellow-brown apedal B horizon by a yellow colour (67.4 %) and some grey (28.6 %). This correlates with dull yellowish brown (10YR4/3), bright brown (7.5YR5/6), light grey (10YR8/2) and pinkish white (2.5YR8/2) colours in the orthic A, yellow-brown apedal B and unspecified material with signs of wetness respectively. The digital calculation identified 3.9 % to 8.5 % black colour in all the horizons of the profile and negligible red colouring. The dominance of grey in the orthic horizon is probably due to short periods of saturation and reduction, followed by vertical leaching of Fe and Mn. This is supported by the Fe and Mn : clay ratios that are fairly low in the A horizon. However the yellow and grey colour domination in the yellow-brown apedal B horizon and the unspecified material with signs of wetness are according to expectation. The nearly 30 % of grey in the yellow-brown apedal B horizon may indicate a significant duration of water saturation. The occurrence of

black colours is probably due to shadows occurring in the photograph. The occurrence of 1 % diagnostic red in the C2 horizon is due to the presence of very small red mottles.

The A horizon of P203 (Tukulu 2100), is also predominantly grey (88.6 %), as observed in P202 (Pinedene). The colour distribution of the neocutanic B horizon and the unspecified material with signs of wetness are very similar, mainly diagnostic yellow (83.1 % and 81.9 % respectively) with some grey, red and black colouring. This correlates with dull yellowish brown (10YR5/3) in the orthic A, dull orange (7.5YR7/4) in the neocutanic B horizon and the unspecified material with signs of wetness (C1), and unspecified material with signs of wetness. The yellow-brown colour count in both horizons is higher than in the yellow-brown apedal B horizon of P202 (Pinedene). The digitally determined colour of the subsoil horizons of the Tukulu is more normally distributed, supporting the variegated colour found in neocutanic horizons. The black colouring may again be shadow.

The colour pattern in P204 (Longlands) is remarkably similar to that in P203 (Tukulu). The digitally calculated colour values change from predominantly grey in the upper two horizons to predominantly yellow-brown and red in the deeper subsoil. The orthic A is also predominantly grey but the E horizon has more diagnostic grey and less diagnostic yellow. This correlates with a greyish brown (7.5YR6/2) orthic A horizon, an orange (7.5YR7/5) E, a light grey (10YR8/2) soft plinthic B (300–470 mm), and a light grey (10YR8/2) G horizon, as determined in the field. The soft plinthic B horizon has 27.0 % diagnostic red colouring, an indication of the Fe oxide mottles present. It therefore supports the classification as a soft plinthic B horizon. The unspecified material with signs of wetness, underlying the soft plinthic B horizon, has a broad normal distribution pattern with 45.1 % diagnostic red, 44.3 % diagnostic yellow and 9.9 % diagnostic grey colouring calculated. The morphology of the deep subsoil is typical of some underlying horizons with very small prominent red spots, where preparation of the profile face resulted

in red streaking. This effect can account for up to 95 % of the red colour in these photographs.

The A (dark greyish yellow [2.5Y5/2]) and G horizons (light grey [2.5Y7/1]) of P205 (Kroonstad 2000) is predominantly diagnostic yellow (87.0 % and 52.5 %), while the E1 (yellowish grey [2.5Y6/1]) and E2 (greyish yellow brown [10YR6/2]) horizons are predominantly diagnostic grey (98.9 % and 91.7 %). The quantified colours therefore support the classification of these horizons. The G horizon has 41.8 % diagnostic red, the reason being the same as discussed for P204 (Longlands).

P206 (Kroonstad 2000) is diagnostic grey throughout the profile (90.3 % – 99.2 % – 98.0 %). This correlates with a brownish grey (10YR5/1) orthic A horizon, a brownish grey (10YR5/1) E and a brownish grey (10YR6/1) G horizon The A horizon has 9.6 % black, which is largely due to the high level of organic material (4.4 % OC in the 0 – 100 mm layer), and shadows in the horizon.

The dominant colours in P207 (Westleigh 1000) are 94.6 % diagnostic grey in the A horizon (greyish yellow brown [10YR6/2]), 71.8 % diagnostic yellow in the soft plinthic B1 horizon (dull yellow orange [10YR6/3]), 70.4 % diagnostic grey in the soft plinthic B2 horizon (light grey [10YR8/1]), and 66.0 % diagnostic grey in the C horizon (light grey [10YR8/2]). The subdominant colour in the B1 horizon is diagnostic grey (27.1 %), while it is diagnostic yellow (26.9 % and 31.1 %) in the B2 and C horizons. The B1 horizon was classified as a soft plinthic B horizon, although it has grey colour, as defined for an E horizon, due to the presence of prominent vesicular mottles. The varied nature of this horizon's colour is clear from the colour classification. The presence of 26.9 % diagnostic yellow in the B2 horizon is due to Fe oxide mottles. It therefore supports the classification as a soft plinthic B horizon. The occurrence of black in these horizons is mainly due to shadows.

The horizon colours of P208 (Kroonstad 1000) are classified as diagnostic grey throughout the profile (92.9 % – 98.7 % – 89.4 % – 96.3 %). This correlates with a brownish grey (10YR6/1) colour in the orthic A, a greyish yellow-brown (10YR6/2) colour in the E, a light grey (10YR7/1) colour in the G1, and a greyish yellow brown (10YR6/2) colour in the G2 horizon. There is 10.3 % diagnostic yellow in the G1 horizon and 2.9 % diagnostic yellow in the G2 horizon. The colours indicate a very wet profile. It also supports the classification of the diagnostic horizons and the profile as a whole. The presence of yellow colours in the G1 is as a result of Fe oxide mottles. The black colours in the G1 and G2 horizons are mainly due to shadows caused by cracks.

Diagnostic grey increases (55.4 % – 54.6 % – 98.4 %) throughout P209 (Katspruit 1000). This correlates with a greyish yellow-brown (10YR5/2) colour in the orthic A horizon, a brownish grey (10YR6/1) colour in the G horizon and a brownish grey (10YR6/1) colour in the saprolite. It has 40.3 % diagnostic yellow in the A and 38.0 % diagnostic yellow as well as 5.5 % diagnostic red in the G horizon. The yellow and red colours in the A and G horizons are due to Fe oxide mottling. The black colours in the A horizon are due to shadows. The increasing area of diagnostic grey as well as yellow mottling might indicate increased durations of water saturation.

P210 (Bloemdal 1100) is the only profile with significant areas of diagnostic red colours. The A1 and A2 horizons are predominantly diagnostic grey (65.3 % and 68.7 %). The B1 horizon has 67.6 % diagnostic yellow and 31.6 % diagnostic red while the B2 horizon has 36.4 % diagnostic yellow and 62.2 % diagnostic red. The underlying unspecified material with signs of wetness has 44.3 % diagnostic yellow and 54.8 % diagnostic red. This correlates with a greyish yellow brown (10YR4/2) orthic A1, a dull yellowish brown (10YR4/3) A2, a brown (7.5YR4/6) red apedal B1, an orange (7.5YR6/6) red apedal B2 and a dull orange (7.5YR6/4) unspecified material with signs of wetness. The colour classification of the B1 and B2 horizons supports the diagnostic horizon classification. The over-estimation of

diagnostic yellow in the B1 horizon might be due to unrefined colour definitions for the colour classification.

## 6.3 Mean horizon colour

The mean colour of each horizon, excluding diagnostic colour classification can be calculated in ArcView as a Zone Summary, or it can be calculated as the product of the percentage diagnostic colour occurrence and the respective R, G or B values. An evaluation of the results provided by the two methods is given in Figure 6.1. It is clear that these two methods are fairly similar ($R^2$ = 0.98), although the weighed mean values are typically 12 units higher for Red, 11 units higher for Blue and one unit lower for Green, than the Zone Summary. The weighed mean values can therefore be used to save time during the calculation process – provided they are corrected, using the proposed equations.

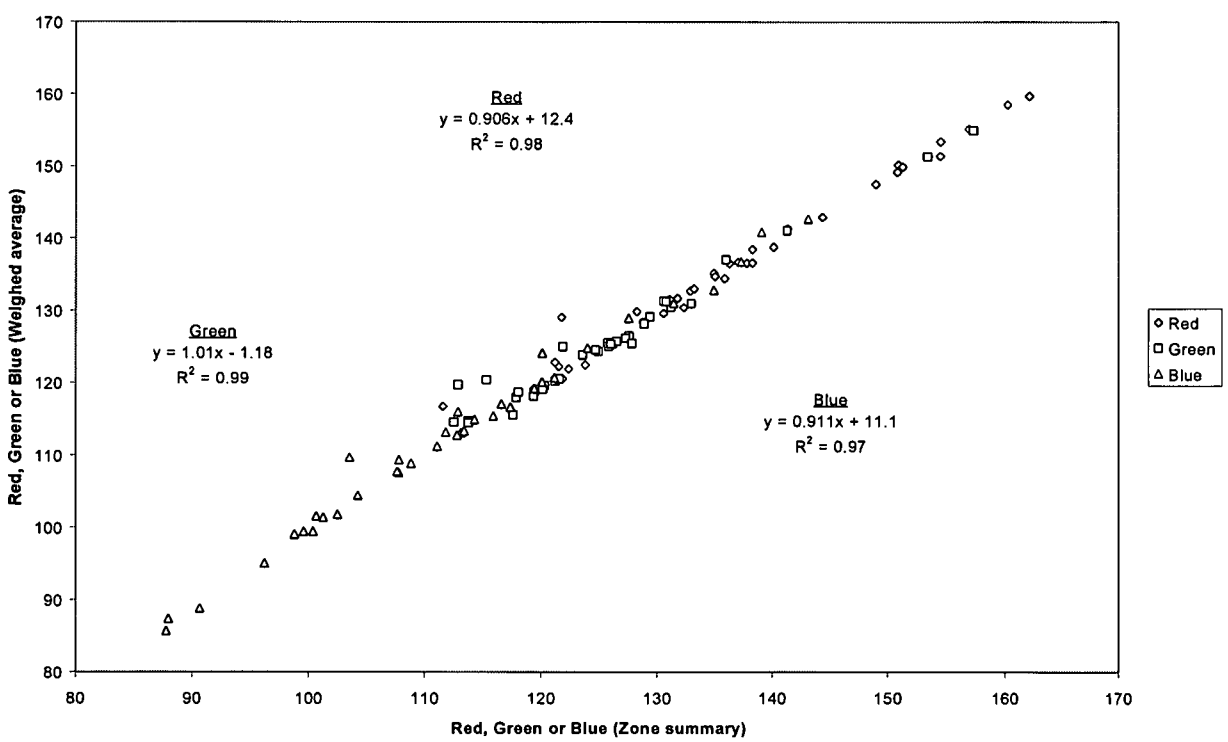


Figure 6.1 The relationship between two methods for determining soil colour.

Results of the corrected mean horizon colours as well as the dry and wet Munsell colour, described during field investigations, are given in Appendix C. An attempt was made to calculate the Munsell colour from the mean RGB horizon colour. This yielded results that were difficult to interpret, due to the continuous nature of the Hue values and the fact that Hue values fell outside that normally expected in soil (Table 6.2). This might be due to the colour classification procedure and the colour correlation programme used (Anon, 2003b). A further disadvantage is that the programme cannot be forced to select a colour within the expected soil colour limits, or within a specific Hue. It is proposed that these issues be researched further, due to the possibilities that they offer for the objective determination of soil colour.

## 6.4 Colour correlations

Although colour correlations were not a specific aim of this research, it would be interesting to evaluate results obtained against published colour indexes. The colour indexes developed by Torrent *et al.,* (1980 and 1983), Mokma & Cremeens (1991) as well as Van Huyssteen (1995), are discussed in paragraph 2.2. These colour indexes were evaluated against colour and soil water data obtained for this study. The colour index developed by Van Huyssteen (1995) gave the best correlation with duration of water saturation with $R^2$ = 0.33. The redness rating developed by Torrent *et al.,* (1980 and 1983), had $R^2$ = 0.16, while the colour index developed by Mokma & Cremeens (1991) had $R^2$ = 0.13. The colour index of Van Huyssteen (1995) also correlated reasonably well with mean $AD_{s>0.7}$ ($R^2$ = 0.35).

Determination of new coefficients for the colour index developed by Van Huyssteen (1995), increases the correlation coefficient to $R^2$ = 0.38. The equation is given by:

$$AD_{s>0.7} \text{ (days year}^{-1}) = -38.6 \times H_d + 35.2 \times V_d + 1.94 \times C_d - 51.3 \qquad (6.1)$$

Where:

$AD_{s>0.7}$ Mean annual duration of water saturation above 0.7 of porosity

$H_d$ = numeric dry colour Hue

$V_d$ = dry colour Value

$C_d$ = dry colour Chroma

Mean Red, Green and Blue values, or combinations thereof, did not correlate with $AD_{s>0.7}$ (Table 6.3). The colour quantification methodology was not studied in further detail, because it would not have had a marked impact on the outcome of this study. It should, however, be studied further to exploit its possibilities for colour quantification and therefore soil classification as well as to aid in correlations with $AD_{s>0.7}$.

Table 6.3 The correlation ($R^2$) of mean photo R, G and B with mean $AD_{s>0.7}$, mean duration and mean frequency of water saturation

| | Red | Green | Blue |
|---|---|---|---|
| Mean $AD_{s>0.7}$ | 0.095 | 0.168 | 0.190 |
| Mean duration | 0.076 | 0.156 | 0.196 |
| Mean frequency | 0.061 | 0.008 | 0.008 |

## 6.5 Summary

The colour variation in digital photographs of soils can be quantified and classified meaningfully, using ArcView SpatialAnalyst. This methodology is, however, not yet sufficiently refined, but holds great promise for the unbiased and quantitative determination of soil and mottle colour properties as well as statistical correlation with related soil conditions.

The black classification was used mainly for the elimination of shaded areas from the photographs. Unfortunately this class includes Mn mottles. This cannot be prevented at this stage. The occurrence of significant amounts of diagnostic red is restricted to P210 (Bloemdal). Where diagnostic red occurs in other profiles, it is associated with Fe oxide mottles. This is the case in P201 (Longlands), P203 (Tukulu), P204 (Longlands), P205 (Kroonstad) and P209 (Katspruit).

Grey and yellow are the dominant colours in the profiles described for this study. For example in P201 (Longlands) and P209 (Katspruit) the amount of

grey increase with depth, at the expense of yellow. The amount of diagnostic grey is, however, much more in the Katspruit than in the Longlands. In P202 (Pinedene) diagnostic grey decreases and then increases with depth. In P203 (Tukulu), P204 (Longlands), P205 (Kroonstad) and P207 (Westleigh) the amount of diagnostic grey decreases with depth. This might indicates a drier subsoil water regime. Artificial increases in the amount of red caused by smearing of Fe oxide mottles during profile preparation explain this feature in P204 (Longlands) and P205 (Kroonstad). Profiles P206 (Kroonstad) and P208 (Kroonstad) are diagnostic grey throughout the profile.

Mean horizon colour can be calculated directly in ArcView, or from the results of diagnostic colour classification. The two methods do not give significantly different results. Results of colour classification do not show great promise regarding correlations with $AD_{s>0.7}$, but can successfully be used in colour determination for diagnostic horizon classification, or for the determination of other soil morphological features.

# 7 PROFILE HYDROLOGY

## 7.1 Introduction

Soil redox reactions are driven by the presence or absence of water. In an aerated environment there is normally sufficient oxygen available for the respiratory demand of microorganisms. As the soil becomes increasingly more saturated, a point is reached where insufficient oxygen is available for microorganism respiration. Some microorganisms then utilize other electron acceptors (*e.g.* $Mn^{4+}$, $Fe^{3+}$) during respiration. This causes the reduction of these elements, their mobilization and an associated reduction in the redox potential of the soil. The long term soil water content is therefore important in any study aiming to relate soil water content to soil morphology. The aim of this chapter is to characterize the long term soil water contents of the ten profiles studied.

The soil was deemed to be sufficiently saturated, for redox reactions to occur, if the degree of saturation was above 0.7 of porosity. This fraction was chosen as a first approximation, based on the following observations. Firstly, experience has shown that the drained upper limit (DUL) of a soil is generally around 0.6 of porosity (Hensley, 2002 personal communication). Since it is reasonable to expect that reduction reactions will only occur to a significant extent above DUL, the critical value for this study needs to be > 0.6 of porosity. Secondly, a study of the degree of water saturation *versus* time graphs in Appendix A (Figures 3, 6, 9, 12, 15, 18, 21, 24, 27, 30) provides the following evidence that 0.7 of porosity is a reasonable first approximation: (a) in horizons that are known to drain rapidly, e.g. the first two horizons in profiles 201 and 210, the water content only exceeds 0.7 of porosity for very short times when normally occur during periods of heavy rainfall; (b) the inflection point in the "water loss" (i.e. drainage + ET) curves of these rapidly drying horizons is always well below 0.7 of porosity, indicating that DUL is < 0.7 of porosity; (c) in horizons that are known to be very wet, e.g. G horizons in

profiles 204, 206, 208 and 209, the water content exceeds 0.7 of porosity for long periods.

Annual and mean annual duration of saturation above 0.7 of porosity ($AD_{s>0.7}$) values are given in Table 7.1. Annual and mean frequency of saturation above 0.7 of porosity ($F_{s>0.7}$) values are given in Table 7.2. Annual and mean duration of saturation events above 0.7 of porosity ($D_{s>0.7}$) values are given in Table 7.3. A summary of mean $AD_{s>0.7}$, $F_{s>0.7}$ and $D_{s>0.7}$ values are given in Table 7.4.

Table 7.1 Annual duration of s>0.7, for profiles 201 to 210, calculated from weekly neutron water meter data from 01/01/1997 until 31/12/2002.

| Profile No | Depth (mm) | Diagnostic horizon | 1997 | 1998 | 1999 | 2000 | 2001 | 2002 | Mean | Median | Std dev |
|---|---|---|---|---|---|---|---|---|---|---|---|
| | | | (days year$^{-1}$) | | | | | | | | |
| 201 | 150 | ot | 0 | 0 | 0 | 29 | 7 | 0 | 6 | 0 | 12 |
| | 450 | gs | 0 | 30 | 22 | 69 | 13 | 10 | 24 | 18 | 24 |
| | 750 | sp | 65 | 96 | 43 | 154 | 58 | 63 | 80 | 64 | 40 |
| 202 | 150 | ot | 0 | 0 | 0 | 0 | 0 | 0 | 0 | 0 | 0 |
| | 450 | ye | 0 | 0 | 0 | 32 | 7 | 0 | 7 | 0 | 13 |
| | 750 | ye | 317 | 357 | 196 | 319 | 319 | 348 | 309 | 319 | 58 |
| | 1050 | on | 352 | 365 | 322 | 365 | 364 | 348 | 353 | 358 | 17 |
| | 1350 | on | 352 | 365 | 308 | 365 | 364 | 348 | 350 | 358 | 22 |
| | 1650 | on | 352 | 365 | 322 | 348 | 364 | 348 | 350 | 350 | 16 |
| 203 | 150 | ot | 0 | 0 | 0 | 0 | 0 | 0 | 0 | 0 | 0 |
| | 450 | ne | 0 | 0 | 0 | 0 | 0 | 0 | 0 | 0 | 0 |
| | 750 | ne | 0 | 6 | 15 | 52 | 57 | 95 | 38 | 34 | 37 |
| | 1050 | on | 127 | 110 | 77 | 231 | 234 | 300 | 180 | 179 | 87 |
| | 1350 | on | 0 | 34 | 0 | 202 | 339 | 187 | 127 | 111 | 138 |
| | 1650 | on | 14 | 34 | 29 | 129 | 304 | 272 | 130 | 82 | 129 |
| 204 | 150 | ot | 12 | 84 | 118 | 68 | 107 | 112 | 84 | 96 | 40 |
| | 450 | sp | 106 | 120 | 118 | 212 | 133 | 106 | 133 | 119 | 40 |
| | 750 | on | 212 | 247 | 189 | 365 | 141 | 336 | 248 | 230 | 87 |
| | 1050 | on | 352 | 365 | 365 | 365 | 361 | 350 | 360 | 363 | 7 |
| 205 | 150 | ot | 21 | 6 | 52 | 40 | 16 | 0 | 23 | 19 | 20 |
| | 450 | gs | 28 | 28 | 75 | 41 | 29 | 0 | 34 | 29 | 24 |
| | 750 | gh | 365 | 343 | 364 | 365 | 233 | 224 | 316 | 354 | 68 |
| | 1050 | gh | 365 | 343 | 364 | 365 | 233 | 224 | 316 | 354 | 68 |
| 206 | 150 | ot | 365 | 365 | 357 | 365 | 365 | 325 | 357 | 365 | 16 |
| | 450 | gs | 365 | 365 | 357 | 365 | 365 | 325 | 357 | 365 | 16 |
| | 750 | gh | 365 | 365 | 357 | 350 | 365 | 325 | 355 | 361 | 16 |
| | 1050 | gh | 365 | 365 | 357 | 365 | 365 | 325 | 357 | 365 | 16 |
| 207 | 150 | ot | 124 | 141 | 110 | 183 | 137 | 249 | 157 | 139 | 51 |
| | 450 | sp | 281 | 175 | 131 | 365 | 143 | 292 | 231 | 228 | 95 |
| 208 | 150 | ot | 225 | 141 | 145 | 326 | 164 | 273 | 212 | 195 | 76 |
| | 450 | gs | 231 | 149 | 145 | 319 | 346 | 279 | 245 | 255 | 85 |
| | 750 | gh | 269 | 213 | 195 | 352 | 345 | 316 | 282 | 293 | 67 |
| | 1050 | gh | 330 | 365 | 362 | 365 | 365 | 343 | 355 | 364 | 15 |
| | 1350 | gh | 317 | 365 | 362 | 365 | 365 | 343 | 353 | 364 | 20 |
| | 1650 | gh | 317 | 365 | 362 | 365 | 365 | 343 | 353 | 364 | 20 |
| 209 | 150 | ot | 262 | 314 | 189 | 263 | 181 | 273 | 247 | 263 | 52 |
| | 450 | gh | 363 | 365 | 357 | 360 | 342 | 238 | 338 | 359 | 49 |
| 210 | 150 | ot | 0 | 16 | 42 | 97 | 118 | 141 | 69 | 70 | 58 |
| | 450 | ot | 0 | 0 | 0 | 35 | 16 | 0 | 9 | 0 | 14 |
| | 750 | re | 0 | 0 | 27 | 21 | 16 | 0 | 11 | 8 | 12 |
| | 1050 | re | 103 | 126 | 77 | 205 | 188 | 270 | 162 | 157 | 72 |
| | 1350 | on | 139 | 142 | 46 | 289 | 365 | 247 | 205 | 195 | 117 |

Table 7.2 Frequency of s>0.7 events per year ($F_{s>0.7}$), for profiles 201 to 210, calculated from weekly neutron water meter data from 01/01/1997 until 31/12/2002.

| Profile No | Depth (mm) | Diagnostic horizon | 1997 | 1998 | 1999 | 2000 | 2001 | 2002 | Mean | Median | Std dev |
|---|---|---|---|---|---|---|---|---|---|---|---|
| | | | (events year$^{-1}$) | | | | | | | | |
| 201 | 150 | ot | 0 | 0 | 0 | 1 | 1 | 0 | 0 | 0 | 1 |
| | 450 | gs | 0 | 2 | 2 | 3 | 1 | 2 | 2 | 2 | 1 |
| | 750 | sp | 3 | 2 | 1 | 3 | 4 | 1 | 2 | 3 | 1 |
| 202 | 150 | ot | 0 | 0 | 0 | 0 | 0 | 0 | 0 | 0 | 0 |
| | 450 | ye | 0 | 0 | 0 | 1 | 1 | 0 | 0 | 0 | 1 |
| | 750 | ye | 1 | 1 | 1 | 5 | 2 | 1 | 2 | 1 | 2 |
| | 1050 | on | 1 | 1 | 1 | 1 | 1 | 1 | 1 | 1 | 0 |
| | 1350 | on | 1 | 1 | 2 | 1 | 1 | 1 | 1 | 1 | 0 |
| | 1650 | on | 1 | 1 | 3 | 3 | 1 | 1 | 2 | 1 | 1 |
| 203 | 150 | ot | 0 | 0 | 0 | 0 | 0 | 0 | 0 | 0 | 0 |
| | 450 | ne | 0 | 0 | 0 | 0 | 0 | 0 | 0 | 0 | 0 |
| | 750 | ne | 0 | 1 | 2 | 2 | 3 | 5 | 2 | 2 | 2 |
| | 1050 | on | 5 | 2 | 1 | 4 | 2 | 1 | 3 | 2 | 2 |
| | 1350 | on | 0 | 3 | 0 | 4 | 2 | 5 | 2 | 3 | 2 |
| | 1650 | on | 2 | 2 | 2 | 6 | 3 | 1 | 3 | 2 | 2 |
| 204 | 150 | ot | 1 | 2 | 1 | 2 | 2 | 1 | 2 | 2 | 1 |
| | 450 | sp | 4 | 3 | 1 | 2 | 2 | 1 | 2 | 2 | 1 |
| | 750 | on | 4 | 7 | 2 | 1 | 1 | 1 | 3 | 2 | 2 |
| | 1050 | on | 1 | 1 | 1 | 1 | 1 | 1 | 1 | 1 | 0 |
| 205 | 150 | ot | 1 | 1 | 1 | 3 | 3 | 0 | 2 | 1 | 1 |
| | 450 | gs | 1 | 3 | 4 | 4 | 3 | 0 | 3 | 3 | 2 |
| | 750 | gh | 1 | 1 | 1 | 1 | 1 | 1 | 1 | 1 | 0 |
| | 1050 | gh | 1 | 1 | 1 | 1 | 1 | 1 | 1 | 1 | 0 |
| 206 | 150 | ot | 1 | 1 | 1 | 1 | 1 | 1 | 1 | 1 | 0 |
| | 450 | gs | 1 | 1 | 1 | 1 | 1 | 1 | 1 | 1 | 0 |
| | 750 | gh | 1 | 1 | 1 | 2 | 1 | 1 | 1 | 1 | 0 |
| | 1050 | gh | 1 | 1 | 1 | 1 | 1 | 1 | 1 | 1 | 0 |
| 207 | 150 | ot | 4 | 4 | 1 | 3 | 2 | 1 | 3 | 3 | 1 |
| | 450 | sp | 3 | 2 | 1 | 1 | 1 | 1 | 2 | 1 | 1 |
| 208 | 150 | ot | 4 | 2 | 1 | 2 | 1 | 1 | 2 | 2 | 1 |
| | 450 | gs | 4 | 2 | 2 | 2 | 2 | 1 | 2 | 2 | 1 |
| | 750 | gh | 2 | 5 | 4 | 2 | 2 | 1 | 3 | 2 | 2 |
| | 1050 | gh | 1 | 1 | 1 | 1 | 1 | 1 | 1 | 1 | 0 |
| | 1350 | gh | 1 | 1 | 1 | 1 | 1 | 1 | 1 | 1 | 0 |
| | 1650 | gh | 1 | 1 | 1 | 1 | 1 | 1 | 1 | 1 | 0 |
| 209 | 150 | ot | 3 | 5 | 3 | 2 | 1 | 1 | 3 | 3 | 2 |
| | 450 | gh | 2 | 1 | 1 | 1 | 1 | 3 | 2 | 1 | 1 |
| 210 | 150 | ot | 0 | 2 | 3 | 5 | 2 | 4 | 3 | 3 | 2 |
| | 450 | ot | 0 | 0 | 0 | 3 | 1 | 0 | 1 | 0 | 1 |
| | 750 | re | 0 | 0 | 1 | 3 | 1 | 0 | 1 | 1 | 1 |
| | 1050 | re | 6 | 5 | 4 | 6 | 2 | 2 | 4 | 5 | 2 |
| | 1350 | on | 6 | 8 | 6 | 5 | 1 | 1 | 5 | 6 | 3 |

Table 7.3 Duration of s>0.7 events, for profiles 201 to 210, calculated from weekly neutron water meter data from 01/01/1997 until 31/12/2002.

| Profile No | Depth (mm) | Diagnostic horizon | 1997 | 1998 | 1999 | 2000 | 2001 | 2002 | Mean | Median | Std dev |
|---|---|---|---|---|---|---|---|---|---|---|---|
| | | | (days event$^{-1}$) | | | | | | | | |
| 201 | 150 | ot | 0 | 0 | 0 | 29 | 7 | 0 | 6 | 0 | 12 |
| | 450 | gs | 0 | 15 | 11 | 23 | 13 | 5 | 14 | 12 | 8 |
| | 750 | sp | 22 | 48 | 43 | 51 | 15 | 63 | 35 | 46 | 19 |
| 202 | 150 | ot | 0 | 0 | 0 | 0 | 0 | 0 | 0 | 0 | 0 |
| | 450 | ye | 0 | 0 | 0 | 32 | 7 | 0 | 7 | 0 | 13 |
| | 750 | ye | 317 | 357 | 196 | 64 | 160 | 348 | 172 | 257 | 119 |
| | 1050 | on | 352 | 365 | 322 | 365 | 364 | 348 | 353 | 358 | 17 |
| | 1350 | on | 352 | 365 | 154 | 365 | 364 | 348 | 292 | 358 | 84 |
| | 1650 | on | 352 | 365 | 107 | 116 | 364 | 348 | 206 | 350 | 127 |
| 203 | 150 | ot | 0 | 0 | 0 | 0 | 0 | 0 | 0 | 0 | 0 |
| | 450 | ne | 0 | 0 | 0 | 0 | 0 | 0 | 0 | 0 | 0 |
| | 750 | ne | 0 | 6 | 8 | 26 | 19 | 19 | 17 | 13 | 10 |
| | 1050 | on | 25 | 55 | 77 | 58 | 117 | 300 | 72 | 67 | 100 |
| | 1350 | on | 0 | 11 | 0 | 51 | 170 | 37 | 55 | 24 | 64 |
| | 1650 | on | 7 | 17 | 15 | 22 | 101 | 272 | 48 | 19 | 104 |
| 204 | 150 | ot | 12 | 42 | 118 | 34 | 54 | 112 | 56 | 48 | 43 |
| | 450 | sp | 27 | 40 | 118 | 106 | 67 | 106 | 60 | 86 | 38 |
| | 750 | on | 53 | 35 | 95 | 365 | 141 | 336 | 92 | 118 | 144 |
| | 1050 | on | 352 | 365 | 365 | 365 | 361 | 350 | 360 | 363 | 7 |
| 205 | 150 | ot | 21 | 6 | 52 | 13 | 5 | 0 | 15 | 10 | 19 |
| | 450 | gs | 28 | 9 | 19 | 10 | 10 | 0 | 14 | 10 | 10 |
| | 750 | gh | 365 | 343 | 364 | 365 | 233 | 224 | 316 | 354 | 68 |
| | 1050 | gh | 365 | 343 | 364 | 365 | 233 | 224 | 316 | 354 | 68 |
| 206 | 150 | ot | 365 | 365 | 357 | 365 | 365 | 325 | 357 | 365 | 16 |
| | 450 | gs | 365 | 365 | 357 | 365 | 365 | 325 | 357 | 365 | 16 |
| | 750 | gh | 365 | 365 | 357 | 175 | 365 | 325 | 296 | 361 | 75 |
| | 1050 | gh | 365 | 365 | 357 | 365 | 365 | 325 | 357 | 365 | 16 |
| 207 | 150 | ot | 31 | 35 | 110 | 61 | 69 | 249 | 63 | 65 | 82 |
| | 450 | sp | 94 | 88 | 131 | 365 | 143 | 292 | 154 | 137 | 115 |
| 208 | 150 | ot | 56 | 71 | 145 | 163 | 164 | 273 | 118 | 154 | 78 |
| | 450 | gs | 58 | 75 | 73 | 160 | 173 | 279 | 111 | 117 | 85 |
| | 750 | gh | 135 | 43 | 49 | 176 | 173 | 316 | 104 | 154 | 101 |
| | 1050 | gh | 330 | 365 | 362 | 365 | 365 | 343 | 355 | 364 | 15 |
| | 1350 | gh | 317 | 365 | 362 | 365 | 365 | 343 | 353 | 364 | 20 |
| | 1650 | gh | 317 | 365 | 362 | 365 | 365 | 343 | 353 | 364 | 20 |
| 209 | 150 | ot | 87 | 63 | 63 | 132 | 181 | 273 | 99 | 109 | 82 |
| | 450 | gh | 182 | 365 | 357 | 360 | 342 | 79 | 225 | 350 | 121 |
| 210 | 150 | ot | 0 | 8 | 14 | 19 | 59 | 35 | 26 | 17 | 21 |
| | 450 | ot | 0 | 0 | 0 | 12 | 16 | 0 | 9 | 0 | 7 |
| | 750 | re | 0 | 0 | 27 | 7 | 16 | 0 | 11 | 4 | 11 |
| | 1050 | re | 17 | 25 | 19 | 34 | 94 | 135 | 39 | 30 | 49 |
| | 1350 | on | 23 | 18 | 8 | 58 | 365 | 247 | 46 | 40 | 150 |

Table 7.4 Mean $AD_{s>0.7}$, mean duration of s>0.7 ($D_{s>0.7}$) and mean frequency of s>0.7 ($F_{s>0.7}$) for profiles 201 to 210, calculated from weekly neutron water meter data from 01/01/1997 until 31/12/2002.

| Profile number | Depth (mm) | Diagnostic horizon | $AD_{s>0.7}$ (days year$^{-1}$) | $F_{s>0.7}$ (events year$^{-1}$) | $D_{s>0.7}$ (days event$^{-1}$) |
|---|---|---|---|---|---|
| 201 | 150 | ot | 6 | < 1 | 6 |
| | 450 | gs | 24 | 2 | 14 |
| | 750 | sp | 80 | 2 | 35 |
| 202 | 150 | ot | 0 | < 1 | 0 |
| | 450 | ye | 7 | < 1 | 7 |
| | 750 | ye | 309 | 2 | 172 |
| | 1050 | on | 353 | 1 | 353 |
| | 1350 | on | 350 | 1 | 292 |
| | 1650 | on | 350 | 2 | 206 |
| 203 | 150 | ot | 0 | < 1 | 0 |
| | 450 | ne | 0 | < 1 | 0 |
| | 750 | ne | 38 | 2 | 17 |
| | 1050 | on | 180 | 3 | 72 |
| | 1350 | on | 127 | 2 | 55 |
| | 1650 | on | 130 | 3 | 48 |
| 204 | 150 | ot | 84 | 2 | 56 |
| | 450 | sp | 133 | 2 | 60 |
| | 750 | on | 248 | 3 | 92 |
| | 1050 | on | 360 | 1 | 360 |
| 205 | 150 | ot | 23 | 2 | 15 |
| | 450 | gs | 34 | 3 | 14 |
| | 750 | gh | 316 | 1 | 316 |
| | 1050 | gh | 316 | 1 | 316 |
| 206 | 150 | ot | 357 | 1 | 357 |
| | 450 | gs | 357 | 1 | 357 |
| | 750 | gh | 355 | 1 | 296 |
| | 1050 | gh | 357 | 1 | 357 |
| 207 | 150 | ot | 157 | 3 | 63 |
| | 450 | sp | 231 | 2 | 154 |
| 208 | 150 | ot | 212 | 2 | 118 |
| | 450 | gs | 245 | 2 | 111 |
| | 750 | gh | 282 | 3 | 104 |
| | 1050 | gh | 355 | 1 | 355 |
| | 1350 | gh | 353 | 1 | 353 |
| | 1650 | gh | 353 | 1 | 353 |
| 209 | 150 | ot | 247 | 3 | 99 |
| | 450 | gh | 338 | 2 | 225 |
| 210 | 150 | ot | 69 | 3 | 26 |
| | 450 | ot | 9 | < 1 | 9 |
| | 750 | re | 11 | < 1 | 11 |
| | 1050 | re | 162 | 4 | 39 |
| | 1350 | on | 205 | 5 | 46 |

## 7.2 P201 (Longlands 2000)

The mean annual duration of saturation above 0.7 of porosity ($AD_{s>0.7}$) increases with depth (Figure 7.1). Two s>0.7 events were measured in the A horizon (0–430 mm) during the six years. In 2000 there was one event of 29 days, and in 2001 one of 7 days. These events correspond to above mean annual rainfall in 2000 and probably also in 2001 (Table 3.1). It is postulated that rainfall in Table 3.1 is under-estimated because of missing data.

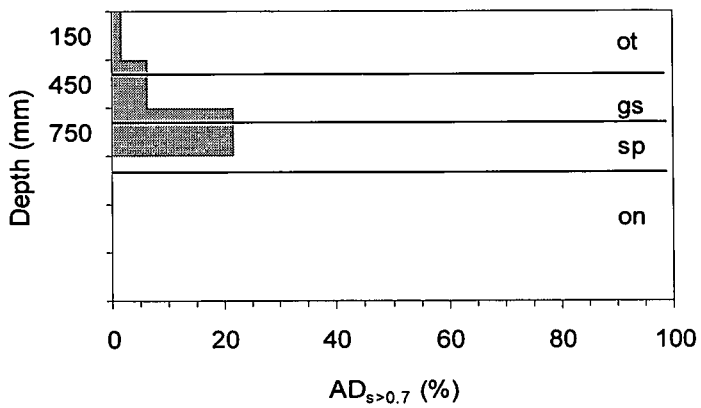


Figure 7.1 Mean $AD_{s>0.7}$ calculated from NWM measurements, for the three measuring depths at P201 (Longlands 2000).

On average, for the E horizon (430–730 mm) s>0.7 occurs 1.7 times during the year, with each event lasting 14 days on average. The mean $AD_{s>0.7}$ is 24 days $year^{-1}$. It ranges from 0 days in 1997 (lowest annual rainfall) to 69 days in 2000, when the highest annual rainfall during the measuring period was recorded. There is a very good relationship ($R^2$ = 0.92) between rainfall and $AD_{s>0.7}$ in the E horizon of profile 201 (Figure 7.2).

In the soft plinthic B horizon (730–980 mm) s>0.7 is slightly more frequent (2.3 times per year), but for a much longer total mean duration of 80 days on average, ranging from 43 days in 1999 to 154 days in 2000. The mean duration of the s>0.7 events is therefore longer (34 days) than in the E horizon (14 days). The longer s>0.7 events in the soft plinthic B can be expected, given the presence of the underlying relatively impermeable saprolite, which impedes further vertical drainage.

Although no water measurements are available for the saprolite horizon, it is expected that the horizon is saturated for longer periods than the soft plinthic B horizon.

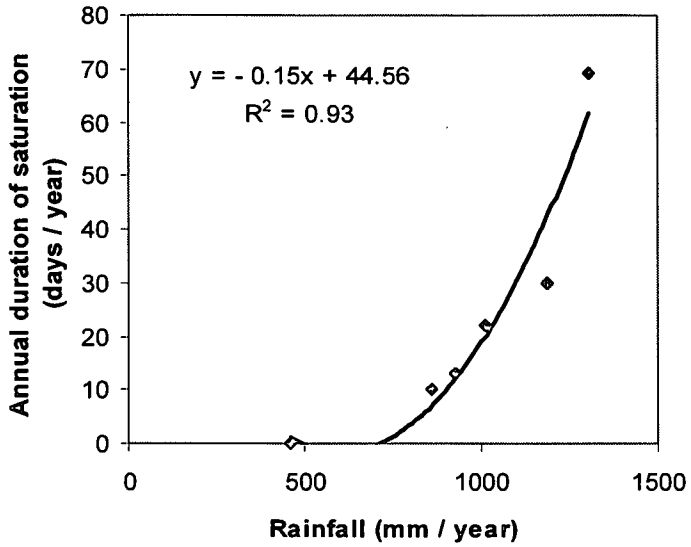


Figure 7.2 The relationship between annual duration of saturation in the E horizon of profile 201 and annual rainfall.

The results indicate adequate hydraulic conductivity in the profile. The underlying saprolite, however, forms an impervious layer, resulting in accumulation of water in the overlying horizons, resulting in redox conditions, leading to the formation of Fe mottles. Rapid lateral drainage in the E horizon results in these being fewer and less prominent than in the underlying horizon. Slower lateral drainage from the soft plinthic B horizon results in increased saturation and reduction, leading to the redistribution of Fe and Mn and the formation of many prominent Fe oxide mottles (Table 5.1).

## 7.3 P202 (Pinedene 1100)

This profile is characterized by a very dry orthic A horizon, dry to variable degree of saturation in the yellow-brown apedal B and almost constant s > 0.7 in the unspecified material with signs of wetness (Figure 7.3). No s>0.7 events were recorded in the A horizon. It therefore seems that short durations (< 7 days) of water saturation are responsible for the grey colour in the orthic A horizon. This is probably as a result of the high organic carbon content, which

gives rise to reduced conditions, even at short periods of water saturation. Two NWM measuring depths (450 mm and 750 mm) are located within the yellow-brown apedal B horizon. At 450 mm the mean $AD_{s>0.7}$ value is 7 days per year. This results from one event in 2000 when with $AD_{s>0.7}$ of 32 days, and one event in 2001 with $AD_{s>0.7}$ of 7 days. Above mean rainfall was recorded in both these years. During the other years there were no s>0.7 events.

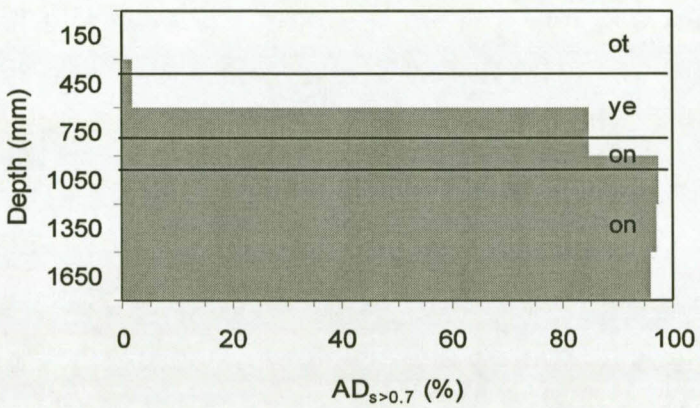


Figure 7.3 Mean $AD_{s>0.7}$ calculated from NWM measurements, for the three measuring depths at P202 (Pinedene 1100).

At 750 mm the yellow-brown apedal B horizon has a mean $AD_{s>0.7}$ value of 309 days $year^{-1}$. The $AD_{s>0.7}$ varies from 196 days in 1999 to 348 days in 2002. At this depth s>0.7 was therefore almost constant. The frequency of s>0.7 events is therefore low (1.8 times $year^{-1}$). It is a result of four dry spells in 2000 and two in 2001. During the other years the water content of the horizon was below 0.7 of porosity only once during the year. One third of the NWM measuring volume at 750 mm lies within the upper part of the C1 horizon. It can therefore be expected that water content will be over-estimated as far as the yellow-brown apedal B is concerned; mean $AD_{s>0.7}$ also corresponds much better to that of the underlying C horizons. If the measurement is assumed to be correct it would indicate that horizons situated deeper in the soil profile (less organic matter and possibly less micro organisms) can be saturated for longer periods before it impacts on the morphology. This is due to the lower organic carbon contents in these

horizons, providing less substrate for microorganisms and therefore resulting in less reduced conditions, even at longer periods of $AD_{s>0.7}$.

In the unspecified material with signs of wetness (1 050, 1 350 and 1 650 mm readings) $AD_{s>0.7}$ was almost continuous, with a mean $AD_{s>0.7}$ of 350 days $year^{-1}$, and mean $F_{s>0.7}$ of less than once per year.

This profile is characterized by mean $AD_{s>0.7}$ being almost continuous in the horizons deeper than 600 mm. There are no s>0.7 events in the A, and minimal (7 days $year^{-1}$) in the B horizon. The increase in $AD_{s>0.7}$ corresponds to an increase in Munsell colour value, clay content and a decrease in the medium and fine sand fractions. It is postulated that water drains fast laterally above the C horizons and that the C horizons drain very slowly due to their high clay content and high bulk density. This is supported by the pH and base saturation that is lower in the yellow-brown apedal B horizon and higher in the unspecified material with signs of wetness.

## 7.4 P203 (Tukulu 2100)

Degree of saturation in this profile is markedly different from the others in that it does not increase with depth. No s>0.7 (Figure 7.4) are recorded at the orthic A horizon (150 mm), or at the orthic A / neocutanic B transition (450 mm). At 750 mm (in the middle of the neocutanic B) the mean $AD_{s>0.7}$ value was 38 days $year^{-1}$. The $AD_{s>0.7}$ ranged from 0 days in 1997 to 95 days in 2002. These occurred as 2.2 s>0.7 events, lasting 17 days each. In the unspecified material with signs of wetness at 1 050 mm the mean $AD_{s>0.7}$ value was 180 days $year^{-1}$. These took place in 2.2 s>0.7 events, and lasted 83 days each. In the unspecified material with signs of wetness (1 350 and 1 650 mm readings) mean $AD_{s>0.7}$ values was 130 days $year^{-1}$.

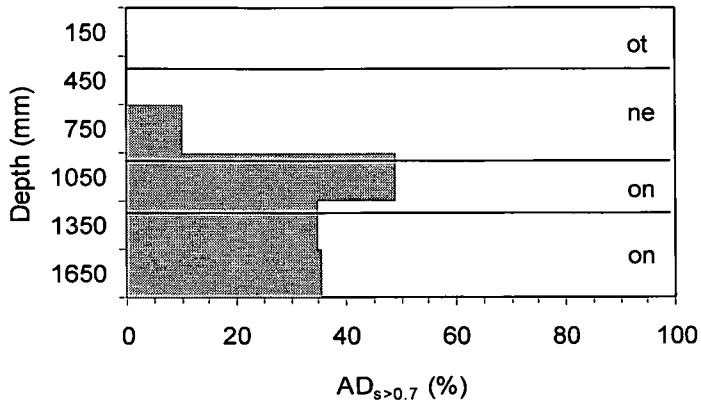


Figure 7.4 Mean $AD_{s>0.7}$ calculated from NWM measurements, for the three measuring depths at P203 (Tukulu 2100).

The high clay content and high bulk density in the C2 probably restricts vertical water movement, causing a longer $AD_{s>0.7}$ value in the C1 horizon. This wetness probably extends into the neocutanic B horizon during wet spells. The result of extended $AD_{s>0.7}$ events in the C1 horizon is evidenced by the occurrence of many Fe oxide mottles.

## 7.5 P204 (Longlands 2000)

Mean $AD_{s>0.7}$ increases with depth (Figure 7.5), similar pattern but with higher values than in P201 (Longlands). At the orthic A/E horizon transition (150 mm) the mean $AD_{s>0.7}$ value is 84 days $year^{-1}$, with a mean of 1.5 s>0.7 events per year, each lasting 56 days each. It seems that this is the minimum duration of water saturation that would result in rusty root channels in orthic A horizons. At the soft plinthic B/G horizon transition (450 mm) the mean $AD_{s>0.7}$ value is 133 days $year^{-1}$, with 2.2 s>0.7 events per year, each lasting 61 days. For the G horizon (750 mm) the mean $AD_{s>0.7}$ value is 250 days $year^{-1}$, with 2.5 s>0.7 events per year on mean, each lasting 100 days. In the lower G horizon (1 050 mm) mean $AD_{s>0.7}$ is almost continuous (361 days $year^{-1}$).

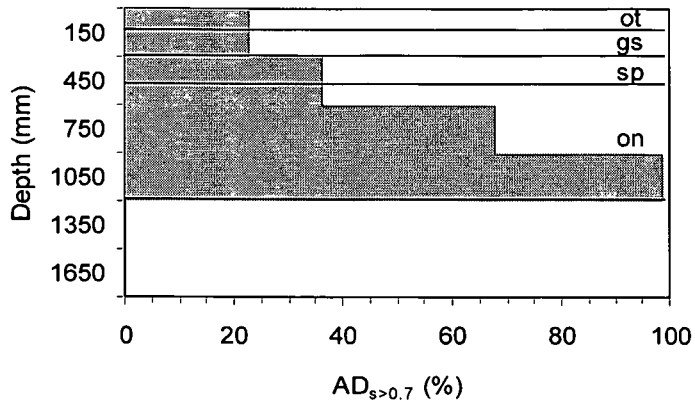


Figure 7.5 Mean $AD_{s>0.7}$ calculated from NWM measurements, for the three measuring depths at P204 (Longlands 2000).

The long $AD_{s>0.7}$ in this profile result in the formation of Fe oxide mottles and a bleached colour. In the orthic A, where s>0.7 events are shortest, there are only a few, fine Fe oxide mottles. This increases to many in the E and common in the soft plinthic B. The E and soft plinthic B horizons also have a pale (10YR8/2) colour, providing evidence that colourants such as Fe and organic matter have been depleted.

This profile is located at the lower end of the upper shelf (Figure 3.3). Here the hard Elliott sandstone (Figure 3.4) prevents downward movement of water. This results in water moving laterally, slowly through the profile, before it cascades over the sandstone shelf.

## 7.6 P205 (Kroonstad 2000)

Mean $AD_{s>0.7}$ increases down the profile (Figure 7.6), similar to the pattern observed for P202 (Pinedene). In the orthic A horizon the mean $AD_{s>0.7}$ value is 28 days $year^{-1}$, with and a mean of 1.5 s>0.7 events per year, each lasting 15 days. In the E1 and E2 horizons the mean $AD_{s>0.7}$ value is 34 days $year^{-1}$, with a mean of 2.5 s>0.7 events per year, each lasting 13 days. The water content of the G horizon is continuously above 0.7 of porosity at the 750 and 1 050 mm measuring depths.

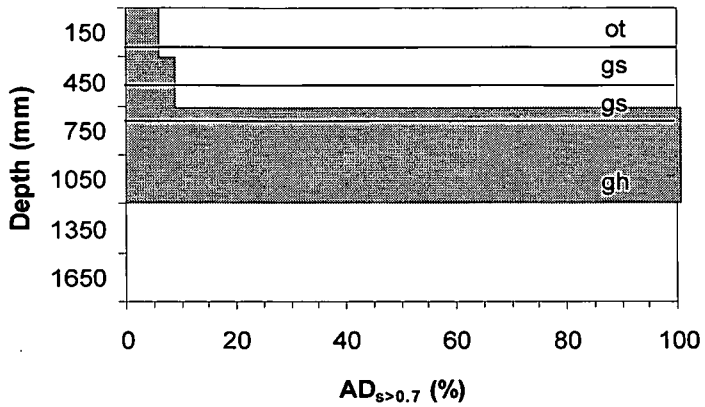


Figure 7.6 Mean $AD_{s>0.7}$ calculated from NWM measurements, for the three measuring depths at P205 (Kroonstad 2000).

The high clay content and high bulk density in the G horizon probably prevents water from draining from the horizon. It might also be responsible for the accumulation of water in the overlying A and E horizons. The location of the profile (Figure 3.3), on a little ridge also causes the A and E horizons to drain faster. The presence of rusty pore coatings in the A, and common and many Fe oxide mottles in the E provide supporting evidence for the relatively high mean $AD_{s>0.7}$ value here, compared to the surface horizons of profiles 201, 202 and 203. The bleached colour as well as common Fe oxide mottles in the G horizon is an indication of the long $AD_{s>0.7}$ in this horizon.

## 7.7 P206 (Kroonstad 1000)

The water content of the whole profile is above 0.7 of porosity for the entire year (Figure 7.7). The frequency of s>0.7 events is therefore once per year, and the mean $AD_{s>0.7}$ is 365 days year$^{-1}$.

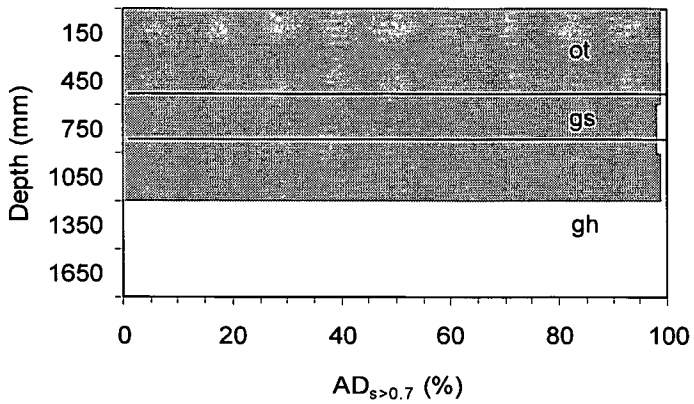


Figure 7.7 Mean $AD_{s>0.7}$ calculated from NWM measurements, for the three measuring depths at P206 (Kroonstad 1000).

The long $AD_{s>0.7}$ in this profile is attributable to the fact that it is situated in a small seep (Figure 3.3). Water from the higher lying soils therefore flows through this profile. The long $AD_{s>0.7}$ resulted in the accumulation of organic matter in the profile, especially at the soil's surface (Figure 5.49) where 4.4 % organic carbon was measured.

## 7.8 P207 (Westleigh 1000)

Although only two depths are measured in P207 (Westleigh), the $AD_{s>0.7}$ looks somewhat similar than that in P208 (Kroonstad) and P209 (Katspruit). The mean $AD_{s>0.7}$ value for the A horizon is 157 days $year^{-1}$ (Figure 7.8). The $AD_{s>0.7}$ range from 110 days in 1999 to 249 days in 2002. On average the s>0.7 events took place 2.5 times per year and each lasted 63 days. In the soft plinthic B1 (at 450 mm) the mean $AD_{s>0.7}$ is 232 days per year. The $AD_{s>0.7}$ varies from 131 days in 1999 to 366 days in 2000. The mean frequency of s>0.7 is 1.5 times per year, each event lasting 174 days. Unfortunately no deeper NWM measurements are available, due to a short pipe installed at this site.

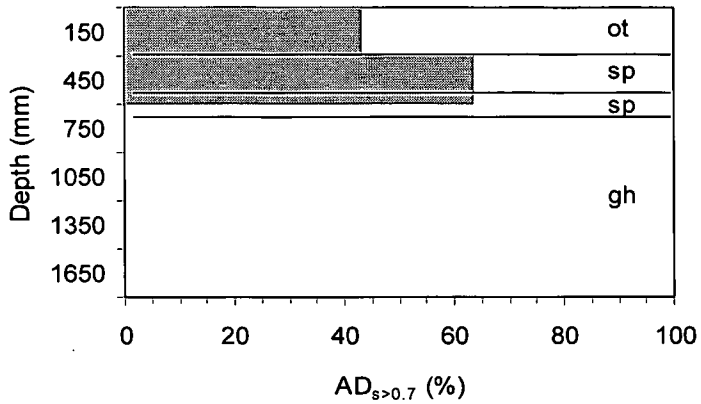


Figure 7.8 Mean $AD_{s>0.7}$ calculated from NWM measurements, for the three measuring depths at P207 (Westleigh 1000).

Fairly high $AD_{s>0.7}$ values in this profile are associated with the occurrence of Fe oxide mottles in the A and B1 horizons. The lack of deeper NWM measurements prevents interpretation of the morphology of the B2 and G horizons.

## 7.9 P208 (Kroonstad 1000)

The mean $AD_{s>0.7}$ value for the orthic A horizon is 212 days per year (Figure 7.9). The $AD_{s>0.7}$ range from 141 days in 1998 to 326 days in 2000. The mean frequency of s>0.7 events is 1.8 per year, with each lasting 127 days. The mean $AD_{s>0.7}$ value for the E horizon is 245 days per year, with $AD_{s>0.7}$ ranging from 145 days in 1999 to 352 days in 2000. The mean frequency of s>0.7 events is 2.2 times per year with each event lasting 122 days. Mean $AD_{s>0.7}$ values for the G horizon are 282 days per year at 750 mm and 354 days per year at 1 050, 1 350 and 1 650 mm. The water content therefore remains above 0.7 of porosity almost continuously at the lower three measuring depths.

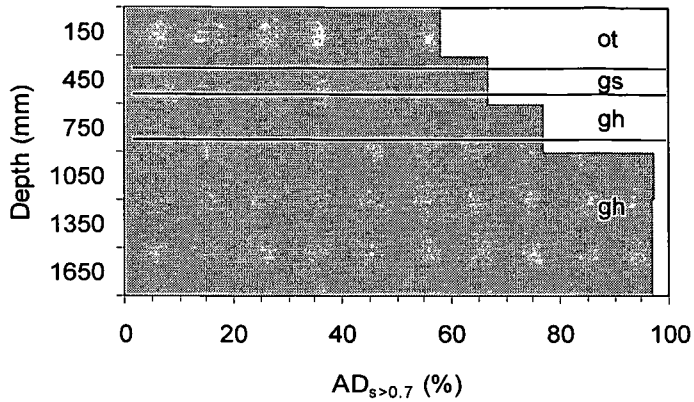


Figure 7.9 Mean $AD_{s>0.7}$ calculated from NWM measurements, for the three measuring depths at P208 (Kroonstad 1000).

This profile lies in a small seep, receiving water from three directions in the landscape. This, linked with high clay content in the G, results in the long periods of wetness. Wetness in the overlying A and E horizons is probably due to the lack of internal drainage. The shorter $AD_{s>0.7}$ in the G1 horizon can be linked to its position in the profile, and / or the slightly lower sand and higher silt content.

## 7.10 P209 (Katspruit 1000)

The mean $AD_{s>0.7}$ value for the orthic A horizon is 247 days per year (Figure 7.10). The $AD_{s>0.7}$ range from 181 days in 2001 to 314 days in 1998. The mean frequency of s>0.7 events is 2.5 per year, with each event lasting 99 days. The mean $AD_{s>0.7}$ at the boundary between the A and the G horizon is 339 days per year, with $AD_{s>0.7}$ ranging from 238 days in 2002 to 365 days in 1998. The mean frequency of s>0.7 events is 1.2 per year, with each event lasting 290 days. This horizon is therefore almost continuously wetter than 0.7 of porosity.

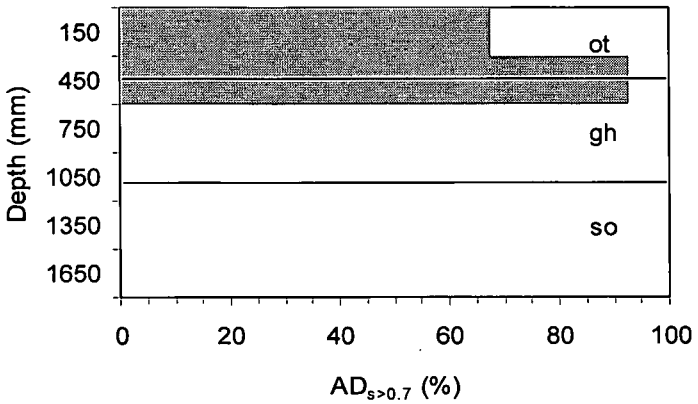


Figure 7.10 Mean $AD_{s>0.7}$ calculated from NWM measurements, for the three measuring depths at P209 (Katspruit 1000).

This profile is subjected to long periods of wetness, probably due to its location (Figure 3.3) in a little seep, just upslope from P208 (Kroonstad). Evidence of s>0.7 is the occurrence of many distinct Fe oxide mottles as well as many bleached and rusty pores in the A horizon. Many prominent Fe oxide mottles, Mn concretions as well as bleached and rusty pores occur in the G horizon.

## 7.11 P210 (Bloemdal 1100)

Annual duration of s>0.7 ($AD_{s>0.7}$) in the A horizon increased continuously from 0 days 1998 to 141 days in 2002 (Figure 7.11). This resulted in a mean $AD_{s>0.7}$ of 69 days per year. Frequency of s>0.7 events was 2.7 per year, with each event lasting 26 days. The reason for the continuous increase in wetness with time is not clear, but human-induced alteration of the surface topography, resulting in increased surface run-on cannot be ruled out. At 450 mm, the A horizon was much drier than at 150 mm (Figure 7.11), with a mean $AD_{s>0.7}$ value of 9 days per year, and $AD_{s>0.7}$ events ranging from 0 to 35 days. The mean $AD_{s>0.7}$ value for the red apedal B1 horizon is 11 days per year, with $AD_{s>0.7}$ ranging from 0 days in 1997 to 27 days in 1999. The mean frequency of s>0.7 events is less than once per year, with each event lasting 11 days. The mean $AD_{s>0.7}$ for the red apedal B2 horizon is 162 days per year, with $AD_{s>0.7}$ ranging from 77 days in 1999 to 270 days in 2002. The mean frequency of s>0.7 events is 4.2 per year, with each event lasting 29 days. At 1 350 mm the unspecified material with signs of wetness has a mean $AD_{s>0.7}$

value of 207 days per year, with $AD_{s>0.7}$ ranging events from 46 days in 1999 to 365 days in 2001. The mean frequency of s>0.7 was 4.5 events per year, lasting 46 days per event.

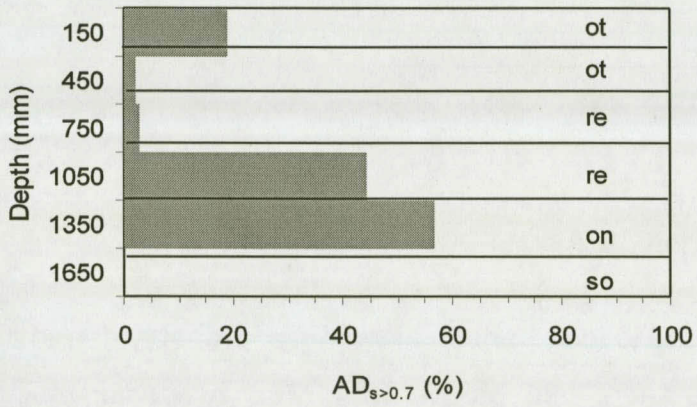


Figure 7.11 Mean $AD_{s>0.7}$ calculated from NWM measurements, for the three measuring depths at P210 (Bloemdal 1100).

Mean $AD_{s>0.7}$ in this profile was highly variable over the six-year study period. This is especially true in the A horizon at 150 mm, where $AD_{s>0.7}$ increased sharply from 0 days per year in 1997 to 141 day per year in 2002. Mean $AD_{s>0.7}$ in the C1 horizon also vary from 46 to 365 days per year. This can, however, be linked to variations in rainfall. The short period of $AD_{s>0.7}$ in the B1 was expected, given the red colour. The long duration $AD_{s>0.7}$ in the B2 was, however, not expected. This might be due to a degree of water accumulation above the unspecified material with signs of wetness that is insufficient to cause reduction and therefore redox morphology. A contributing factor may be wetness caused by oxygenated water that provides an electron acceptor for microorganisms and / or the absence of organic matter that inhibits the activity of microorganisms.

## 7.12 Summary

There is a good correlation between soil classification and soil profile hydrology. The hydromorphic P205 (Kroonstad), P206 (Kroonstad), P208 (Kroonstad) and P209 (Katspruit) soils have very high mean $AD_{s>0.7}$ values and are therefore almost continuously saturated above 0.7 of porosity. There are significant variations in the mean $AD_{s>0.7}$ values of the A horizons in these profiles. This seems to be linked to surface topography and is manifested in horizon morphology. The A horizons of profiles occurring in local seeps, normally in lower concave slope positions have high mean $AD_{s>0.7}$ values (212 – 365 days $year^{-1}$), and have common and many Fe oxide mottles. A horizons of profiles occurring in lower slope positions on local ridges have lower mean $AD_{s>0.7}$ values (< 25 days $year^{-1}$), and lack clear mottling.

The chromatic soils [P202 (Pinedene), P203 (Tukulu) and P210 (Bloemdal)] have yellow-brown apedal B, neocutanic B or red apedal B horizons respectively as the second horizon in the profile. These soils are much drier than the previous hydromorphic group. The A and B1 horizons have mean $AD_{s>0.7}$ values of less than 40 days per year, and mean $AD_{s>0.7}$ values in the underlying unspecified material with signs of wetness vary from 130 to 350 days per year. Some of these horizons can, however, be as saturated as unspecified material with signs of wetness. They normally occur deeper in the profile and have unspecified material with signs of wetness as the underlying horizon. For example, the measurement at 750 mm of P202 (Pinedene) encompassing the yellow-brown apedal B / unspecified material with signs of wetness transition has $AD_{s>0.7}$ of 309 days $year^{-1}$, while the red apedal B of the P210 (Bloemdal) is saturated for 162 days $year^{-1}$ at 1 050 mm. These horizons have a low organic carbon content and are therefore saturated for longer periods before reduced conditions occur.

P201 (Longlands), P204 (Longlands) and P207 (Westleigh) are characterised by the presence of a soft plinthic B horizon and have intermediate mean $AD_{s>0.7}$ values. It increases from 84 to 157 days per year in the orthic A horizon, to 80 – 232 days per year in the soft plinthic B horizon, and 365 days

per year in the underlying unspecified material with signs of wetness. The Longlands at P201 is much drier than the other profiles in this group. Its morphology and hydrology seem to correlate much better with the chromatic soils. This is expressed by the fact that the colour of the E horizon is on the boundary with that of the yellow-brown apedal B horizon.

It is clear from the above that soil form is a very good indicator of soil profile hydrology and can therefore be used as a first approximation of duration of wetness. These results do, however, not necessarily hold true beyond the boundaries of this catchment.

Most soil profiles have an aquic soil moisture regime, depending on the definition of the soil moisture control section (Soil Survey Staff, 1999). It is only P202 (Pinedene), P203 (Tukulu) and P210 (Bloemdal) that have an udic moisture regime. The aquic moisture regimes can be endosaturated or episaturated, depending on the time of year and the type of rain (Lorentz, 2003 personal communication).

# 8 DIAGNOSTIC HORIZON CHARACTERIZATION

## 8.1 Introduction

Duration of s>0.7 can be described in relation to soil profiles, or it can be described for each individual diagnostic horizon group. The South African soil classification system (Soil Classification Working Group, 1991) gives high priority to horizon identification in profiles. This makes it possible to characterize the diagnostic horizons in terms of diagnostic and non-diagnostic soil qualities. The aim of this chapter is to characterize diagnostic horizon hydrology and to propose subdivisions, when appropriate.

Due to the few individual horizons available in this study, the red apedal B, yellow-brown apedal B and neocutanic B horizons were grouped to form the chromatic horizons.

The means and standard errors of the means per diagnostic horizon group for $AD_{s>0.7}$ is given in Figure 8.1, for clay content in Figure 8.2, for texture in Figure 8.3, for organic carbon content in Figure 8.4, for sum of basic cations in Figure 8.5, for nitrogen content in Figure 8.6, for pH in Figure 8.7, for Fe content in Figure 8.8, for Mn content in Figure 8.9 and for base saturation in Figure 8.10.

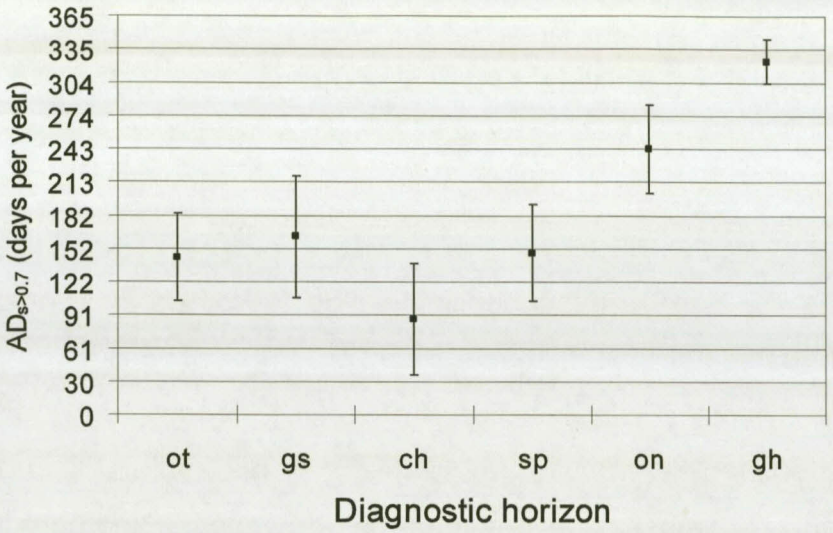


Figure 8.1 Mean and standard error of mean $AD_{s>0.7}$ per diagnostic horizon group.

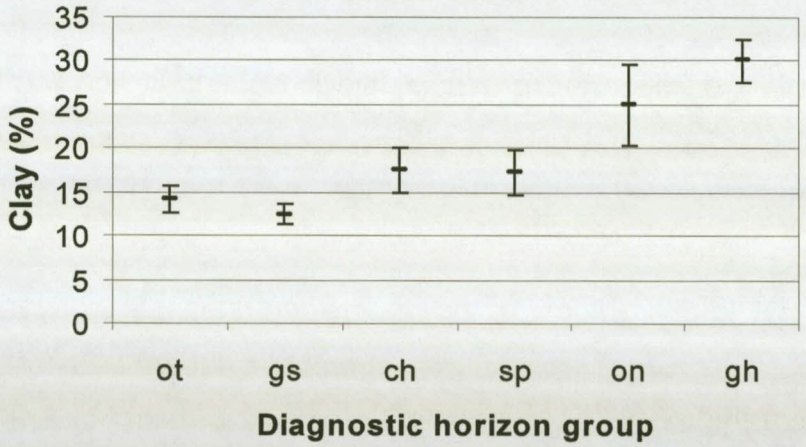


Figure 8.2 Mean and standard error of clay content, per diagnostic horizon group.

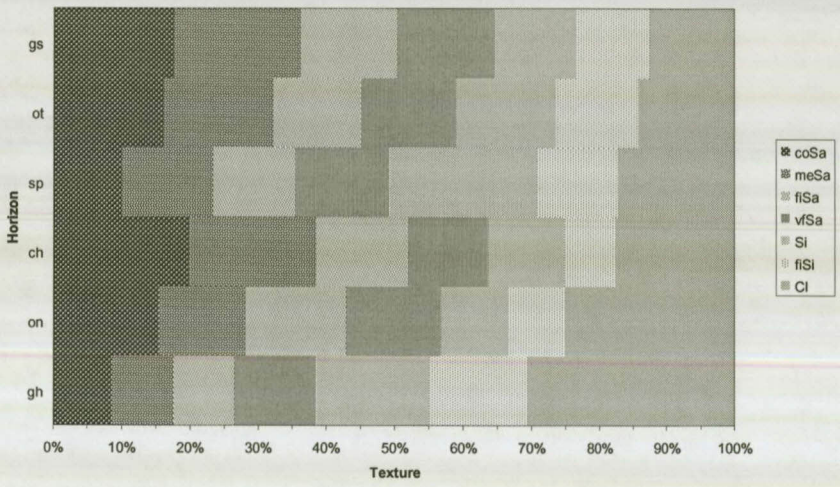


Figure 8.3 Mean texture for the diagnostic horizon groups.

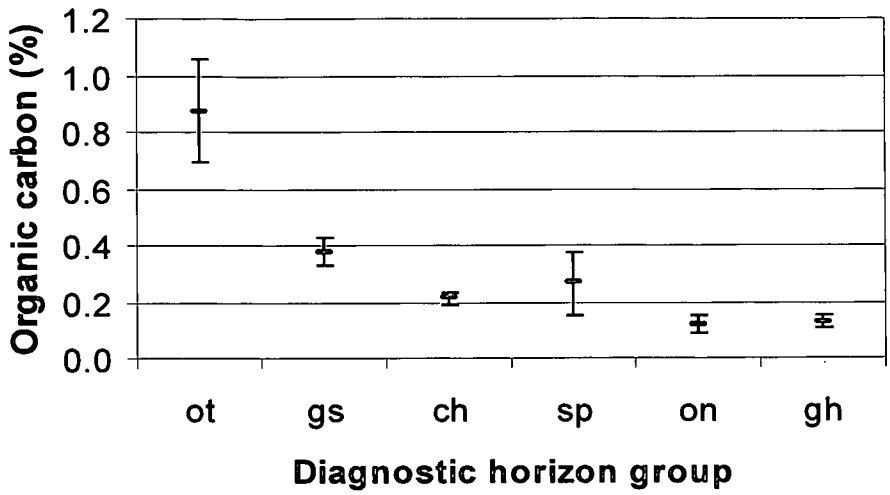


Figure 8.4 Organic carbon mean and standard error, per diagnostic horizon group.

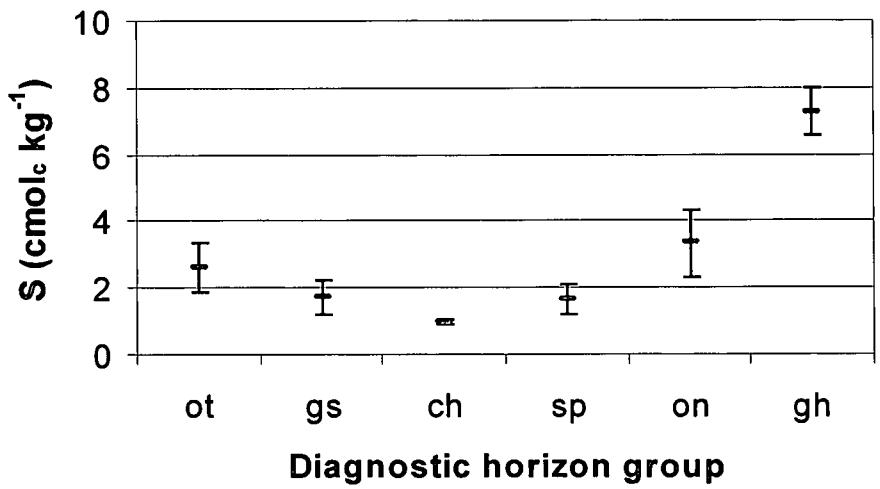


Figure 8.5 Mean and standard error of the sum of basic cations (S), per diagnostic horizon group.

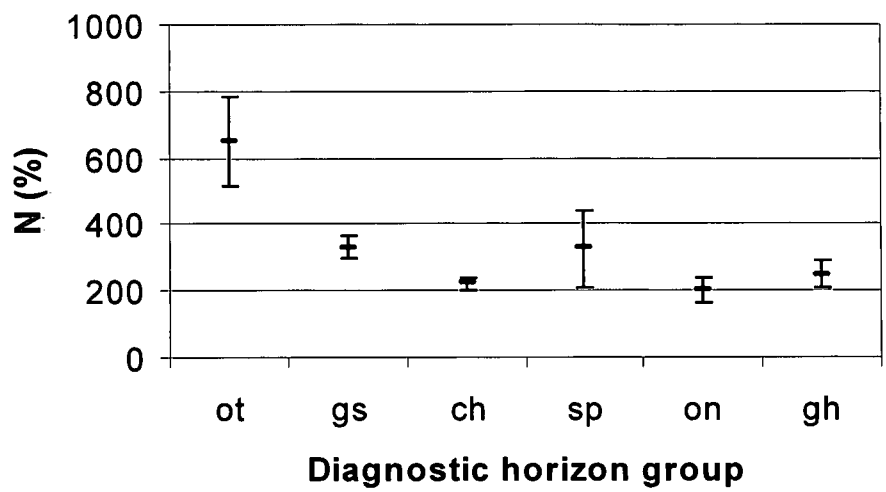


Figure 8.6 Nitrogen (N) mean and standard error, per diagnostic horizon group.

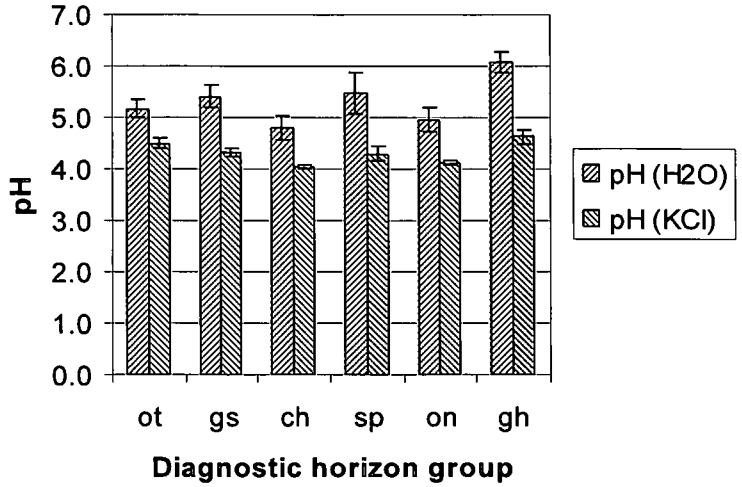


Figure 8.7 Mean and standard error of pH, per diagnostic horizon group.

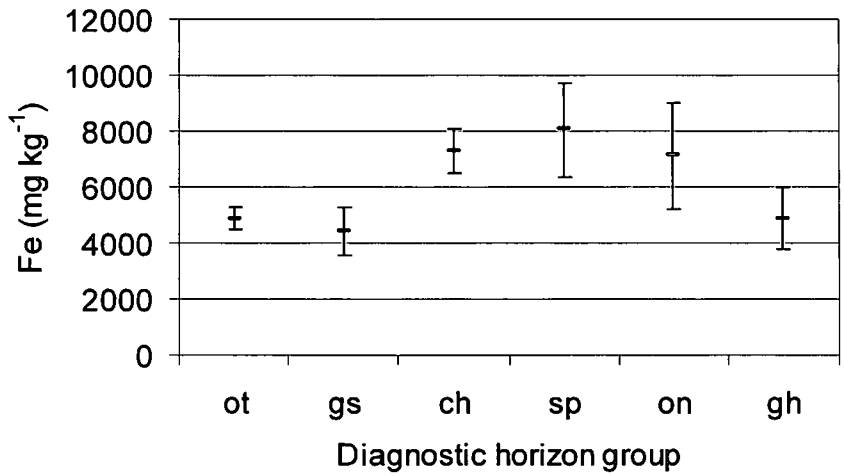


Figure 8.8 Mean and standard error of Fe, per diagnostic horizon group.

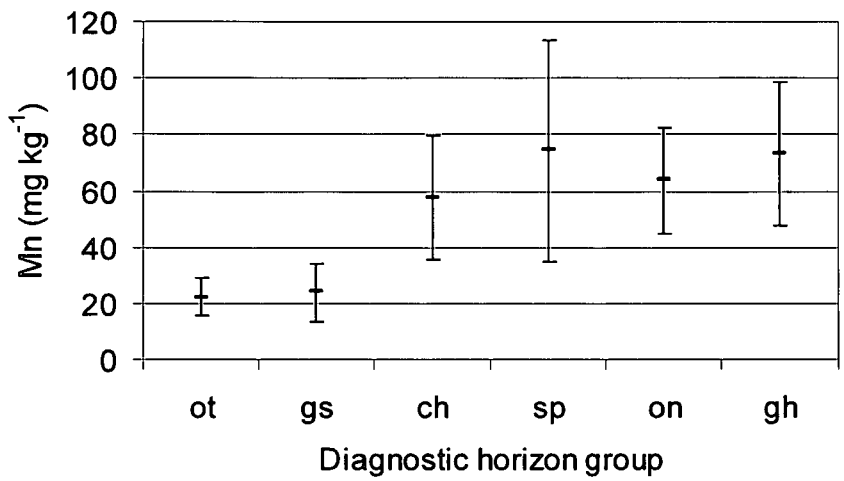


Figure 8.9 Mean and standard error of Mn, per diagnostic horizon group.

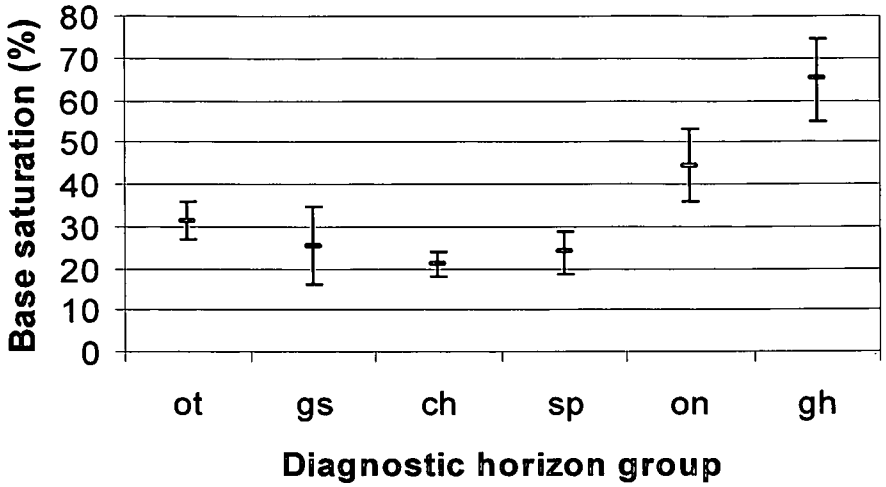


Figure 8.10 Base saturation mean and standard error, per diagnostic horizon group.

## 8.2 Orthic A horizons

Orthic A horizons (ot) have varying properties, including degrees of wetness. This is mainly due to the definition by which all non-organic, vertic, humic or melanic A horizons are classified as orthic A horizons (Soil Classification Working Group, 1991). The properties of orthic A horizons can, however, largely be determined by inference from the underlying horizons (Le Roux *et al,* 1999).

Eleven orthic A horizons are included in this study. One from each of the ten profiles, and with two (0-300 mm and 300-600 mm) described for profile 210. The varied nature of orthic A horizons is clear from the soils used in this study. Mean $AD_{s>0.7}$ range from 0 to 360 days per year (Figure 8.1), clay content from 8 to 23 % (Figure 8.2 and Figure 8.3) and organic carbon content from 0.3 to 4.4 % (Figure 8.4).

The mean value of the sum of basic cations (2.58 $cmol_c\ kg^{-1}$ with standard error of 0.74 $cmol_c\ kg^{-1}$), is significantly higher in the orthic A horizons, than in the soft plinthic B, or chromatic horizons (Figure 8.5). This is probably due to biocycling, resulting in the accumulation of organic matter and basic cations in the topsoil. The higher organic carbon content could also result in a higher CEC, resulting in increased adsorption of basic cations. Basic cation

concentration in the orthic A horizon is, however, lower than in the G horizons or unspecified material with signs of wetness. This is largely due to cation accumulation in these horizons, due to lateral leaching from up-slope profiles and vertical leaching from the overlying horizons.

Organic carbon and nitrogen are higher in the orthic A horizons than in E, chromatic, soft plinthic B, G horizons or unspecified material with signs of wetness (Figure 8.4 & Figure 8.6). The higher organic carbon and nitrogen contents are most probably due to the proliferation of plant roots in the topsoil, followed by the accumulation of organic matter upon humification and slow mineralization thereof.

$pH_{KCl}$ in orthic A horizons is third lowest, and $pH_{Water}$ second lowest of the diagnostic horizon groups (Figure 8.7). This indicates increased residual acidity in orthic A horizons, probably due to the accumulated organic matter. The lower pH points to increased leaching of basic cations from the orthic A horizons as well as the increased acidity of organic matter, that is higher in these horizons. Other variables did not differ significantly between orthic A and the other horizons.

Wetness classes (in terms of duration) as defined by the USDA's Soil Survey Division Staff (1993) are presented in Table 8.1. The degree of saturation (volumetric water as a fraction of porosity) where the soil is considered to be wet was, however, not specified. The orthic A horizons of this study are ranked according to these classes in Table 8.2. There is a reasonably good agreement between the defined Soil Survey Division Staff (1993) wetness classes and the measured mean $AD_{s>0.7}$ for orthic A horizons in this study.

There is also a good relationship between defined wetness classes of the orthic A horizons and nature of the underlying horizon. Wetness class A has yellow-brown apedal B, red apedal B and neocutanic B horizons as the underlying horizon. The occurrence of the second E horizon in profile 201 in wetness class A can be explained by the fact that it is a border-line case as far

as colour is concerned and at least one researcher classified it as yellow-brown apedal B (Roberts *et al.*, 1996).

This wetness class had no mottles, except for profile 201 where few, and for profile 209, where many mottles were described.

Wetness classes B, C and D seem to be restricted to orthic A horizons overlying E, soft plinthic B and G horizons. There does not seem to be a meaningful differentiation in terms of underlying horizon between these wetness classes. The occurrence of mottles and matrix colour can, however, be used as a further differentiation.

Orthic A horizons in the B wetness class are those in profiles 210 and 204. The mean $AD_{s>0.7}$ data for profile 210 at 150 mm is highly suspect, as it increases yearly (Table 7.1). It seems that the pale colour (Chroma = 2) of these orthic A horizons might be indicative of the longer duration of water saturation. The orthic A horizons in the C wetness class had few and many mottles, with matrix Chroma equal to 1 and 2.

Table 8.1 Classes of duration of the wet state (Soil Survey Division Staff, 1993)

| Wetness class | Description | Saturation | |
|---|---|---|---|
| | | (months year$^{-1}$) | (days year$^{-1}$) |
| A | Well drained | < 1 | < 30 |
| B | Moderately well drained | 1 – 4 | 30 – 122 |
| C | Moderately to poorly drained | 4 – 6 | 122 – 183 |
| D | Poorly drained | > 6 | > 183 |

Wetness class D had either common or no mottles described. No mottles were described in the A horizon of profile 205. This horizon does, however, have a very pale colour with a chroma of 1.

Table 8.2 Classification of mean $AD_{s>0.7}$ in orthic A horizons according to the wetness classes of Soil Survey Division Staff (1993)

| Profile No | Depth (mm) | Diagnostic horizon | Mean $AD_{s>0.7}$ (days $year^{-1}$) | Wetness class | (days $year^{-1}$) | Underlying horizon | Occurrence of mottles |
|---|---|---|---|---|---|---|---|
| 202 | 150 | ot | 0 | A | | ye | none |
| 203 | 150 | ot | 0 | A | | ne | none |
| 201 | 150 | ot | 7 | A | < 30 | gs | few |
| 210 | 450 | ot | 9 | A | | re | none |
| 205 | 150 | ot | 23 | A | | gs | none |
| 210 | 150 | ot | 69 | B | 30-122 | ot | none |
| 204 | 150 | ot/gs | 84 | B | | gs | few |
| 207 | 150 | ot | 157 | C | 122-183 | sp | common |
| 208 | 150 | ot | 212 | D | | gs | common |
| 209 | 150 | ot | 339 | D | > 183 | ot/gh | many |
| 209 | 450 | ot/gh | 339 | D | | gh | many |
| 206 | 150 | ot | 361 | D | | gs | few |

## 8.3 E horizons

E horizons (gs) are *inter alia* defined as a grey horizon, having undergone marked *in situ* nett removal of colloidal material, defined as Fe oxides, silicate clays and organic matter (Soil Classification Working Group, 1991).

The mean $AD_{s>0.7}$ in E horizons (Table 8.3) varies from 24 days per year in profile 201 to 361 days per year in profile 206 (Table 7.4), with a group mean of 163 days per year and standard error of 56 days per year. The colour of the E horizon in profile 201 is close to that of a yellow-brown apedal B horizon. It can therefore be expected to have a relatively dry water regime. The mottles in this horizon are bleached, indicating somewhat more Fe oxide removal than Fe oxide accumulation, as in the other E horizons.

The relatively dry E horizon (Table 7.4) of profile 205 (mean $AD_{s>0.7}$ = 34 days per year) can only be attributed to the location of the profile on a local ridge. It is possible that the water regime in this profile has changed over time, as the local drainage lines shifted. This horizon is characterized by many Fe oxide mottles and a very pale 2.5Y6/1 colour.

Table 8.3 Classification of mean $AD_{s>0.7}$ in E horizons (gs) using the wetness classes of the Soil Survey Division Staff (1993)

| Profile No | Depth (mm) | Diagnostic horizon | Mean $AD_{s>0.7}$ (days year$^{-1}$) | Wetness class | Underlying horizon | Mottle occurrence |
|---|---|---|---|---|---|---|
| 201 | 450 | gs | 24 | A | sp | many |
| 205 | 450 | gs | 34 | A | gh | many |
| 204 | 150 | gs | 84 | B | sp | many |
| 208 | 450 | gs | 245 | D | gh | many |
| 206 | 450 | gs | 361 | D | gh | common |

The E horizons in profile 206 and 208 have mean $AD_{s>0.7}$ larger than 232 days per year. They therefore fall into the "poorly drained" wetness class (Soil Survey Division Staff (1993). These horizons also occur exclusively on G horizons, or unspecified material with signs of wetness. These horizons have common or many Fe oxide mottles. The colour is mainly pale (10YR5/1, 10YR6/3 and 10YR6/2). It is therefore proposed that E horizons occurring on G horizons and unspecified material with signs of wetness should be classified as poorly drained, while those occurring on soft plinthic B horizons should be classified as well and moderately well drained.

The sum of basic cations (1.71 $cmol_c\ kg^{-1}$ with standard error of 0.54 $cmol_c\ kg^{-1}$) is significantly lower in E horizons than in G horizons or unspecified material with signs of wetness (Figure 8.5). The sum of basic cations (S) is higher in E than in chromatic horizons. The sum of basic cations is equal in E and soft plinthic B horizons. These relationships are indicative of accumulation of basic cations in G horizons and unspecified material with signs of wetness, with associated removal from orthic A, E and soft plinthic B horizons.

The clay content in E horizons, with a mean of 12.5 % and standard error of 1.1 %, (Figure 8.2) is significantly lower than in the other horizons, except for the orthic A horizons, which have a similar clay content. The mean CBD extractable Fe (4 444 mg $kg^{-1}$, with standard error of 859 mg $kg^{-1}$), and Mn (23.8 mg $kg^{-1}$, with standard error of 10.2 mg $kg^{-1}$), is also significantly lower in E horizons than in the chromatic, soft plinthic B and unspecified material

with signs of wetness (Figure 8.8 & Figure 8.9). Mn in E horizons is also significantly lower than in the G horizons. This supports their classification which stipulates net removal of colloidal material relative to the over and underlying horizons (Soil Classification Working Group, 1991). Because the clay content is not significantly lower in the E than in the orthic A, this criterion is the only one not met for these E horizons. Both the other specified components of "colloidal matter", viz. Fe oxides and organic matter, are considerably lower in E horizons than in the orthic A horizons. It might also be that orthic A horizons have undergone clay removal, in association with E horizons, through increased reduction and leaching of Fe oxides, causing clay degradation through ferrolysis (Brinkman, 1979). It should also be kept in mind that data for the orthic A horizons includes all orthic A horizons and not only those that occur above E horizons.

## 8.4 G horizons

G horizons (gh) are saturated for long periods and have grey colours on the macro pore and ped surfaces. They have not undergone marked removal of colloidal material, as in the case of E horizons, but are rather characterized by the accumulation of colloidal material, as defined by the Soil Classification Working Group (1991).

With a mean $AD_{s>0.7}$ of 324 days per year, with standard error of 20 days per year, the G horizons have significantly longer mean $AD_{s>0.7}$ than all other diagnostic horizons (Figure 8.1). This is a result of the high clay content and high bulk density in these horizons, as well as the position of the horizons in the landscape, normally as the end member in a catena. All G horizons fall into the "poorly drained" wetness class (Table 8.4), with the exception of the upper G horizon (450 mm) in P204 (Longlands).

The sum of basic cations (7.26 $cmol_c\ kg^{-1}$, with standard error of 0.70 $cmol_c\ kg^{-1}$), as well as base saturation (65 %, with standard error of 10 %) is significantly higher than in the other horizons (Figure 8.5 & Figure 8.10). Clay

content in the G horizons (30.0 %, with standard error of 2.3 %) is also significantly higher than in orthic A, E, soft plinthic B or chromatic horizons (Figure 8.2). The CBD extractable Fe is significantly lower than in the soft plinthic B and chromatic horizons, while the CBD extractable Mn is significantly higher than E and orthic A horizons (Figure 8.8 & Figure 8.9). The data presented here designates horizons where clay and Mn accumulate, while Fe is removed to some extent. The accumulation of clay and Mn therefore conforms to the diagnostic criteria of G horizons (Soil Classification Working Group, 1991), requiring accumulation of colloidal matter, except for Fe that is removed to some extent.

Table 8.4 Classification of mean $AD_{s>0.7}$ in G horizons (gh) according to the wetness classes of Soil Survey Division Staff (1993)

| Profile No | Depth (mm) | Diagnostic horizon | Mean $AD_{s>0.7}$ (days $year^{-1}$) | Wetness class | Occurrence of mottles | Type of mottles |
|---|---|---|---|---|---|---|
| 208 | 750 | gh | 282 | D | common | Fe |
| 209 | 450 | gh | 339 | D | many | Fe |
| 208 | 1350 | gh | 354 | D | many | Fe |
| 208 | 1650 | gh | 354 | D | many | Fe |
| 208 | 1050 | gh | 356 | D | many | Fe |
| 206 | 750 | gh | 359 | D | many | Fe |
| 206 | 1050 | gh | 361 | D | many | Fe |
| 205 | 750 | gh | 369 | D | common | Fe |
| 205 | 1050 | gh | 369 | D | common | Fe |
| Mean | | | 324 | D | | |

## 8.5 Chromatic (re, ye, ne) horizons

The red apedal B (re) and yellow-brown apedal (ye) B horizons are defined by virtue of their high chroma (typically a chroma of 3 or 5 or more). They lack structure and are non-calcareous. The neocutanic B horizon (ne) is defined as being non-calcareous and having undergone limited pedogenesis (Soil Classification Working Group, 1991). In this study, it is grouped with the red apedal B and yellow-brown apedal B horizons due to its dull orange colour (it meets the colour requirements for a yellow E horizon, but lacks the required removal of colloidal material). This group is termed the chromatic horizons (ch). It is postulated that the lack of pedogenesis in neocutanic B horizons is

the result of the dry water regime in these horizons (Figure 8.1). This does not explain the grey (bleached) colours in the neocutanic B horizon. The lack of redness may be due either to the lack of Fe in the parent material, or the possibility that Fe has not yet been released from the parent material.

Mean $AD_{s>0.7}$ in chromatic horizons is 88 days $year^{-1}$, with a standard error of 51 days $year^{-1}$. It is the driest diagnostic horizon group, although it is not significantly different from the E, soft plinthic B and orthic A horizons. Chromatic horizons fall into the A, B, C and D wetness classes (Table 8.5). The wetter chromatic horizons are typically deeper than 600 mm, and occur on unspecified material with signs of wetness.

Table 8.5 Classification of mean $AD_{s>0.7}$ in red apedal B (re), yellow-brown apedal B (ye) and neocutanic B (ne) horizons, according to the wetness classes of Soil Survey Division Staff (1993)

| Profile No | Depth (mm) | Diagnostic horizon | Mean $AD_{s>0.7}$ (days $year^{-1}$) | Wetness class | Occurrence of mottles | Type of mottles |
|---|---|---|---|---|---|---|
| 203 | 450 | ne | 0 | A | common | Fe |
| 202 | 450 | ye | 7 | A | few | Fe |
| 210 | 750 | re | 11 | A | many | humus |
| 203 | 750 | ne | 38 | B | common | Fe |
| 210 | 1050 | re | 162 | C | many | humus |
| 202 | 750 | ye | 309 | D | few | Fe |
| Mean | | | 88 | B | | |

Only the G horizons and unspecified material with signs of wetness have significantly higher clay content (Figure 8.2) than the chromatic horizons (17.5 % with standard error of 2.5 %). The clay content in the chromatic horizons is significantly higher than in the E horizons, but it is not significantly different to the clay content in soft plinthic B or orthic A horizons. The difference in clay content between chromatic horizons on the one hand and G horizons as well as unspecified material with signs of wetness on the other hand, is probably due to clay accumulation in the latter, in contrast to clay removal from the former.

The sum of basic cations (0.97 $cmol_c\ kg^{-1}$, with standard error of 0.07 $cmol_c\ kg^{-1}$), and base saturation (21 %, with standard error of 3 %) are significantly lower in the chromatic horizons than in orthic A, G horizons and unspecified material with signs of wetness, but not significantly different to in the soft plinthic B and E horizons (Figure 8.5 & Figure 8.10).

The organic carbon content in chromatic horizons (0.21 %, with standard error 0.02 %), is extremely low (Figure 8.4). It is significantly lower than in orthic A or E horizons, but significantly higher than in G horizons and unspecified material with signs of wetness. It does not differ significantly from the organic carbon content in soft plinthic B horizons. The low organic carbon content can be expected in subsoil horizons, where plant roots are less prolific than at the soil's surface. The expected better aeration (lower degree of water saturation) in chromatic horizons would also lead to increased organic matter mineralization and therefore a lower organic carbon content.

CBD extractable Fe (7 295 $mg\ kg^{-1}$, with standard error 1 681 $mg\ kg^{-1}$) is significantly higher in chromatic horizons than in orthic A, E and G horizons (Figure 8.8). It does not differ significantly from the Fe content in soft plinthic B horizons and unspecified material with signs of wetness. The higher Fe content explains the high chroma of these horizons. It is indicative of less removal of Fe from the chromatic horizons than from the orthic A, E or G horizons.

CBD extractable Mn (57.6 $mg\ kg^{-1}$, with standard error 22.1 $mg\ kg^{-1}$) is not significantly different to that in soft plinthic B, G horizons and unspecified material with signs of wetness (Figure 8.9). It is, however, significantly higher than in orthic A and E horizons. The high Mn content in chromatic horizons is indicative of less removal of Mn from the chromatic horizons than from orthic A of E horizons.

## 8.6 Soft plinthic B horizons

Soft plinthic B horizons (sp) form due to the localisation and accumulation of Fe and Mn oxides under a fluctuating water table (Soil Classification Working Group, 1991).

Soft plinthic B horizons have mean $AD_{s>0.7}$ of 148 days per year, with a standard error of 45 days per year. This is significantly lower than in G horizons and unspecified material with signs of wetness (Figure 8.1). It does, however, not differ significantly from the mean $AD_{s>0.7}$ in orthic A, E and chromatic horizons. Soft plinthic B horizons fall into the B, C and D wetness classes (Table 8.6).

Table 8.6 Classification of mean $AD_{s>0.7}$ in soft plinthic B horizons according to the wetness classes of Soil Survey Division Staff (1993)

| Profile No | Depth (mm) | Diagnostic horizon | Mean $AD_{s>0.7}$ (days $year^{-1}$) | Wetness class | Occurrence of mottles | Type of mottles |
|---|---|---|---|---|---|---|
| 201 | 750 | sp | 80 | B | many | Fe |
| 204 | 450 | sp | 133 | C | common | Fe |
| 207 | 450 | sp | 232 | D | many | Fe |
| Mean | | | 148 | C | | |

The clay content in soft plinthic B horizons (17.3 % with standard error of 2.6 %) is significantly lower than in G horizons or unspecified material with signs of wetness (Figure 8.2). It is significantly higher than the clay content in E horizons, but does not differ significantly from the clay content in orthic A or chromatic horizons.

The sum of basic cations in soft plinthic B horizons (1.64 $cmol_c\ kg^{-1}$ with standard error of 0.44 $cmol_c\ kg^{-1}$) is significantly lower than in G horizons or unspecified material with signs of wetness; lower than in orthic A horizons, but not significantly so; significantly higher than in chromatic horizons (Figure 8.5). Base saturation follows the same trend (Figure 8.10).

Organic carbon in soft plinthic B horizons (0.26 %, with standard error of 0.11 %) is significantly lower than in orthic A horizons and significantly higher

than in G horizons or unspecified material with signs of wetness (Figure 8.4). It does, however, not differ significantly from the organic carbon content in E or chromatic horizons. There is therefore more organic substrate available for micro organisms, that could lead to reduction under anaerobic conditions, in soft plinthic B horizons than in G horizons or unspecified material with signs of wetness. This would indicate that, given the same $AD_{s>0.7}$ values, soft plinthic horizons will be subjected to more reduced conditions than the G horizons or unspecified material with signs of wetness.

CBD extractable Fe in soft plinthic B horizons (8 069 mg $kg^{-1}$, with standard error 1 681 mg $kg^{-1}$) is significantly higher than in orthic A, E or G horizons (Figure 8.8). It does, however, not differ significantly from the CBD extractable Fe in unspecified material with signs of wetness or chromatic horizons. The high CBD extractable Fe supports the underlying pedogenic concept, expressed in the definition for soft plinthic B horizons, i.e. the localization and accumulation of Fe under conditions of a fluctuating water table (Soil Classification Working Group, 1991).

CBD extractable Mn in soft plinthic B horizons (74.3 mg $kg^{-1}$, with standard error 39.4 mg $kg^{-1}$) is significantly higher than in orthic A and E horizons, but does not, however, differ significantly from the values for G and chromatic horizons or unspecified material with signs of wetness (Figure 8.9). The high CBD extractable Mn content in soft plinthic B horizons also supports the pedogenic concept of soft plinthic B horizons.

## 8.7 Unspecified material with signs of wetness

The properties of unspecified material with signs of wetness (on) vary considerably. The main diagnostic criterion is the presence of grey, low chroma matrix colours due to the reduction and loss of Fe oxides (Soil Classification Working Group, 1991). It is therefore analogous to the G horizons and unconsolidated material with signs of wetness (Soil Classification Working Group, 1991), the main difference being its occurrence under a red

apedal, neocutanic or neocarbonate B horizon. In this study, the material underlying a soft plinthic B was also included into this group.

The mean $AD_{s>0.7}$ in unspecified material with signs of wetness is 243 days per year with a standard error of 40 days per year (Figure 8.1). This is significantly higher than the value for the soft plinthic B, orthic A and chromatic horizons, and significantly lower than the value in G horizons. Although the mean $AD_{s>0.7}$ is higher than in E horizons, the difference is not significant. Unspecified material with signs of wetness fall into the C and D wetness classes (Table 8.7).

Table 8.7 Classification of mean $AD_{s>0.7}$ in unspecified material with signs of wetness (on) according to the wetness classes of Soil Survey Division Staff (1993)

| Profile No | Depth (mm) | Diagnostic horizon | Mean $AD_{s>0.7}$ (days $year^{-1}$) | Wetness class | Occurrence of mottles | Type of mottles |
|---|---|---|---|---|---|---|
| 203 | 1350 | on | 127 | C | many | Fe |
| 203 | 1650 | on | 130 | C | many | Fe |
| 203 | 1050 | on | 180 | C | many | Fe |
| 210 | 1350 | on | 207 | D | none | Fe |
| 202 | 1650 | on | 350 | D | many | Fe |
| 202 | 1350 | on | 354 | D | many | Fe |
| 202 | 1050 | on | 356 | D | many | Fe |
| Mean | | | 243 | D | | |

The clay content in unspecified material with signs of wetness (24.9 % with a standard error of 4.7 %) is significantly higher than in orthic A, soft plinthic B, chromatic or E horizons (Figure 8.2). It does not differ significantly from the clay content in G horizons. The high clay content is indicative of a cumulative environment, similar to that of G horizons.

The sum of basic cations in unspecified material with signs of wetness (3.32 $cmol_c\ kg^{-1}$ with standard error of 1.00 $cmol_c\ kg^{-1}$) is significantly lower than in G horizons (Figure 8.5). It is significantly higher than in soft plinthic B, E and chromatic horizons and does not differ significantly from that in orthic A horizons. Base saturation follows the same trend, except that it is significantly higher in unspecified material with signs of wetness than in orthic A, soft

plinthic B, E or chromatic horizons, and significantly lower than in G horizons (Figure 8.10).

Organic carbon content (Figure 8.4) is very low in unspecified material with signs of wetness (0.12 % with standard error of 0.11 %). It is significantly lower than in orthic A, soft plinthic B, E, or chromatic horizons, but does not differ significantly from the organic carbon content in G horizons. The low organic carbon content in G horizons and unspecified material with signs of wetness is possibly a result of the location of these horizons lower down in profiles, where plant root activity is lower than in the surface horizons. It could further be indicative of saturated conditions in these horizons that would restrict root development due to anaerobic conditions.

CBD extractable Fe (7 116 mg $kg^{-1}$ with standard error of 1 880 mg $kg^{-1}$) is higher in unspecified material with signs of wetness than in orthic A, E or G horizons, but the difference is not significant (Figure 8.8). The value is similar to that in soft plinthic B and chromatic horizons. The higher Fe content in unspecified material with signs of wetness indicates a cumulative environment, similar to that of G horizons.

CBD extractable Mn (63.9 mg $kg^{-1}$ with standard error of 18.8 mg $kg^{-1}$) is significantly higher in unspecified material with signs of wetness than in orthic A or E horizons; and similar to soft plinthic B, G and chromatic horizons (Figure 8.9). The relatively high Mn content indicates a cumulative environment, as is the case with the higher Fe content.

## 8.8 Summary

Orthic A horizons can be meaningfully subdivided, to differentiate between wetness classes. Subdivision is mainly on the nature of the underlying horizon, with orthic A horizons on red apedal B, yellow-brown apedal B and neocutanic horizons classified in the A wetness class (Table 8.1). Orthic A horizons in the B wetness class occur on E horizons and have either no or few

mottles. Orthic A horizons in the C wetness class occur on E and G horizons and have few to many mottles. The orthic A horizons in the D wetness class occur on soft plinthic B and E horizons and have common mottles.

As expected, the orthic A horizons have the highest organic carbon and nitrogen content. The organic carbon content is lowest in G horizons and unspecified material with signs of wetness. There is no significant difference in the organic carbon content of soft plinthic B, E or chromatic horizons. The nitrogen content is also similar between soft plinthic B, E, G and chromatic horizons as well as unspecified material with signs of wetness.

Sum of bases is only significantly higher in orthic A horizons than in the chromatic horizons and is significantly lower than in G horizons. There is no significant difference in sum of basic cations between orthic A, soft plinthic B and E horizons or unspecified material with signs of wetness.

The clay content does not differ significantly between soft plinthic B, orthic A or chromatic horizons. It is, however, significantly higher in G horizons and unspecified material with signs of wetness and is lowest in E horizons.

Total Fe content is higher in soft plinthic B and chromatic horizons as well as unspecified material with signs of wetness. It is lower in orthic A, E and G horizons. Total Mn content shows the same trend as the total Fe content, except that two clear groups can be distinguished. Soft plinthic B, G, chromatic horizons and unspecified material with signs of wetness, have a higher total Mn content, while orthic A, E and G horizons have a significantly lower Mn content.

The chemical and physical analyses as well as mean $AD_{s>0.7}$ generally support the classification of diagnostic horizons (Soil Classification Working Group, 1991). This implies that diagnostic horizons can be used to infer these properties, within the current research environment.

# 9 CONCLUSIONS AND RECOMMENDATIONS

The aim of this study was to characterize and quantify the soil water regime and soil profile morphology in the Weatherley catchment, situated close to Maclear in the northern Eastern Cape Province, and to determine the relationship between soil water regime and soil profile morphology.

The parent material in the catchment consists of Elliott and Molteno sandstone. Mean annual rainfall is 741 mm while Class A-pan evaporation is 1 490 mm. Ten soil profiles in the catchment were described and analysed in detail. The results of neutron water meter measurements from January 1997 until December 2002 are included in this study.

Profile morphology indicates that $AD_{s>0.7}$ increases from P201 (Longlands) to P204 (Longlands), situated on the first upslope part of the eastern catena. Soils down this catena become more clayey, CEC and base saturation increases. $CEC_{soil}$ increases from approximately 3.5 $cmol_c\ kg^{-1}$ in P201 (Longlands) to 11.5 $cmol_c\ kg^{-1}$ in P204 (Longlands). The base saturation increases from 25 % in P201 to 44 % in the subsoil of P204 (Longlands), while the underlying unspecified material with signs of wetness and G horizons also occur closer to the soil surface.

Profiles P205 (Kroonstad), P206 (Kroonstad), P208 (Kroonstad) and P209 (Katspruit) are in lower slope positions relative to the crest of the watershed. P205, P206 and P208 were classified as Kroonstad, while P209 was classified as Katspruit. These profiles are similar in the sense that they develop in wet, cumulative environments. $CEC_{soil}$ (10 – 15 $cmol_c\ kg^{-1}$), base saturation (> 50 %) and $pH_{Water}$ (> 5.5) therefore tend to be higher than in the other higher lying profiles.

P207 (Westleigh) is somewhat of an outlier, since it is situated close to the stream and is therefore characterized by a highly variable parent material. $CEC_{soil}$ is

between 10 and 15 $cmol_c\ kg^{-1}$, while the base saturation is between 25 and 60 %. It seems that this profile has undergone localization and accumulation of Fe to form a soft plinthic B horizon. The CBD extractable Fe content increases from < 4 000 mg $kg^{-1}$ in the overlying horizon to 12 600 mg $kg^{-1}$ in the soft plinthic B horizon and then decreases to < 4 000 mg $kg^{-1}$ in the underlying horizon.

P210 (Bloemdal), in an upslope position (Figure 3.3), seems to have the driest water regime in terms of its morphology. It is sandy in nature (< 20 % clay) and is therefore well drained, except for the underlying unspecified material with signs of wetness. The profile has a characteristic red colour, which is pale in the dry state. Clay content, $CEC_{soil}$ (< 6.0 $cmol_c\ kg^{-1}$), base saturation (< 30 %) and $pH_{Water}$ (< 5.3) are indicative of a well leached profile. The accumulation of Fe and Mn relative to clay at 1 000 to 1 100 mm depth indicates that it was subjected to plinthitisation for at least short periods.

The water content in subsoils of the Kroonstad and Katspruit soils (P205, P206, P208 and P209) is almost continuously above 0.7 of porosity, while significant variations occur in their orthic A horizons. This seems to be linked to surface topography and is manifested in horizon morphology. Orthic A horizons that occur in local seeps have high mean $AD_{s>0.7}$ (212 – 365 days $year^{-1}$) and have common and many Fe oxide mottles, while those occurring on local ridges have lower mean $AD_{s>0.7}$ (< 25 days $year^{-1}$), and lack clear mottling.

The Longlands (P201 and P204) and Westleigh (P207) soils, characterized by the occurrence of a soft plinthic B horizon, have intermediate mean $AD_{s>0.7}$. Mean $AD_{s>0.7}$ in these soils increases from 84 to 157 days per year in the A, to 232 days per year in the soft plinthic B, and then to 365 days per year in the underlying unspecified material with signs of wetness. The Longlands profile (P201) is much drier than the other profiles in this group, and its degree of wetness is similar to the chromatic soils. This is expressed by the colour of the E horizon which is on the colour definition boundary with that of the yellow-brown apedal B horizon.

The chromatic soils [P202 (Pinedene), P203 (Tukulu) and P210 (Bloemdal)] have yellow-brown apedal B, neocutanic B or red apedal B horizons respectively as the second horizon in the profile. These soils have the driest water regime of the soils studied. The A and B1 horizons have mean $AD_{s>0.7}$ of less than 40 days per year, while in the underlying unspecified material with signs of wetness mean $AD_{s>0.7}$ varies from 130 to 350 days per year.

Soil profile morphology, as described by the soil form during soil classification, is therefore a very good indicator of soil profile hydrology and can be used as a first approximation of the mean $AD_{s>0.7}$. The results will not necessarily hold true outside the boundary of this study, because climate, topography and parent material also impacts significantly on soil morphology and therefore the relationship with hydrology will not necessarily be the same in other catchments.

Orthic A horizons can be subdivided, using the nature of the underlying horizon, to differentiate between wetness classes. Orthic A horizons in the well drained wetness class occur on red apedal B, yellow-brown apedal B and neocutanic B horizons. Orthic A horizons in the moderately well drained wetness class occur on E horizons and have either no or few mottles. Orthic A horizons in the moderately to poorly drained wetness class occur on E and G horizons and have few or many mottles. The orthic A horizons in the poorly drained wetness class occur on soft plinthic B and E horizons and have common mottles.

Table 9.1 lists the means of selected soil properties, grouped per diagnostic horizon. Orthic A horizons have the highest organic carbon (0.87 ± 0.18 %) and nitrogen content. Organic carbon content is lower in E, chromatic and soft plinthic B horizons (0.38 ± 0.05 %, 0.26 ± 0.11 % and 0.21 ± 0.02 % respectively). The organic carbon content is lowest in G horizons (0.13 ± 0.03 %) and unspecified material with signs of wetness (0.12 ± 0.03 %). It is therefore proposed that sufficient organic material is available throughout the profile to supply a substrate for microorganisms which leads to reduction in the event of water saturation. It should be borne in mind, however, that the threshold carbon and water content for reduction are interdependent. It therefore seems that the higher the degree of

water saturation, the less carbon is required for redox conditions to occur, and *vice versa*. The nitrogen content is also similar in soft plinthic B, E, G, chromatic horizons, and unspecified material with signs of wetness.

The sum of basic cations is highest in G horizons (7.26 ± 0.70 $cmol_c\ kg^{-1}$). It then decreases in the following order: unspecified material with signs of wetness (3.32 ± 1.00 $cmol_c\ kg^{-1}$); orthic A (2.58 ± 0.74 $cmol_c\ kg^{-1}$); E (1.71 ± 0.54 $cmol_c\ kg^{-1}$); soft plinthic B (1.64 ± 0.44 $cmol_c\ kg^{-1}$); chromatic horizons (0.97 ± 0.07 $cmol_c\ kg^{-1}$). The difference in sum of basic cations is, however, not significant between these horizons. The high sum of bases in the G horizon indicates a cumulative environment. Similarly, the low sum of bases in the E, soft plinthic B and chromatic horizons indicates leaching and removal of basic cations. It is especially $Ca^{2+}$ and $Mg^{2+}$ that differ between the diagnostic horizons, whereas $K^+$ and $Na^+$ remain almost constant throughout the profiles.

The clay content is significantly higher in G horizons (30.0 ± 2.3 %) and unspecified material with signs of wetness (24.9 ± 4.7 %), than in chromatic (17.5 ± 2.5 %), soft plinthic B (17.3 ± 2.6 %) and orthic A horizons (14.2 ± 1.7 %). It is lowest in E horizons (12.5 ± 1.1 %). The pattern in clay content substantiates the process of clay accumulation in the G horizon and luviation from the E and soft plinthic B horizons.

Table 9.1 Mean of selected soil properties, grouped per diagnostic horizon. Shaded areas group values that are not significantly different

| Hor | Clay | S | $CEC_{soil}$ | $CEC_{clay}$ | BS | OC | N | $pH_{Water}$ | $pH_{KCl}$ | CBD Fe | CBD Mn | Mean $AD_{s>0.7}$ |
|---|---|---|---|---|---|---|---|---|---|---|---|---|
| | (%) | ($cmol_c\ kg^{-1}$) | | | | (%) | | | | (mg $kg^{-1}$) | | (days $year^{-1}$) |
| ot | 14.2 | 2.6 | 7.8 | 36.9 | 31.3 | 0.87 | 652 | 5.18 | 4.48 | 4878 | 22.4 | 144 |
| gs | 12.5 | 1.7 | 8.7 | 64.1 | 25.1 | 0.38 | 330 | 5.42 | 4.33 | 4444 | 23.8 | 163 |
| ch | 17.5 | 1.0 | 4.9 | 25.4 | 21.0 | 0.21 | 222 | 4.80 | 4.03 | 7295 | 57.6 | 88 |
| sp | 17.3 | 1.6 | 7.3 | 39.0 | 23.7 | 0.26 | 325 | 5.49 | 4.29 | 8069 | 74.3 | 148 |
| on | 24.9 | 3.3 | 6.9 | 26.6 | 44.4 | 0.12 | 202 | 4.96 | 4.14 | 7116 | 63.9 | 243 |
| gh | 30.0 | 7.3 | 11.7 | 38.4 | 64.8 | 0.13 | 250 | 6.08 | 4.63 | 4873 | 73.1 | 324 |

Total Fe content (CBD extractable) is highest in soft plinthic B (8 069 ± 1 681 mg $kg^{-1}$), chromatic horizons (7 295 ± 776 mg $kg^{-1}$), and unspecified material with

signs of wetness (7 116 ± 1 880 mg $kg^{-1}$). It is lowest in orthic A (4 878 ± 390 mg $kg^{-1}$), E (4 444 ± 859 mg $kg^{-1}$) and G horizons (4 873 ± 1 121 mg $kg^{-1}$).

Total Mn content shows the same trend as the total Fe content, except that two clear groups can be distinguished. Soft plinthic B (74.3 ± 39.4 mg $kg^{-1}$), G (73.1 ± 25.3 mg $kg^{-1}$), unspecified material with signs of wetness (63.9 ± 18.8 mg $kg^{-1}$) and chromatic horizons (57.6 ± 22.1 mg $kg^{-1}$) have the highest total Mn (CBD extractable) content, while orthic A (22.4 ± 7.0 mg $kg^{-1}$) and E (23.8 ± 10.2 mg $kg^{-1}$) horizons have a significantly lower Mn content.

G horizons (324 ± 20 days $year^{-1}$) and unspecified material with signs of wetness (243 ± 40 days $year^{-1}$) have the highest mean $AD_{s>0.7}$. Mean $AD_{s>0.7}$ is lower in E (163 ± 56 days $year^{-1}$), soft plinthic B (148 ± 45 days $year^{-1}$) and orthic A horizons (144 ± 40 days $year^{-1}$), although there is no significant difference within the latter group. Chromatic horizons (88 ± 51 days $year^{-1}$) have the lowest mean $AD_{s>0.7}$.

Digital classification of digital photographs of soil horizons for colour classification can be done with reasonable accuracy. Results have shown that digital photographs can be quantified and classified meaningfully using ArcView SpatialAnalyst. This methodology holds great promise for the unbiased quantitative determination of soil colour and mottles, but will need further refinement before it can be implemented.

The following equations can be used to classify digital (RGB) photographs:

Between grey and yellow: Photo Green = 0.95 * Photo Red − 3.7 (9.1)

Between yellow and red: Photo Green = 0.85 * Photo Red − 9.7 (9.2)

Black can be classified as those cells having Red and Green values < 75

These equations include a correction factor to correct for the fact that there exists a difference between the photographed and calculated relation between RGB and Munsell notations. Elimination of black is necessary to remove shaded areas from the photographs. Unfortunately this also excluded Mn mottles, but could not be prevented.

The following are some results obtained by quantifying colour from digital colour photographs of soil horizons in this study. Grey and yellow are the dominant colours in the profiles described, with the exception of P210 (Bloemdal) which is classified as red. In P201 (Longlands) and P209 (Katspruit) the amount of grey increases with depth, with an associated decrease in yellow. The amount of diagnostic grey is, however, much more in the Katspruit than in the Longlands. In P202 (Pinedene) diagnostic grey decreases initially and then increases with depth. In P203 (Tukulu), P204 (Longlands), P205 (Kroonstad) and P207 (Westleigh) the amount of diagnostic grey decreases with depth. This might point to a drier subsoil water regime, or an artificial increase amount of red caused during profile preparation. Profiles P206 (Kroonstad) and P208 (Kroonstad) are diagnostic grey throughout the profile. The occurrence of red Fe oxide mottles in P201 (Longlands), P203 (Tukulu), P204 (Longlands), P205 (Kroonstad) and P209 (Katspruit) was clearly highlighted and quantified by the colour classification.

Colour indexes, used to predict duration of s>0.7 from morphological data did not yield meaningful correlations in this study. The following equation yielded the best correlation ($R^2 = 0.38$):

$$AD_{s>0.7}\ (\text{days year}^{-1}) = -38.6 \times H_d + 35.2 \times V_d + 1.94 \times C_d - 51.3 \qquad (9.3)$$

Where:

$AD_{s>0.7}$ = mean annual duration of water saturation above 0.7 of porosity
$H_d$ = dry colour (numeric) Hue
$V_d$ = dry colour Value
$C_d$ = dry colour Chroma

A summary of correlation coefficients for selected soil properties is given in Appendix C.

Chemical and physical analyses as well as mean $AD_{s>0.7}$ generally support the classification of diagnostic horizons in Soil Classification – A Taxonomic System for South Africa (Soil Classification Working Group, 1991). This implies that

diagnostic horizons can be used to infer these properties within the current research environment. These relationships could be extrapolated, with caution, to other catchments having similar climate and geology. The hypothesis regarding these relationships and the effect of lithology, topography and time on it should receive further scrutiny.

The possibilities of digital photograph interpretation should be investigated further. It is especially the effect of different cameras and lighting conditions that should receive attention. The relationship between Munsell Hue, Value and Chroma on the one hand and RGB on the other should also be investigated, for example the difference between look-up tables and computer programs. Meaningful differentiation between diagnostic red, yellow and grey colours, as well as the interpretation of dry and wet photographs should also be investigated.

Since this study is concerned with soils that have developed in sandy parent material, the effect of different parent materials on Fe supply, and hence soil colour should be researched. The same is true for climate. Similar studies should be carried out under different climatic conditions. The predictive value of diagnostic horizon and soil form characterization in relation to hydrology should also be evaluated by verification against other profiles in other catchments.

There is a need to investigate the utilisation of the relationship between soil morphology and soil hydrology to support the definition and delineation of hydrological response units from detailed soil maps. Estimation of the rate and volume of water discharged by these hydrological response units can be improved. This could contribute towards modelling the low flow of water in a catchment, a very important hydrological parameter.

# 10 REFERENCES


Adderley, W.P., I.A. Simpson and A. Davidson. 2002. Colour description and quantification in mosaic images of soil thin sections. *Geoderma* 108:181–195.

Amerman, C.R. 1973. Field soil water regime. In: R.R. Bruce, K.W. Flach, H.M. Taylor, M. Stelly, R.C. Dinauer and J.M. Hoch (Eds.) Hydrology and soil science. SSSA 9. Madison.

Anon., 2003A. http://developer.apple.com/documentation/mac/ACI/ACI-48.html. 17/09/2003.

Anon., 2003b. Munsell Conversion Program Version 6.22. http://Standards. GretagMacbeth.com/Munsell/Color%20Conversion.htm. 15/09/2003.

BEEH. 2003. Weatherley Database V1.0. School of Bioresources Engineering and Environmental Hydrology, University of Natal, South Africa.

Bennie, A.T.P., M.G. Strydom and H.S. Vrey. 1998. Gebruik van rekenaar modelle vir landboukundige waterbestuur op ekotoopvlak. WRC Report No. TT 102/98. WRC, Pretoria.

Blake, G.R. and K.H. Hartge. 1986. Bulk density. In. A. Klute (Ed.) Methods of soil analysis. Part 1. Physical and mineralogical methods. 2nd ed. ASA, Madison.

Blavet, D., E. Mathe and J.C. Leprun. 2000. Relations between soil colour and waterlogging duration in a representative hillside of the West African granito-gneissic bedrock. *Geoderma* 39:187–210.

Blavet, D., J.C. Leprun, and M. Pansu. 2002. Soil colour variables as simple indicators of duration of soil waterlogging in a West African catena. 17th WCSS Conference. 14–21 August 2002, Thailand.

Boggeaard, O.K. 1983. The influence of iron oxides on phosphate adsorption by soil. *J. Soil Sci.* 34:333–341.

Bohn, H. L., B. L. McNeal and G. A. O'Connor. 1985. Soil chemistry. John Wiley & Sons, New York.

Brady, N.C. and R.R. Weil. 1996. The nature and properties of soils. Prentice Hall, New Jersey.

Brindley, G.W. and G. Brown. 1980. X-Ray diffraction procedures for clay mineral identification. In: G.W. Brindley and G. Brown (Eds.) Crystal structures of clay minerals and their X-ray identification. Mineralogical Society, London.

Brinkman, R. 1979. Ferrolysis, a soil forming process in hydromorphic conditions. Centre Agric. Publ. and Docum., Wageningen.

Buol, S.W., F.D. Hole and R.J. McCracken. 1989. Soil genesis and classification. 3rd ed. Iowa State University Press, Ames.

Chief Director of Surveys and Mapping. 1993. South Africa 1:50 000 sheet 3128AB Maclear. Chief Director of Surveys and Mapping, Mowbray.

Cogger, C.G. and P.E. Kennedy. 1992. Seasonally saturated soils in the Paget Lowland. I. Saturation, reduction and color patterns. *Soil Sci.* 153:421–433.

Cutler, E.J.B. 1983. Soil classification in New Zealand. Lincoln College, Canterbury.

De Decker, R.H. 1981. 1:250 000 Geological series 3028 Kokstad. Council for Geoscience, Pretoria.

Desphande, T.L., D.J. Greenland and J.P. Quirk. 1964. Role of iron oxides in the bonding of soil particles. *Nature*. 201:107–108.

Desphande, T.L., D.J. Greenland and J.P. Quirk. 1968. Changes in soil properties associated with the removal of iron and aluminium oxides. *J. Soil Sci.* 19:108–122.

De Villiers, J.M. 1965. Present soil-forming factors and processes in tropical and subtropical regions. *Soil Sci.* 99:50–57.

Donkin, M.J. and M.V. Fey. 1991. Factor analysis of familiar properties of some Natal soils with the potential for afforestation. *Geoderma* 48:297–304.

Esprey, L.J. 1997. Hillslope experiments in the North Eastern Cape to measure and model subsurface flow processes. M.Sc Thesis. University of Natal, Pietermaritzburg.

ESRI. 2000. ArcView GIS 3.2a. Environmental Research Institute Inc., Redlands.

Evans, C.V. and D.P. Franzmeier. 1986. Saturation, aeration and color patterns in a toposequence of soils in north central Indiana. *Soil Sci. Soc. Am. J.* 50:975–980.

Evans, C.V. and D.P. Franzmeier. 1988. Color index values to represent wetness and aeration in some Indiana soils. *Geoderma* 41:353–368.

FAO. 1998a. Crop evapotranspiration: Guidelines for computing crop water requirements. FAO Irrigation and Drainage Paper No. 56. FAO, Rome.

FAO. 1998b. World Reference Base For Soil Resources. World Soil Resources Reports 84. FAO, Rome.

Fiedler, S., H.P.F. Jungkunst, R. Jahn, M. Kleber, M. Sommer and K. Stahr. 2002. Linking soil classification and soil dynamics – pedological and ecological perspectives. *J. Plant Nutr. Soil Sci.* 165:517–529.

Fitzpatrick, E.A. 1980. Soils: Their formation, classification and distribution. Longman, London.

Fitzpatrick, R.W. and U. Schwertmann. 1982. Al-substituted goethite – an indicator of pedogenic and other weathering environments in South-Africa. *Geoderma* 27:335–347.

Flugel, W.A. 1993. GIS-analysis to derive Hydrological Response Units (HRU's) for regional modelling using PRMS. In: Proc. International workshop on scale issues in hydrological / environmental modelling. Robertson, Australia.

Franson, M.A.H., A.E. Greenberg, R.R. Trussell and L.S. Clesceri. 1995. Standard methods for the examination of water and wastewater. American Public Health Association, Washington DC.

FSD. 1995. Forest industry soils database (FSD) co-operative. Soil surveys standards for consultants. Version 1.2.

Fujihara Industry Company. 1967. Revised standard soil colour charts. Fujihara Industry Company, Tokyo.

Godlove, I.H. 1951. Improved color-difference formula, with applications to the perceptibility and acceptability of fadings. *J. Otical Soc. Am.* 41:760–772.

Henning, J.A.G. and H.J. von M. Harmse. 1993. Die invloed van golwende onderliggende paleosols op seisoenale fluktuasies van vrywatervlakke in eoliese sand van die noordwestelike Oranje-Vrystaat. *S. Afr. J. Plant Soil* 10:105–109.

Hickson, R. M. 2000. Defining small catchment runoff responses using hillslope hydrological process observations. M.Sc. Thesis. University of Natal, Pietermaritzburg.

Hillel, D. 1980. Fundamentals of soil physics. Academic Press, New York.

Jury, W.A., W.R. Gardner and W.H. Gardner. 1991. Soil physics. John Wiley & Sons, New York.

Land-Use and Wetland/Riparian Habitat Working Group. 2000. Wetland/riparian habitats: A practical field procedure for identification and delineation. Mondi Forests, Pietermaritzburg.

Le Roux, P.A.L. 1996. Die aard, verspreiding en genese van geselekteerde redoksmorfe gronde in Suid-Afrika. Ph.D. Dissertation. University of the Orange Free State, Bloemfontein.

Le Roux, P.A.L., F. Ellis, F.R. Merryweather, J.L. Schoeman, K. Snyman, P.W. van Deventer and E. Verster. 1999. Guidelines for the mapping and interpretation of soils in South Africa. University of the Free State, Bloemfontein.

Le Roux, P.A.L., C.W. van Huyssteen and M. Hensley. 2003. Soil properties and hill slope hydrology in the Weatherley catchment. 50th Conference of the Soil Science Society of South Africa. 20-25 January 2003, Stellenbosch.

Loeppert, R.H. and W.P. Inskeep. 1996. Iron. In. D.L. Sparks (Ed.) Methods of soil analysis. Part 3. Chemical methods. SSSA, Madison.

Lorentz, S. 2001. Hydrological systems modelling research programme: Hydrological processes. WRC Report No. 637/1/01. WRC, Pretoria.

Lorentz, S. and L. Esprey. 1998. Baseline hillslope study prior to afforestation in the Umzimvubu headwaters of the North East Cape Province, South Africa. Hydrology, Water Resources and Ecology in Headwaters. Processdings of the HeadWater '98 Conference held in Meran/Merano, Italy, 20–23 April 1998. IAHS Publ. No. 248.

Lorentz, S. and R. Hickson. 2001. Applying hillslope hydrology observations to catchment modelling in Molteno formations. Tenth SA National Hydrology Symposium. 26 to 28 September 2001, Pietermaritzburg.

Lorentz, S., P. Goba and J. Pretorius. 2001. Hydrological processes research: Experiments and measurements of soil hydraulic characteristics. WRC Report No. 744/1/01. WRC, Pretoria.

MacVicar, C.N. 1978. Advances in soil classification and genesis in southern Africa. Proceedings 8th National Congress of the Soil Science Society of Southern Africa. Tech. Comm. No. 165. *Dept. Agric. Tech Serv.*, Pretoria.

MacVicar, C.N., D.M. Scotney, T.E. Skinner, H.S. Niehaus and J.H. Loubser. 1974. A classification of land (climate, terrain form, soil) primarily for rain fed agriculture. *S. Afr. J. Agric. Extension* 3:22–24.

McCarthy G.W. and J.M. Bremner. 1992. Availability of carbon for denitrification of nitrate in subsoils. *Biol. Fertil. Soils.* 14:219–222.

McKeague, J.A., J.E. Brydon and N.M. Miles. 1971. Differentiation of forms of extractable iron and aluminium in soils. *Soil Sci. Soc. Am. Proc.* 35:33–38.

Mehra, O.P. and M.L. Jackson. 1960. Iron oxide removal from soils and clays by a dithionite-citrite system buffered with sodium bicarbonate. In: A. Swinefored (Ed.) Proc. 7th Clays Clay Miner. Conf. Washington D.C., 1958. Pergamon Press, New York.

Melville, M.D. and G. Atkinson. 1985. Soil Colour: Its measurement and its designation in models of uniform colour space. *J. Soil Sci.* 36:495–512.

Mokma, D.L. & D.L. Cremeens. 1991. Relationships of saturation and B horizon colour patterns in soils of three hydrosequences in south-central Michigan, USA. *Soil use and management.* 7:56–61.

Munsell Color Company. 1975. Munsell soil color charts. Munsell Color, Baltimore.

Munsell Color Company. 1980. Munsell book of color. Munsell Color, Baltimore.

Norrish, K. and R.M. Taylor. 1961. The isomorphous replacement of iron by aluminium in soil goethites. *J. Soil Sci.* 13:294–306.

Ottow, J.C.G. and H. Glathe. 1971. Isolation and identification of iron-reducing bacteria from gley soils. *Soil Bio. Geochem.* 3:43–55.

Poynton, C. 1999. Frequently asked questions about color. http://www.inforamp.net/~poynton/notes/colour_and_gamma/ColorFAQ.txt. 16/09/2002.

Reginato, R. and F.S. Nakayama. 1987. Plastic standards for transferring neutron probe calibrations. In: R.J. Hanks (Ed.) Proc. Int. Conf. Meas. Soil Plant Water Status. Logan, 6–10 Jul. 1987. Utah State University, Logan.

Roberts, V.G., M. Hensley, A.L. Smith-Baillie and D.G. Patterson. 1996. Detailed soil survey of the Weatherley catchment. ISCW Report No. GW/A/96/33. ARC-ISCW, Pretoria.

Snedecor, G.W. and Cochran, W.G. 1989. Statistical Methods. 8th Ed. Iowa State University Press, Ames.

Schulze, D.G. and J.B. Dixon. 1979. High gradient magnetic separation of iron oxides and magnetic minerals from soil clays. *Soil Sci. Soc. Am. J.* 43:793–799.

Schulze, R.E. 1995. Hydrology and agrohydrology: A text to accompany the ACRU 3.00 agrohydrological modelling system. WRC Report No 63/2/84. WRC, Pretoria.

Schwertmann, U. 1971. Transformation of hematite to goethite in soils. *Nature* 232:624–625.

Schwertmann, U. 1985. The effect of pedogenic environments on iron oxide minerals. *Advances in Soil Science* 1:171–200.

Schwertmann, U. 1993. Relations between iron oxides, soil color and soil formation. In. J.M. Bigham and E.J. Coilkosz (Eds.) Soil color. SSSA Spec. Publ. 31. SSSA, Madison.

Schwertmann, U. and N. Kämpf. 1985. Properties of goethite and hematite in kaolinitic soils of Southern and Central Brazil. *Soil Sci.* 139:344–350.

Schwertmann, U. and R.M. Taylor. 1989. Iron oxides. In: J.B. Dixon and S.B. Weed (Eds.) Minerals in soil environments. SSSA, Madison.

Schwertmann, U., P. Cambier and E. Murad. 1985. Properties of goethites of varying crystallinity. *Clays Clay Miner.* 33:369–378.

Shadfan, H., J.B. Dixon and F.C. Calhoun. 1985. Iron oxide properties versus strength of ferruginous crust and iron-glaebules in soils. *Soil Sci.* 140:317–325.

Soil Science Society of America. 2001. Internet Glossary of Soil Science Terms. http://www.soils.org/sssagloss/index.html. 02/02/2004.

Soil Classification Working Group. 1991. Soil classification – A taxonomic system for South Africa. *Mem. agric. nat. Resour. S. Afr.* No. 15. Dept. Agric. Dev., Pretoria.

Soil Survey Division Staff. 1993. Soil survey manual. Handbook no. 18. United States Department of Agriculture, Washington DC.

Soil Survey Staff. 1975. Soil Taxonomy – A basic system of soil classification for making and interpreting soil surveys. U.S. Govt. Printing Office, Washington DC.

Soil Survey Staff. 1999. Soil Taxonomy – A basic system of soil classification for making and interpreting soil surveys. U.S. Govt. Printing Office, Washington DC.

Tarekegne, A. 2001. Studies on genotypic variability and inheritance of waterlogging tolerance in wheat. Ph.D. Thesis, University of the Free State, Bloemfontein.

Taylor, R.M. and U. Schwertmann. 1978. The influence of aluminium on iron oxides. Part I. The influence of Al on Fe-oxide formation from the Fe(II) system. *Clays Clay Min.* 26:373–383.

The Non-Affiliated Soil Analysis Work Committee. 1990. Handbook of standard soil testing methods for advisory purposes. SSSSA, Pretoria.

Torrent, J. and U. Schwertmann. 1987. Influence of hematite on the color of red beds. *J. Sed. Petr.* 57:682–686.

Torrent, J., R. Guzmann and M.A. Parra. 1982. Influence of relative humidity on the crystallization of Fe(III) oxides from ferrihydrite. *Clays Clay Min.* 30:337–340.

Torrent, J., U. Schwertmann and D.G. Schulze. 1980. Iron oxide mineralogy of some soils of two terrace sequences in Spain. *Geoderma* 23:191–208.

Torrent, J., U. Schwertmann, H. Fetcher and F. Alfrez. 1983. Quantitative relationships between soil color and hematite content. *Soil Sci.* 136:354–358.

Turner, D.P. 1991. A procedure for describing soil profiles. ISCW report No. GB/A/91/67. ARC-ISCW, Pretoria.

Van der Watt, H.V.H. and T.H. van Rooyen. 1995. A glossary of soil science. 2nd ed. SSSSA, Pretoria.

Van Huyssteen, C.W. 1995. The relationship between subsoil colour and degree of wetness in a suite of soils in the Grabouw district, Western Cape. M.Sc. Agric. Thesis, University of Stellenbosch.

Van Huyssteen, C.W., M. Hensley, P.A.L. le Roux, L.F. Joseph and C.C. du Preez. 2003a. The relationship between soil water regime and soil profile morphology in the Weatherley catchment, an afforestation area in the North Eastern Cape. First progress report on WRC project No K5/1317. WRC, Pretoria.

Van Huyssteen, C.W., M. Hensley and P.A.L. le Roux. 2002. Correlating soil hydrology with soil morphology for improved technology transfer. A report to the WRC on project No. K8/419. WRC, Pretoria.

Van Huyssteen, C.W., M. Hensley and P.A.L. le Roux. 2003b. Correlating soil hydrology with soil morphology. 50th Conference of the Soil Science Society of South Africa. 20-25 January 2003, Stellenbosch.

Van Huyssteen, C.W., M. Hensley & P.A.L. le Roux. 2003c. Correlating soil hydrology with soil morphology. 11th SANCIAHS National Hydrology Symposium. 3-5 September 2003, Port Elizabeth.

Weaver, J.M.C. 1992. Ground water sampling. A comprehensive guide for sampling methods. WRC Project No 339. TT 54/92. WRC, Pretoria.

# APPENDIX A

## Photographs, profile descriptions, chemical and physical analyses as well as seasonal volumetric water contents and degrees of water saturation for profiles P201 to P210

Data for profiles 201 to 210, grouped per profile and given in the following sequence:

a) Photograph of the profile, including horizon demarcations, location of piezometer pipes, tensiometers and NWM measurements.
b) Profile description.
c) Chemical and physical analyses.
d) Volumetric water content and daily rainfall from 1 January 1997 until 31 December 2002.
e) Degree of water saturation and daily rainfall from 1 January 1997 until 31 December 2002.

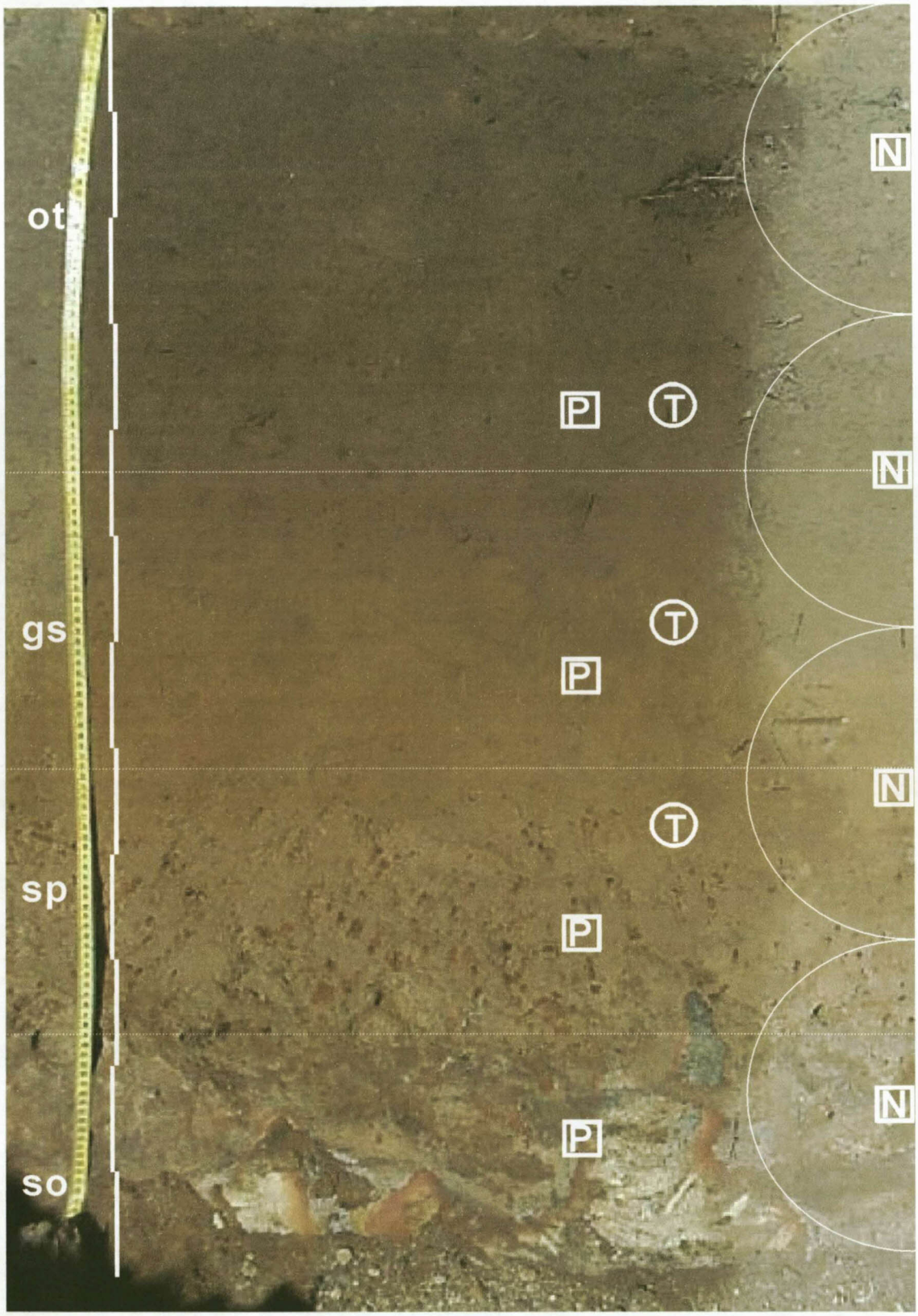


Figure 1 Profile 201 (Longlands 2000), indicating diagnostic horizons as well as measurement depths for tensiometers [T], neutron water meter [N] and piezometers [P].

## Table 1 Profile description for profile 201 (Longlands 2000)

**Profile No:** 201
**Map/photo:** 3128AB
**Latitude & Longitude:** 31° 06' 06.0" / 28° 20' 18.0"
**Surface stoniness:** None
**Altitude:** 1 337 m
**Terrain unit:** Upper midslope
**Slope:** 4 %
**Slope shape:** Convex
**Aspect:** West
**Microrelief:** None
**Parent material solum:** Origin single, solid rock
**Underlying material:** Feldspathic sandstone
**Geological Group:** Elliot

**Soil form:** Longlands
**Soil family: 2000**
**Surface rockiness:** None
**Occurrence of flooding:** None
**Wind erosion:** None
**water erosion:** None
**Vegetation / Land use:** Grassveld, closed
**Water table:** None
**Described by:** C.W. van Huyssteen & W. Boshoff
**Date described:** 19/06/2001
**Weathering of underlying material:** Weak physical, weak chemical
**Alteration of underlying material:** Ferruginised

| Horizon | Depth(mm) | Description | Diagnostic horizons |
|---|---|---|---|
| A | 0 – 430 | **Moisture status:** dry; **dry colour:** 10YR4/4 (80 %), 10YR4/2 (20 %); **moist colour:** 10YR3/3 (80 %), 10YR3/2 (20 %); 8.9 % clay; coarse sandy loam; few fine faint 10YR4/2 dry, 10YR3/2 moist, geogenic and biological mottles; apedal massive; soft, friable, non-sticky, non-plastic; no fine and very fine pores; common normal medium and coarse pores; no slickensides; no cracks; no cutans; no coarse fragments; water absorption 1 second(s); many normal roots; gradual smooth transition | orthic A horizon |
| E | 430 – 730 | **Moisture status:** moist; **dry colour:** 7.5YR6/4 (95 %), 10YR4/4 (5 %); **moist colour:** 10YR4/4 (95 %), 10YR4/4 (5 %); 11.9 % clay; coarse sandy loam; common medium distinct 10YR4/4 dry, 10YR3/3 moist, Illuvial humus mottles; common fine distinct 2.5YR4/8 dry, 10R4/8 moist, iron oxide mottles; apedal massive; soft, friable, non-sticky, non-plastic; no fine and very fine pores; few normal medium and coarse pores; no slickensides; no cracks; no cutans; no coarse fragments; water absorption 1 second(s); many normal roots; gradual smooth transition | E horizon |
| B | 730 – 980 | **Moisture status:** moist; **dry colour:** 7.5YR6/4 (100 %); **moist colour:** 10YR4/4 (100 %); 12.6 % clay; coarse sandy loam; many fine prominent 2.5YR4/8 dry, 10R4/8 moist, iron oxide mottles; few fine distinct 2.5YR3/0 dry, 2.5YR2.5/0 moist, manganese mottles; apedal massive; soft, friable, non-sticky, non-plastic; few normal fine and very fine pores; no medium and coarse pores; no slickensides; no cracks; no cutans; very few 6-25 mm mixed shaped stones; water absorption 1 second(s); many normal roots; gradual tonguing transition; Remark: B2 horizon has tongues of sandstone saprolite, with manganese concretions and red surfaces, surrounded by grey sillans. | soft plinthic B horizon |
| C | 980 – 1210 | **Moisture status:** moist; **dry colour:** 7.5YR7/2 (40 %), 10YR4/8 (10 %), 10YR8/4 (50 %); **moist colour:** 7.5YR4/4 (40 %), 10R4/6 (10 %), 7.5YR6/8 (50 %); 11.4 % clay; coarse sandy loam; no mottles; apedal massive; soft, friable, non-sticky, non-plastic; no fine and very fine pores; no medium and coarse pores; many slickensides; no cracks; no cutans; no coarse fragments; water absorption 1 second(s); no normal roots; transition not reached; Remark: 870 to 1000 mm is wavy transition between the soft plinthic B horizon and rock horizons. Cores are grey and yellow with red mottles. | saprolite / rock |

Table 2 Soil analyses for profile 201 (Longlands 2000)

| Horizon | Depth | Diagnostic horizon | Gravel | Texture of the fine earth | | | | | | | Exchangeable cations | | | | | CEC soil | CEC clay | Base sat |
|---|---|---|---|---|---|---|---|---|---|---|---|---|---|---|---|---|---|---|
| | | | | coSa | meSa | fiSa | vfSa | coSi | fiSi | Cl | Ca | Mg | K | Na | S | | | |
| | mm | | % | % | | | | | | | $cmol_c\ kg^{-1}$ | | | | | | | % |
| A | 0-100 | ot | 3.4 | 20.4 | 30.6 | 14.3 | 8.5 | 7.9 | 8.8 | 9.2 | 1.38 | 0.48 | 0.16 | 0.11 | 2.14 | 4.84 | 52.6 | 44 |
| | 100-200 | | 5.8 | 26.9 | 30.8 | 12.4 | 7.4 | 6.7 | 7.3 | 7.7 | 1.21 | 0.47 | 0.09 | 0.12 | 1.89 | 4.47 | 58.0 | 42 |
| | 200-300 | | 1.7 | 25.4 | 30.3 | 12.9 | 7.4 | 6.6 | 7.8 | 8.4 | | | | | | | | |
| | 300-400 | | 2.2 | 21.9 | 30.4 | 13.9 | 8.7 | 6.9 | 7.5 | 10.2 | 0.45 | 0.22 | 0.10 | 0.10 | 0.87 | 3.75 | 36.8 | 23 |
| E | 400-500 | gs | 1.6 | 26.2 | 31.0 | 12.5 | 7.3 | 2.6 | 9.8 | 10.0 | 0.31 | 0.15 | 0.13 | 0.09 | 0.67 | 3.04 | 30.5 | 22 |
| | 500-600 | | 3.8 | 17.7 | 30.0 | 15.1 | 10.4 | 7.1 | 6.6 | 12.8 | 0.24 | 0.10 | 0.11 | 0.11 | 0.55 | 2.83 | 22.1 | 19 |
| | 600-700 | | 6.7 | 17.7 | 30.0 | 15.1 | 10.4 | 7.1 | 6.6 | 12.8 | 0.25 | 0.11 | 0.07 | 0.09 | 0.51 | 3.43 | 26.8 | 15 |
| B | 700-800 | sp | 13.7 | 20.6 | 28.8 | 12.6 | 10.3 | 5.5 | 7.0 | 13.7 | 0.26 | 0.13 | 0.05 | 0.12 | 0.56 | 2.66 | 19.5 | 21 |
| | 800-900 | | 17.3 | 19.0 | 28.6 | 12.7 | 11.0 | 7.7 | 7.0 | 12.8 | 0.26 | 0.16 | 0.04 | 0.09 | 0.55 | 3.10 | 24.2 | 18 |
| | 900-1000 | | 44.2 | 16.4 | 30.8 | 13.2 | 11.8 | 6.4 | 8.4 | 11.4 | 0.28 | 0.17 | 0.03 | 0.11 | 0.59 | 2.34 | 20.5 | 25 |

| Horizon | Depth | Bulk density | pH | | Org C | N | C:N | Fe | | | Mn | | | Mineralogy |
|---|---|---|---|---|---|---|---|---|---|---|---|---|---|---|
| | | | | | | | | CBD | Ox | Piro | CBD | Ox | Piro | |
| | mm | $Mg\ m^{-3}$ | $H_2O$ | KCl | % | $mg\ kg^{-1}$ | | $mg\ kg^{-1}$ | | | | | | < 0,002mm |
| A | 0-100 | 1.53 | 4.73 | 4.54 | 0.99 | 625 | 15.9 | 4510 | 474 | 1362 | 31.5 | 33.5 | 20.4 | |
| | 100-200 | | 4.65 | 4.51 | 0.96 | 554 | 17.2 | 4750 | 477 | 1456 | 21.5 | 18.0 | 12.0 | |
| | 200-300 | | 4.43 | 4.28 | 0.61 | 516 | 11.8 | 5030 | 517 | 1643 | 14.0 | 7.5 | 8.7 | |
| | 300-400 | 1.57 | 4.55 | 4.20 | 0.43 | 423 | 10.0 | 5180 | 400 | 1476 | 9.0 | 2.5 | 7.0 | |
| E | 400-500 | | 4.49 | 4.17 | 0.68 | 360 | 18.9 | 5425 | 431 | 1944 | 8.5 | 1.5 | 7.0 | |
| | 500-600 | | 4.44 | 4.19 | 0.29 | 260 | 11.2 | 5470 | 528 | 1526 | 8.0 | 1.5 | 6.7 | |
| | 600-700 | 1.65 | 4.36 | 4.14 | 0.21 | 234 | 9.1 | 6875 | 322 | 1205 | 15.5 | 1.5 | 6.5 | |
| B | 700-800 | | 4.30 | 4.13 | 0.14 | 196 | 7.3 | 5385 | 325 | 834 | 15.5 | 2.0 | 18.1 | |
| | 800-900 | | 4.35 | 4.15 | 0.33 | 156 | 20.9 | 3900 | 374 | 509 | 26.0 | 7.0 | 11.0 | |
| | 900-1000 | 1.84 | 4.52 | 4.14 | 0.11 | 116 | 9.6 | 4295 | 362 | 487 | 19.5 | 19.0 | 12.0 | |

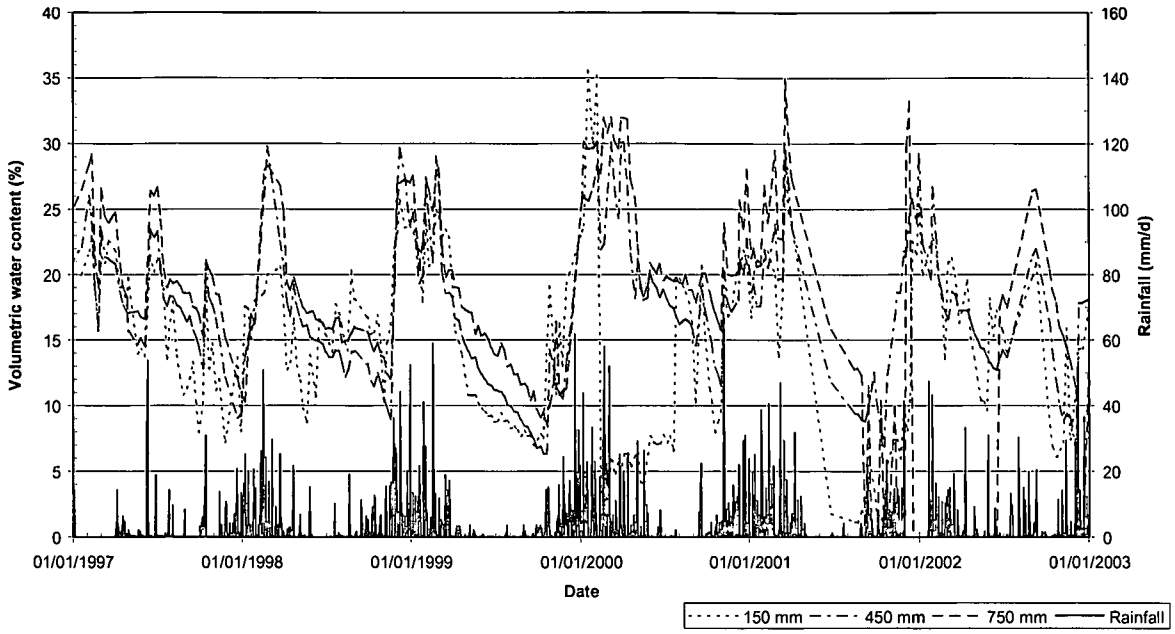


Figure 2 Volumetric water content and daily rainfall from 1 January 1997 until 31 December 2002 for profile 201.

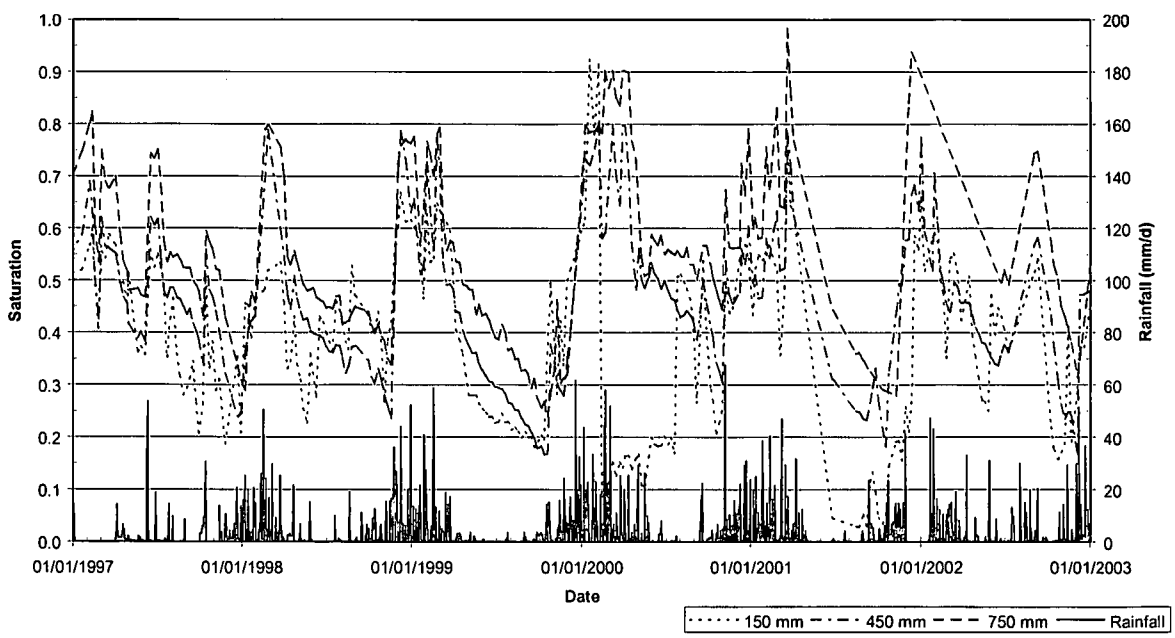


Figure 3 Degree of water saturation and daily rainfall from 1 January 1997 until 31 December 2002 for profile 201.

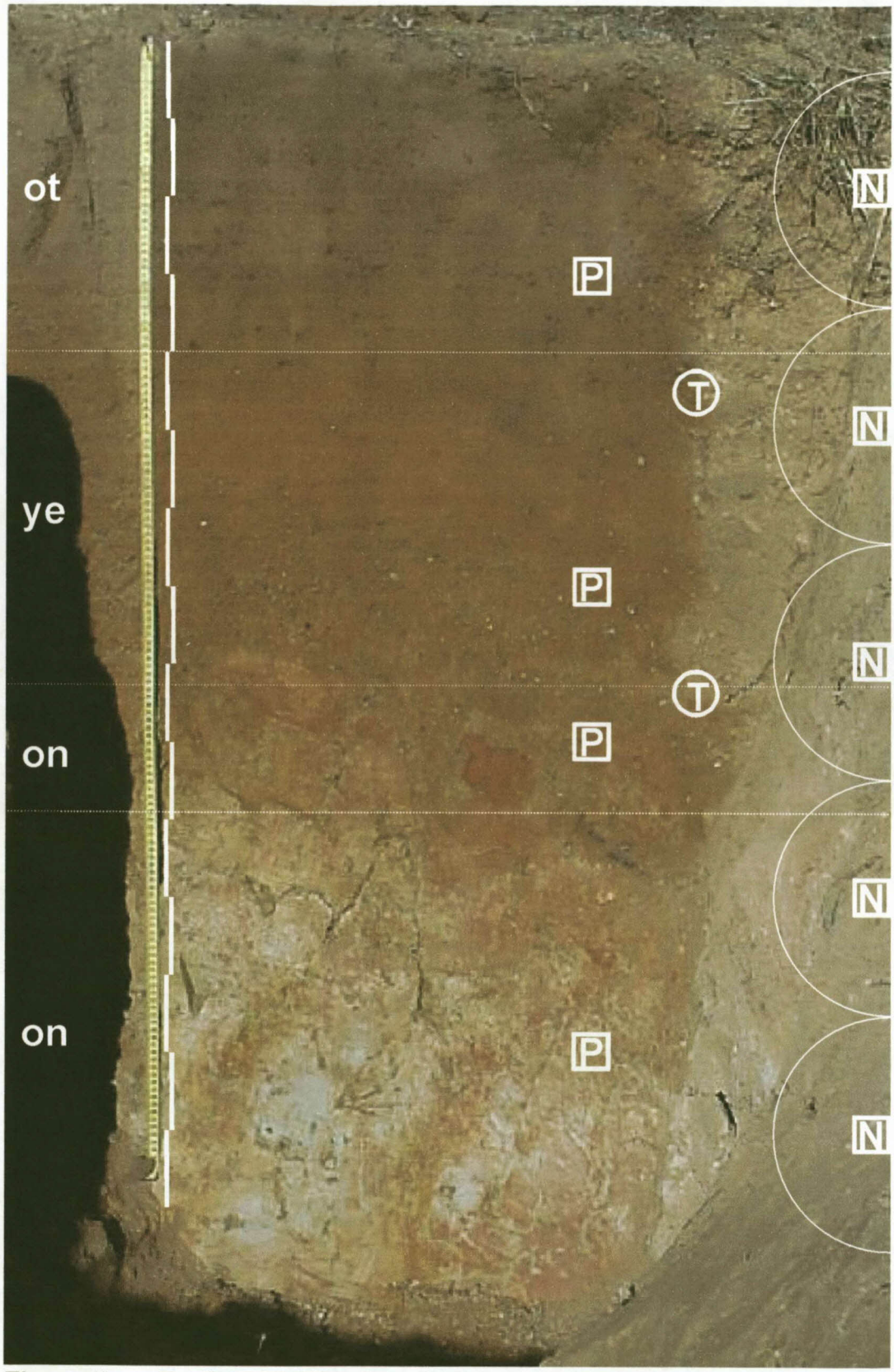


Figure 4 Profile 202 (Pinedene 1100), indicating diagnostic horizons as well as measurement depths for tensiometers [T], neutron water meter [N] and piezometers [P].

## Table 3 Profile description for profile 202 (Pinedene 1100)

**Profile No:** 202
**Map/photo:** 3128AB
**Latitude & Longitude:** 31° 06' 06.0" / 28° 20' 15.1"
**Surface stoniness:** None
**Altitude:** 1 329 m
**Terrain unit:** Upper midslope
**Slope:** 4 %
**Slope shape:** Convex
**Aspect:** West
**Microrelief:** None
**Parent material solum:** Origin binary, local colluvium, solid rock
**Underlying material:** Mudstone
**Geological Group:** Elliot

**Soil form:** Pinedene
**Soil family:** 1100
**Surface rockiness:** None
**Occurrence of flooding:** None
**Wind erosion:** None
**Water erosion:** Slight, partially stabilised
**Vegetation / Land use:** Grassveld, open
**Water table:** None
**Described by:** M. Hensley & M. Smit
**Date described:** 19/06/2001
**Weathering of underlying material:** Moderate physical, strong chemical
**Alteration of underlying material:** Ferruginised

| Horizon | Depth(mm) | Description | Diagnostic horizons |
|---|---|---|---|
| A | 0 - 400 | **Moisture status:** dry; **dry colour:** 10YR4/3 (100 %); **moist colour:** 10YR3/3 (100 %); 10.1 % clay; medium sandy loam; no mottles; weak fine subangular blocky; soft, friable, non-sticky, non-plastic; many normal fine and very fine pores; many normal medium and coarse pores; no slickensides; no cracks; no cutans; no coarse fragments; water absorption 1 second(s); many normal roots; clear smooth transition; | orthic A horizon |
| B | 400 - 820 | **Moisture status:** dry; **dry colour:** 7.5YR5/6 (95 %), 7.5YR6/8 (5 %); **moist colour:** 7.5YR4/6 (95 %), 7.5YR4/4 (5 %); 16.1 % clay; medium sandy loam; few medium faint 7.5Y6/4 dry, 7.5YR6/8 moist, iron oxide mottles; few fine faint 7.5YR6/8 dry, 7.5YR4/4 moist, iron oxide mottles; weak fine subangular blocky; soft, friable, non-sticky, non-plastic; many normal fine and very fine pores; many normal medium and coarse pores; no slickensides; no cracks; no cutans; common 2-6 mm round stones; water absorption 3 second(s); many normal roots; clear smooth transition; | yellow-brown apedal B horizon |
| C1 | 820 - 990 | **Moisture status:** moist; **dry colour:** 10YR8/2 (90 %), 7.5YR5/8 (5 %), 7.5YR6/8 (5 %); **moist colour:** 7.5YR6/6 8(5 %), 7.5YR5/6 (5 %), 7.5YR7/4 (10 %); 19.9 % clay; fine sandy loam; common medium faint 5YR4/6 dry, 5YR4/6 moist, iron oxide mottles; common medium faint 7.5YR5/6 dry, 7.5YR5/8 moist, iron oxide mottles; apedal massive; hard, friable, non-sticky, non-plastic; many normal fine and very fine pores; no medium and coarse pores; no slickensides; no cracks; no cutans; common 25-75 mm round stones; water absorption 1 second(s); many normal roots; abrupt smooth transition; | unspecified material with signs of wetness |
| C2 | 990 - 1500 | **Moisture status:** moist; **dry colour:** 2.5Y8/2 (70 %), 7.5YR5/8 (20 %), 10YR4/8 (10 %); **moist colour:** 2.5Y6/2 (70 %), 10YR5/8 (20 %), 10R4/6 (10 %); 24.7 % clay; fine sandy clay loam; few fine prominent 2.5YR4/6 dry, 2.5YR4/4 moist, iron oxide mottles; many fine prominent 10YR6/8 dry, 10YR5/8 moist, iron oxide mottles; moderate coarse prismatic; very hard, friable, very sticky, slightly plastic; few normal fine and very fine pores; few bleached medium and coarse pores; no slickensides; fine cracks; very many silica cutans; no coarse fragments; water absorption 2 second(s); few bleached roots; transition not reached; | unspecified material with signs of wetness |

Table 4 Soil analyses for profile 202 (Pinedene 1100)

| Horizon | Depth mm | Diagnostic horizon | Gravel | Texture of the fine earth | | | | | | | Exchangeable cations | | | | | CEC soil | CEC clay | Base sat |
|---|---|---|---|---|---|---|---|---|---|---|---|---|---|---|---|---|---|---|
| | | | | coSa | meSa | fiSa | vfSa | coSi | fiSi | Cl | Ca | Mg | K | Na | S | | | |
| | | | % | % | | | | | | | cmolc kg$^{-1}$ soil | | | | | | | % |
| A | 0-100 | ot | 2.7 | 11.2 | 30.6 | 22.8 | 13.7 | 4.4 | 6.5 | 9.9 | 0.74 | 0.22 | 0.10 | 0.11 | 1.17 | 3.32 | 33.5 | 35 |
| | 100-200 | | 2.9 | 13.9 | 31.6 | 21.5 | 12.1 | 10.6 | 1.1 | 8.5 | 0.59 | 0.20 | 0.13 | 0.12 | 1.04 | 3.31 | 38.9 | 31 |
| | 200-300 | | 5.0 | 12.1 | 30.2 | 22.2 | 15.7 | 4.0 | 3.9 | 11.1 | 0.51 | 0.20 | 0.16 | 0.10 | 0.97 | 3.64 | 32.8 | 27 |
| | 300-400 | | 11.3 | 10.9 | 29.9 | 22.8 | 14.0 | 5.0 | 5.5 | 11.0 | 0.47 | 0.17 | 0.16 | 0.11 | 0.91 | 2.83 | 25.7 | 32 |
| B | 400-500 | ye | 13.7 | 11.7 | 27.9 | 21.3 | 16.1 | 2.8 | 1.3 | 16.4 | 0.44 | 0.18 | 0.16 | 0.11 | 0.89 | 2.56 | 15.6 | 35 |
| | 500-550 | | 14.4 | 10.5 | 24.6 | 20.7 | 14.5 | 7.2 | 5.3 | 17.2 | 0.44 | 0.20 | 0.16 | 0.12 | 0.93 | 3.86 | 22.4 | 24 |
| | 550-600 | | 23.2 | 15.7 | 23.3 | 18.2 | 14.2 | 5.5 | 6.7 | 16.3 | 0.43 | 0.22 | 0.16 | 0.10 | 0.91 | 3.52 | 21.6 | 26 |
| | 600-700 | | 31.7 | 13.0 | 21.9 | 19.5 | 15.4 | 6.6 | 5.9 | 15.8 | 0.44 | 0.23 | 0.16 | 0.11 | 0.94 | 3.97 | 25.1 | 24 |
| | 700-800 | | 34.3 | 13.2 | 20.8 | 20.2 | 15.2 | 6.4 | 8.3 | 14.8 | 0.41 | 0.24 | 0.13 | 0.11 | 0.88 | 2.72 | 18.4 | 32 |
| C1 | 800-850 | on | 11.2 | 13.3 | 14.9 | 23.0 | 19.8 | 1.5 | 9.7 | 17.0 | 0.65 | 0.48 | 0.09 | 0.13 | 1.37 | 4.02 | 23.7 | 34 |
| | 850-900 | | 2.2 | 4.1 | 9.6 | 22.0 | 23.3 | 6.9 | 10.6 | 21.2 | 0.87 | 0.68 | 0.11 | 0.13 | 1.79 | 4.41 | 20.8 | 41 |
| | 900-1000 | | 2.3 | 6.2 | 9.4 | 21.9 | 18.0 | 10.6 | 10.6 | 21.5 | 1.44 | 0.94 | 0.12 | 0.13 | 2.63 | 5.65 | 26.3 | 47 |
| C2 | 1000-1100 | on | 1.6 | 11.1 | 7.5 | 21.4 | 17.3 | 7.6 | 10.8 | 26.1 | 1.61 | 1.41 | 0.16 | 0.15 | 3.34 | 8.10 | 31.0 | 41 |
| | 1100-1300 | | 1.8 | 9.0 | 4.9 | 26.0 | 18.1 | 6.5 | 7.2 | 26.0 | 1.76 | 1.79 | 0.24 | 0.16 | 3.95 | 9.68 | 37.2 | 41 |
| | 1300-1600 | | 2.1 | 8.7 | 4.8 | 26.0 | 21.5 | 7.5 | 6.4 | 23.8 | 2.78 | 2.68 | 0.25 | 0.16 | 5.86 | 8.04 | 33.8 | 73 |
| | 1600+ | | 0.2 | 8.5 | 4.6 | 30.0 | 18.7 | 7.8 | 7.9 | 22.9 | 2.92 | 2.72 | 0.27 | 0.16 | 6.07 | 8.21 | 35.9 | 74 |

| Horizon | Depth | Bulk | pH | | Org C | N | C:N | Fe | | | Mn | | | Mineralogy |
|---|---|---|---|---|---|---|---|---|---|---|---|---|---|---|
| | | | | | | | | CBD | Ox | Pyro | CBD | Ox | Pyro | |
| | mm | Mg m$^{-3}$ | $H_2O$ | KCl | % | mg kg$^{-1}$ | | mg kg$^{-1}$ | | | | | | < 0.002mm |
| A | 0-100 | 1.68 | 4.54 | 4.19 | 0.76 | 410 | 18.6 | 5165 | 268 | 663 | 13.5 | 7.5 | 13.1 | |
| | 100-200 | | 4.65 | 4.25 | 0.75 | 373 | 20.2 | 4960 | 296 | 689 | 11.0 | 4.5 | 11.0 | |
| | 200-300 | | 4.67 | 4.21 | 0.83 | 358 | 23.1 | 3945 | 283 | 723 | 12.0 | 3.5 | 11.0 | |
| | 300-400 | | 4.65 | 4.20 | 0.42 | 261 | 16.0 | 3420 | 290 | 718 | 9.5 | 4.0 | 11.0 | |
| B | 400-500 | 1.61 | 4.49 | 4.12 | 0.13 | 228 | 5.5 | 6010 | 383 | 796 | 15.0 | 4.0 | 11.0 | |
| | 500-550 | | 4.46 | 4.10 | 0.21 | 218 | 9.6 | 7305 | 479 | 695 | 16.0 | 4.5 | 11.0 | |
| | 550-600 | | 4.44 | 4.06 | 0.22 | 229 | 9.6 | 6610 | 519 | 730 | 16.5 | 7.0 | 12.0 | |
| | 600-700 | 1.72 | 4.44 | 4.09 | 0.10 | 206 | 4.8 | 7455 | 528 | 530 | 40.0 | 24.5 | 17.1 | |
| | 700-800 | | 4.42 | 4.12 | 0.16 | 192 | 8.3 | 7845 | 552 | 420 | 61.0 | 49.0 | 21.1 | |
| C1 | 800-850 | | 4.50 | 4.14 | 0.10 | 163 | 6.4 | 12200 | 1085 | 306 | 98.0 | 60.0 | 21.1 | |
| | 850-900 | | 4.50 | 4.09 | 0.19 | 209 | 9.2 | 17850 | 1145 | 277 | 57.5 | 32.0 | 20.1 | |
| | 900-1000 | 1.71 | 4.52 | 4.08 | 0.14 | 230 | 6.2 | 16750 | 1345 | 264 | 69.5 | 50.5 | 17.1 | |
| | 1000-1100 | | 4.53 | 4.03 | 0.13 | 272 | 4.8 | 15250 | 1030 | 239 | 44.0 | 18.0 | 14.1 | |
| C2 | 1100-1300 | | 4.59 | 4.02 | 0.11 | 281 | 4.1 | 7800 | 558 | 223 | 57.0 | 62.0 | 16.1 | |
| | 1300-1600 | 1.72 | 4.52 | 4.11 | 0.14 | 238 | 5.8 | 3055 | 592 | 217 | 8.0 | 13.0 | 12.0 | |
| | 1600+ | | 4.67 | 4.15 | 0.04 | 209 | 1.9 | 8185 | 2065 | 215 | 7.0 | 3.5 | 11.0 | |

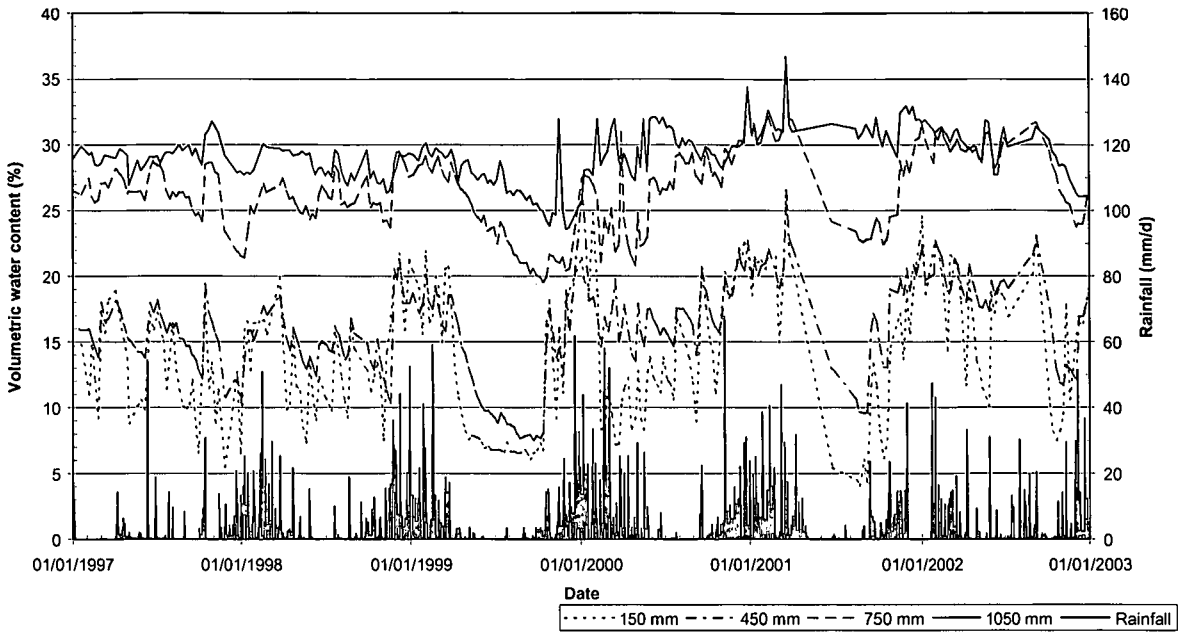


Figure 5 Volumetric water content and daily rainfall from 1 January 1997 until 31 December 2002 for profile 202.

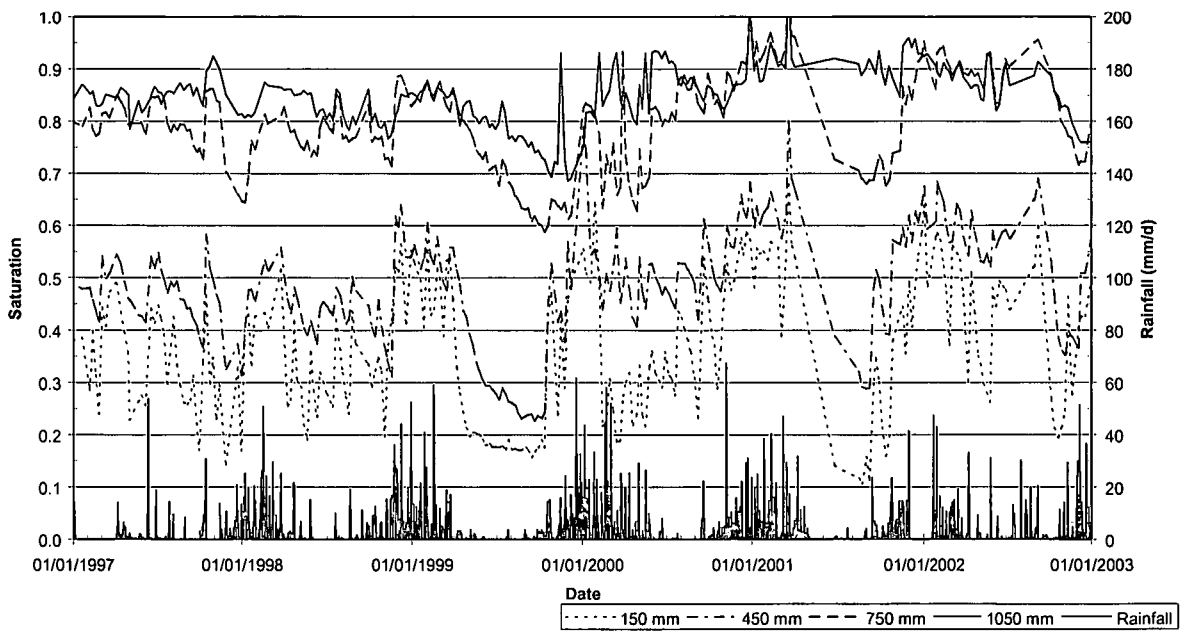


Figure 6 Degree of water saturation and daily rainfall from 1 January 1997 until 31 December 2002 for profile 202.

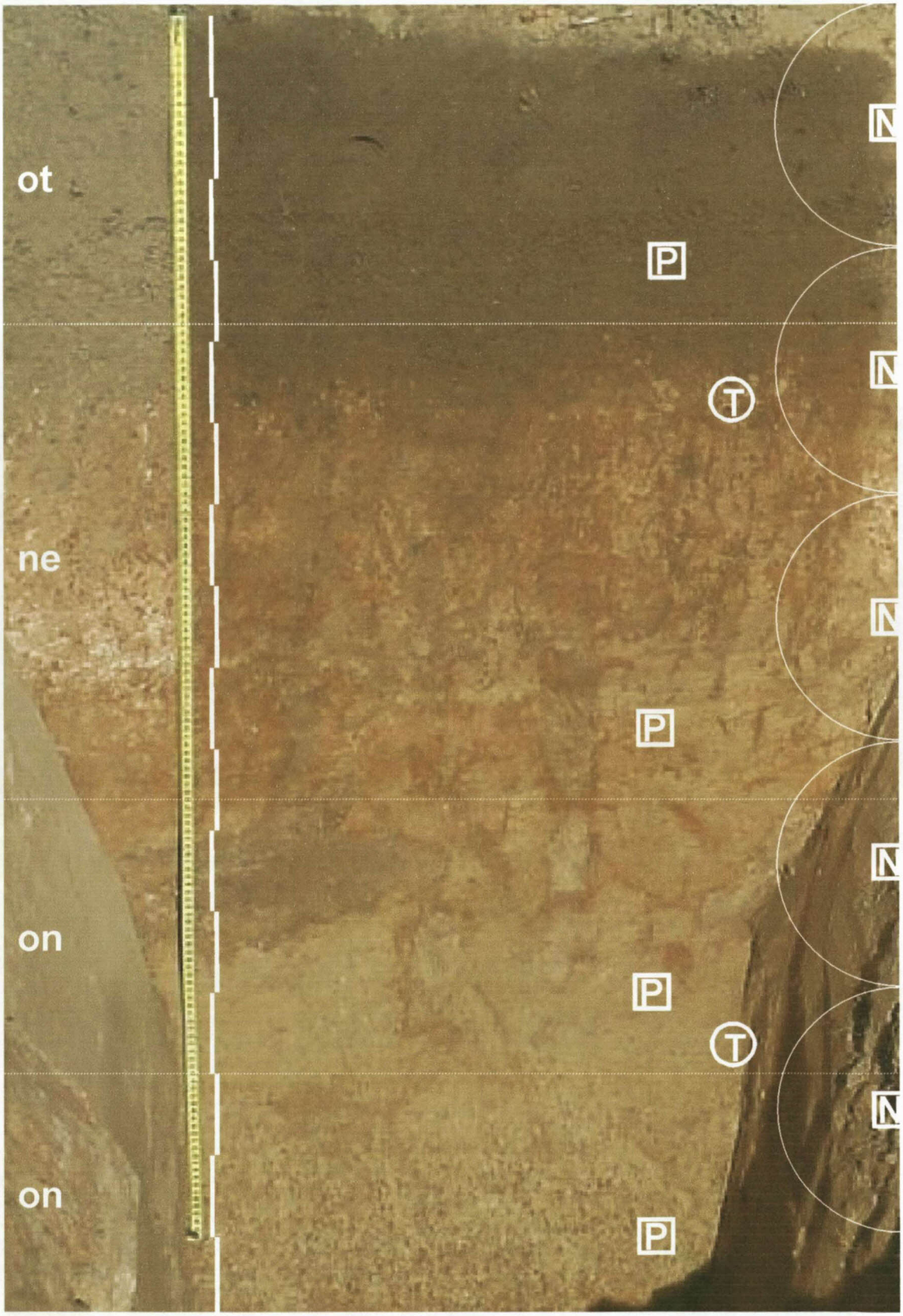


Figure 7 Profile 203 (Tukulu 2110), indicating diagnostic horizons as well as measurement depths for tensiometers [T], neutron water meter [N] and piezometers [P].

## Table 5 Profile description for profile 203 (Tukulu 2100)

**Profile No:** 203
**Map/photo:** 3128AB
**Latitude & Longitude:** 31° 06' 05.9" / 28° 20' 13.0"
**Surface stoniness:** None
**Altitude:** 1 322 m
**Terrain unit:** Midslope
**Slope:** 8 %
**Slope shape:** Convex
**Aspect:** West
**Microrelief:** None
**Parent material solum:** Single, solid rock
**Underlying material:** Feldspathic sandstone
**Geological Group:** Elliot

**Soil form:** Tukulu
**Soil family:** 2110
**Surface rockiness:** None
**Occurrence of flooding:** None
**Wind erosion:** None
**Water erosion:** None
**Vegetation / Land use:** Grassveld, open
**Water table:** None
**Described by:** P.A.L. le Roux & D. Scholtz
**Date described:** 19/06/2001
**Weathering of underlying material:** Strong physical, strong chemical
**Alteration of underlying material:** Ferruginised

| Horizon | Depth(mm) | Description | Diagnostic horizons |
|---|---|---|---|
| A | 0 - 380 | **Moisture status:** dry; **dry colour:** 10YR5/3 (100 %); **moist colour:** 7.5YR3/2 (100 %); 9.8 % clay; coarse sandy loam; no mottles; weak fine subangular blocky; slightly hard, friable, non-sticky, non-plastic; many normal fine and very fine pores; few normal medium and coarse pores; no slickensides; no cracks; no cutans; many 2-6 mm round stones; water absorption 2 second(s); many normal roots; gradual smooth transition; | orthic A horizon |
| B | 380 - 960 | **Moisture status:** dry; **dry colour:** 7.5YR7/4 (90 %), 7.5YR5/6 (10 %); **moist colour:** 7.5YR6/6 (90 %), 2.5YR5/8 (10 %); 12.5 % clay; medium sandy loam; common coarse prominent 2.5YR5/8 dry, 2.5YR4/8 moist, iron oxide mottles; common coarse prominent 5YR7/4 dry, 5YR6/4 moist, iron oxide mottles; weak fine subangular blocky; very hard, friable, non-sticky, non-plastic; many normal fine and very fine pores; few normal medium and coarse pores; no slickensides; no cracks; no cutans; no coarse fragments; water absorption 2 second(s); common normal roots; gradual smooth transition; | neocutanic B horizon |
| C1 | 960 - 1300 | **Moisture status:** moist; **dry colour:** 7.5YR7/4 (90 %), 7.5YR6/6 (10 %); **moist colour:** 5YR5/6 (90 %), 2.5YR4/8 (10 %); 13.8 % clay; coarse sandy clay loam; many medium distinct 5YR5/8 dry, 5YR4/6 moist, iron oxide mottles; few medium distinct 5YR6/8 dry, 5YR5/8 moist, iron oxide mottles; apedal massive; very hard, friable, non-sticky, non-plastic; common normal fine and very fine pores; few normal medium and coarse pores; no slickensides; no cracks; no cutans; no coarse fragments; water absorption 3 second(s); few normal roots; gradual smooth transition; | unspecified material with signs of wetness |
| C2 | 1300 - 1500 | **Moisture status:** moist; **dry colour:** 7.5YR8/2 (40 %), 7.5YR5/6 (40 %), 7.5YR6/8 (20 %); **moist colour:** 5YR7/2 (40 %), 5YR5/6 (40 %), 2.5YR4/8 (20 %); 27.8 % clay; coarse sandy clay loam; many fine prominent 2.5YR5/8 dry, 2.5YR4/6 moist, iron oxide mottles; many fine prominent 10YR5/6 dry, 7.5YR6/8 moist, iron oxide mottles; apedal massive; very hard, friable, non-sticky, non-plastic; few normal fine and very fine pores; no medium and coarse pores; no slickensides; no cracks; no cutans; no coarse fragments; water absorption 6 second(s); few normal roots; transition not reached; | unspecified material with signs of wetness |

Table 6 Soil analyses for profile 203 (Tukulu 2100)

| Horizon | Depth | Diagnostic horizon | Gravel | Texture of the fine earth | | | | | | | Exchangeable cations | | | | | CEC soil | CEC clay | Base sat |
|---|---|---|---|---|---|---|---|---|---|---|---|---|---|---|---|---|---|---|
| | | | | coSa | meSa | fiSa | vfSa | coSi | fiSi | Cl | Ca | Mg | K | Na | S | | | |
| | mm | | % | % | | | | | | | $cmol_c\ kg^{-1}$ | | | | | | | % |
| A | 0-100 | ot | 5.5 | 15.4 | 26.6 | 23.2 | 15.4 | 5.3 | 9.2 | 3.7 | 0.53 | 0.18 | 0.05 | 0.10 | 0.87 | 3.74 | 101.1 | 23 |
| | 100-200 | | 9.3 | 16.3 | 25.4 | 20.9 | 14.7 | 5.5 | 5.1 | 10.9 | 0.68 | 0.31 | 0.06 | 0.12 | 1.17 | 2.77 | 25.4 | 42 |
| | 200-300 | | 9.4 | 14.0 | 22.9 | 21.8 | 17.6 | 5.4 | 4.6 | 12.3 | 0.58 | 0.29 | 0.05 | 0.15 | 1.07 | 2.62 | 21.3 | 41 |
| | 300-400 | | 7.1 | 21.3 | 27.1 | 20.5 | 13.7 | 0.9 | 1.9 | 12.2 | 0.56 | 0.29 | 0.06 | 0.15 | 1.06 | 2.61 | 21.4 | 41 |
| B | 400-500 | ne | 4.9 | 14.8 | 25.9 | 21.4 | 14.8 | 9.4 | 1.2 | 12.1 | 0.39 | 0.36 | 0.08 | 0.14 | 0.96 | 6.37 | 52.7 | 15 |
| | 500-600 | | 6.4 | 16.0 | 26.0 | 20.5 | 14.1 | 9.7 | 5.2 | 10.7 | 0.51 | 0.40 | 0.09 | 0.13 | 1.13 | 4.51 | 42.2 | 25 |
| | 600-800 | | 13.3 | 13.3 | 26.4 | 21.9 | 15.7 | 5.5 | 4.3 | 13.4 | 0.43 | 0.40 | 0.09 | 0.13 | 1.06 | 6.14 | 45.9 | 17 |
| C1 | 900-1200 | on | 5.6 | 15.6 | 25.4 | 20.3 | 15.1 | 4.5 | 4.0 | 13.8 | 0.46 | 0.46 | 0.09 | 0.13 | 1.14 | 5.93 | 43.0 | 19 |
| C2 | 1200+ | | 20.9 | 18.4 | 18.0 | 11.5 | 10.0 | 5.1 | 8.7 | 27.8 | 1.63 | 2.05 | 0.23 | 0.16 | 4.06 | 5.93 | 21.3 | 69 |

| Horizon | Depth | Bulk density | pH | | Org C | N | C:N | Fe | | | Mn | | | Mineralogy |
|---|---|---|---|---|---|---|---|---|---|---|---|---|---|---|
| | | | | | | | | CBD | Ox | Piro | CBD | Ox | Piro | |
| | mm | $Mg\ m^{-3}$ | $H_2O$ | KCl | % | $mg\ kg^{-1}$ | | $mg\ kg^{-1}$ | | | | | | < 0,002mm |
| A | 0-100 | 1.65 | 4.25 | 4.06 | 0.31 | 231 | 13.3 | 4975 | 513 | 379 | 17.5 | 5.0 | 13.1 | |
| | 100-200 | | 4.24 | 4.06 | 0.27 | 229 | 11.7 | 4630 | 515 | 334 | 19.5 | 11.0 | 17.1 | |
| | 200-300 | | 4.28 | 4.02 | 0.21 | 130 | 16.4 | 4500 | 430 | 303 | 17.0 | 9.0 | 14.1 | |
| | 300-400 | 1.74 | | | 0.25 | 147 | 17.2 | 5250 | 440 | 287 | 19.0 | 8.0 | 14.1 | |
| B | 400-500 | | 4.30 | 4.00 | 0.19 | 205 | 9.3 | 5715 | 424 | 388 | 15.0 | 5.5 | 13.1 | |
| | 500-600 | | 4.35 | 4.15 | 0.27 | 206 | 13.1 | 5630 | 481 | 399 | 17.5 | 5.5 | 14.1 | |
| | 600-800 | 1.62 | 4.21 | 4.15 | 0.27 | 121 | 22.4 | 4975 | 432 | 373 | 11.5 | 3.5 | 11.0 | |
| C1 | 900-1200 | 1.75 | 4.48 | 4.07 | 0.08 | 121 | 7.0 | 5110 | 376 | 271 | 17.0 | 5.0 | 11.0 | |
| C2 | 1200+ | 1.77 | 4.82 | 4.17 | 0.04 | 149 | 2.4 | 8100 | 590 | 211 | 36.5 | 17.0 | 16.1 | |

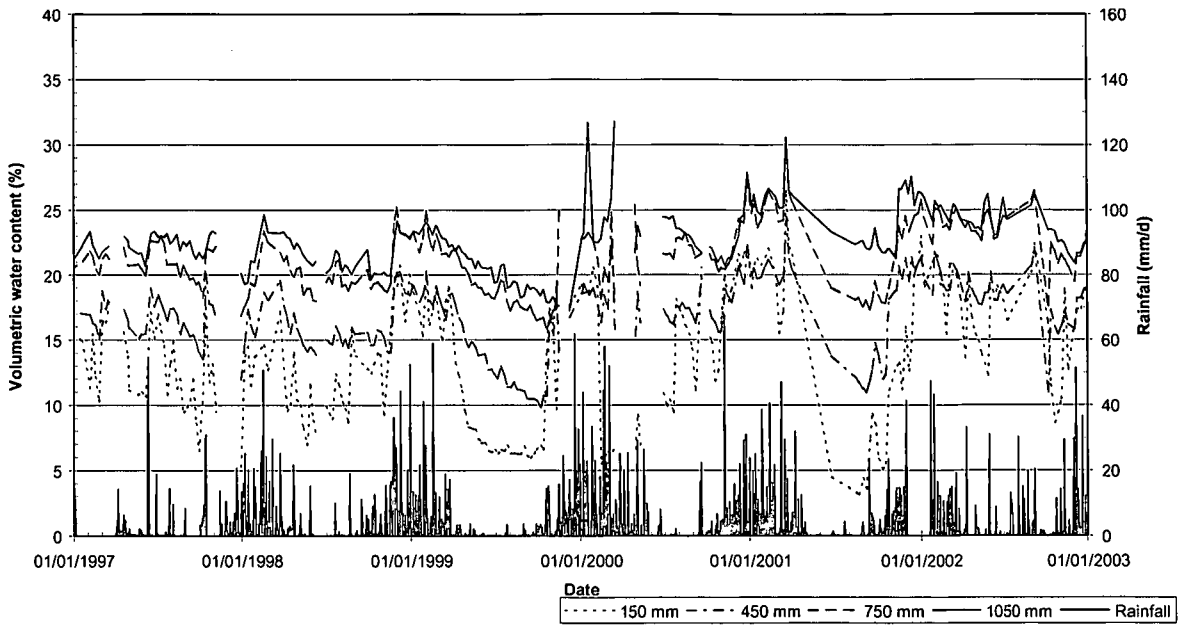


Figure 8 Volumetric water content and daily rainfall from 1 January 1997 until 31 December 2002 for profile 203.

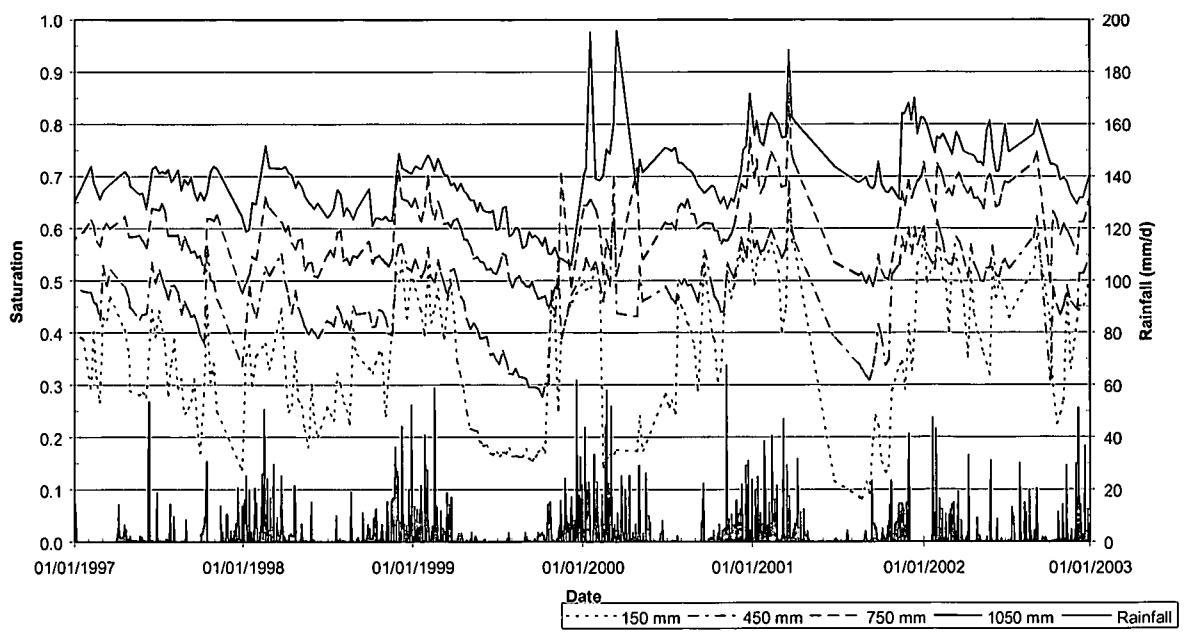


Figure 9 Degree of water saturation and daily rainfall from 1 January 1997 until 31 December 2002 for profile 203.

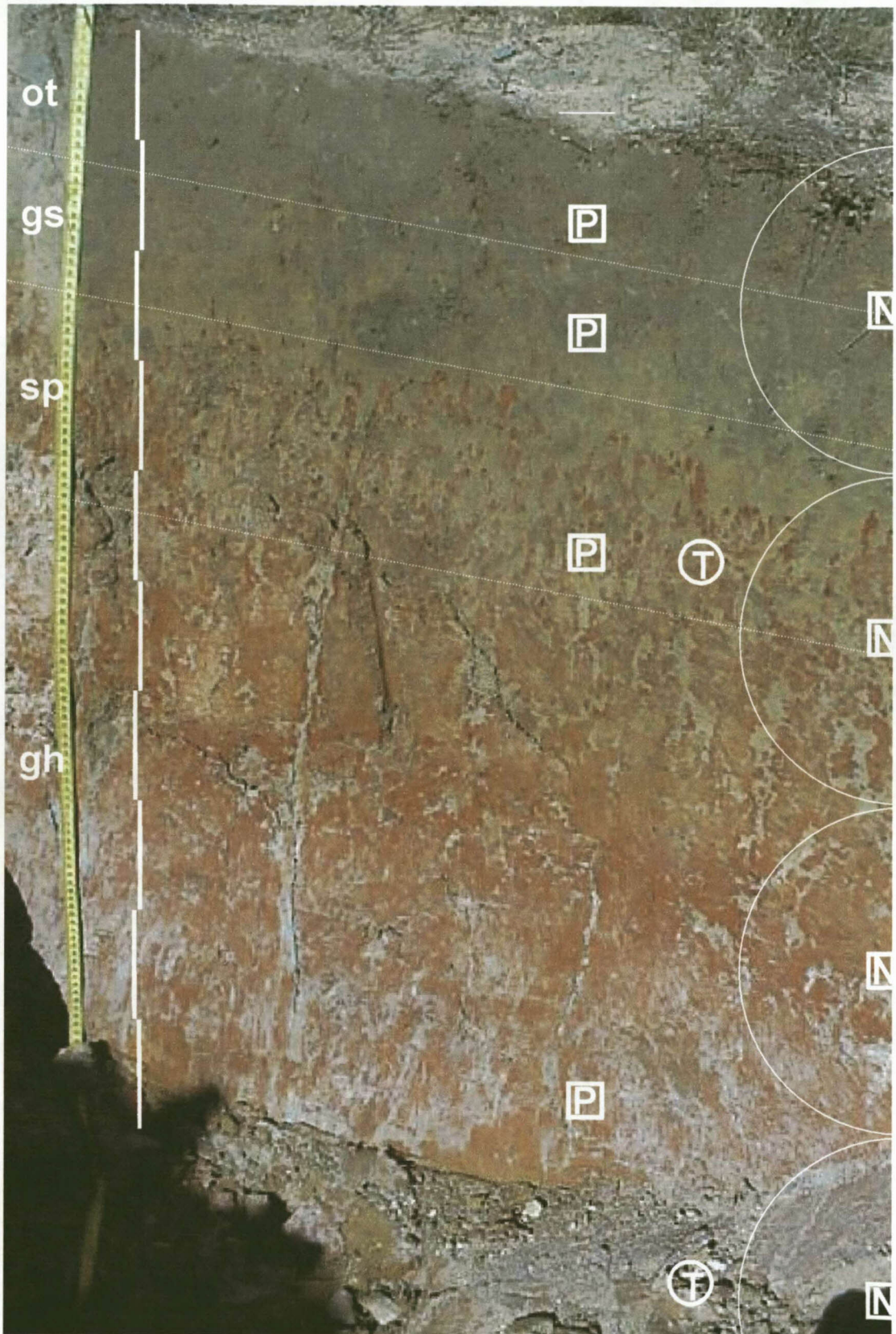


Figure 10 Profile 204 (Longlands 2000), indicating diagnostic horizons as well as measurement depths for tensiometers [T], neutron water meter [N] and piezometers [P].

## Table 7 Profile description for profile 204 (Longlands 2000)

**Profile No:** 204
**Map/photo:** 3128AB
**Latitude & Longitude:** 31° 06' 06.0" / 28° 20' 11.1"
**Surface stoniness:** None
**Altitude:** 1 317 m
**Terrain unit:** Crest / footslope
**Slope:** 2 %
**Slope shape:** Straight
**Aspect:** West
**Microrelief:** Terracettes, 2 %
**Parent material solum:** Origin single, solid rock
**Underlying material:** Mudstone
**Geological Group:** Elliot

**Soil form:** Longlands
**Soil family:** 2000
**Surface rockiness:** None
**Occurrence of flooding:** None
**Wind erosion:** None
**Water erosion:** None
**Vegetation / Land use:** Grassveld, open
**Water table:** None
**Described by:** P.A.L. le Roux & M. Scholtz
**Date described:** 19/06/2001
**Weathering of underlying material:** Advanced physical, strong chemical
**Alteration of underlying material:** Ferruginised

| Horizon | Depth(mm) | Description | Diagnostic horizons |
|---|---|---|---|
| A | 0 - 140 | **Moisture status:** moist; **dry colour:** 7.5YR6/2 (50 %), 7.5YR7/2 (50 %); **moist colour:** 10YR3/3 (50 %), 10YR6/6 (50 %); 7.9 % clay; loam medium sand; few fine prominent 5YR5/8 dry, 2.5YR4/8 moist, iron oxide mottles; apedal massive; loose, loose, non-sticky, non-plastic; many rusty fine and very fine pores; no medium and coarse pores; no slickensides; no cracks; few sesquioxide cutans; no coarse fragments; water absorption 1 second(s); many rusty roots; clear smooth transition; Remark: clear difference in consistency and structure between horizon 3 and 4. | orthic A horizon |
| E | 140 - 300 | **Moisture status:** moist; **dry colour:** 7.5YR7/5 (60 %), 7.5YR7/2 (40 %); **moist colour:** 10YR6/6 (60 %), 2.5YR2/4 (40 %); 9.5 % clay; fine sandy loam; many medium distinct 5YR5/8 dry, 2.5YR4/8 moist, iron oxide mottles; apedal massive; soft, friable, non-sticky, non-plastic; many rusty fine and very fine pores; no medium and coarse pores; no slickensides; no cracks; few sesquioxide cutans; no coarse fragments; water absorption 1 second(s); many rusty roots; clear smooth transition; | E horizon |
| B | 300 - 470 | **Moisture status:** moist; **dry colour:** 10YR8/2 (40 %), 2.5YR5/8 (40 %), 2.5YR6/4 (20 %); **moist colour:** 10YR6/4 (40 %), 2.5YR4/8 (40 %), 2.5YR5/4 (20 %); 13.6 % clay; fine sandy loam; common coarse prominent 2.5YR4/8 dry, 2.5YR4/8 moist, iron oxide mottles; common coarse prominent 10YR4/8 dry, 7.5YR8/3 moist, mottles; apedal massive; very hard, very firm, non-sticky, non-plastic; no fine and very fine pores; few bleached medium and coarse pores; no slickensides; coarse cracks; few silica cutans; very few 75-250 mm round & flat stones; water absorption 2 second(s); few bleached roots; gradual smooth transition; | soft plinthic B horizon |
| G | 470 - 1000 | **Moisture status:** moist; **dry colour:** 10YR8/2 (90 %), 2.5YR5/8 (10 %); **moist colour:** 10YR7/2 (90 %), 2.5YR4/8 (10 %); 29.5 % clay; coarse sandy loam; many fine prominent 2.5YR4/8 dry, 2.5YR4/8 moist, geogenic iron mottles; strong coarse angular blocky; very hard, very firm, very sticky, very plastic; no fine and very fine pores; few bleached medium and coarse pores; no slickensides; coarse cracks; common silica cutans; no coarse fragments; water absorption 8 second(s); few bleached roots; transition not reached; | G horizon |

Table 8 Soil analyses for profile 204 (Longlands 2000)

| Horizon | Depth | Diagnostic horizon | Gravel | Texture of the fine earth | | | | | | | Exchangeable cations | | | | | CEC soil | CEC clay | Base sat |
|---|---|---|---|---|---|---|---|---|---|---|---|---|---|---|---|---|---|---|
| | | | | coSa | meSa | fiSa | vfSa | coSi | fiSi | Cl | Ca | Mg | K | Na | S | | | |
| | mm | | % | % | | | | | | | cmolc $kg^{-1}$ soil | | | | | | | % |
| A | 0-100 | ot | 5.5 | 11.9 | 21.3 | 28.5 | 21.6 | 5.1 | 4.3 | 7.5 | 0.48 | 0.24 | 0.06 | 0.13 | 0.91 | 7.72 | 102.9 | 12 |
| E | 100-200 | gs | 7.6 | 11.8 | 22.7 | 27.7 | 20.4 | 4.8 | 4.9 | 8.2 | 0.41 | 0.25 | 0.05 | 0.12 | 0.82 | 10.28 | 125.3 | 8 |
| | 200-300 | | 9.7 | 9.4 | 20.4 | 27.4 | 22.3 | 2.2 | 5.4 | 9.5 | 0.36 | 0.26 | 0.06 | 0.12 | 0.79 | 9.62 | 101.3 | 8 |
| B | 300-400 | sp | 4.0 | 8.4 | 20.3 | 26.1 | 22.3 | 6.2 | 7.5 | 12.1 | 0.43 | 0.44 | 0.06 | 0.14 | 1.05 | 11.15 | 92.1 | 9 |
| | 400-500 | | 3.4 | 5.0 | 12.3 | 31.6 | 23.1 | 4.9 | 5.6 | 15.1 | 0.58 | 0.71 | 0.07 | 0.13 | 1.5 | 11.04 | 73.1 | 14 |
| G | 500-800 | gh | 2.5 | 5.8 | 14.3 | 22.9 | 17.3 | 18.1 | 7.3 | 11.6 | 1.18 | 1.13 | 0.09 | 0.14 | 2.55 | 8.97 | 77.3 | 28 |
| | 800-1100 | | 3.9 | 3.2 | 7.0 | 12.3 | 9.2 | 5.3 | 9.3 | 52.1 | 6.97 | 6.51 | 0.43 | 0.30 | 14.2 | 20.77 | 39.9 | 68 |
| | 1100+ | | 68.8 | 28.0 | 20.5 | 10.0 | 5.6 | 2.7 | 5.4 | 24.8 | 1.93 | 2.13 | 0.09 | 0.13 | 4.27 | 11.91 | 48.0 | 36 |

| Horizon | Depth | Bulk density | pH | | Org C | N | C:N | Fe | | | Mn | | | Mineralogy |
|---|---|---|---|---|---|---|---|---|---|---|---|---|---|---|
| | | | | | | | | CBD | Ox | Piro | CBD | Ox | Piro | |
| | mm | Mg $m^{-3}$ | $H_2O$ | KCl | % | mg $kg^{-1}$ | | mg $kg^{-1}$ | | | | | | < 0,002mm |
| A | 0-100 | 1.60 | 4.96 | 4.44 | 0.50 | 394 | 12.6 | 4130 | 1060 | 613 | 8.5 | 5.0 | 13.1 | |
| E | 100-200 | | 6.06 | 4.43 | 0.45 | 344 | 13.1 | 2590 | 472 | 605 | 5.0 | 2.5 | 12.0 | |
| | 200-300 | | 5.80 | 4.65 | 0.31 | 290 | 10.5 | 7145 | 720 | 534 | 54.5 | 4.5 | 12.0 | |
| B | 300-400 | 1.74 | 5.47 | 4.80 | 0.09 | 125 | 6.9 | 12600 | 1170 | 312 | 3.5 | 41.5 | 16.1 | |
| | 400-500 | | 5.69 | 4.62 | 0.03 | 133 | 2.0 | 12600 | 1265 | 603 | 22.0 | 60.0 | 18.1 | |
| G | 500-800 | 1.82 | 5.41 | 4.38 | 0.06 | 146 | 4.0 | 3560 | 462 | 261 | 28.5 | 13.5 | 14.1 | |
| | 800-1100 | 1.82 | 5.45 | 4.36 | 0.09 | 265 | 3.4 | 2865 | 257 | 200 | 16.5 | 1.0 | 12.0 | |
| | 1100+ | | | | 0.04 | 125 | 2.9 | 3665 | 213 | 275 | 8.5 | 21.5 | 12.0 | |

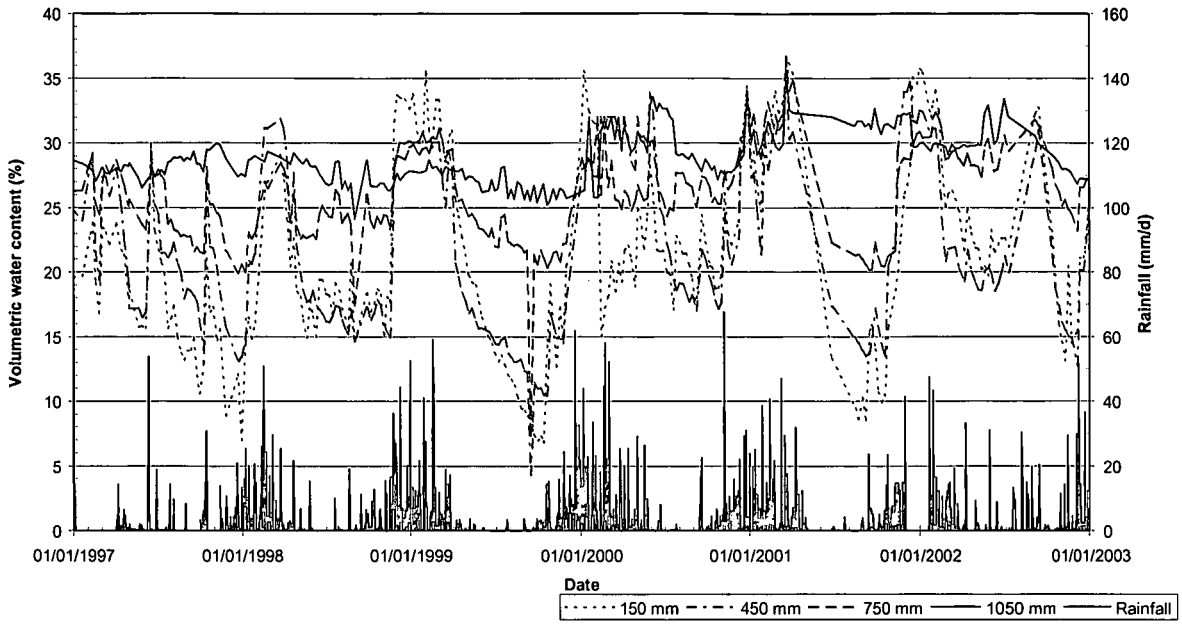


Figure 11 Volumetric water content and daily rainfall from 1 January 1997 until 31 December 2002 for profile 204.

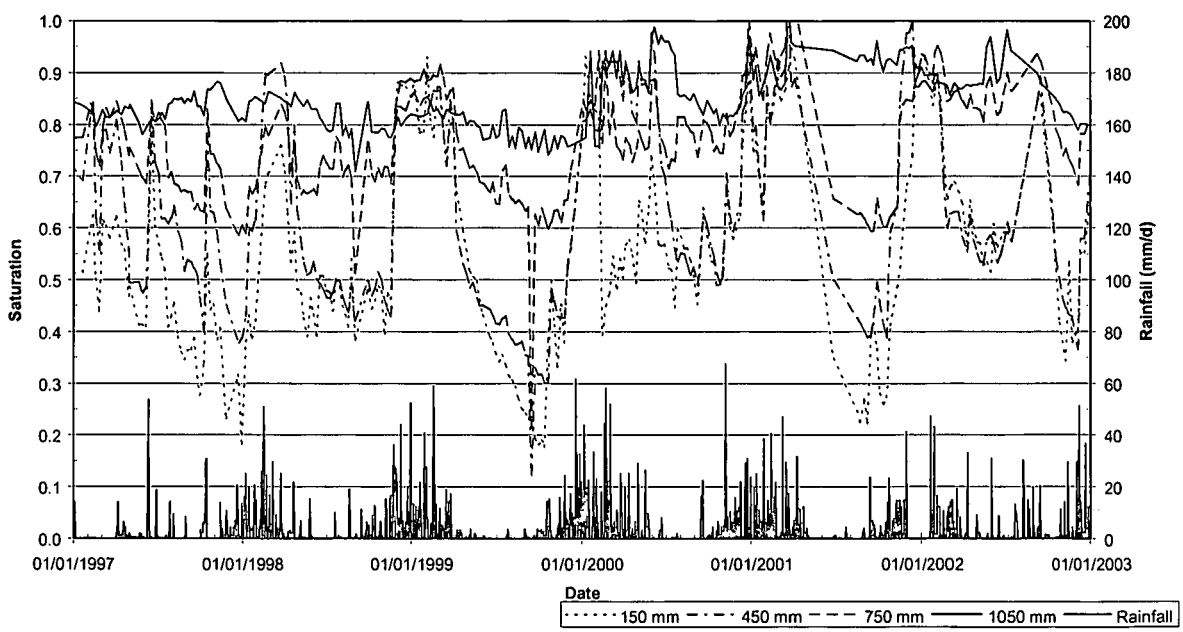


Figure 12 Degree of water saturation and daily rainfall from 1 January 1997 until 31 December 2002 for profile 204.

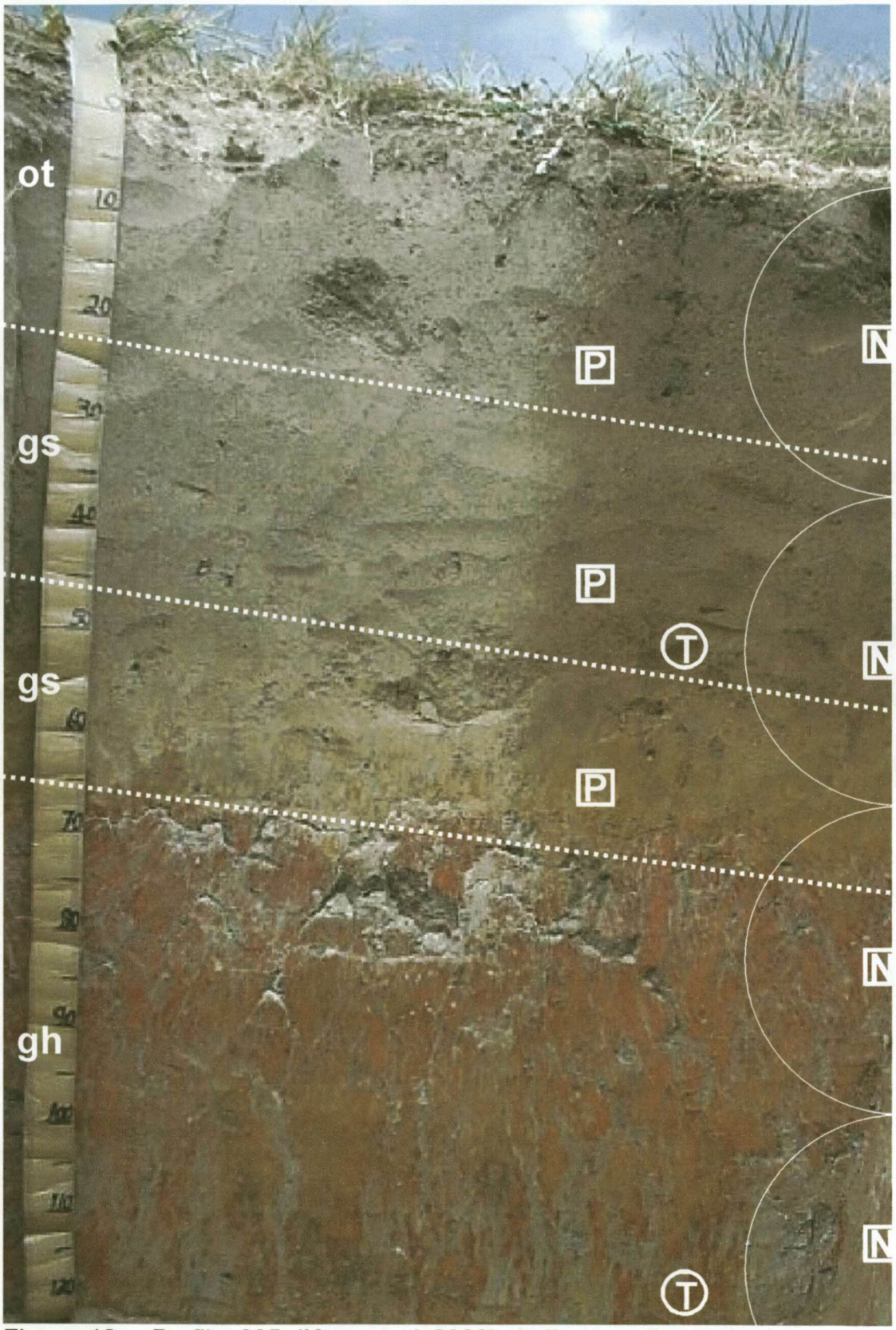


Figure 13 Profile 205 (Kroonstad 2000), indicating diagnostic horizons as well as measurement depths for tensiometers [T], neutron water meter [N] and piezometers [P].

## Table 9 Profile description for profile 205 (Kroonstad 2000)

**Profile No:** 205
**Map/photo:** 3128AB
**Latitude & Longitude:** 31° 06' 07.9" / 28° 20' 03.4"
**Surface stoniness:** None
**Altitude:** 1 286 m
**Terrain unit:** Lower midslope
**Slope:** 7 %
**Slope shape:** Concave
**Aspect:** North-west
**Microrelief:** None
**Parent material solum:** Origin single, solid rock
**Underlying material:** Mudstone
**Geological Group:** Molteno

**Soil form:** Kroonstad
**Soil family:** 2000
**Surface rockiness:** None
**Occurrence of flooding:** None
**Wind erosion:** None
**Water erosion:** None
**Vegetation / Land use:** Grassveld, closed
**Water table:** None
**Described by:** D. Scholtz & T.B. Zere
**Date described:** 19/06/2001
**Weathering of underlying material:** Moderate physical, strong chemical
**Alteration of underlying material:** Ferruginised

| Horizon | Depth(mm) | Description | Diagnostic horizons |
|---|---|---|---|
| A | 0 - 220 | Moisture status: moist; dry colour: 2.5Y5/2 (100 %); moist colour: 2.5Y3/2 (100 %); 13.1 % clay; coarse sandy loam; no mottles; weak fine subangular blocky; hard, friable, non-sticky, non-plastic; many rusty fine and very fine pores; few bleached medium and coarse pores; no slickensides; no cracks; no cutans; no coarse fragments; water absorption 1 second(s); many normal roots; diffuse smooth transition; | orthic A horizon |
| E1 | 220 - 460 | **Moisture status:** moist; **dry colour:** 2.5Y6/1 (70 %), 10YR6/6 (30 %); **moist colour:** 10YR3/3 (70 %), 10YR4/6 (30 %); 11.0 % clay; coarse sandy loam; many medium distinct 10YR6/6 dry, 10YR4/6 moist, iron oxide mottles; common medium distinct 2.5Y4/2 dry, 2.5Y3/2 moist, humus mottles; weak fine granular; hard, friable, non-sticky, non-plastic; many rusty fine and very fine pores; no medium and coarse pores; no slickensides; no cracks; no cutans; no coarse fragments; water absorption 2 second(s); many normal roots; clear smooth transition; | E horizon |
| E2 | 460 - 660 | **Moisture status:** moist; **dry colour:** 10YR6/2 (80 %), 10YR5/8 (10 %), 10YR5/2 (10 %); **moist colour:** 10YR5/2 (80 %), 7.5YR5/8 (10 %), 10YR4/3 (10 %); 11.0 % clay; coarse sandy loam; common medium distinct 10YR6/8 dry, 7.5YR5/8 moist, iron oxide mottles; common medium prominent 2.5Y4/2 dry, 2.5Y3/2 moist, humus mottles; weak fine granular; hard, friable, slightly sticky, slightly plastic; many rusty fine and very fine pores; no medium and coarse pores; no slickensides; no cracks; no cutans; no coarse fragments; water absorption 4 second(s); common normal roots; abrupt smooth transition; | E horizon |
| G | 660 - 1400 | **Moisture status:** moist; **dry colour:** 2.5Y7/1 (70 %), 10YR4/8 (30 %); **moist colour:** 2.5Y6/2 (70 %), 10YR4/8 (30 %); 28.0 % clay; coarse sandy loam; common fine prominent 2.5YR4/8 dry, 10R4/8 moist, iron oxide mottles; common medium prominent 10YR6/8 dry, 7.5YR4/8 moist, iron oxide mottles; strong coarse angular blocky; very hard, very firm, sticky, plastic; common normal fine and very fine pores; no medium and coarse pores; many slickensides; fine cracks; common silica cutans; few 2-6 mm round stones; water absorption 8 second(s); few normal roots; transition not reached; | G horizon |

Table 10 Soil analyses for profile 205 (Kroonstad 2000)

| Horizon | Depth | Diagnostic horizon | Gravel | Texture of the fine earth | | | | | | | Exchangeable cations | | | | | CEC soil | CEC clay | Base sat |
|---|---|---|---|---|---|---|---|---|---|---|---|---|---|---|---|---|---|---|
| | | | | coSa | meSa | fiSa | vfSa | coSi | fiSi | Cl | Ca | Mg | K | Na | S | | | |
| | mm | | % | % | | | | | | | cmolc $kg^{-1}$ | | | | | | | % |
| A | 0-100 | ot | 7.1 | 28.1 | 23.6 | 12.7 | 11.0 | 4.7 | 8.8 | 9.5 | 1.40 | 0.55 | 0.16 | 0.10 | 2.21 | 10.49 | 110.5 | 21 |
| | 100-200 | | 5.6 | 29.2 | 23.2 | 12.5 | 11.7 | 3.6 | 9.1 | 10.0 | 1.35 | 0.56 | 0.15 | 0.13 | 2.18 | 10.17 | 101.7 | 21 |
| E1 | 200-300 | gs | 3.5 | 32.8 | 22.0 | 11.9 | 10.8 | 3.5 | 8.4 | 9.8 | 0.68 | 0.42 | 0.08 | 0.11 | 1.3 | 11.85 | 121.0 | 11 |
| | 300-400 | | 5.4 | 34.0 | 22.7 | 11.1 | 9.9 | 4.5 | 7.8 | 9.4 | 0.71 | 0.27 | 0.09 | 0.11 | 1.18 | 14.30 | 152.1 | 8 |
| | 400-500 | | 7.7 | 33.5 | 22.2 | 11.3 | 9.6 | 4.8 | 8.7 | 10.2 | 0.70 | 0.34 | 0.11 | 0.13 | 1.28 | 15.66 | 153.5 | 8 |
| E2 | 500-600 | gs | 5.4 | 23.6 | 23.2 | 14.0 | 11.7 | 4.8 | 8.7 | 12.3 | 0.66 | 0.42 | 0.10 | 0.14 | 1.32 | 15.17 | 123.3 | 9 |
| | 600-700 | | 6.4 | 24.8 | 23.3 | 13.3 | 12.8 | 3.7 | 8.6 | 13.4 | 0.63 | 0.44 | 0.07 | 0.12 | 1.26 | 12.29 | 91.7 | 1 |
| G | 700-800 | gh | 11.9 | 17.7 | 22.1 | 13.8 | 13.8 | 5.7 | 9.1 | 17.0 | 1.11 | 0.79 | 0.10 | 0.16 | 2.16 | 15.99 | 94.0 | 14 |
| | 800-950 | | 11.7 | 17.5 | 15.1 | 7.9 | 10.1 | 4.0 | 10.0 | 33.7 | 2.38 | 2.13 | 0.20 | 0.18 | 4.9 | 15.17 | 45.0 | 32 |
| | 950-1100 | | 20.1 | 6.0 | 12.1 | 13.9 | 6.2 | 7.9 | 10.7 | 40.1 | 1.74 | 1.48 | 0.17 | 0.16 | 3.55 | 17.63 | 44.0 | 2 |
| | 1100-1400 | | 63.0 | 13.2 | 18.5 | 9.9 | 16.5 | 4.5 | 9.9 | 25.7 | 1.87 | 1.30 | 0.11 | 0.16 | 3.44 | 13.54 | 52.7 | 25 |
| | 1400+ | | 24.2 | 9.3 | 11.1 | 4.9 | 3.5 | 14.1 | 31.8 | 23.5 | 6.45 | 4.27 | 0.22 | 0.23 | 11.17 | 14.03 | 59.7 | 8 |

| Horizon | Depth | Bulk density | pH | | Org C | N | C:N | Fe | | | Mn | | | Mineralogy |
|---|---|---|---|---|---|---|---|---|---|---|---|---|---|---|
| | | | | | | | | CBD | Ox | Piro | CBD | Ox | Piro | |
| | mm | Mg $m^{-3}$ | $H_2O$ | KCl | % | mg $kg^{-1}$ | | mg $kg^{-1}$ | | | | | | < 0,002mm |
| A | 0-100 | 1.66 | 5.38 | 4.57 | 0.78 | 680 | 11.5 | 5385 | 665 | 798 | 4.5 | 16.5 | 26.1 | |
| | 100-200 | | 5.32 | 4.37 | 0.79 | 609 | 12.9 | 4075 | 1460 | 784 | 5.0 | 13.0 | 17.1 | |
| E1 | 200-300 | | 5.37 | 4.31 | 0.53 | 503 | 10.6 | 4245 | 1390 | 872 | 4.0 | 5.0 | 14.1 | |
| | 300-400 | 1.69 | 5.35 | 4.20 | 0.54 | 426 | 12.6 | 5625 | 1500 | 822 | 3.5 | 3.0 | 13.1 | |
| | 400-500 | | 5.41 | 4.27 | 0.78 | 431 | 18.0 | 3865 | 1760 | 681 | 11.0 | 2.5 | 12.0 | |
| E2 | 500-600 | | 5.40 | 4.21 | 0.35 | 431 | 8.0 | 4285 | 1640 | 643 | 46.0 | 1.5 | 11.0 | |
| | 600-700 | 1.72 | 5.52 | 4.28 | 0.31 | 330 | 9.3 | 5855 | 1170 | 584 | 69.0 | 1.5 | 11.0 | |
| G | 700-800 | | 5.67 | 4.20 | 0.16 | 295 | 5.4 | 7145 | 587 | 427 | 10.5 | 1.0 | 11.0 | |
| | 800-950 | | 5.86 | 5.82 | 0.20 | 383 | 5.1 | 4285 | 369 | 297 | 2.5 | 5.0 | 11.0 | |
| | 950-1100 | 1.79 | 5.66 | 4.22 | 0.38 | 486 | 7.8 | 5855 | 692 | 363 | 30.5 | 1.0 | 11.0 | |
| | 1100-1400 | | 5.92 | 4.31 | 0.09 | 234 | 3.6 | 1260 | 280 | 240 | 75.0 | 18.0 | 13.1 | |
| | 1400+ | 1.73 | 5.97 | 4.40 | 0.08 | 289 | 2.9 | 5420 | 249 | 228 | 47.0 | 61.0 | 15.1 | |

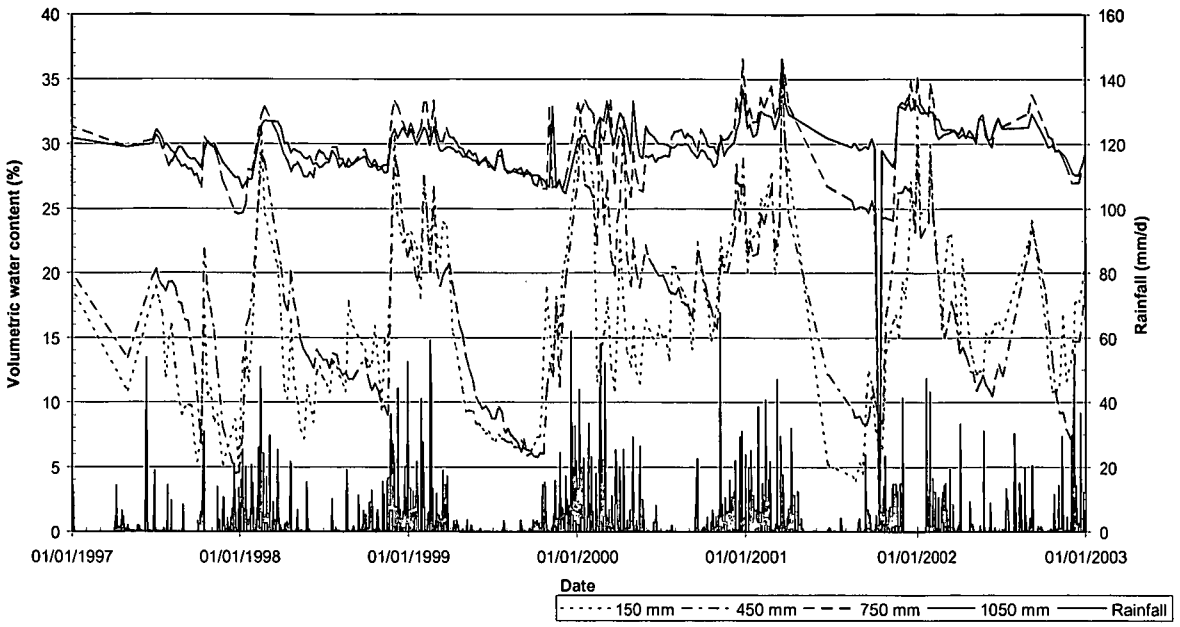


Figure 14 Volumetric water content and daily rainfall from 1 January 1997 until 31 December 2002 for profile 205.

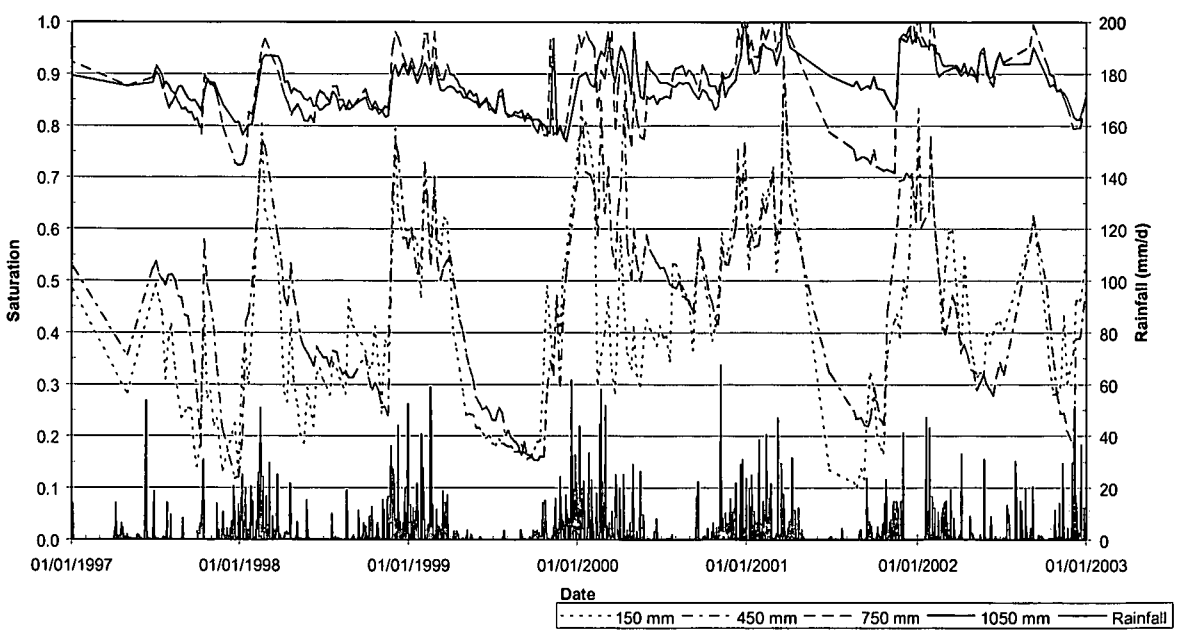


Figure 15 Degree of water saturation and daily rainfall from 1 January 1997 until 31 December 2002 for profile 205.

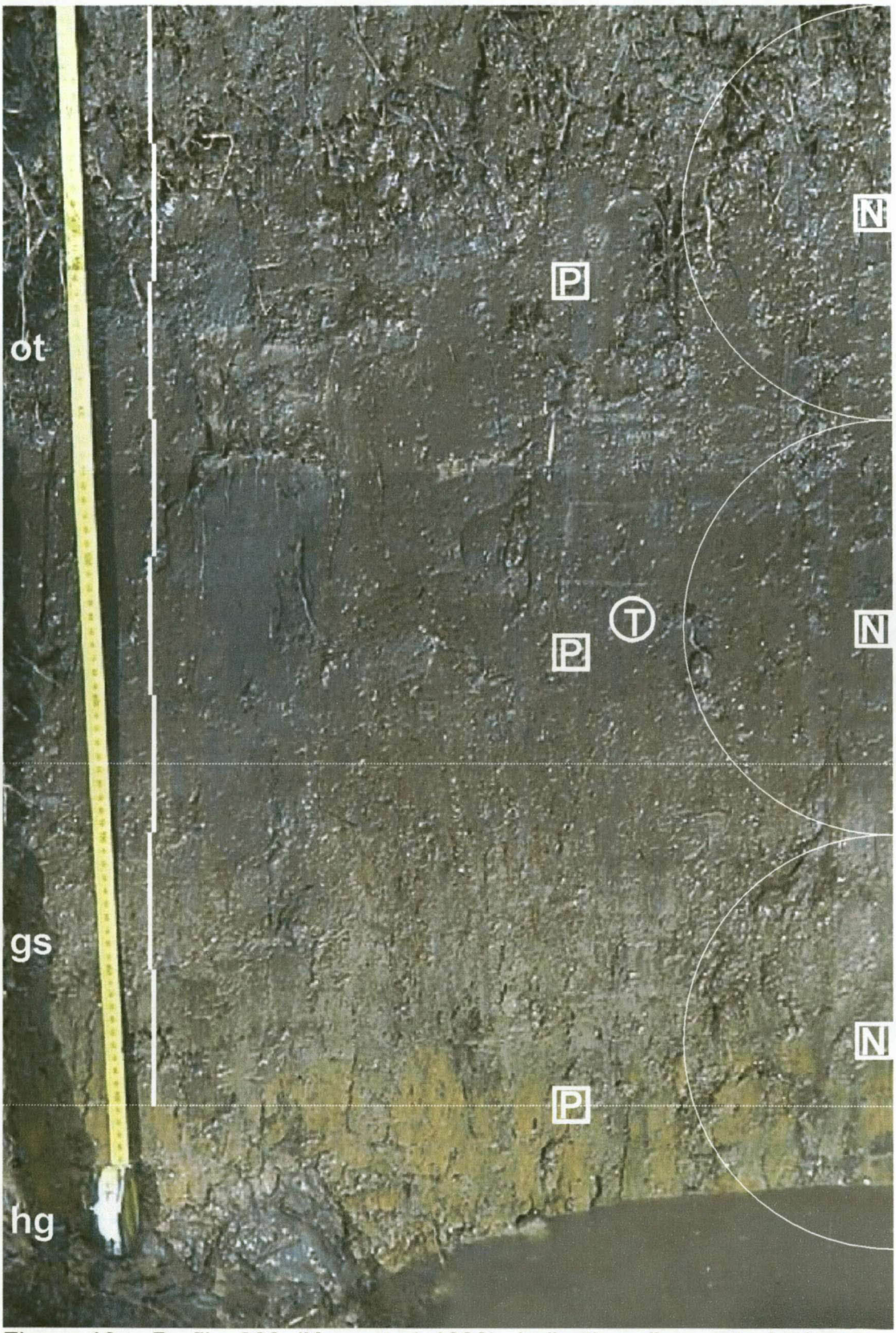


Figure 16 Profile 206 (Kroonstad 1000), indicating diagnostic horizons as well as measurement depths for tensiometers [T], neutron water meter [N] and piezometers [P].

## Table 11 Profile description for profile 206 (Kroonstad 1000)

**Profile No:** 206
**Map/photo:** 3128AB
**Latitude & Longitude:** 31° 06' 07.9" / 28° 20' 00.9"
**Surface stoniness:** None
**Altitude:** 1 281 m
**Terrain unit:** Lower footslope
**Slope:** 3 %
**Slope shape:** Straight
**Aspect:** North-west
**Microrelief:** 10 % mole mounds, 0,6 m high, profile between features
**Parent material solum:** Single, local colluvium
**Underlying material:** Mudstone
**Geological Group:** Molteno

**Soil form:** Kroonstad
**Soil family:** 1000
**Surface rockiness:** None
**Occurrence of flooding:** None
**Wind erosion:** None
**Water erosion:** None
**Vegetation / Land use:** Grassveld, closed
**Water table:** 200 mm
**Described by:** D. Scholtz & T.B. Zere
**Date described:** 19/06/2001
**Weathering of underlying material:** Advanced physical, strong chemical
**Alteration of underlying material:** Ferruginised

| Horizon | Depth(mm) | Description | Diagnostic horizons |
|---|---|---|---|
| A | 0 - 550 | **Moisture status:** Wet; **dry colour:** 10YR5/1 (100 %); **moist colour:** 10YR3/1 (100 %); 21.7 % clay; loam; few fine distinct 7.5YR5/8 dry, 10YR4/6 moist, iron oxide mottles; weak medium granular; hard, friable, sticky, plastic; common normal fine and very fine pores; few rusty medium and coarse pores; no slickensides; no cracks; no cutans; no coarse fragments; water absorption 1 second(s); many rusty roots; clear smooth transition; | orthic A horizon |
| E | 550 - 800 | **Moisture status:** Wet; **dry colour:** 10YR5/1 (95 %), 7.5YR5/8 (5 %); **moist colour:** 10YR2/1 (95 %), 10YR4/6 (5 %), 16.6 % clay; loam; common fine prominent 7.5YR5/8 dry, 10YR4/6 moist, iron oxide mottles; few fine prominent 10YR2/1 dry, 10YR2/1 moist, manganese mottles; apedal massive; very hard, friable, non-sticky, non-plastic; few normal fine and very fine pores; few bleached medium and coarse pores; no slickensides; no cracks; no cutans; few 2-6 mm mixed shaped stones; water absorption 1 second(s); few bleached roots; clear smooth transition; | E horizon |
| G | 800 - 1100 | **Moisture status:** Wet; **dry colour:** 10YR6/1 (90 %), 7.5YR5/8 (10 %); **moist colour:** 10YR4/1 (90 %), 10YR5/8 (10 %); 38.0 % clay; clay loam; many medium prominent 7.5YR5/8 dry, 10YR5/8 moist, iron oxide mottles; moderate coarse subangular blocky; very hard, firm, sticky, plastic; few bleached fine and very fine pores; few bleached medium and coarse pores; no slickensides; medium cracks; common silica cutans; very few 6-25 mm mixed shaped stones; water absorption 8 second(s); few bleached roots; transition not reached; | G horizon |

Table 12 Soil analyses for profile 206 (Kroonstad 1000)

| Horizon | Depth | Diagnostic horizon | Gravel | Texture of the fine earth | | | | | | | Exchangeable cations | | | | | CEC soil | CEC clay | Base sat |
|---|---|---|---|---|---|---|---|---|---|---|---|---|---|---|---|---|---|---|
| | | | | coSa | meSa | fiSa | vfSa | coSi | fiSi | Cl | Ca | Mg | K | Na | S | | | |
| | mm | | % | % | | | | | | | cmolc $kg^{-1}$ | | | | | | | % |
| A | 0-100 | ot | 13.3 | 6.9 | 6.6 | 10.1 | 11.5 | 7.4 | 32.9 | 23.2 | 8.91 | 3.27 | 0.29 | 0.33 | 12.81 | 30.99 | 134.0 | 41 |
| | 100-200 | | 15.4 | 7.0 | 6.8 | 7.8 | 15.8 | 13.4 | 27.0 | 23.9 | 9.95 | 2.78 | 0.19 | 0.30 | 13.21 | 19.19 | 80.3 | 69 |
| | 200-300 | | 7.2 | 8.1 | 7.3 | 7.8 | 14.0 | 15.8 | 21.9 | 24.6 | 5.91 | 2.06 | 0.15 | 0.27 | 8.39 | 15.77 | 64.1 | 53 |
| | 300-400 | | 2.0 | 9.4 | 8.1 | 9.7 | 13.8 | 22.1 | 17.2 | 18.7 | 3.93 | 1.17 | 0.07 | 0.20 | 5.37 | 15.12 | 80.8 | 36 |
| | 400-500 | | 1.6 | 10.1 | 8.1 | 11.7 | 16.0 | 13.3 | 20.0 | 18.1 | 4.21 | 1.16 | 0.07 | 0.27 | 5.7 | 10.66 | 58.9 | 53 |
| E | 500-600 | gs | 2.9 | 10.0 | 9.6 | 9.9 | 16.2 | 17.9 | 17.9 | 15.6 | 3.97 | 0.98 | 0.10 | 0.27 | 5.31 | 9.79 | 62.7 | 54 |
| | 600-700 | | 4.3 | 11.5 | 10.0 | 9.9 | 14.9 | 19.2 | 15.7 | 15.9 | 3.07 | 0.92 | 0.11 | 0.24 | 4.34 | 6.96 | 43.8 | 62 |
| | 700-800 | | 4.8 | 10.6 | 9.4 | 10.2 | 15.6 | 23.0 | 16.2 | 17.3 | 2.67 | 1.02 | 0.14 | 0.23 | 4.06 | 6.42 | 37.1 | 63 |
| G | 800-1000 | gh | 5.7 | 8.0 | 8.0 | 7.8 | 11.3 | 14.8 | 8.9 | 38.0 | 5.21 | 2.37 | 0.29 | 0.29 | 8.17 | 12.78 | 33.6 | 64 |

| Horizon | Depth | Bulk density | pH | | Org C | N | C:N | Fe | | | Mn | | | Mineralogy |
|---|---|---|---|---|---|---|---|---|---|---|---|---|---|---|
| | | | | | | | | CBD | Ox | Piro | CBD | Ox | Piro | |
| | mm | Mg $m^{-3}$ | $H_2O$ | KCl | % | mg $kg^{-1}$ | | mg $kg^{-1}$ | | | | | | < 0,002mm |
| A | 0-100 | 0.99 | 6.13 | 5.66 | 4.40 | 2648 | 16.6 | 7975 | 7960 | 3524 | 41.0 | 46.5 | 27.1 | |
| | 100-200 | | 6.23 | 5.72 | 2.91 | 2747 | 10.6 | 2290 | 13050 | 2560 | 15.0 | 35.0 | 25.1 | |
| | 200-300 | | 5.76 | 5.39 | 2.80 | 2052 | 13.7 | 5635 | 5935 | 2902 | 11.0 | 13.0 | 21.1 | |
| | 300-400 | 1.76 | 5.82 | 4.78 | 1.26 | 968 | 13.0 | 2985 | 2700 | 847 | 9.5 | 9.0 | 18.1 | |
| | 400-500 | | 6.00 | 4.63 | 1.12 | 830 | 13.4 | 2275 | 1965 | 660 | 6.0 | 7.0 | 16.1 | |
| E | 500-600 | | 5.77 | 4.74 | 0.91 | 587 | 15.5 | 2285 | 2320 | 564 | 4.0 | 5.0 | 15.1 | |
| | 600-700 | 1.66 | 5.87 | 4.49 | 0.42 | 274 | 15.3 | 1815 | 1890 | 396 | 4.0 | 4.5 | 13.1 | |
| | 700-800 | | 5.70 | 4.42 | 0.18 | 201 | 8.9 | 2435 | 1595 | 327 | 8.5 | 3.5 | 13.1 | |
| G | 800-1000 | 1.70 | 5.83 | 4.28 | 0.16 | 264 | 5.9 | 1240 | 1520 | 407 | 147.0 | 3.5 | 17.1 | |

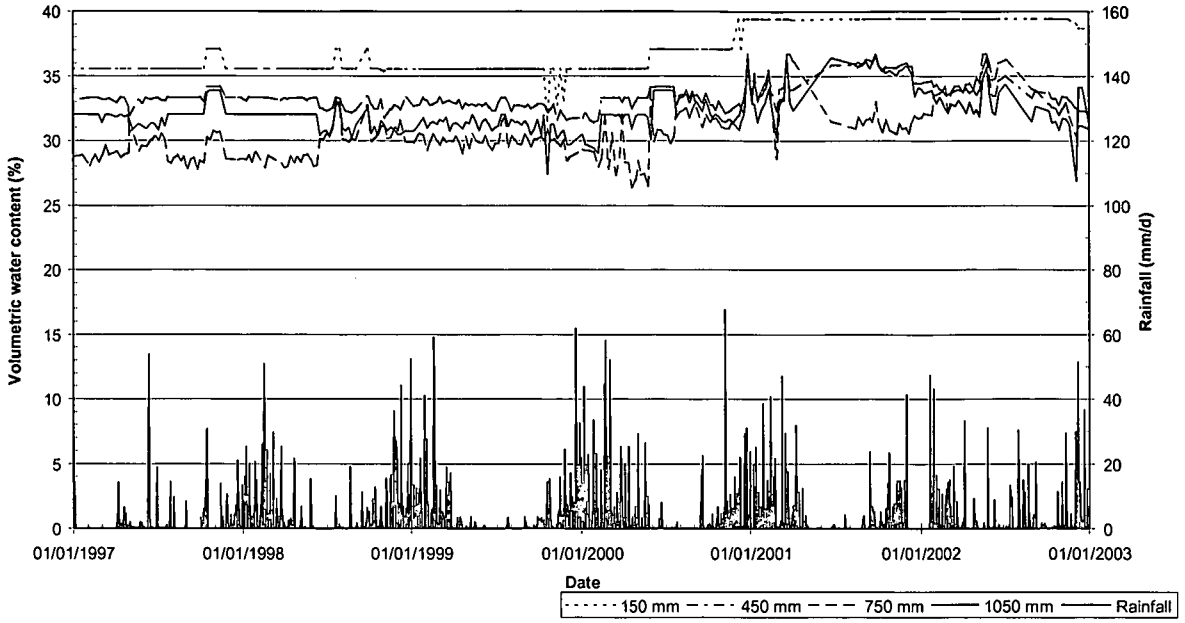


Figure 17 Volumetric water content and daily rainfall from 1 January 1997 until 31 December 2002 for profile 206.

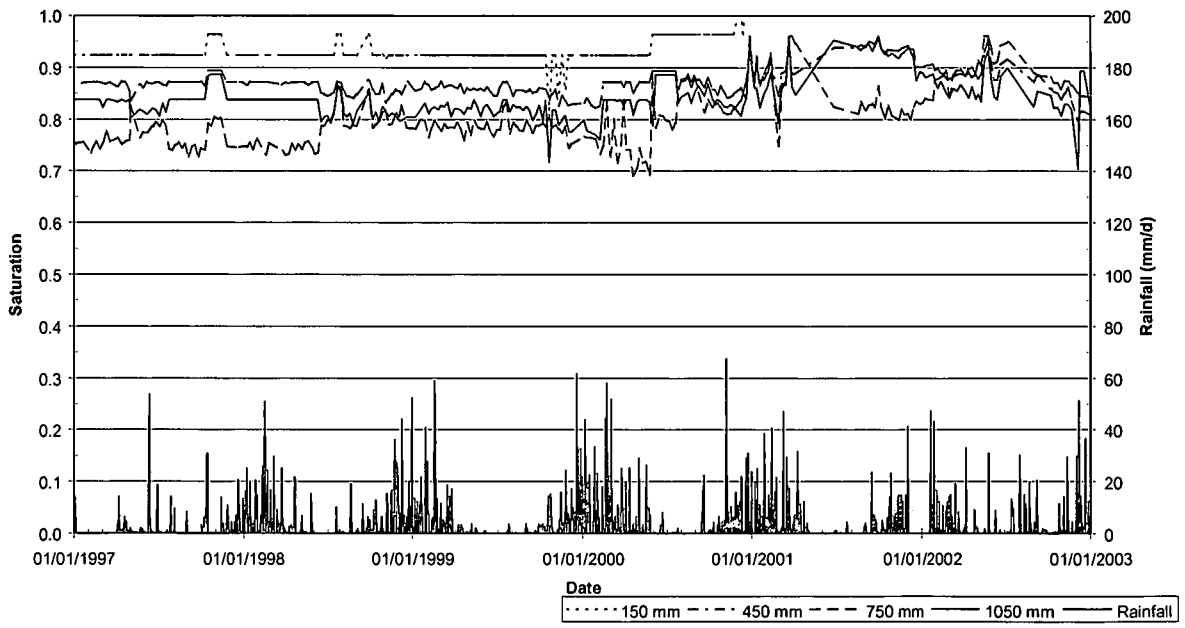


Figure 18 Degree of water saturation and daily rainfall from 1 January 1997 until 31 December 2002 for profile 206.

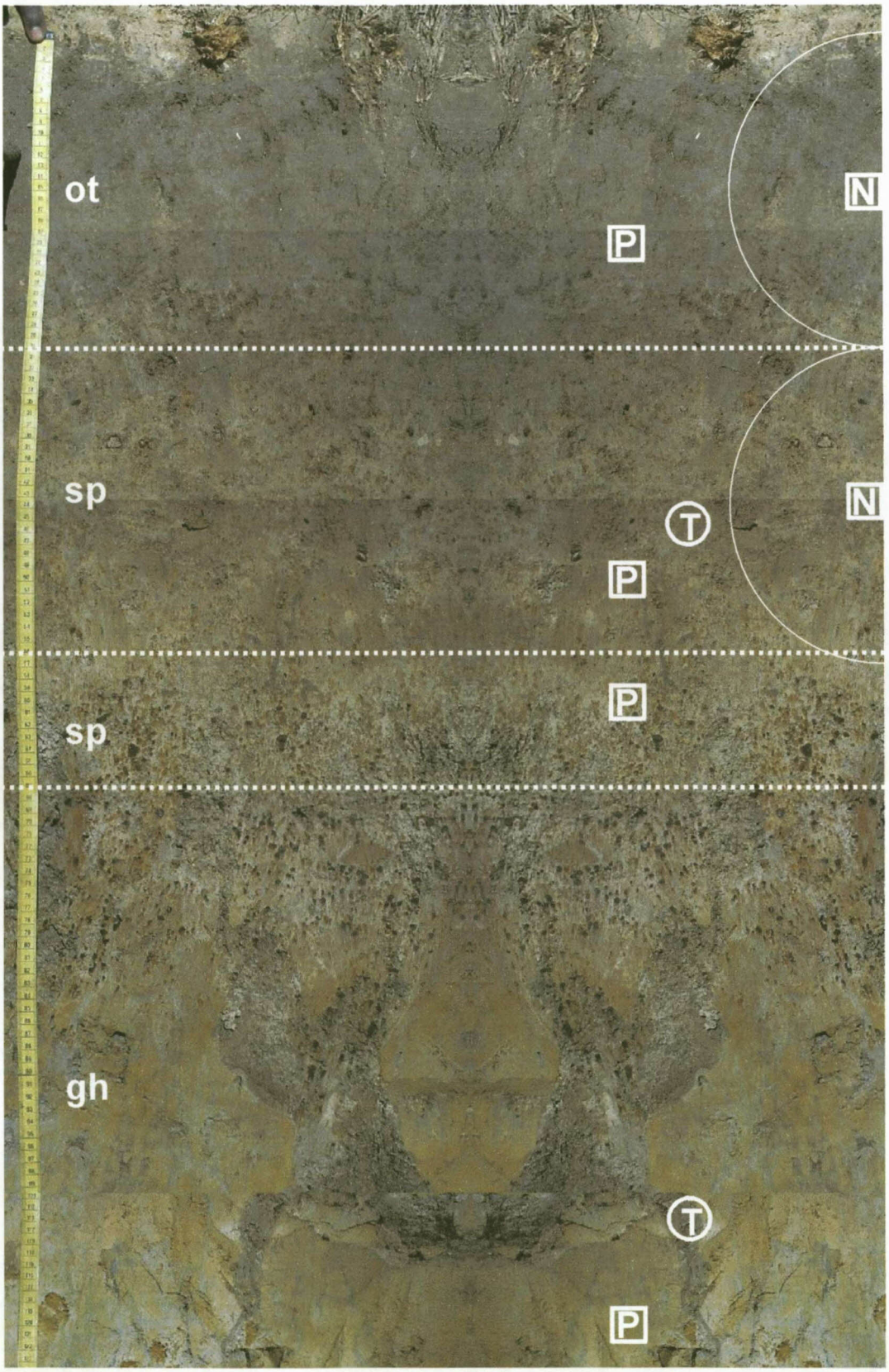


Figure 19 Profile 207 (Westleigh 1000), indicating diagnostic horizons as well as measurement depths for tensiometers [T], neutron water meter [N] and piezometers [P].

## Table 13 Profile description for profile 207 (Westleigh 1000)

**Profile No:** 207
**Map/photo:** 3128AB
**Latitude & Longitude:** 31° 06' 10.2" / 28° 19' 49.0"
**Surface stoniness:** None
**Altitude:** 1 269 m
**Terrain unit:** Valley bottom
**Slope:** 3 %
**Slope shape:** Concave
**Aspect:** West
**Microrelief:** 1 % mole mounds, 0.5 m height, profile between features
**Parent material solum:** Origin single, solid rock
**Underlying material:** Feldspathic sandstone
**Geological Group:** Molteno

**Soil form:** Westleigh
**Soil family:** 1000
**Surface rockiness:** None
**Occurrence of flooding:** Occasional
**Wind erosion:** None
**Water erosion:** None
**Vegetation / Land use:** Grassveld, closed
**Water table:** None
**Described by:** C.W. van Huyssteen & M. Smit
**Date described:** 19/06/2001
**Weathering of underlying material:** Weak physical, weak chemical
**Alteration of underlying material:** Ferruginised

| Horizon | Depth(mm) | Description | Diagnostic horizons |
|---|---|---|---|
| A | 0 - 300 | **Moisture status:** moist; **dry colour:** 10YR6/2 (100 %); **moist colour:** 7.5YR4/3 (100 %); 22.5 % clay; silty loam; common fine distinct 10YR5/7 dry, 10YR4/6 moist, iron oxide mottles; moderate fine subangular blocky; hard, friable, slightly sticky, slightly plastic; many rusty fine and very fine pores; many rusty medium and coarse pores; no slickensides; fine cracks; no cutans; common 6-25 mm round biocasts; water absorption 5 second(s); many rusty roots; clear smooth transition; | orthic A horizon |
| B1 | 300 - 560 | **Moisture status:** moist; **dry colour:** 10YR6/3 (90 %), 10YR5/7 (10 %); **moist colour:** 7.5YR5/2 (90 %), 10YR4/6 (10 %); 23.6 % clay; silty loam; many medium distinct 10YR5/7 dry, 10YR4/6 moist, iron oxide mottles; moderate fine angular blocky; hard, friable, slightly sticky, plastic; many rusty fine and very fine pores; many rusty medium and coarse pores; no slickensides; no cracks; no cutans; common 6-25 mm round biocasts; water absorption 6 second(s); common bleached roots; clear smooth transition; | soft plinthic B horizon |
| B2 | 560 - 670 | **Moisture status:** moist; **dry colour:** 10YR8/1 (80 %), 10YR5/6 (20 %); **moist colour:** 10YR6/2 (80 %), 10YR4/6 (20 %); 19.4 % clay; silty loam; common medium prominent 10YR5/6 dry, 10YR4/6 moist, iron oxide mottles; moderate fine angular blocky; hard, friable, slightly sticky, slightly plastic; common rusty fine and very fine pores; few rusty medium and coarse pores; no slickensides; no cracks; no cutans; many 2-6 mm round stones; water absorption 3 second(s); few bleached roots; clear smooth transition; Remark: B2 horizon tongues into G | soft plinthic B horizon |
| G | 670 - 1300 | **Moisture status:** Wet; **dry colour:** 10YR8/2 (60 %), 10YR6/8 (40 %); **moist colour:** 10YR7/2 (60 %), 10YR4/6 (40 %); 45.9 % clay; clay; many fine prominent 10YR6/8 dry, 10YR4/6 moist, iron oxide mottles; strong coarse prismatic; very hard, firm, very sticky, plastic; many bleached fine and very fine pores; few bleached medium and coarse pores; few slickensides; no cracks; many silica cutans; very few >250 mm angular stones; water absorption 5 second(s); no roots; transition not reached; | unspecified material with signs of wetness |

Table 14 Soil analyses for profile 207 (Westleigh 1000)

| Horizon | Depth | Diagnostic horizon | Gravel | Texture of the fine earth | | | | | | | Exchangeable cations | | | | | CEC soil | CEC clay | Base sat |
|---|---|---|---|---|---|---|---|---|---|---|---|---|---|---|---|---|---|---|
| | | | | coSa | meSa | fiSa | vfSa | coSi | fiSi | Cl | Ca | Mg | K | Na | S | | | |
| | mm | | % | % | | | | | | | cmolc kg$^{-1}$ | | | | | | | % |
| A | 0-100 | ot | 5.3 | 4.3 | 3.8 | 3.8 | 10.2 | 33.9 | 20.5 | 20.9 | 2.29 | 1.17 | 0.31 | 0.18 | 3.94 | 10.44 | 50.0 | 38 |
| | 100-200 | | 2.3 | 3.9 | 3.8 | 3.9 | 11.6 | 31.2 | 20.4 | 23.9 | 1.98 | 1.02 | 0.25 | 0.20 | 3.46 | 10.66 | 44.6 | 32 |
| | 200-300 | | 0.9 | 4.7 | 3.7 | 3.3 | 11.7 | 32.3 | 21.0 | 22.8 | 1.58 | 0.90 | 0.17 | 0.23 | 2.88 | 9.08 | 39.8 | 32 |
| B1 | 300-400 | sp | 0.7 | 5.0 | 3.4 | 3.2 | 11.7 | 35.4 | 15.1 | 23.8 | 1.27 | 0.78 | 0.15 | 0.23 | 2.43 | 9.30 | 39.1 | 26 |
| | 400-560 | | 3.1 | 6.6 | 3.7 | 3.2 | 11.4 | 37.7 | 16.7 | 23.4 | 1.23 | 0.77 | 0.16 | 0.20 | 2.36 | 8.37 | 35.8 | 28 |
| B2 | 560-670 | sp | 8.2 | 9.3 | 4.1 | 3.8 | 10.5 | 37.8 | 18.5 | 19.4 | 1.18 | 0.79 | 0.15 | 0.20 | 2.33 | 6.74 | 34.8 | 35 |
| G | 670-800 | gh | 29.3 | 4.4 | 3.4 | 3.4 | 10.9 | 29.1 | 7.8 | 41.4 | 2.91 | 1.90 | 0.20 | 0.30 | 5.32 | 10.77 | 26.0 | 49 |
| | 800-900 | | 7.7 | 3.8 | 3.1 | 3.2 | 9.1 | 21.5 | 6.0 | 50.4 | 4.83 | 2.86 | 0.23 | 0.39 | 8.30 | 14.68 | 29.1 | 57 |

| Horizon | Depth | Bulk density | pH | | Org C | N | C:N | Fe | | | Mn | | | Mineralogy |
|---|---|---|---|---|---|---|---|---|---|---|---|---|---|---|
| | | | | | | | | CBD | Ox | Piro | CBD | Ox | Piro | |
| | mm | Mg m$^{-3}$ | $H_2O$ | KCl | % | mg kg$^{-1}$ | | mg kg$^{-1}$ | | | | | | < 0,002mm |
| A | 0-100 | 1.58 | 5.35 | 4.29 | 1.61 | 1109 | 14.5 | 8200 | 1160 | 754 | 103.0 | 3.0 | 49.2 | |
| | 100-200 | | 3.63 | 4.21 | 1.24 | 1031 | 12.1 | 6025 | 1975 | 811 | 88.5 | 3.0 | 32.1 | |
| | 200-300 | | 5.69 | 4.36 | 0.87 | 770 | 11.3 | 8075 | 6560 | 796 | 58.5 | 7.0 | 26.1 | |
| B1 | 300-400 | 1.63 | 5.74 | 4.14 | 0.72 | 694 | 10.3 | 6825 | 230 | 1098 | 50.0 | 6.5 | 25.1 | |
| | 400-560 | | 5.71 | 4.07 | 0.46 | 527 | 8.7 | 7515 | 395 | 945 | 111.0 | 125.0 | 22.1 | |
| B2 | 560-670 | 1.68 | 6.27 | 4.20 | 0.21 | 404 | 5.3 | 7980 | 405 | 610 | 183.5 | 110.0 | 20.1 | |
| G | 670-800 | | 5.83 | 4.19 | 0.27 | 360 | 7.4 | 1145 | 2255 | 329 | 229.0 | 90.0 | 19.1 | |
| | 800-900 | | 6.36 | 4.46 | 0.21 | 375 | 5.6 | 2905 | 2090 | 286 | 37.5 | 71.5 | 14.1 | |

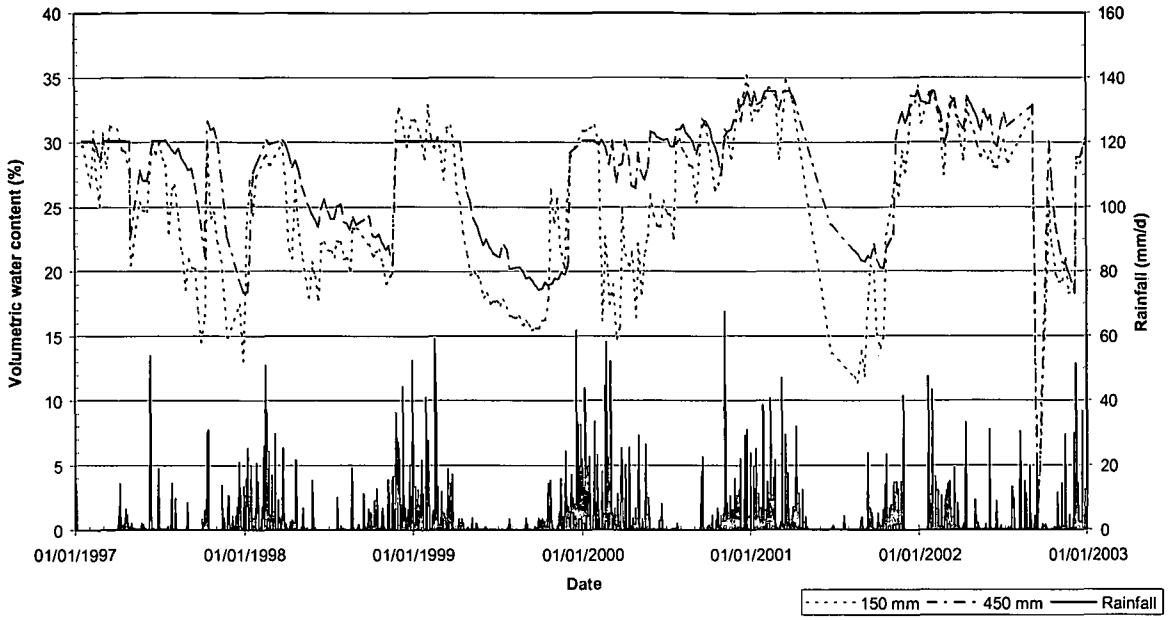


Figure 20 Volumetric water content and daily rainfall from 1 January 1997 until 31 December 2002 for profile 207.

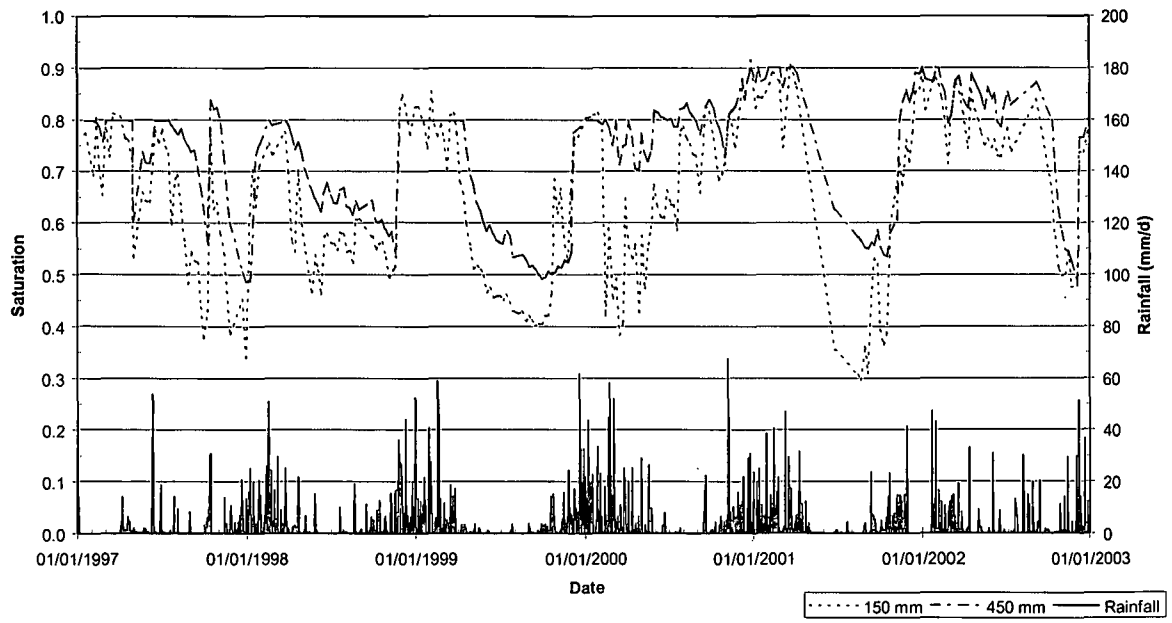


Figure 21 Degree of water saturation and daily rainfall from 1 January 1997 until 31 December 2002 for profile 207.

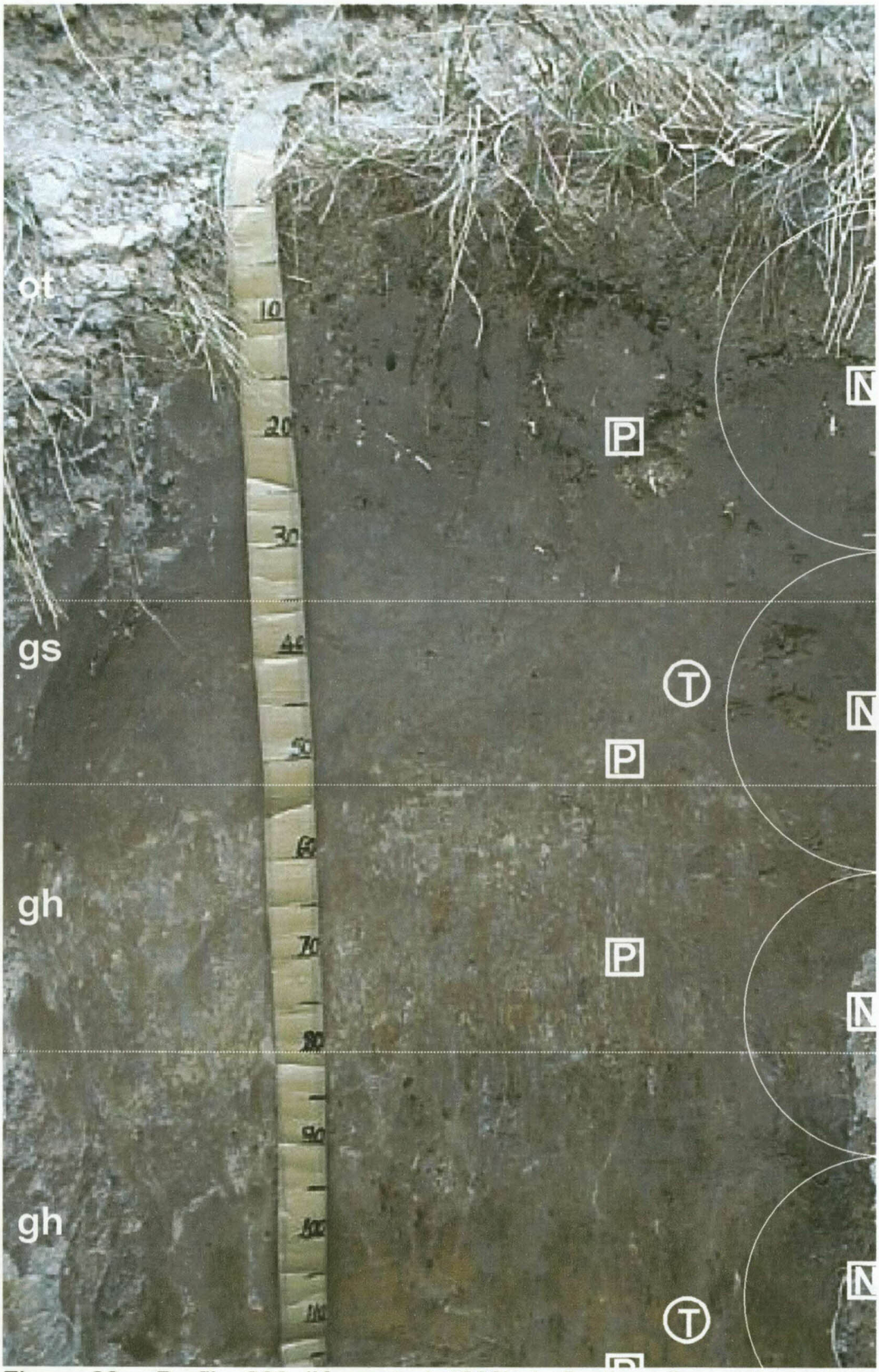


Figure 22 Profile 208 (Kroonstad 1000), indicating diagnostic horizons as well as measurement depths for tensiometers [T], neutron water meter [N] and piezometers [P].

## Table 15 Profile description for profile 208 (Kroonstad 1000)

**Profile No:** 208
**Map/photo:** 3128AB
**Latitude & Longitude:** 31° 06' 10.2" / 28° 19' 44.8"
**Surface stoniness:** None
**Altitude:** 1 272 m
**Terrain unit:** Lower footslope
**Slope:** 1 %
**Slope shape:** Concave
**Aspect:** East
**Microrelief:** None
**Parent material solum:** Origin single, local colluvium
**Underlying material:** Mudstone
**Geological Group:** Molteno

**Soil form:** Kroonstad
**Soil family:** 1000
**Surface rockiness:** None
**Occurrence of flooding:** None
**Wind erosion:** None
**Water erosion:** None
**Vegetation / Land use:** Grassveld, closed
**Water table:** None
**Described by:** M. Hensley & A.Q. Weldeyohannes
**Date described:** 19/06/2001
**Weathering of underlying material:** Moderate physical, moderate chemical
**Alteration of underlying material:** Ferruginised

| Horizon | Depth(mm) | Description | Diagnostic horizons |
|---|---|---|---|
| A1 | 0 - 350 | **Moisture status:** moist; **dry colour:** 10YR6/1 (100 %); **moist colour:** 10YR4/1 (100 %); 13.9 % clay; silty loam; common fine distinct 10YR5/8 dry, 10YR4/6 moist, iron oxide mottles; weak coarse granular; hard, friable, non-sticky, non-plastic; many rusty fine and very fine pores; few rusty medium and coarse pores; no slickensides; no cracks; no cutans; no coarse fragments; water absorption 1 second(s); many bleached roots; gradual smooth transition; | orthic A horizon |
| E | 350 - 530 | **Moisture status:** moist; **dry colour:** 10YR6/2 (90 %), 10YR5/8 (10 %); **moist colour:** 10YR4/1 (90 %), 10YR4/6 (10 %); 13.1 % clay; loam; many medium distinct 10YR5/8 dry, 10YR4/6 moist, iron oxide mottles; weak medium subangular blocky; hard, friable, non-sticky, non-plastic; many rusty fine and very fine pores; few rusty medium and coarse pores; no slickensides; no cracks; few clay cutans; no coarse fragments; water absorption 1 second(s); many bleached roots; gradual smooth transition; | E horizon |
| G1 | 530 - 800 | **Moisture status:** moist; **dry colour:** 10YR7/1 (80 %), 10YR6/6 (20 %); **moist colour:** 10YR5/2 (80 %), 10YR4/6 (20 %); 23.7 % clay; loam; common medium distinct 10YR6/6 dry, 10YR4/6 moist, iron oxide mottles; apedal massive; very hard, firm, sticky, slightly plastic; many bleached fine and very fine pores; few dark medium and coarse pores; no slickensides; no cracks; few clay cutans; no coarse fragments; water absorption 1 second(s); common bleached roots; clear smooth transition; Remark: This horizon forms the transition between B and G | G horizon |
| G2 | 800 - 1700 | **Moisture status:** moist; **dry colour:** 10YR6/2 (70 %), 10YR5/8 (20 %), 10YR8/1 (10 %); **moist colour:** 10YR5/2 (70 %), 10YR4/6 (20 %), 10YR7/1 (10 %); 25.1 % clay; loam; many medium distinct 10YR5/8 dry, 10YR5/6 moist, iron oxide mottles; common medium distinct 10YR4/3 dry, 10YR4/2 moist, humus mottles; few fine prominent 10YR2/1 dry, 10YR2/1 moist, manganese mottles; strong coarse prismatic; very hard, very firm, very sticky, plastic; common normal fine and very fine pores; common dark medium and coarse pores; many slickensides; no cracks; very many clay cutans; no coarse fragments; water absorption 10 second(s); few bleached roots; transition not reached; | G horizon |

Table 16 Soil analyses for profile 208 (Kroonstad 1000)

| Horizon | Depth | Diagnostic horizon | Gravel | Texture of the fine earth | | | | | | | Exchangeable cations | | | | | CEC soil | CEC clay | Base sat |
|---|---|---|---|---|---|---|---|---|---|---|---|---|---|---|---|---|---|---|
| | | | | coSa | meSa | fiSa | vfSa | coSi | fiSi | Cl | Ca | Mg | K | Na | S | | | |
| | mm | | % | % | | | | | | | $cmol_c\ kg^{-1}$ | | | | | | | % |
| A | 0-100 | ot | 2.1 | 5.4 | 5.9 | 7.9 | 15.6 | 37.4 | 18.7 | 11.7 | 1.60 | 0.83 | 0.10 | 0.17 | 2.69 | 10.11 | 86.4 | 27 |
| | 100-200 | | 8.0 | 5.7 | 6.0 | 8.4 | 17.1 | 46.4 | 1.7 | 16.3 | 1.50 | 0.78 | 0.10 | 0.22 | 2.59 | 9.08 | 55.7 | 29 |
| | 200-300 | | 3.1 | 6.5 | 6.2 | 8.0 | 18.0 | 31.8 | 17.9 | 13.7 | 1.14 | 0.59 | 0.10 | 0.22 | 2.04 | 6.85 | 50.0 | 3 |
| E | 300-400 | gs | 3.4 | 6.2 | 6.2 | 7.8 | 16.1 | 32.7 | 20.8 | 12.0 | 0.92 | 0.51 | 0.05 | 0.16 | 1.64 | 5.06 | 42.1 | 32 |
| | 400-500 | | 3.6 | 6.4 | 5.2 | 8.0 | 16.0 | 34.3 | 19.2 | 14.1 | 1.17 | 0.71 | 0.06 | 0.18 | 2.12 | 4.89 | 34.7 | 43 |
| G1 | 500-600 | gh | 4.8 | 6.5 | 6.2 | 7.7 | 15.6 | 27.3 | 18.0 | 19.2 | 2.18 | 1.39 | 0.14 | 0.27 | 3.99 | 6.96 | 36.3 | 57 |
| | 600-650 | | 2.7 | 6.7 | 6.0 | 7.4 | 14.3 | 26.7 | 16.8 | 21.6 | 2.58 | 1.40 | 0.15 | 0.23 | 4.36 | 7.45 | 34.5 | 59 |
| | 650-700 | | 20.3 | 5.7 | 5.5 | 6.6 | 12.4 | 23.9 | 20.0 | 24.0 | 2.82 | 1.81 | 0.18 | 0.26 | 5.07 | 8.43 | 35.1 | 6 |
| | 700-800 | | 16.3 | 5.6 | 5.2 | 6.1 | 11.3 | 24.3 | 19.4 | 25.5 | 4.04 | 2.55 | 0.25 | 0.33 | 7.17 | 9.62 | 37.7 | 74 |
| G2 | 800-900 | gh | 11.3 | 6.0 | 5.2 | 6.0 | 11.5 | 17.9 | 22.3 | 27.8 | 3.90 | 2.45 | 0.23 | 0.27 | 6.85 | 10.00 | 36.0 | 68 |
| | 900-1000 | | 4.2 | 4.4 | 8.0 | 10.1 | 11.9 | 23.6 | 18.4 | 26.4 | 5.06 | 3.11 | 0.26 | 0.35 | 8.77 | 10.93 | 41.4 | 8 |
| | 1000-1100 | | 1.6 | 6.1 | 7.1 | 7.4 | 11.1 | 21.3 | 19.0 | 26.3 | 5.29 | 3.18 | 0.25 | 0.35 | 9.07 | 11.25 | 42.8 | 81 |
| | 1100-1200 | | 11.6 | 13.1 | 9.6 | 11.0 | 14.2 | 16.0 | 12.4 | 22.0 | 4.78 | 2.93 | 0.23 | 0.32 | 8.26 | 9.08 | 41.3 | 91 |
| | 1400+ | | 36.9 | 7.7 | 6.8 | 10.1 | 18.0 | 19.5 | 13.0 | 22.8 | 5.03 | 3.03 | 0.19 | 0.32 | 8.56 | 8.70 | 38.2 | 98 |

| Horizon | Depth | Bulk density | pH | | Org C | N | C:N | Fe | | | Mn | | | Mineralogy |
|---|---|---|---|---|---|---|---|---|---|---|---|---|---|---|
| | | | | | | | | CBD | Ox | Piro | CBD | Ox | Piro | |
| | mm | $Mg\ m^{-3}$ | $H_2O$ | KCl | % | $mg\ kg^{-1}$ | | $mg\ kg^{-1}$ | | | | | | < 0,002mm |
| A | 0-100 | 1.44 | 5.76 | 4.59 | 1.12 | 806 | 13.9 | 2955 | 705 | 1186 | 1.5 | 23.5 | 22.1 | |
| | 100-200 | | 5.63 | 4.32 | 0.95 | 659 | 14.5 | 3115 | 1645 | 706 | 2.0 | 40.0 | 12.0 | |
| | 200-300 | | 5.17 | 4.05 | 0.71 | 631 | 11.2 | 2220 | 1465 | 649 | 4.5 | 35.0 | 11.0 | |
| E | 300-400 | 1.62 | 5.28 | 4.08 | 0.57 | 496 | 11.6 | 2380 | 1430 | 577 | 7.0 | 273.0 | 9.0 | |
| | 400-500 | | 5.64 | 4.23 | 0.30 | 336 | 9.0 | 1820 | 796 | 521 | 8.0 | 184.0 | 7.0 | |
| G1 | 500-600 | | 6.03 | 4.21 | 0.17 | 233 | 7.1 | 3440 | 2115 | 361 | 1.5 | 48.0 | 7.0 | |
| | 600-650 | 1.76 | 6.26 | 4.25 | 0.11 | 204 | 5.6 | 4220 | 7185 | 339 | 20.0 | 10.0 | 7.0 | |
| | 650-700 | | 5.52 | 4.65 | 0.07 | 189 | 3.5 | 4620 | 5920 | 409 | 32.0 | 7.5 | 7.0 | |
| | 700-800 | | 6.48 | 4.55 | 0.11 | 151 | 7.0 | 7555 | 2260 | 408 | 109.0 | 4.0 | 8.0 | |
| G2 | 800-900 | | 6.62 | 4.48 | 0.08 | 176 | 4.6 | 1335 | 2310 | 348 | 191.5 | 1.0 | 11.0 | |
| | 900-1000 | 1.75 | 6.74 | 5.18 | 0.08 | 170 | 4.9 | 2905 | 661 | 296 | 118.0 | 0.5 | 14.1 | |
| | 1000-1100 | | 6.77 | 5.02 | 0.06 | 168 | 3.7 | 7150 | 316 | 282 | 359.5 | 0.5 | 12.0 | |
| | 1100-1200 | | 6.99 | 5.24 | 0.06 | 134 | 4.6 | 7840 | 218 | 284 | 15.0 | 31.5 | 10.0 | |
| | 1400+ | 1.74 | 7.13 | 5.43 | 0.02 | 118 | 1.4 | 4905 | 455 | 311 | 98.5 | 42.0 | 7.0 | |

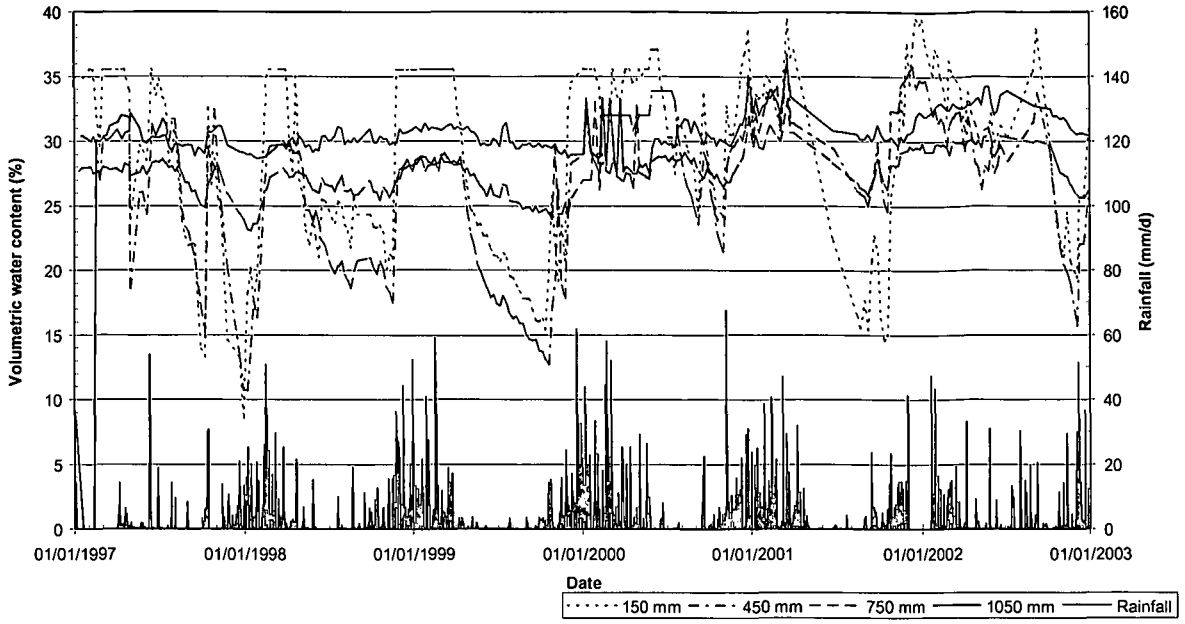


Figure 23 Volumetric water content and daily rainfall from 1 January 1997 until 31 December 2002 for profile 208.

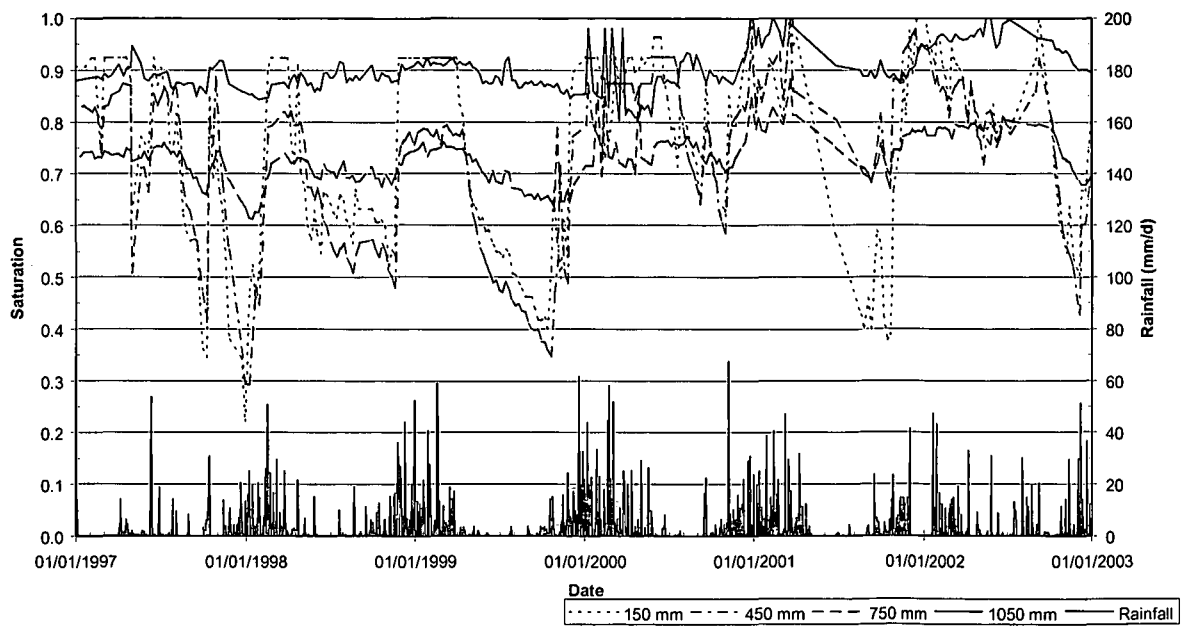


Figure 24 Degree of water saturation and daily rainfall from 1 January 1997 until 31 December 2002 for profile 208.

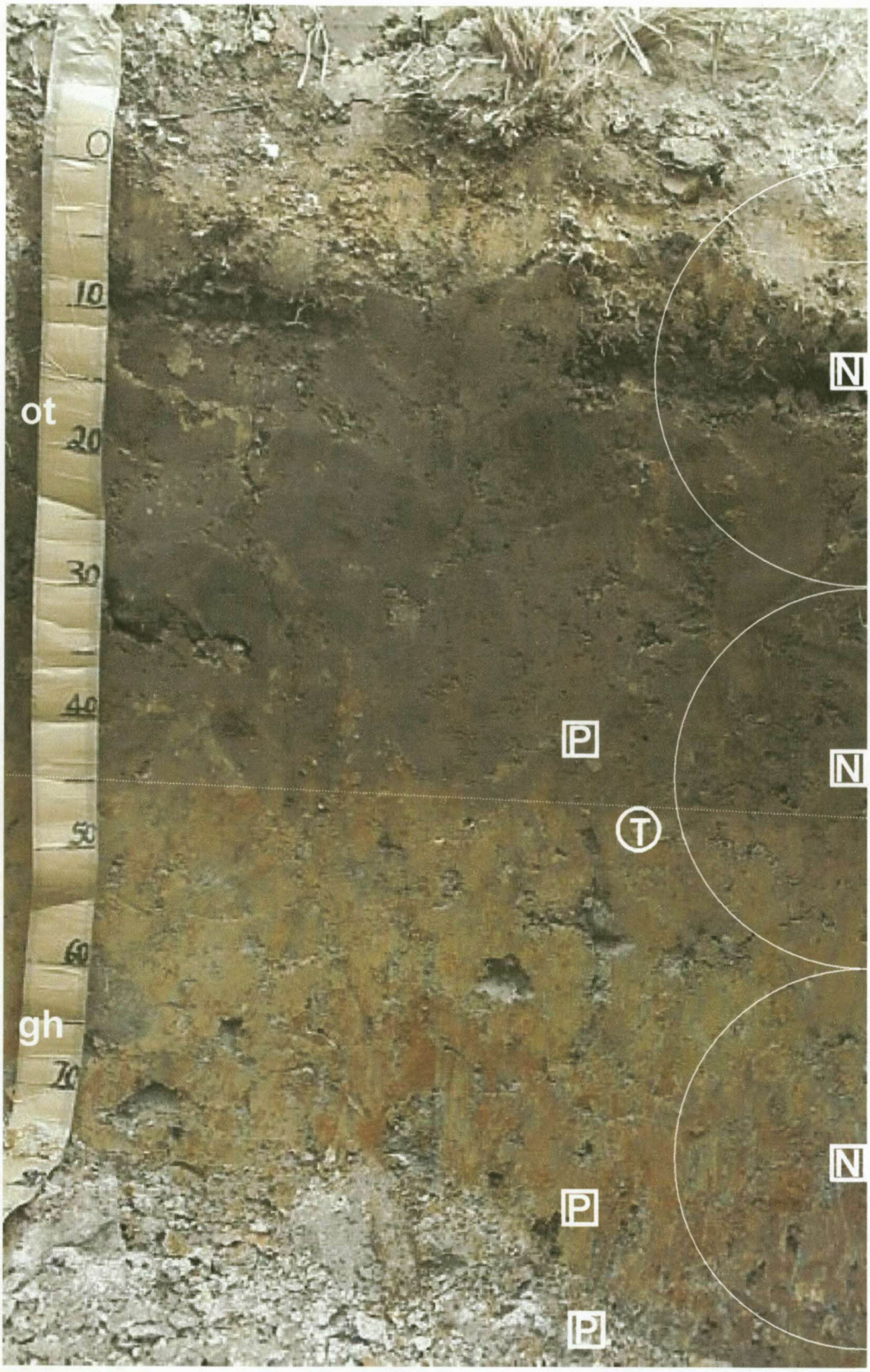


Figure 25 Profile 209 (Katspruit 1000), indicating diagnostic horizons as well as measurement depths for tensiometers [T], neutron water meter [N] and piezometers [P].

## Table 17 Profile description for profile 209 (Katspruit 1000)

**Profile No:** 209
**Map/photo:** 3128AB
**Latitude & Longitude:** 31° 06' 10.3" / 28° 19' 39.6"
**Surface stoniness:** None
**Altitude:** 1 285 m
**Terrain unit:** Upper midslope
**Slope:** 8 %
**Slope shape:** Concave
**Aspect:** East
**Microrelief:** None
**Parent material solum:** Origin binary, local colluvium, solid rock
**Underlying material:** Mudstone
**Geological Group:** Molteno

**Soil form:** Katspruit
**Soil family:** 1000
**Surface rockiness:** None
**Occurrence of flooding:** None
**Wind erosion:** None
**Water erosion:** None
**Vegetation / Land use:** Grassveld, closed
**Water table:** None
**Described by:** M. Hensley, W. Boshoff
**Date described:** 19/06/2001
**Weathering of underlying material:** Weak physical, weak chemical
**Alteration of underlying material:** Ferruginised

| Horizon | Depth(mm) | Description | Diagnostic horizons |
|---|---|---|---|
| A | 0 - 450 | **Moisture status:** moist; **dry colour:** 10YR5/2 (90 %), 7.5YR4/6 (10 %); **moist colour:** 10YR3/2 (90 %), 7.5YR3/4 (10 %); 16.3 % clay; loam; many fine distinct 7.5YR4/6 dry, 7.5YR3/4 moist, iron oxide mottles; moderate coarse granular; hard, slightly firm, non-sticky, non-plastic; many bleached and rusty fine and very fine pores; many bleached and rusty medium and coarse pores; no slickensides; fine cracks; no cutans; very few 6-25 mm mixed shaped stones; water absorption 2 second(s); many bleached roots; clear smooth transition; Remark: ±70 m to dolerite outcrop. Rocks in 2 layers at 700 and 900 mm. | orthic A horizon |
| G | 450 - 1100 | **Moisture status:** moist; **dry colour:** 10YR6/1 (90 %), 7.5YR6/8 (10 %); **moist colour:** 10YR5/1 (90 %), 7.5YR5/8 (10 %); 35.7 % clay; clay loam; many fine prominent 10YR6/8 dry, 7.5YR5/8 moist, iron oxide mottles; strong coarse prismatic; very hard, very firm, very sticky, plastic; common bleached fine and very fine pores; few bleached and rusty medium and coarse pores; many slickensides; medium cracks; very many clay cutans; common 75-250 mm mixed shaped stones; very few 2-6 mm round manganese concretions; water absorption 6 second(s); few bleached roots; clear smooth transition; Remark: root channels are always dark gray (10YR4/1). Vertical streaking light to dark gray. | G horizon |
| C | 1100 - 1400 | **Moisture status:** moist; **dry colour:** 10YR6/1 (90 %), 7.5YR5/8 (10 %); **moist colour:** 10YR5/1 (90 %), 7.5YR4/6 (10 %); 35.7 % clay; clay loam; many fine distinct 7.5YR5/8 dry, 7.5YR4/6 moist, iron oxide mottles; strong coarse prismatic; very hard, very firm, very sticky, plastic; few bleached fine and very fine pores; few bleached and rusty medium and coarse pores; many slickensides; medium cracks; very many silica & clay cutans; many 75-250 mm mixed shaped stones; water absorption 6 second(s); common bleached roots; transition not reached; Remark: C horizon is horizontally layered mudstone. | saprolite |

Table 18 Soil analyses for profile 209 (Katspruit 1000)

| Horizon | Depth | Diagnostic horizon | Gravel | Texture of the fine earth | | | | | | | Exchangeable cations | | | | | CEC soil | CEC clay | Base sat |
|---|---|---|---|---|---|---|---|---|---|---|---|---|---|---|---|---|---|---|
| | | | | coSa | meSa | fiSa | vfSa | coSi | fiSi | Cl | Ca | Mg | K | Na | S | | | |
| | mm | | % | % | | | | | | | $cmol_c\ kg^{-1}$ | | | | | | | % |
| A | 0-100 | ot | 3.8 | 3.7 | 3.0 | 10.1 | 25.4 | 23.8 | 17.9 | 16.5 | 2.98 | 1.55 | 0.23 | 0.20 | 4.96 | 9.41 | 57.0 | 53 |
| | 100-200 | | 4.1 | 4.2 | 3.0 | 8.6 | 26.7 | 25.9 | 16.0 | 16.2 | 2.95 | 1.57 | 0.15 | 0.23 | 4.9 | 8.32 | 51.4 | 59 |
| | 200-300 | | 1.8 | 3.8 | 2.9 | 8.5 | 26.9 | 22.6 | 18.9 | 16.2 | 2.75 | 1.52 | 0.16 | 0.22 | 4.66 | 8.81 | 54.4 | 53 |
| | 300-400 | | 3.9 | 4.1 | 3.0 | 8.5 | 27.2 | 22.0 | 20.8 | 14.8 | 2.80 | 1.56 | 0.15 | 0.28 | 4.78 | 7.99 | 54.0 | 60 |
| | 400-450 | | 18.4 | 4.2 | 3.2 | 8.6 | 25.9 | 23.4 | 16.4 | 17.9 | 2.08 | 1.56 | 0.15 | 0.25 | 4.04 | 5.71 | 31.9 | 71 |
| G | 450-500 | gh | 7.0 | 5.4 | 3.2 | 8.0 | 23.8 | 21.0 | 14.2 | 22.5 | 2.41 | 2.07 | 0.17 | 0.28 | 4.93 | 6.80 | 30.2 | 73 |
| | 500-600 | | 9.0 | 6.5 | 2.9 | 5.6 | 18.6 | 25.6 | 13.7 | 28.8 | 3.22 | 2.51 | 0.19 | 0.32 | 6.24 | 6.42 | 22.3 | 97 |
| | 600-850 | | 31.7 | 4.0 | 2.0 | 4.1 | 14.6 | 22.6 | 13.9 | 35.2 | 4.30 | 3.10 | 0.20 | 0.33 | 7.92 | 7.61 | 21.6 | 104 |
| | 850-900 | | 27.6 | 1.2 | 0.6 | 1.7 | 8.2 | 25.8 | 12.8 | 47.6 | 10.25 | 6.03 | 0.30 | 0.39 | 16.97 | 13.05 | 27.4 | 130 |
| | 900-1000 | | 36.5 | 7.0 | 4.8 | 4.1 | 9.7 | 16.7 | 21.0 | 35.7 | 5.97 | 2.94 | 0.27 | 0.36 | 9.54 | 7.72 | 21.6 | 124 |
| | 1000-1100 | | 25.5 | 0.5 | 0.5 | 0.8 | 3.2 | 13.5 | 37.0 | 44.2 | 2.83 | 7.86 | 0.28 | 0.39 | 11.36 | 17.83 | 40.4 | 64 |

| Horizon | Depth | Bulk density | pH | | Org C | N | C:N | Fe | | | Mn | | | Mineralogy |
|---|---|---|---|---|---|---|---|---|---|---|---|---|---|---|
| | | | | | | | | CBD | Ox | Piro | CBD | Ox | Piro | |
| | mm | $Mg\ m^{-3}$ | $H_2O$ | KCl | % | $mg\ kg^{-1}$ | | $mg\ kg^{-1}$ | | | | | | < 0,002mm |
| A | 0-100 | 1.45 | 5.60 | 4.74 | 1.43 | 866 | 16.5 | 5155 | 253 | 1069 | 82.0 | 97.5 | 51.2 | |
| | 100-200 | | 5.78 | 4.71 | 0.76 | 671 | 11.3 | 4720 | 327 | 678 | 61.0 | 190.5 | 23.1 | |
| | 200-300 | | 5.98 | 4.88 | 0.81 | 611 | 13.3 | 4525 | 296 | 562 | 48.5 | 134.5 | 17.1 | |
| | 300-400 | 1.65 | 5.93 | 4.66 | 0.57 | 539 | 10.6 | 6945 | 262 | 508 | 8.0 | 263.0 | 16.1 | |
| | 400-450 | | 6.22 | 4.68 | 0.43 | 487 | 8.8 | 7180 | 197 | 468 | 26.0 | 14.0 | 13.1 | |
| G | 450-500 | | 6.22 | 4.63 | 0.31 | 412 | 7.6 | 44940 | 179 | 375 | 5.5 | 104.0 | 8.0 | |
| | 500-600 | | 6.36 | 4.69 | 0.35 | 350 | 10.0 | 1460 | 2250 | 314 | 6.0 | 65.5 | 7.0 | |
| | 600-850 | 1.64 | 6.49 | 4.90 | 0.26 | 378 | 6.9 | 1370 | 2505 | 300 | 47.5 | 46.5 | 6.0 | |
| | 850-900 | | 6.51 | 5.23 | 0.16 | 389 | 4.1 | 390 | 2875 | 235 | 10.5 | 37.5 | 8.0 | |
| | 900-1000 | 1.73 | 6.59 | 5.21 | 0.08 | 351 | 2.3 | 1145 | 2940 | 288 | 95.5 | 18.0 | 6.0 | |
| | 1000-1100 | | 6.64 | 5.35 | 0.08 | 430 | 1.8 | 7975 | 2775 | 302 | 18.5 | 5.5 | 8.0 | |

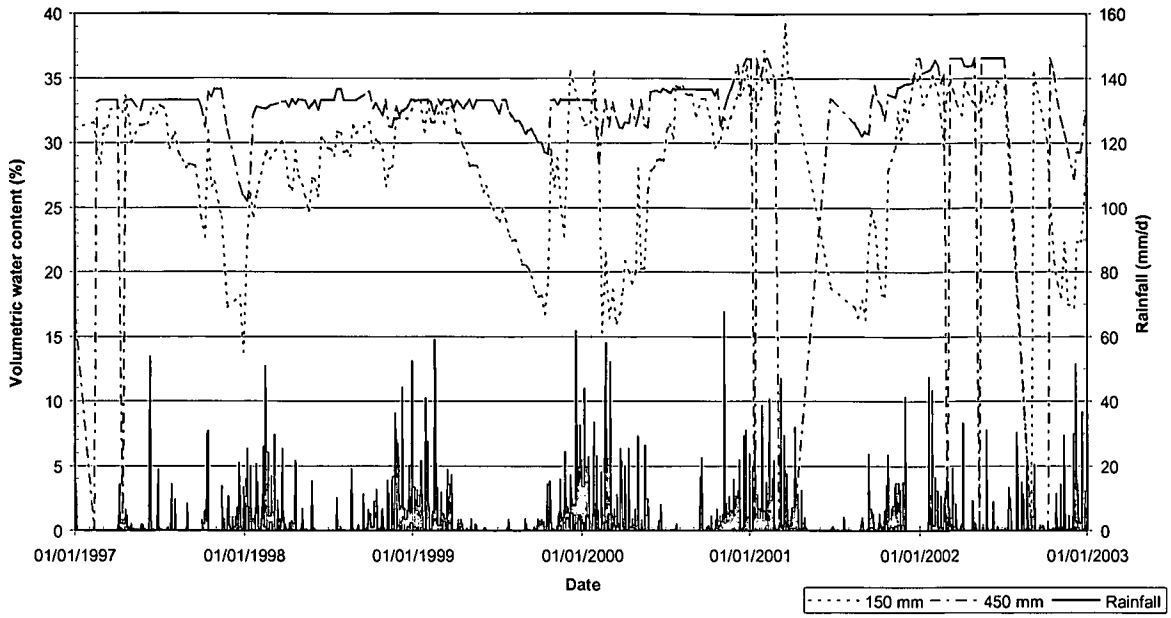


Figure 26 Volumetric water content and daily rainfall from 1 January 1997 until 31 December 2002 for profile 209.

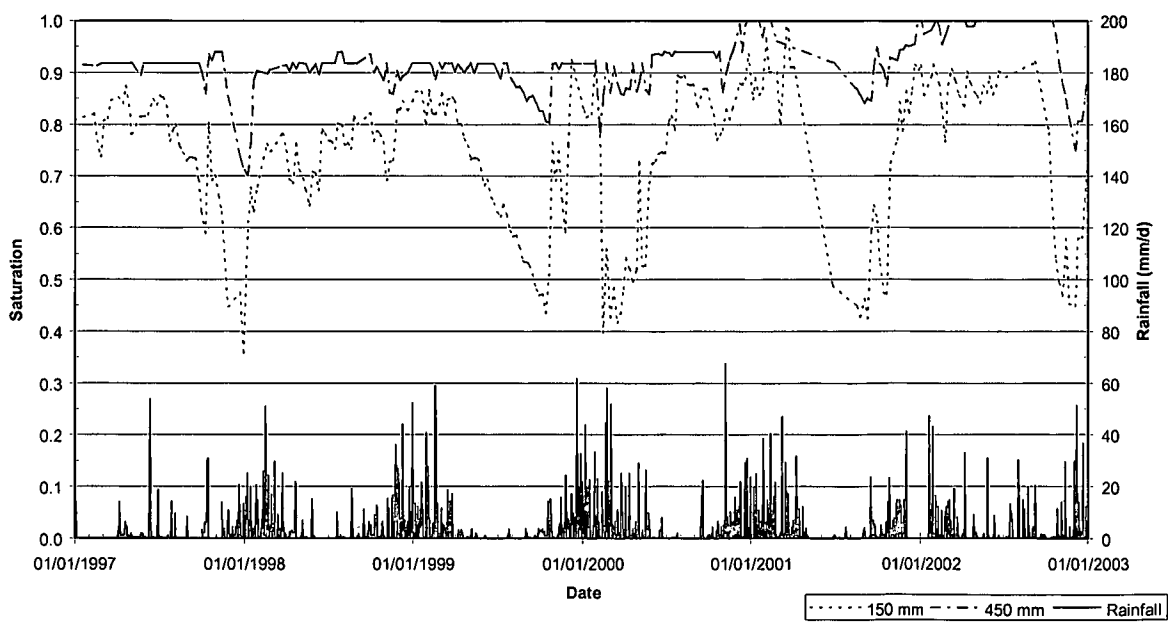


Figure 27 Degree of water saturation and daily rainfall from 1 January 1997 until 31 December 2002 for profile 209.

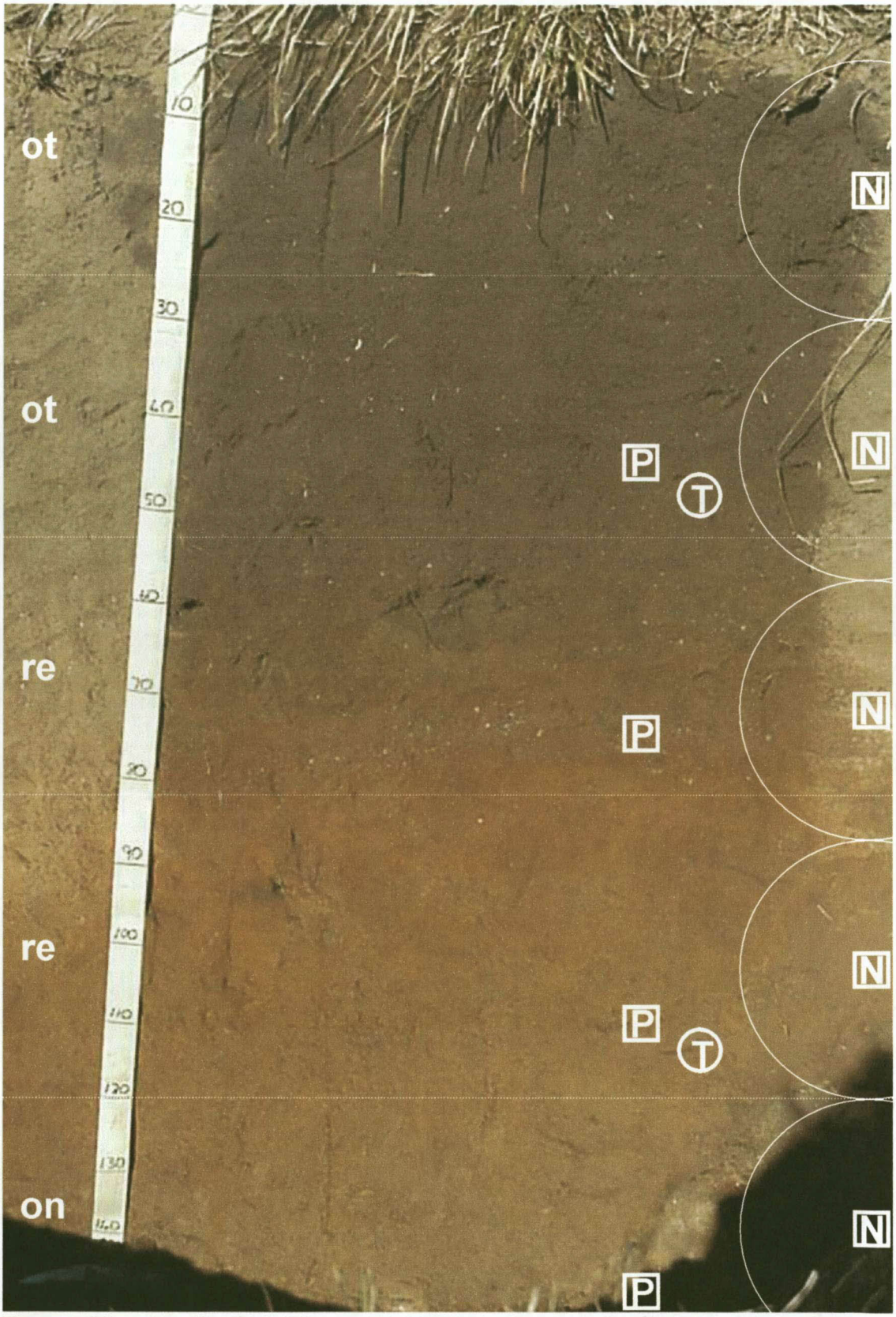


Figure 28 Profile 210 (Bloemdal 1100), indicating diagnostic horizons as well as measurement depths for tensiometers [T], neutron water meter [N] and piezometers [P].

## Table 19 Profile description for profile 210 (Bloemdal 1100)

**Profile No:** 210
**Map/photo:** 3128AB
**Latitude & Longitude:** 31° 06' 10.5" / 28° 19' 34.9"
**Surface stoniness:** None
**Altitude:** 1 306 m
**Terrain unit:** Upper midslope
**Slope:** 5 %
**Slope shape:** Convex
**Aspect:** East
**Microrelief:** None
**Parent material solum:** Origin single, solid rock
**Underlying material:** Feldspathic sandstone
**Geological Group:** Molteno

**Soil form:** Bloemdal
**Soil family:** 1100
**Surface rockiness:** None
**Occurrence of flooding:** None
**Wind erosion:** None
**Water erosion:** None
**Vegetation / Land use:** Grassveld, closed
**Water table:** None
**Described by:** M. Hensley & T.B. Zere
**Date described:** 19/06/2001
**Weathering of underlying material:** Strong physical, strong chemical
**Alteration of underlying material:** Ferruginised

| Horizon | Depth(mm) | Description | Diagnostic horizons |
|---|---|---|---|
| A1 | 0 - 260 | **Moisture status:** dry; **dry colour:** 10YR4/2 (100 %); **moist colour:** 10YR3/2 (100 %); 19.0 % clay; clay loam; no mottles; moderate fine subangular blocky; slightly hard, loose, non-sticky, non-plastic; many normal fine and very fine pores; few normal medium and coarse pores; no slickensides; no cracks; no cutans; no coarse fragments; water absorption 2 second(s); many normal roots; gradual smooth transition; | orthic A horizon |
| A2 | 260 - 530 | **Moisture status:** dry; **dry colour:** 10YR4/3 (100 %); **moist colour:** 7.5YR3/2 (100 %); 16.7 % clay; loam; no mottles; moderate fine subangular blocky; soft, loose, non-sticky, non-plastic; many normal fine and very fine pores; few normal medium and coarse pores; no slickensides; no cracks; no cutans; no coarse fragments; water absorption 1 second(s); many normal roots; gradual smooth transition; Remark: This horizon forms the transition between orthic A horizon and re. | orthic A horizon |
| B1 | 530 - 810 | **Moisture status:** dry; **dry colour:** 7.5YR4/6 (90 %), 7.5YR4/2 (10 %); **moist colour:** 5YR4/6 (90 %), 7.5YR3/2 (10 %); 23.9 % clay; loam; many medium distinct 7.5YR4/2 dry, 7.5YR3/2 moist, humus mottles; weak fine subangular blocky; slightly hard, loose, non-sticky, non-plastic; many normal fine and very fine pores; few normal medium and coarse pores; no slickensides; no cracks; no cutans; common 2-6 mm round stones; very few 6-25 mm round biocasts; water absorption 2 second(s); many normal roots; gradual smooth transition; Remark: Gravel layer at 830 mm. | red apedal B horizon |
| B2 | 810 - 1200 | **Moisture status:** moist; **dry colour:** 7.5YR6/6 (90 %), 5YR4/6 (10 %); **moist colour:** 5YR4/4 (90 %), 5YR4/4 (10 %); 18.0 % clay; loam; many fine distinct 7.5YR4/2 dry, 7.5YR3/2 moist, humus mottles; apedal massive; hard, friable, non-sticky, non-plastic; many normal fine and very fine pores; few normal medium and coarse pores; no slickensides; no cracks; no cutans; common 2-6 mm round stones; very few 6-25 mm round biocasts; water absorption 3 second(s); common normal roots; gradual smooth transition; Remark: humus in channels between 600 and 1200 mm. | red apedal B horizon |
| C1 | 1200 - 1580 | **Moisture status:** moist; **dry colour:** 10YR6/4 (100 %); **moist colour:** 7.5YR3/4 (100 %); 17.3 % clay; coarse sandy loam; no mottles; apedal massive; hard, friable, non-sticky, non-plastic; many normal fine and very fine pores; few normal medium and coarse pores; no slickensides; no cracks; no cutans; very few 2-6 mm round stones; water absorption 2 second(s); few normal roots; clear smooth transition; | unspecified material with signs of wetness |
| C2 | 1580 - 1750 | **Moisture status:** moist; **dry colour:** 2.5YR3/6 100 %; **moist colour:** 5YR6/2 100 %; 20.1 % clay; loam; no mottles; strong coarse prismatic; hard, firm, sticky, plastic; few normal fine and very fine pores; few normal medium and coarse pores; no slickensides; no cracks; common silica cutans; no coarse fragments; water absorption 7 second(s); no roots; transition not reached; | saprolite |

Table 20 Soil analyses for profile 210 (Bloemdal 1100)

| Horizon | Depth | Diagnostic horizon | Gravel | Texture of the fine earth | | | | | | | Exchangeable cations | | | | | CEC soil | CEC clay | Base sat |
|---|---|---|---|---|---|---|---|---|---|---|---|---|---|---|---|---|---|---|
| | | | | coSa | meSa | fiSa | vfSa | coSi | fiSi | Cl | Ca | Mg | K | Na | S | | | |
| | mm | | % | % | | | | | | | $cmol_c\ kg^{-1}$ | | | | | | | % |
| A | 0-130 | ot | 3.7 | 0.5 | 0.5 | 0.8 | 3.2 | 13.5 | 37.0 | 18.9 | 0.76 | 0.51 | 0.10 | 0.13 | 1.5 | 6.58 | 14.9 | 23 |
| | 130-260 | | 6.5 | 29.1 | 12.8 | 6.2 | 7.8 | 11.5 | 12.8 | 19.2 | 0.54 | 0.44 | 0.10 | 0.14 | 1.23 | 6.14 | 32.0 | 20 |
| | 260-370 | | 18.5 | 33.4 | 11.6 | 5.3 | 7.1 | 12.0 | 14.1 | 14.5 | 0.36 | 0.33 | 0.09 | 0.13 | 0.91 | 6.09 | 42.0 | 15 |
| | 370-550 | | 11.1 | 31.9 | 13.3 | 6.3 | 7.2 | 13.2 | 9.2 | 18.8 | 0.24 | 0.23 | 0.10 | 0.14 | 0.72 | 5.44 | 28.9 | 13 |
| B1 | 530-650 | re | 15.3 | 26.2 | 12.0 | 5.9 | 8.1 | 12.7 | 14.3 | 18.6 | 0.22 | 0.22 | 0.11 | 0.14 | 0.69 | 5.27 | 28.4 | 13 |
| | 650-750 | | 9.2 | 27.4 | 12.7 | 6.0 | 7.2 | 23.0 | 7.1 | 16.6 | 0.23 | 0.25 | 0.13 | 0.14 | 0.76 | 5.82 | 35.1 | 13 |
| | 750-810 | | 5.4 | 24.8 | 11.3 | 5.3 | 7.6 | 11.3 | 2.4 | 36.4 | 0.30 | 0.36 | 0.14 | 0.15 | 0.94 | 5.17 | 14.2 | 18 |
| B2 | 810-910 | re | 6.8 | 27.4 | 11.6 | 5.4 | 7.5 | 21.3 | 7.5 | 18.5 | 0.28 | 0.35 | 0.13 | 0.16 | 0.91 | 5.60 | 30.3 | 16 |
| | 910-1010 | | 7.7 | 26.9 | 11.8 | 5.0 | 7.9 | 12.7 | 15.9 | 17.5 | 0.28 | 0.34 | 0.12 | 0.17 | 0.91 | 5.38 | 30.8 | 17 |
| | 1010-1100 | | 5.7 | 30.1 | 12.0 | 5.4 | 8.0 | 13.0 | 18.1 | 12.5 | 0.28 | 0.34 | 0.11 | 0.16 | 0.9 | 5.17 | 41.3 | 17 |
| | 1100-1200 | | 13.9 | 16.0 | 14.4 | 9.4 | 13.0 | 11.9 | 11.1 | 23.5 | 0.59 | 0.88 | 0.07 | 0.16 | 1.71 | 4.51 | 19.2 | 38 |
| C1 | 1200-1300 | uw | 10.1 | 31.5 | 10.9 | 5.3 | 7.7 | 14.3 | 11.0 | 19.0 | 0.24 | 0.23 | 0.12 | 0.14 | 0.73 | 5.17 | 27.2 | 14 |
| | 1300-1400 | | 9.8 | 30.7 | 13.1 | 5.9 | 8.6 | 14.5 | 7.7 | 18.8 | 0.23 | 0.21 | 0.11 | 0.15 | 0.7 | 2.39 | 12.7 | 29 |
| | 1400-1500 | | 7.4 | 42.0 | 10.6 | 4.5 | 7.8 | 11.1 | 6.9 | 15.5 | 0.23 | 0.19 | 0.09 | 0.14 | 0.65 | 3.04 | 19.7 | 21 |
| | 1500-1600 | | 25.5 | 42.2 | 10.7 | 4.4 | 7.0 | 3.2 | 15.8 | 15.7 | 0.23 | 0.21 | 0.11 | 0.16 | 0.71 | 2.83 | 18.0 | 25 |
| C2 | 1600-1700 | so | 43.6 | 36.2 | 9.3 | 4.4 | 9.2 | 12.1 | 10.7 | 16.3 | 0.38 | 0.41 | 0.08 | 0.13 | 1 | 3.15 | 19.4 | 32 |
| | 1900-2000 | | 33.8 | 26.2 | 10.0 | 4.9 | 8.6 | 13.6 | 12.5 | 23.8 | 1.01 | 0.74 | 0.18 | 0.15 | 2.08 | 7.94 | 33.4 | 26 |

| Horizon | Depth | Bulk density | pH | | Org C | N | C:N | Fe | | | Mn | | | Mineralogy |
|---|---|---|---|---|---|---|---|---|---|---|---|---|---|---|
| | | | | | | | | CBD | Ox | Piro | CBD | Ox | Piro | |
| | mm | $Mg\ m^{-3}$ | $H_2O$ | KCl | % | $mg\ kg^{-1}$ | | $mg\ kg^{-1}$ | | | | | | < 0.002mm |
| A | 0-130 | 1.39 | 5.09 | 5.10 | 1.00 | 686 | 14.5 | 7020 | 513 | 1184 | 11.5 | 2.5 | 11.0 | |
| | 130-260 | | 5.15 | 4.41 | 0.86 | 510 | 16.8 | 3860 | 396 | 1151 | 19.5 | 3.0 | 9.0 | |
| | 260-370 | 1.62 | 5.21 | 4.10 | 0.33 | 430 | 7.6 | 7880 | 457 | 1204 | 13.5 | 34.5 | 9.0 | |
| | 370-550 | | 5.29 | 4.92 | 0.33 | 354 | 9.3 | 4150 | 336 | 1331 | 29.5 | 9.0 | 9.0 | |
| B1 | 530-650 | | 5.20 | 3.85 | 0.39 | 305 | 12.7 | 7145 | 3090 | 1272 | 48.0 | 105.5 | 11.0 | |
| | 650-750 | 1.72 | 5.11 | 3.91 | 0.14 | 247 | 5.5 | 5450 | 717 | 994 | 80.0 | 11.5 | 10.0 | |
| | 750-810 | | 5.15 | 3.93 | 0.23 | 246 | 9.2 | 9850 | 1250 | 950 | 94.5 | 9.0 | 12.0 | |
| B2 | 810-910 | | 5.20 | 3.96 | 0.31 | 304 | 10.3 | 6750 | 1620 | 654 | 106.0 | 13.0 | 14.1 | |
| | 910-1010 | 1.70 | 5.24 | 3.97 | 0.17 | 230 | 7.4 | 8100 | 3680 | 390 | 112.0 | 14.0 | 11.0 | |
| | 1010-1100 | | 5.22 | 4.04 | 0.10 | 216 | 4.5 | 13950 | 1575 | 580 | 112.0 | 18.5 | 15.1 | |
| | 1100-1200 | | 5.60 | 4.14 | 0.12 | 171 | 6.8 | 8060 | 1830 | 423 | 118.0 | 37.0 | 13.1 | |
| C1 | 1200-1300 | 1.82 | 5.24 | 4.02 | 0.21 | 169 | 12.3 | 6570 | 165 | 470 | 102.0 | 54.5 | 14.1 | |
| | 1300-1400 | | 5.28 | 4.11 | 0.09 | 109 | 8.6 | 4280 | 2515 | 298 | 106.0 | 119.5 | 11.0 | |
| | 1400-1500 | | 5.29 | 4.12 | 0.12 | 115 | 10.5 | 5830 | 1910 | 305 | 109.5 | 124.5 | 12.0 | |
| | 1500-1600 | – | 5.21 | 4.05 | 0.06 | 125 | 5.2 | 5385 | 1695 | 369 | 72.5 | 107.5 | 14.1 | |
| C2 | 1600-1700 | | 5.45 | 4.08 | 0.03 | 132 | 2.5 | 5660 | 1260 | 296 | 49.0 | 108.5 | 12.0 | |
| | 1900-2000 | | 5.18 | 4.12 | 0.61 | 438 | 13.8 | 10650 | 2310 | 1025 | 145.5 | 105.0 | 15.1 | |

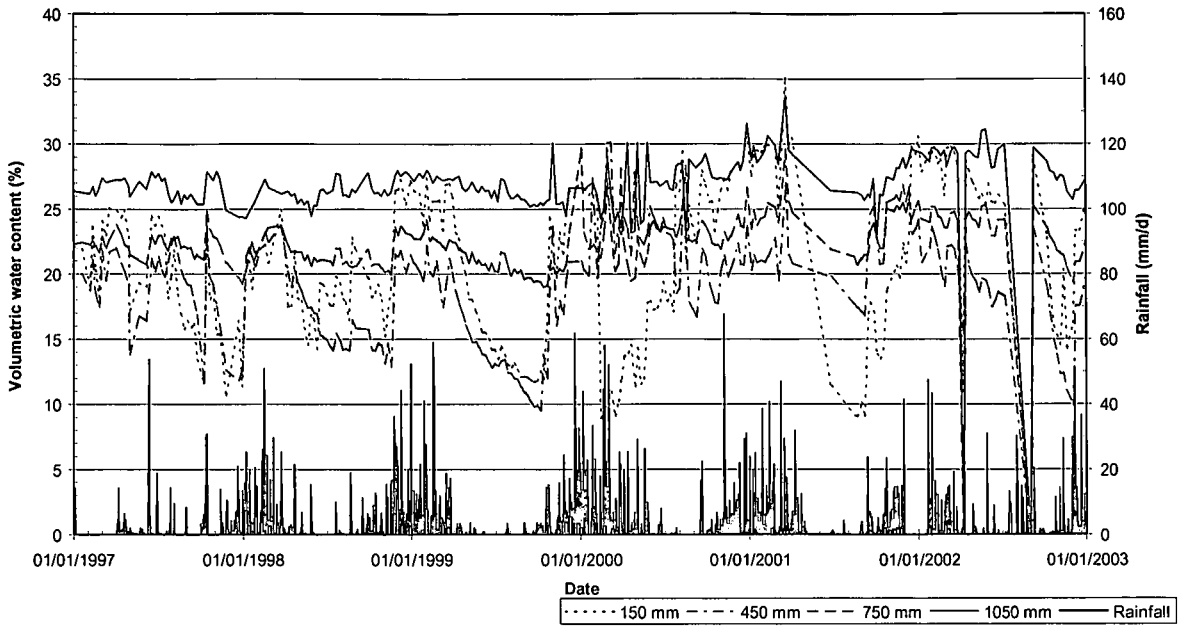


Figure 29 Volumetric water content and daily rainfall from 1 January 1997 until 31 December 2002 for profile 210.

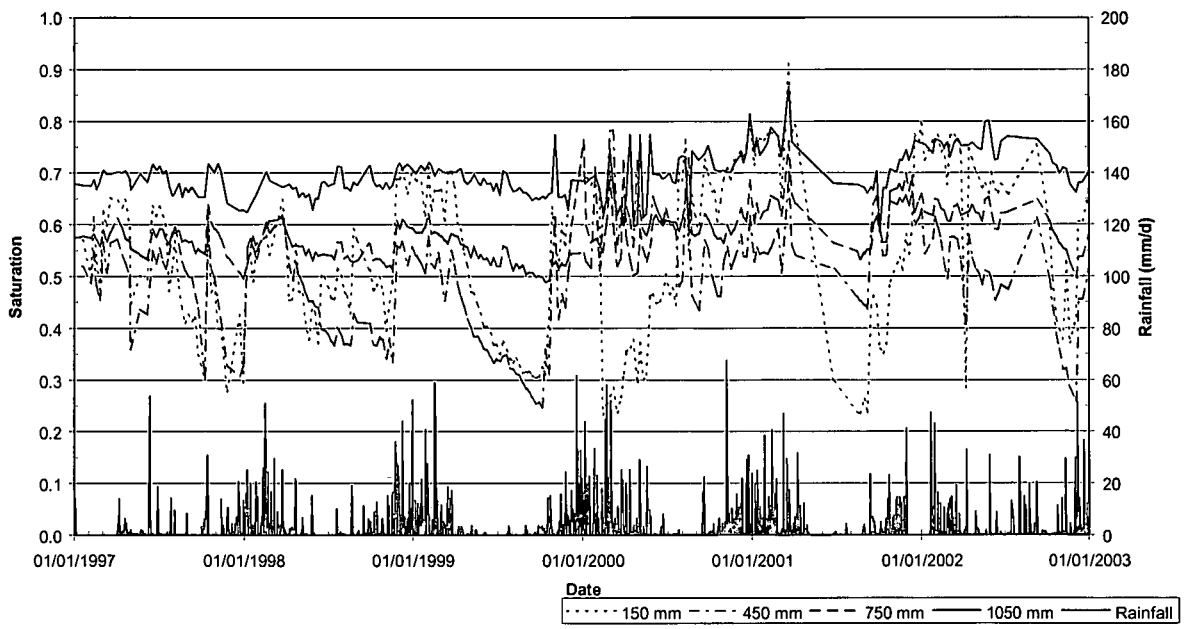


Figure 30 Degree of water saturation and daily rainfall from 1 January 1997 until 31 December 2002 for profile 210.

# APPENDIX B

## Results of digital photo colour quantification

Table 1 Statistics for RGB values calculated from diagnostic grey, yellow and red classification (Soil Classification Working Group, 1991) as well as black, from digital horizon photographs

| Profile | Form | Horizon | Depth (mm) | Colour | Quantity (%) | Count (cells) | RGB | RGB colour statistics | | | | | | | | |
|---|---|---|---|---|---|---|---|---|---|---|---|---|---|---|---|---|
| | | | | | | | | Min | Max | Range | Mean | Std | Variety | Majority | Minority | Median |
| P201 | Lo | ot | 430 | grey | 3.0 | 13095 | Red | 75 | 255 | 180 | 128 | 18 | 172 | 126 | 75 | 126 |
| | | | | | | | Green | 68 | 253 | 185 | 119 | 17 | 173 | 116 | 68 | 117 |
| | | | | | | | Blue | 55 | 240 | 185 | 104 | 16 | 169 | 104 | 186 | 102 |
| | | | | yellow | 96.9 | 426980 | Red | 75 | 244 | 169 | 133 | 12 | 162 | 134 | 214 | 133 |
| | | | | | | | Green | 57 | 228 | 171 | 118 | 11 | 161 | 119 | 57 | 118 |
| | | | | | | | Blue | 32 | 213 | 181 | 99 | 10 | 172 | 99 | 32 | 99 |
| | | | | red | 0.0 | 33 | Red | 83 | 191 | 108 | 161 | 27 | 22 | 173 | 83 | 173 |
| | | | | | | | Green | 56 | 150 | 94 | 125 | 22 | 23 | 135 | 56 | 135 |
| | | | | | | | Blue | 37 | 118 | 81 | 96 | 23 | 21 | 108 | 37 | 108 |
| | | | | black | 0.1 | 500 | Red | 8 | 74 | 66 | 58 | 16 | 62 | 73 | 8 | 64 |
| | | | | | | | Green | 0 | 69 | 69 | 46 | 16 | 65 | 57 | 2 | 51 |
| | | | | | | | Blue | 0 | 60 | 60 | 32 | 16 | 60 | 0 | 4 | 34 |
| P201 | Lo | gs | 730 | grey | 0.0 | 117 | Red | 81 | 255 | 174 | 173 | 49 | 74 | 255 | 81 | 165 |
| | | | | | | | Green | 74 | 254 | 180 | 162 | 48 | 75 | 118 | 74 | 154 |
| | | | | | | | Blue | 46 | 227 | 181 | 133 | 46 | 81 | 157 | 46 | 126 |
| | | | | yellow | 98.6 | 699491 | Red | 75 | 255 | 180 | 150 | 17 | 178 | 163 | 239 | 151 |
| | | | | | | | Green | 55 | 236 | 181 | 126 | 15 | 180 | 130 | 214 | 126 |
| | | | | | | | Blue | 9 | 206 | 197 | 88 | 11 | 189 | 87 | 9 | 88 |
| | | | | red | 1.3 | 9181 | Red | 75 | 190 | 115 | 136 | 22 | 115 | 143 | 186 | 139 |
| | | | | | | | Green | 41 | 150 | 109 | 105 | 19 | 107 | 113 | 41 | 107 |
| | | | | | | | Blue | 0 | 107 | 107 | 61 | 18 | 108 | 66 | 0 | 63 |
| | | | | black | 0.1 | 519 | Red | 10 | 74 | 64 | 54 | 17 | 63 | 74 | 10 | 58 |
| | | | | | | | Green | 0 | 62 | 62 | 34 | 16 | 63 | 45 | 12 | 37 |
| | | | | | | | Blue | 0 | 46 | 46 | 9 | 12 | 45 | 0 | 35 | 2 |
| P201 | Lo | sp | 1000 | grey | 78.5 | 352476 | Red | 63 | 255 | 192 | 135 | 15 | 189 | 136 | 63 | 136 |
| | | | | | | | Green | 68 | 253 | 185 | 130 | 15 | 183 | 128 | 237 | 130 |
| | | | | | | | Blue | 49 | 255 | 206 | 126 | 16 | 204 | 128 | 49 | 126 |
| | | | | yellow | 19.4 | 87062 | Red | 75 | 209 | 134 | 124 | 18 | 123 | 125 | 191 | 126 |
| | | | | | | | Green | 55 | 194 | 139 | 111 | 18 | 128 | 115 | 179 | 113 |
| | | | | | | | Blue | 38 | 197 | 159 | 107 | 18 | 143 | 110 | 38 | 109 |
| | | | | red | 0.5 | 2168 | Red | 75 | 160 | 85 | 109 | 18 | 82 | 123 | 148 | 110 |
| | | | | | | | Green | 42 | 125 | 83 | 80 | 16 | 79 | 91 | 42 | 81 |
| | | | | | | | Blue | 35 | 123 | 88 | 78 | 15 | 80 | 81 | 35 | 80 |
| | | | | black | 1.6 | 7116 | Red | 0 | 74 | 74 | 55 | 17 | 75 | 74 | 0 | 60 |
| | | | | | | | Green | 0 | 74 | 74 | 45 | 18 | 75 | 57 | 74 | 49 |
| | | | | | | | Blue | 0 | 96 | 96 | 45 | 19 | 94 | 56 | 95 | 49 |

| Profile | Form | Horizon | Depth (mm) | Colour | Quantity (%) | Count (cells) | RGB | RGB colour statistics | | | | | | | | |
|---|---|---|---|---|---|---|---|---|---|---|---|---|---|---|---|---|
| | | | | | | | | Min | Max | Range | Mean | Std | Variety | Majority | Minority | Median |
| P201 | Lo | so | 1210 | grey | 90.9 | 242031 | Red | 59 | 255 | 196 | 139 | 22 | 195 | 135 | 59 | 138 |
| | | | | | | | Green | 68 | 254 | 186 | 139 | 23 | 187 | 138 | 68 | 138 |
| | | | | | | | Blue | 58 | 255 | 197 | 143 | 24 | 197 | 144 | 58 | 141 |
| | | | | yellow | 8.1 | 21466 | Red | 75 | 227 | 152 | 144 | 21 | 145 | 140 | 212 | 143 |
| | | | | | | | Green | 59 | 211 | 152 | 126 | 19 | 143 | 121 | 61 | 126 |
| | | | | | | | Blue | 53 | 224 | 171 | 129 | 19 | 151 | 137 | 53 | 130 |
| | | | | red | 0.1 | 298 | Red | 76 | 176 | 100 | 145 | 17 | 68 | 146 | 76 | 146 |
| | | | | | | | Green | 55 | 140 | 85 | 111 | 15 | 64 | 106 | 55 | 111 |
| | | | | | | | Blue | 64 | 154 | 90 | 118 | 17 | 73 | 111 | 64 | 116 |
| | | | | black | 0.9 | 2354 | Red | 0 | 74 | 74 | 51 | 19 | 75 | 68 | 2 | 57 |
| | | | | | | | Green | 0 | 74 | 74 | 50 | 20 | 75 | 70 | 9 | 56 |
| | | | | | | | Blue | 0 | 101 | 101 | 56 | 21 | 99 | 67 | 95 | 61 |
| P202 | Pn | ot | 400 | grey | 91.0 | 652303 | Red | 57 | 251 | 194 | 125 | 20 | 185 | 130 | 57 | 126 |
| | | | | | | | Green | 68 | 255 | 187 | 126 | 21 | 176 | 127 | 234 | 126 |
| | | | | | | | Blue | 50 | 255 | 205 | 126 | 22 | 198 | 128 | 50 | 126 |
| | | | | yellow | 3.5 | 25372 | Red | 75 | 194 | 119 | 110 | 18 | 111 | 105 | 172 | 110 |
| | | | | | | | Green | 58 | 180 | 122 | 99 | 17 | 112 | 96 | 58 | 99 |
| | | | | | | | Blue | 48 | 177 | 129 | 94 | 17 | 117 | 104 | 48 | 95 |
| | | | | red | 0.0 | 0 | Red | 0 | 0 | 0 | 0 | 0 | 0 | 0 | 0 | 0 |
| | | | | | | | Green | 0 | 0 | 0 | 0 | 0 | 0 | 0 | 0 | 0 |
| | | | | | | | Blue | 0 | 0 | 0 | 0 | 0 | 0 | 0 | 0 | 0 |
| | | | | black | 5.4 | 38887 | Red | 0 | 74 | 74 | 47 | 20 | 75 | 67 | 2 | 52 |
| | | | | | | | Green | 0 | 74 | 74 | 46 | 20 | 75 | 68 | 2 | 50 |
| | | | | | | | Blue | 0 | 88 | 88 | 47 | 21 | 89 | 56 | 88 | 50 |
| P202 | Pn | ye | 820 | grey | 14.5 | 158764 | Red | 66 | 255 | 189 | 141 | 24 | 188 | 147 | 66 | 141 |
| | | | | | | | Green | 68 | 255 | 187 | 134 | 24 | 188 | 136 | 248 | 134 |
| | | | | | | | Blue | 49 | 255 | 206 | 125 | 25 | 206 | 118 | 241 | 123 |
| | | | | yellow | 34.3 | 374676 | Red | 75 | 252 | 177 | 134 | 21 | 169 | 141 | 225 | 136 |
| | | | | | | | Green | 55 | 232 | 177 | 118 | 21 | 173 | 125 | 213 | 120 |
| | | | | | | | Blue | 32 | 231 | 199 | 105 | 21 | 187 | 110 | 197 | 106 |
| | | | | red | 0.0 | 481 | Red | 75 | 165 | 90 | 99 | 18 | 71 | 76 | 120 | 96 |
| | | | | | | | Green | 48 | 131 | 83 | 73 | 16 | 67 | 54 | 48 | 70 |
| | | | | | | | Blue | 26 | 121 | 95 | 62 | 18 | 83 | 47 | 26 | 59 |
| | | | | black | 2.0 | 21739 | Red | 0 | 74 | 74 | 51 | 18 | 75 | 72 | 2 | 56 |
| | | | | | | | Green | 0 | 74 | 74 | 40 | 18 | 75 | 57 | 74 | 44 |
| | | | | | | | Blue | 0 | 81 | 81 | 31 | 18 | 82 | 0 | 80 | 33 |

| Profile | Form | Horizon | Depth (mm) | Colour | Quantity (%) | Count (cells) | RGB | RGB colour statistics | | | | | | | | |
|---|---|---|---|---|---|---|---|---|---|---|---|---|---|---|---|---|
| | | | | | | | | Min | Max | Range | Mean | Std | Variety | Majority | Minority | Median |
| P202 | Pn | on | 820 | grey | 14.5 | 158764 | Red | 66 | 255 | 189 | 141 | 24 | 188 | 147 | 66 | 141 |
| | | | | | | | Green | 68 | 255 | 187 | 134 | 24 | 188 | 136 | 248 | 134 |
| | | | | | | | Blue | 49 | 255 | 206 | 125 | 25 | 206 | 118 | 241 | 123 |
| | | | | yellow | 34.3 | 374676 | Red | 75 | 252 | 177 | 134 | 21 | 169 | 141 | 225 | 136 |
| | | | | | | | Green | 55 | 232 | 177 | 118 | 21 | 173 | 125 | 213 | 120 |
| | | | | | | | Blue | 32 | 231 | 199 | 105 | 21 | 187 | 110 | 197 | 106 |
| | | | | red | 0.0 | 481 | Red | 75 | 165 | 90 | 99 | 18 | 71 | 76 | 120 | 96 |
| | | | | | | | Green | 48 | 131 | 83 | 73 | 16 | 67 | 54 | 48 | 70 |
| | | | | | | | Blue | 26 | 121 | 95 | 62 | 18 | 83 | 47 | 26 | 59 |
| | | | | black | 2.0 | 21739 | Red | 0 | 74 | 74 | 51 | 18 | 75 | 72 | 2 | 56 |
| | | | | | | | Green | 0 | 74 | 74 | 40 | 18 | 75 | 57 | 74 | 44 |
| | | | | | | | Blue | 0 | 81 | 81 | 31 | 18 | 82 | 0 | 80 | 33 |
| P202 | Pn | on | 960 | grey | 64.2 | 262138 | Red | 67 | 255 | 188 | 144 | 25 | 187 | 148 | 246 | 146 |
| | | | | | | | Green | 75 | 252 | 177 | 136 | 24 | 153 | 145 | 215 | 140 |
| | | | | | | | Blue | 76 | 165 | 89 | 126 | 21 | 85 | 142 | 80 | 131 |
| | | | | yellow | 27.2 | 111219 | Red | 0 | 74 | 74 | 43 | 19 | 75 | 34 | 2 | 42 |
| | | | | | | | Green | 49 | 255 | 206 | 135 | 27 | 204 | 133 | 49 | 135 |
| | | | | | | | Blue | 41 | 229 | 188 | 110 | 21 | 165 | 116 | 195 | 113 |
| | | | | red | 0.1 | 478 | Red | 33 | 118 | 85 | 85 | 18 | 77 | 105 | 33 | 89 |
| | | | | | | | Green | 0 | 86 | 86 | 33 | 19 | 84 | 0 | 86 | 33 |
| | | | | | | | Blue | 68 | 255 | 187 | 141 | 26 | 187 | 143 | 249 | 142 |
| | | | | black | 8.5 | 34597 | Red | 55 | 233 | 178 | 121 | 22 | 158 | 131 | 201 | 124 |
| | | | | | | | Green | 49 | 128 | 79 | 96 | 18 | 75 | 113 | 49 | 101 |
| | | | | | | | Blue | 0 | 74 | 74 | 36 | 19 | 75 | 27 | 73 | 35 |
| P202 | Pn | on | 1500 | grey | 74.7 | 457313 | Red | 53 | 253 | 200 | 139 | 22 | 184 | 139 | 53 | 141 |
| | | | | | | | Green | 68 | 255 | 187 | 138 | 23 | 182 | 140 | 235 | 139 |
| | | | | | | | Blue | 37 | 255 | 218 | 128 | 25 | 208 | 128 | 37 | 128 |
| | | | | yellow | 17.3 | 105707 | Red | 75 | 214 | 139 | 129 | 18 | 124 | 133 | 199 | 131 |
| | | | | | | | Green | 55 | 199 | 144 | 113 | 17 | 131 | 115 | 174 | 114 |
| | | | | | | | Blue | 31 | 192 | 161 | 95 | 18 | 148 | 90 | 31 | 94 |
| | | | | red | 1.0 | 6186 | Red | 75 | 165 | 90 | 124 | 13 | 90 | 129 | 159 | 125 |
| | | | | | | | Green | 42 | 131 | 89 | 92 | 12 | 84 | 95 | 42 | 94 |
| | | | | | | | Blue | 25 | 121 | 96 | 72 | 11 | 91 | 72 | 25 | 72 |
| | | | | black | 7.0 | 42794 | Red | 0 | 74 | 74 | 42 | 19 | 75 | 24 | 2 | 42 |
| | | | | | | | Green | 0 | 74 | 74 | 37 | 19 | 75 | 19 | 4 | 36 |
| | | | | | | | Blue | 0 | 90 | 90 | 31 | 18 | 89 | 0 | 85 | 30 |

| Profile | Form | Horizon | Depth (mm) | Colour | Quantity (%) | Count (cells) | RGB | RGB colour statistics | | | | | | | | |
|---|---|---|---|---|---|---|---|---|---|---|---|---|---|---|---|---|
| | | | | | | | | Min | Max | Range | Mean | Std | Variety | Majority | Minority | Median |
| P203 | Tu | ot | 380 | grey | 88.6 | 618347 | Red | 61 | 255 | 194 | 129 | 21 | 195 | 130 | 61 | 130 |
| | | | | | | | Green | 68 | 255 | 187 | 126 | 21 | 188 | 130 | 245 | 126 |
| | | | | | | | Blue | 52 | 255 | 203 | 123 | 21 | 203 | 124 | 52 | 124 |
| | | | | yellow | 4.5 | 31115 | Red | 75 | 218 | 143 | 112 | 21 | 129 | 123 | 188 | 113 |
| | | | | | | | Green | 56 | 202 | 146 | 102 | 20 | 131 | 113 | 58 | 102 |
| | | | | | | | Blue | 42 | 191 | 149 | 98 | 20 | 143 | 111 | 42 | 99 |
| | | | | red | 0.0 | 0 | Red | 0 | 0 | 0 | 0 | 0 | 0 | 0 | 0 | 0 |
| | | | | | | | Green | 0 | 0 | 0 | 0 | 0 | 0 | 0 | 0 | 0 |
| | | | | | | | Blue | 0 | 0 | 0 | 0 | 0 | 0 | 0 | 0 | 0 |
| | | | | black | 6.9 | 48200 | Red | 0 | 74 | 74 | 47 | 20 | 75 | 74 | 2 | 51 |
| | | | | | | | Green | 0 | 74 | 74 | 43 | 20 | 75 | 64 | 2 | 47 |
| | | | | | | | Blue | 0 | 87 | 87 | 42 | 20 | 87 | 0 | 87 | 45 |
| P203 | Tu | ne | 960 | grey | 2.7 | 33671 | Red | 75 | 255 | 180 | 142 | 29 | 181 | 132 | 251 | 138 |
| | | | | | | | Green | 68 | 253 | 185 | 134 | 28 | 185 | 122 | 249 | 130 |
| | | | | | | | Blue | 42 | 246 | 204 | 123 | 27 | 197 | 113 | 42 | 119 |
| | | | | yellow | 27.7 | 341711 | Red | 75 | 255 | 180 | 148 | 26 | 181 | 154 | 247 | 149 |
| | | | | | | | Green | 55 | 238 | 183 | 128 | 25 | 184 | 129 | 238 | 128 |
| | | | | | | | Blue | 29 | 233 | 204 | 112 | 25 | 201 | 110 | 29 | 112 |
| | | | | red | 2.0 | 24511 | Red | 75 | 205 | 130 | 132 | 24 | 127 | 137 | 195 | 135 |
| | | | | | | | Green | 30 | 164 | 134 | 99 | 21 | 126 | 113 | 30 | 101 |
| | | | | | | | Blue | 9 | 148 | 139 | 81 | 20 | 128 | 92 | 9 | 82 |
| | | | | black | 0.9 | 11132 | Red | 3 | 74 | 71 | 53 | 16 | 71 | 74 | 3 | 57 |
| | | | | | | | Green | 0 | 73 | 73 | 38 | 17 | 74 | 48 | 73 | 41 |
| | | | | | | | Blue | 0 | 71 | 71 | 28 | 16 | 71 | 0 | 69 | 29 |
| P203 | Tu | on | 1300 | grey | 9.2 | 53728 | Red | 75 | 249 | 174 | 154 | 21 | 158 | 166 | 222 | 158 |
| | | | | | | | Green | 68 | 233 | 165 | 145 | 20 | 154 | 154 | 214 | 148 |
| | | | | | | | Blue | 37 | 220 | 183 | 125 | 19 | 165 | 133 | 37 | 126 |
| | | | | yellow | 81.9 | 479503 | Red | 75 | 255 | 180 | 141 | 23 | 168 | 152 | 227 | 143 |
| | | | | | | | Green | 55 | 238 | 183 | 122 | 23 | 168 | 124 | 213 | 123 |
| | | | | | | | Blue | 9 | 228 | 219 | 98 | 22 | 190 | 98 | 9 | 98 |
| | | | | red | 4.2 | 24350 | Red | 75 | 180 | 105 | 116 | 22 | 103 | 124 | 178 | 116 |
| | | | | | | | Green | 38 | 143 | 105 | 86 | 20 | 104 | 96 | 38 | 87 |
| | | | | | | | Blue | 7 | 126 | 119 | 63 | 18 | 111 | 70 | 7 | 63 |
| | | | | black | 4.7 | 27587 | Red | 4 | 74 | 70 | 51 | 16 | 70 | 74 | 4 | 53 |
| | | | | | | | Green | 0 | 74 | 74 | 34 | 15 | 75 | 45 | 72 | 35 |
| | | | | | | | Blue | 0 | 63 | 63 | 22 | 13 | 64 | 0 | 62 | 22 |

| Profile | Form | Horizon | Depth (mm) | Colour | Quantity (%) | Count (cells) | RGB | RGB colour statistics | | | | | | | | |
|---|---|---|---|---|---|---|---|---|---|---|---|---|---|---|---|---|
| | | | | | | | | Min | Max | Range | Mean | Std | Variety | Majority | Minority | Median |
| P204 | Lo | ot | 140 | grey | 92.4 | 209521 | Red | 65 | 255 | 190 | 131 | 18 | 189 | 129 | 65 | 129 |
| | | | | | | | Green | 68 | 255 | 187 | 127 | 19 | 187 | 123 | 222 | 124 |
| | | | | | | | Blue | 50 | 255 | 205 | 118 | 20 | 203 | 110 | 50 | 114 |
| | | | | yellow | 6.5 | 14840 | Red | 75 | 214 | 139 | 123 | 17 | 126 | 124 | 178 | 123 |
| | | | | | | | Green | 56 | 198 | 142 | 111 | 16 | 127 | 113 | 56 | 112 |
| | | | | | | | Blue | 37 | 199 | 162 | 100 | 16 | 142 | 103 | 37 | 101 |
| | | | | red | 0.0 | 17 | Red | 86 | 130 | 44 | 102 | 12 | 16 | 86 | 88 | 102 |
| | | | | | | | Green | 59 | 101 | 42 | 75 | 11 | 14 | 59 | 61 | 74 |
| | | | | | | | Blue | 40 | 83 | 43 | 57 | 12 | 15 | 40 | 42 | 57 |
| | | | | black | 1.1 | 2462 | Red | 0 | 74 | 74 | 56 | 16 | 74 | 74 | 0 | 62 |
| | | | | | | | Green | 0 | 74 | 74 | 52 | 17 | 75 | 64 | 2 | 57 |
| | | | | | | | Blue | 0 | 77 | 77 | 47 | 18 | 78 | 59 | 77 | 50 |
| P204 | Lo | gs | 300 | grey | 63.5 | 169336 | Red | 75 | 255 | 180 | 135 | 14 | 170 | 132 | 216 | 135 |
| | | | | | | | Green | 68 | 255 | 187 | 127 | 13 | 176 | 125 | 207 | 127 |
| | | | | | | | Blue | 42 | 243 | 201 | 111 | 13 | 183 | 110 | 42 | 111 |
| | | | | yellow | 35.7 | 95116 | Red | 75 | 231 | 156 | 137 | 15 | 129 | 142 | 193 | 138 |
| | | | | | | | Green | 58 | 212 | 154 | 124 | 15 | 130 | 131 | 58 | 126 |
| | | | | | | | Blue | 30 | 205 | 175 | 104 | 13 | 138 | 109 | 30 | 106 |
| | | | | red | 0.2 | 650 | Red | 76 | 179 | 103 | 127 | 19 | 90 | 127 | 79 | 129 |
| | | | | | | | Green | 39 | 140 | 101 | 92 | 18 | 89 | 86 | 39 | 92 |
| | | | | | | | Blue | 12 | 113 | 101 | 57 | 19 | 95 | 53 | 14 | 56 |
| | | | | black | 0.6 | 1635 | Red | 4 | 74 | 70 | 56 | 17 | 71 | 71 | 4 | 61 |
| | | | | | | | Green | 0 | 72 | 72 | 47 | 17 | 73 | 62 | 72 | 53 |
| | | | | | | | Blue | 0 | 67 | 67 | 34 | 16 | 64 | 0 | 62 | 38 |
| P204 | Lo | sp | 470 | grey | 9.6 | 36028 | Red | 75 | 255 | 180 | 160 | 22 | 172 | 167 | 236 | 161 |
| | | | | | | | Green | 68 | 253 | 185 | 151 | 21 | 176 | 155 | 230 | 152 |
| | | | | | | | Blue | 39 | 240 | 201 | 131 | 22 | 186 | 132 | 39 | 131 |
| | | | | yellow | 62.6 | 233714 | Red | 75 | 255 | 180 | 153 | 19 | 174 | 153 | 234 | 154 |
| | | | | | | | Green | 55 | 238 | 183 | 131 | 19 | 175 | 133 | 215 | 132 |
| | | | | | | | Blue | 20 | 226 | 206 | 106 | 19 | 197 | 105 | 20 | 106 |
| | | | | red | 27.0 | 100940 | Red | 75 | 218 | 143 | 143 | 17 | 136 | 149 | 216 | 145 |
| | | | | | | | Green | 27 | 175 | 148 | 104 | 17 | 140 | 106 | 27 | 106 |
| | | | | | | | Blue | 0 | 149 | 149 | 75 | 16 | 143 | 79 | 2 | 76 |
| | | | | black | 0.8 | 2828 | Red | 5 | 74 | 69 | 53 | 17 | 69 | 74 | 5 | 57 |
| | | | | | | | Green | 0 | 71 | 71 | 36 | 17 | 72 | 0 | 69 | 39 |
| | | | | | | | Blue | 0 | 61 | 61 | 21 | 15 | 62 | 0 | 60 | 21 |

| Profile | Form | Horizon | Depth (mm) | Colour | Quantity (%) | Count (cells) | RGB | RGB colour statistics | | | | | | | | |
|---|---|---|---|---|---|---|---|---|---|---|---|---|---|---|---|---|
| | | | | | | | | Min | Max | Range | Mean | Std | Variety | Majority | Minority | Median |
| P204 | Lo | gh | 1000 | grey | 9.9 | 53268 | Red | 69 | 255 | 186 | 163 | 24 | 186 | 168 | 70 | 165 |
| | | | | | | | Green | 68 | 255 | 187 | 157 | 25 | 188 | 161 | 255 | 159 |
| | | | | | | | Blue | 51 | 255 | 204 | 153 | 27 | 200 | 157 | 51 | 155 |
| | | | | yellow | 44.3 | 237314 | Red | 75 | 255 | 180 | 159 | 19 | 181 | 160 | 251 | 160 |
| | | | | | | | Green | 55 | 238 | 183 | 134 | 19 | 183 | 133 | 227 | 134 |
| | | | | | | | Blue | 35 | 237 | 202 | 124 | 21 | 197 | 123 | 35 | 124 |
| | | | | red | 45.1 | 241809 | Red | 75 | 218 | 143 | 151 | 14 | 140 | 155 | 209 | 153 |
| | | | | | | | Green | 29 | 171 | 142 | 111 | 14 | 136 | 115 | 166 | 112 |
| | | | | | | | Blue | 14 | 164 | 150 | 95 | 16 | 147 | 95 | 14 | 95 |
| | | | | black | 0.6 | 3210 | Red | 0 | 74 | 74 | 47 | 20 | 75 | 68 | 0 | 49 |
| | | | | | | | Green | 0 | 73 | 73 | 32 | 19 | 74 | 0 | 70 | 34 |
| | | | | | | | Blue | 0 | 83 | 83 | 25 | 18 | 77 | 0 | 75 | 25 |
| P205 | Kd | ot | 220 | grey | 10.6 | 46425 | Red | 68 | 255 | 187 | 149 | 33 | 187 | 146 | 68 | 146 |
| | | | | | | | Green | 68 | 255 | 187 | 141 | 32 | 188 | 135 | 242 | 137 |
| | | | | | | | Blue | 48 | 251 | 203 | 125 | 31 | 203 | 117 | 48 | 121 |
| | | | | yellow | 87.0 | 382052 | Red | 75 | 255 | 180 | 133 | 20 | 181 | 139 | 249 | 134 |
| | | | | | | | Green | 55 | 238 | 183 | 118 | 20 | 184 | 121 | 231 | 119 |
| | | | | | | | Blue | 30 | 233 | 203 | 101 | 20 | 193 | 103 | 30 | 101 |
| | | | | red | 0.1 | 462 | Red | 75 | 144 | 69 | 97 | 14 | 58 | 110 | 118 | 96 |
| | | | | | | | Green | 47 | 113 | 66 | 70 | 12 | 54 | 54 | 49 | 70 |
| | | | | | | | Blue | 19 | 82 | 63 | 49 | 11 | 56 | 49 | 19 | 49 |
| | | | | black | 2.3 | 10113 | Red | 3 | 74 | 71 | 59 | 13 | 71 | 74 | 3 | 63 |
| | | | | | | | Green | 0 | 74 | 74 | 47 | 13 | 75 | 57 | 2 | 50 |
| | | | | | | | Blue | 0 | 79 | 79 | 35 | 13 | 79 | 40 | 78 | 37 |
| P205 | Kd | gs | 460 | grey | 98.9 | 418970 | Red | 68 | 254 | 186 | 122 | 12 | 145 | 126 | 68 | 123 |
| | | | | | | | Green | 68 | 250 | 182 | 120 | 12 | 143 | 122 | 186 | 121 |
| | | | | | | | Blue | 54 | 249 | 195 | 114 | 13 | 153 | 112 | 55 | 114 |
| | | | | yellow | 0.4 | 1819 | Red | 75 | 148 | 73 | 115 | 14 | 74 | 123 | 147 | 119 |
| | | | | | | | Green | 65 | 134 | 69 | 105 | 13 | 70 | 114 | 132 | 109 |
| | | | | | | | Blue | 53 | 134 | 81 | 99 | 13 | 75 | 101 | 61 | 102 |
| | | | | red | 0.0 | 0 | Red | 0 | 0 | 0 | 0 | 0 | 0 | 0 | 0 | 0 |
| | | | | | | | Green | 0 | 0 | 0 | 0 | 0 | 0 | 0 | 0 | 0 |
| | | | | | | | Blue | 0 | 0 | 0 | 0 | 0 | 0 | 0 | 0 | 0 |
| | | | | black | 0.7 | 2865 | Red | 0 | 74 | 74 | 48 | 19 | 75 | 71 | 0 | 51 |
| | | | | | | | Green | 0 | 74 | 74 | 47 | 19 | 75 | 60 | 25 | 51 |
| | | | | | | | Blue | 0 | 82 | 82 | 44 | 18 | 80 | 44 | 82 | 47 |

| Profile | Form | Horizon | Depth (mm) | Colour | Quantity (%) | Count (cells) | RGB | RGB colour statistics | | | | | | | | |
|---|---|---|---|---|---|---|---|---|---|---|---|---|---|---|---|---|
| | | | | | | | | Min | Max | Range | Mean | Std | Variety | Majority | Minority | Median |
| P205 | Kd | gs | 660 | grey | 91.7 | 381174 | Red | 70 | 228 | 158 | 135 | 11 | 145 | 134 | 70 | 135 |
| | | | | | | | Green | 68 | 232 | 164 | 130 | 11 | 144 | 130 | 184 | 130 |
| | | | | | | | Blue | 45 | 233 | 188 | 114 | 11 | 166 | 115 | 45 | 114 |
| | | | | yellow | 8.1 | 33711 | Red | 75 | 190 | 115 | 138 | 11 | 112 | 143 | 187 | 140 |
| | | | | | | | Green | 62 | 174 | 112 | 124 | 10 | 109 | 128 | 62 | 126 |
| | | | | | | | Blue | 26 | 168 | 142 | 100 | 14 | 133 | 106 | 26 | 102 |
| | | | | red | 0.1 | 332 | Red | 76 | 160 | 84 | 130 | 19 | 70 | 140 | 76 | 137 |
| | | | | | | | Green | 45 | 126 | 81 | 99 | 18 | 70 | 109 | 45 | 105 |
| | | | | | | | Blue | 18 | 124 | 106 | 63 | 16 | 71 | 72 | 18 | 65 |
| | | | | black | 0.1 | 416 | Red | 5 | 74 | 69 | 56 | 16 | 65 | 69 | 5 | 62 |
| | | | | | | | Green | 0 | 74 | 74 | 52 | 18 | 67 | 59 | 5 | 59 |
| | | | | | | | Blue | 0 | 79 | 79 | 41 | 21 | 75 | 0 | 4 | 47 |
| P205 | Kd | gh | 1400 | grey | 5.1 | 28560 | Red | 75 | 255 | 180 | 173 | 31 | 181 | 166 | 79 | 173 |
| | | | | | | | Green | 68 | 255 | 187 | 163 | 30 | 188 | 158 | 68 | 163 |
| | | | | | | | Blue | 41 | 248 | 207 | 145 | 31 | 201 | 132 | 41 | 144 |
| | | | | yellow | 52.5 | 293480 | Red | 75 | 255 | 180 | 160 | 24 | 181 | 163 | 254 | 162 |
| | | | | | | | Green | 55 | 238 | 183 | 137 | 23 | 184 | 137 | 55 | 137 |
| | | | | | | | Blue | 25 | 228 | 203 | 112 | 23 | 200 | 109 | 27 | 112 |
| | | | | red | 41.8 | 233675 | Red | 75 | 242 | 167 | 156 | 15 | 159 | 158 | 225 | 158 |
| | | | | | | | Green | 29 | 191 | 162 | 114 | 15 | 155 | 113 | 29 | 115 |
| | | | | | | | Blue | 0 | 168 | 168 | 84 | 16 | 158 | 81 | 0 | 84 |
| | | | | black | 0.6 | 3138 | Red | 3 | 74 | 71 | 56 | 15 | 69 | 70 | 8 | 60 |
| | | | | | | | Green | 0 | 74 | 74 | 41 | 16 | 71 | 57 | 72 | 44 |
| | | | | | | | Blue | 0 | 59 | 59 | 23 | 14 | 58 | 0 | 53 | 25 |
| P206 | Kd | ot | 550 | grey | 90.3 | 665283 | Red | 55 | 255 | 200 | 124 | 33 | 199 | 112 | 55 | 118 |
| | | | | | | | Green | 68 | 255 | 187 | 128 | 33 | 188 | 115 | 68 | 122 |
| | | | | | | | Blue | 57 | 255 | 198 | 132 | 33 | 199 | 118 | 58 | 127 |
| | | | | yellow | 0.1 | | Red | 75 | 255 | 180 | 107 | 27 | 112 | 79 | 145 | 101 |
| | | | | | | | Green | 60 | 237 | 177 | 96 | 26 | 112 | 75 | 63 | 90 |
| | | | | | | | Blue | 51 | 246 | 195 | 99 | 27 | 121 | 87 | 51 | 93 |
| | | | | red | 0.0 | 1 | Red | 76 | 76 | 0 | 76 | 0 | 1 | 76 | 76 | 76 |
| | | | | | | | Green | 55 | 55 | 0 | 55 | 0 | 1 | 55 | 55 | 55 |
| | | | | | | | Blue | 62 | 62 | 0 | 62 | 0 | 1 | 62 | 62 | 62 |
| | | | | black | 9.6 | 70861 | Red | 0 | 74 | 74 | 47 | 20 | 75 | 66 | 2 | 52 |
| | | | | | | | Green | 0 | 74 | 74 | 49 | 20 | 75 | 72 | 4 | 54 |
| | | | | | | | Blue | 0 | 93 | 93 | 52 | 21 | 93 | 70 | 91 | 57 |

| Profile | Form | Horizon | Depth (mm) | Colour | Quantity (%) | Count (cells) | RGB | RGB colour statistics | | | | | | | | |
|---|---|---|---|---|---|---|---|---|---|---|---|---|---|---|---|---|
| | | | | | | | | Min | Max | Range | Mean | Std | Variety | Majority | Minority | Median |
| P206 | Kd | gs | 800 | grey | 99.2 | 261739 | Red | 67 | 255 | 188 | 142 | 22 | 188 | 142 | 67 | 142 |
| | | | | | | | Green | 68 | 255 | 187 | 142 | 22 | 188 | 143 | 68 | 142 |
| | | | | | | | Blue | 54 | 255 | 201 | 137 | 22 | 198 | 139 | 54 | 138 |
| | | | | yellow | 0.2 | 519 | Red | 75 | 184 | 109 | 124 | 23 | 99 | 124 | 75 | 124 |
| | | | | | | | Green | 67 | 170 | 103 | 112 | 21 | 92 | 113 | 67 | 113 |
| | | | | | | | Blue | 54 | 160 | 106 | 105 | 21 | 95 | 89 | 54 | 104 |
| | | | | red | 0.0 | 0 | Red | 0 | 0 | 0 | 0 | 0 | 0 | 0 | 0 | 0 |
| | | | | | | | Green | 0 | 0 | 0 | 0 | 0 | 0 | 0 | 0 | 0 |
| | | | | | | | Blue | 0 | 0 | 0 | 0 | 0 | 0 | 0 | 0 | 0 |
| | | | | black | 0.6 | 1614 | Red | 0 | 74 | 74 | 60 | 13 | 69 | 72 | 0 | 63 |
| | | | | | | | Green | 2 | 74 | 72 | 60 | 13 | 68 | 72 | 5 | 63 |
| | | | | | | | Blue | 0 | 82 | 82 | 56 | 14 | 76 | 62 | 7 | 59 |
| P206 | Kd | gh | 1100 | grey | 98.0 | 86815 | Red | 70 | 255 | 185 | 154 | 20 | 186 | 158 | 70 | 155 |
| | | | | | | | Green | 69 | 255 | 186 | 152 | 19 | 187 | 157 | 240 | 154 |
| | | | | | | | Blue | 33 | 255 | 222 | 132 | 19 | 212 | 134 | 33 | 132 |
| | | | | yellow | 1.7 | 1493 | Red | 76 | 205 | 129 | 166 | 21 | 117 | 177 | 76 | 170 |
| | | | | | | | Green | 66 | 190 | 124 | 152 | 20 | 115 | 153 | 66 | 156 |
| | | | | | | | Blue | 36 | 164 | 128 | 115 | 16 | 107 | 118 | 36 | 117 |
| | | | | red | 0.0 | 0 | Red | 0 | 0 | 0 | 0 | 0 | 0 | 0 | 0 | 0 |
| | | | | | | | Green | 0 | 0 | 0 | 0 | 0 | 0 | 0 | 0 | 0 |
| | | | | | | | Blue | 0 | 0 | 0 | 0 | 0 | 0 | 0 | 0 | 0 |
| | | | | black | 0.3 | 300 | Red | 3 | 74 | 71 | 55 | 18 | 61 | 73 | 9 | 60 |
| | | | | | | | Green | 0 | 74 | 74 | 54 | 18 | 68 | 68 | 0 | 59 |
| | | | | | | | Blue | 0 | 68 | 68 | 40 | 18 | 62 | 0 | 3 | 44 |
| P207 | We | ot | 300 | grey | 94.6 | 749582 | Red | 63 | 255 | 192 | 130 | 16 | 188 | 131 | 63 | 130 |
| | | | | | | | Green | 68 | 255 | 187 | 126 | 16 | 188 | 127 | 251 | 126 |
| | | | | | | | Blue | 43 | 255 | 212 | 121 | 16 | 208 | 124 | 43 | 122 |
| | | | | yellow | 3.6 | 28351 | Red | 75 | 254 | 179 | 125 | 24 | 177 | 125 | 234 | 125 |
| | | | | | | | Green | 55 | 233 | 178 | 112 | 23 | 173 | 114 | 55 | 113 |
| | | | | | | | Blue | 23 | 225 | 202 | 103 | 22 | 190 | 113 | 23 | 104 |
| | | | | red | 0.0 | 228 | Red | 75 | 166 | 91 | 104 | 23 | 74 | 82 | 96 | 97 |
| | | | | | | | Green | 43 | 131 | 88 | 76 | 20 | 70 | 55 | 43 | 70 |
| | | | | | | | Blue | 12 | 111 | 99 | 52 | 20 | 75 | 37 | 12 | 47 |
| | | | | black | 1.8 | 13995 | Red | 0 | 74 | 74 | 50 | 19 | 75 | 74 | 0 | 54 |
| | | | | | | | Green | 0 | 74 | 74 | 43 | 20 | 75 | 64 | 74 | 47 |
| | | | | | | | Blue | 0 | 82 | 82 | 38 | 20 | 80 | 0 | 78 | 41 |

| Profile | Form | Horizon | Depth (mm) | Colour | Quantity (%) | Count (cells) | RGB | RGB colour statistics | | | | | | | | |
|---|---|---|---|---|---|---|---|---|---|---|---|---|---|---|---|---|
| | | | | | | | | Min | Max | Range | Mean | Std | Variety | Majority | Minority | Median |
| P207 | We | sp | 560 | grey | 27.1 | 138829 | Red | 75 | 255 | 180 | 144 | 19 | 180 | 146 | 236 | 145 |
| | | | | | | | Green | 68 | 255 | 187 | 135 | 19 | 181 | 135 | 228 | 136 |
| | | | | | | | Blue | 43 | 246 | 203 | 117 | 19 | 201 | 117 | 46 | 117 |
| | | | | yellow | 71.8 | 367762 | Red | 75 | 254 | 179 | 135 | 16 | 162 | 138 | 210 | 136 |
| | | | | | | | Green | 55 | 237 | 182 | 122 | 16 | 165 | 124 | 55 | 123 |
| | | | | | | | Blue | 20 | 230 | 210 | 101 | 16 | 172 | 102 | 20 | 102 |
| | | | | red | 0.0 | 34 | Red | 75 | 122 | 47 | 92 | 14 | 23 | 77 | 78 | 90 |
| | | | | | | | Green | 51 | 93 | 42 | 67 | 12 | 21 | 55 | 51 | 66 |
| | | | | | | | Blue | 18 | 62 | 44 | 38 | 12 | 25 | 34 | 22 | 37 |
| | | | | black | 1.1 | 5439 | Red | 6 | 74 | 68 | 58 | 13 | 68 | 74 | 6 | 60 |
| | | | | | | | Green | 0 | 72 | 72 | 47 | 13 | 73 | 61 | 71 | 49 |
| | | | | | | | Blue | 0 | 65 | 65 | 33 | 13 | 65 | 36 | 61 | 35 |
| P207 | We | sp | 670 | grey | 70.4 | 225207 | Red | 66 | 244 | 178 | 144 | 21 | 161 | 150 | 66 | 146 |
| | | | | | | | Green | 68 | 241 | 173 | 138 | 20 | 165 | 139 | 216 | 140 |
| | | | | | | | Blue | 35 | 232 | 197 | 125 | 21 | 189 | 128 | 35 | 126 |
| | | | | yellow | 26.9 | 86028 | Red | 75 | 221 | 146 | 133 | 22 | 143 | 141 | 209 | 135 |
| | | | | | | | Green | 55 | 204 | 149 | 119 | 21 | 146 | 129 | 55 | 121 |
| | | | | | | | Blue | 21 | 190 | 169 | 99 | 22 | 163 | 103 | 23 | 101 |
| | | | | red | 0.1 | 388 | Red | 75 | 164 | 89 | 103 | 17 | 70 | 97 | 121 | 101 |
| | | | | | | | Green | 48 | 130 | 82 | 76 | 14 | 65 | 65 | 48 | 74 |
| | | | | | | | Blue | 10 | 95 | 85 | 44 | 14 | 62 | 45 | 12 | 44 |
| | | | | black | 2.6 | 8185 | Red | 0 | 74 | 74 | 57 | 15 | 75 | 74 | 2 | 60 |
| | | | | | | | Green | 0 | 74 | 74 | 50 | 15 | 75 | 61 | 6 | 52 |
| | | | | | | | Blue | 0 | 77 | 77 | 40 | 15 | 78 | 50 | 77 | 42 |
| P207 | We | on | 1300 | grey | 66.0 | 1043845 | Red | 65 | 255 | 190 | 139 | 20 | 183 | 146 | 65 | 141 |
| | | | | | | | Green | 68 | 249 | 181 | 134 | 20 | 181 | 135 | 242 | 135 |
| | | | | | | | Blue | 29 | 246 | 217 | 118 | 21 | 210 | 115 | 29 | 118 |
| | | | | yellow | 31.1 | 492440 | Red | 75 | 217 | 142 | 133 | 18 | 141 | 142 | 211 | 135 |
| | | | | | | | Green | 55 | 201 | 146 | 119 | 18 | 146 | 128 | 195 | 121 |
| | | | | | | | Blue | 0 | 184 | 184 | 93 | 17 | 180 | 94 | 0 | 93 |
| | | | | red | 0.1 | 1758 | Red | 75 | 166 | 91 | 115 | 19 | 90 | 121 | 156 | 118 |
| | | | | | | | Green | 45 | 131 | 86 | 86 | 17 | 85 | 90 | 45 | 89 |
| | | | | | | | Blue | 0 | 88 | 88 | 47 | 18 | 85 | 41 | 3 | 47 |
| | | | | black | 2.8 | 44188 | Red | 0 | 74 | 74 | 53 | 17 | 75 | 73 | 2 | 56 |
| | | | | | | | Green | 0 | 74 | 74 | 47 | 17 | 75 | 58 | 1 | 50 |
| | | | | | | | Blue | 0 | 82 | 82 | 38 | 18 | 83 | 0 | 82 | 40 |

| Profile | Form | Horizon | Depth (mm) | Colour | Quantity (%) | Count (cells) | RGB | RGB colour statistics | | | | | | | | |
|---|---|---|---|---|---|---|---|---|---|---|---|---|---|---|---|---|
| | | | | | | | | Min | Max | Range | Mean | Std | Variety | Majority | Minority | Median |
| P208 | Kd | ot | 350 | grey | 92.9 | 492665 | Red | 59 | 255 | 196 | 119 | 23 | 196 | 119 | 60 | 117 |
| | | | | | | | Green | 68 | 255 | 187 | 119 | 23 | 188 | 122 | 68 | 118 |
| | | | | | | | Blue | 54 | 255 | 201 | 122 | 23 | 199 | 123 | 54 | 121 |
| | | | | yellow | 0.6 | 3094 | Red | 75 | 254 | 179 | 109 | 28 | 146 | 101 | 168 | 103 |
| | | | | | | | Green | 57 | 236 | 179 | 97 | 26 | 149 | 92 | 57 | 92 |
| | | | | | | | Blue | 43 | 226 | 183 | 95 | 26 | 152 | 79 | 43 | 90 |
| | | | | red | 0.0 | 60 | Red | 89 | 151 | 62 | 120 | 15 | 40 | 102 | 89 | 121 |
| | | | | | | | Green | 63 | 115 | 52 | 88 | 13 | 36 | 83 | 65 | 88 |
| | | | | | | | Blue | 42 | 105 | 63 | 68 | 13 | 33 | 62 | 42 | 68 |
| | | | | black | 6.5 | 34515 | Red | 0 | 74 | 74 | 55 | 15 | 75 | 69 | 2 | 59 |
| | | | | | | | Green | 0 | 74 | 74 | 55 | 15 | 75 | 69 | 1 | 59 |
| | | | | | | | Blue | 0 | 86 | 86 | 56 | 16 | 87 | 68 | 86 | 60 |
| P208 | Kd | gs | 530 | grey | 98.7 | 207515 | Red | 70 | 255 | 185 | 132 | 13 | 163 | 136 | 194 | 134 |
| | | | | | | | Green | 69 | 255 | 186 | 132 | 13 | 162 | 137 | 189 | 134 |
| | | | | | | | Blue | 54 | 255 | 201 | 134 | 13 | 177 | 138 | 54 | 136 |
| | | | | yellow | 0.1 | 236 | Red | 75 | 162 | 87 | 116 | 20 | 75 | 103 | 76 | 118 |
| | | | | | | | Green | 65 | 150 | 85 | 105 | 19 | 71 | 102 | 65 | 108 |
| | | | | | | | Blue | 56 | 138 | 82 | 102 | 20 | 73 | 123 | 56 | 103 |
| | | | | red | 0.0 | 0 | Red | 0 | 0 | 0 | 0 | 0 | 0 | 0 | 0 | 0 |
| | | | | | | | Green | 0 | 0 | 0 | 0 | 0 | 0 | 0 | 0 | 0 |
| | | | | | | | Blue | 0 | 0 | 0 | 0 | 0 | 0 | 0 | 0 | 0 |
| | | | | black | 1.2 | 2437 | Red | 0 | 74 | 74 | 55 | 15 | 75 | 72 | 2 | 59 |
| | | | | | | | Green | 0 | 74 | 74 | 55 | 15 | 72 | 69 | 3 | 58 |
| | | | | | | | Blue | 0 | 82 | 82 | 55 | 16 | 81 | 62 | 8 | 59 |
| P208 | Kd | gh | 800 | grey | 89.4 | 511448 | Red | 69 | 250 | 181 | 138 | 17 | 167 | 132 | 69 | 137 |
| | | | | | | | Green | 68 | 247 | 179 | 133 | 17 | 169 | 125 | 223 | 133 |
| | | | | | | | Blue | 53 | 241 | 188 | 128 | 18 | 180 | 123 | 53 | 127 |
| | | | | yellow | 10.3 | 58933 | Red | 75 | 208 | 133 | 127 | 13 | 112 | 125 | 182 | 126 |
| | | | | | | | Green | 62 | 193 | 131 | 115 | 12 | 112 | 115 | 164 | 114 |
| | | | | | | | Blue | 39 | 173 | 134 | 102 | 11 | 118 | 103 | 39 | 102 |
| | | | | red | 0.0 | 0 | Red | 0 | 0 | 0 | 0 | 0 | 0 | 0 | 0 | 0 |
| | | | | | | | Green | 0 | 0 | 0 | 0 | 0 | 0 | 0 | 0 | 0 |
| | | | | | | | Blue | 0 | 0 | 0 | 0 | 0 | 0 | 0 | 0 | 0 |
| | | | | black | 0.2 | 1429 | Red | 0 | 74 | 74 | 57 | 16 | 73 | 72 | 0 | 62 |
| | | | | | | | Green | 0 | 74 | 74 | 53 | 17 | 74 | 65 | 7 | 58 |
| | | | | | | | Blue | 0 | 77 | 77 | 49 | 17 | 78 | 63 | 75 | 53 |

| Profile | Form | Horizon | Depth (mm) | Colour | Quantity (%) | Count (cells) | RGB | RGB colour statistics | | | | | | | | |
|---|---|---|---|---|---|---|---|---|---|---|---|---|---|---|---|---|
| | | | | | | | | Min | Max | Range | Mean | Std | Variety | Majority | Minority | Median |
| P208 | Kd | gh | 1700 | grey | 96.3 | 593645 | Red | 61 | 255 | 194 | 132 | 17 | 192 | 130 | 61 | 132 |
| | | | | | | | Green | 69 | 255 | 186 | 132 | 18 | 185 | 134 | 245 | 132 |
| | | | | | | | Blue | 45 | 255 | 210 | 131 | 19 | 211 | 127 | 45 | 129 |
| | | | | yellow | 2.9 | 17763 | Red | 75 | 187 | 112 | 130 | 14 | 108 | 125 | 182 | 130 |
| | | | | | | | Green | 57 | 173 | 116 | 118 | 13 | 111 | 115 | 57 | 117 |
| | | | | | | | Blue | 33 | 154 | 121 | 103 | 11 | 112 | 100 | 33 | 103 |
| | | | | red | 0.0 | 0 | Red | 0 | 0 | 0 | 0 | 0 | 0 | 0 | 0 | 0 |
| | | | | | | | Green | 0 | 0 | 0 | 0 | 0 | 0 | 0 | 0 | 0 |
| | | | | | | | Blue | 0 | 0 | 0 | 0 | 0 | 0 | 0 | 0 | 0 |
| | | | | black | 0.8 | 5191 | Red | 0 | 74 | 74 | 46 | 21 | 75 | 0 | 13 | 52 |
| | | | | | | | Green | 0 | 74 | 74 | 48 | 21 | 75 | 69 | 16 | 54 |
| | | | | | | | Blue | 0 | 92 | 92 | 50 | 23 | 93 | 61 | 91 | 56 |
| P209 | Kd | ot | 450 | grey | 55.4 | 448871 | Red | 71 | 255 | 184 | 138 | 39 | 185 | 114 | 72 | 126 |
| | | | | | | | Green | 68 | 255 | 187 | 131 | 39 | 188 | 107 | 68 | 118 |
| | | | | | | | Blue | 42 | 255 | 213 | 122 | 36 | 211 | 107 | 42 | 110 |
| | | | | yellow | 40.3 | 326854 | Red | 75 | 255 | 180 | 124 | 29 | 181 | 121 | 253 | 119 |
| | | | | | | | Green | 55 | 238 | 183 | 112 | 27 | 184 | 111 | 55 | 107 |
| | | | | | | | Blue | 26 | 228 | 202 | 100 | 24 | 198 | 102 | 26 | 97 |
| | | | | red | 0.0 | 146 | Red | 78 | 192 | 114 | 132 | 33 | 79 | 163 | 80 | 134 |
| | | | | | | | Green | 52 | 154 | 102 | 100 | 28 | 74 | 60 | 52 | 101 |
| | | | | | | | Blue | 29 | 141 | 112 | 78 | 26 | 76 | 62 | 29 | 76 |
| | | | | black | 4.3 | 34897 | Red | 5 | 74 | 69 | 59 | 12 | 70 | 74 | 5 | 62 |
| | | | | | | | Green | 0 | 74 | 74 | 52 | 12 | 75 | 61 | 1 | 55 |
| | | | | | | | Blue | 0 | 98 | 98 | 47 | 13 | 98 | 52 | 95 | 48 |
| P209 | Kd | gh | 1100 | grey | 54.6 | 752806 | Red | 60 | 255 | 195 | 138 | 22 | 195 | 146 | 61 | 140 |
| | | | | | | | Green | 68 | 255 | 187 | 135 | 22 | 188 | 138 | 247 | 136 |
| | | | | | | | Blue | 36 | 255 | 219 | 124 | 22 | 216 | 118 | 36 | 123 |
| | | | | yellow | 38.0 | 523652 | Red | 75 | 229 | 154 | 139 | 17 | 148 | 145 | 211 | 140 |
| | | | | | | | Green | 55 | 212 | 157 | 121 | 17 | 152 | 125 | 192 | 122 |
| | | | | | | | Blue | 15 | 205 | 190 | 101 | 15 | 167 | 102 | 15 | 102 |
| | | | | red | 5.5 | 75295 | Red | 75 | 194 | 119 | 139 | 15 | 116 | 144 | 189 | 141 |
| | | | | | | | Green | 33 | 154 | 121 | 103 | 13 | 118 | 102 | 33 | 104 |
| | | | | | | | Blue | 2 | 135 | 133 | 81 | 12 | 118 | 81 | 2 | 82 |
| | | | | black | 2.0 | 27765 | Red | 0 | 74 | 74 | 49 | 20 | 75 | 72 | 2 | 55 |
| | | | | | | | Green | 0 | 74 | 74 | 46 | 20 | 75 | 64 | 3 | 51 |
| | | | | | | | Blue | 0 | 86 | 86 | 42 | 21 | 86 | 0 | 81 | 45 |

| Profile | Form | Horizon | Depth (mm) | Colour | Quantity (%) | Count (cells) | RGB | RGB colour statistics | | | | | | | | |
|---|---|---|---|---|---|---|---|---|---|---|---|---|---|---|---|---|
| | | | | | | | | Min | Max | Range | Mean | Std | Variety | Majority | Minority | Median |
| P209 | Kd | so | 1400 | grey | 98.4 | 251901 | Red | 62 | 245 | 183 | 152 | 21 | 178 | 162 | 62 | 155 |
| | | | | | | | Green | 68 | 254 | 186 | 156 | 22 | 176 | 165 | 234 | 159 |
| | | | | | | | Blue | 37 | 251 | 214 | 144 | 24 | 198 | 150 | 37 | 145 |
| | | | | yellow | 1.1 | 2849 | Red | 75 | 199 | 124 | 146 | 17 | 114 | 145 | 76 | 145 |
| | | | | | | | Green | 64 | 185 | 121 | 131 | 17 | 108 | 134 | 65 | 131 |
| | | | | | | | Blue | 34 | 165 | 131 | 103 | 16 | 117 | 110 | 34 | 104 |
| | | | | red | 0.0 | 0 | Red | 0 | 0 | 0 | 0 | 0 | 0 | 0 | 0 | 0 |
| | | | | | | | Green | 0 | 0 | 0 | 0 | 0 | 0 | 0 | 0 | 0 |
| | | | | | | | Blue | 0 | 0 | 0 | 0 | 0 | 0 | 0 | 0 | 0 |
| | | | | black | 0.5 | 1205 | Red | 0 | 74 | 74 | 49 | 22 | 74 | 66 | 2 | 58 |
| | | | | | | | Green | 0 | 74 | 74 | 51 | 22 | 75 | 74 | 22 | 60 |
| | | | | | | | Blue | 0 | 84 | 84 | 45 | 23 | 82 | 0 | 16 | 52 |
| P210 | Bd | ot | 260 | grey | 65.3 | 373388 | Red | 67 | 255 | 188 | 127 | 24 | 188 | 126 | 68 | 126 |
| | | | | | | | Green | 68 | 255 | 187 | 121 | 24 | 188 | 116 | 241 | 120 |
| | | | | | | | Blue | 57 | 255 | 198 | 120 | 24 | 199 | 117 | 57 | 119 |
| | | | | yellow | 32.3 | 184667 | Red | 75 | 249 | 174 | 117 | 19 | 162 | 121 | 226 | 116 |
| | | | | | | | Green | 58 | 230 | 172 | 105 | 18 | 164 | 111 | 59 | 105 |
| | | | | | | | Blue | 49 | 228 | 179 | 103 | 18 | 170 | 105 | 49 | 103 |
| | | | | red | 0.0 | 1 | Red | 122 | 122 | 0 | 122 | 0 | 1 | 122 | 122 | 122 |
| | | | | | | | Green | 94 | 94 | 0 | 94 | 0 | 1 | 94 | 94 | 94 |
| | | | | | | | Blue | 90 | 90 | 0 | 90 | 0 | 1 | 90 | 90 | 90 |
| | | | | black | 2.3 | 13336 | Red | 0 | 74 | 74 | 63 | 10 | 71 | 74 | 12 | 66 |
| | | | | | | | Green | 0 | 74 | 74 | 57 | 11 | 75 | 62 | 5 | 59 |
| | | | | | | | Blue | 0 | 89 | 89 | 57 | 11 | 89 | 62 | 1 | 59 |
| P210 | Bd | ot | 530 | grey | 68.7 | 462570 | Red | 73 | 255 | 182 | 129 | 24 | 183 | 126 | 73 | 126 |
| | | | | | | | Green | 68 | 255 | 187 | 121 | 23 | 188 | 116 | 243 | 119 |
| | | | | | | | Blue | 52 | 255 | 203 | 116 | 23 | 204 | 115 | 52 | 113 |
| | | | | yellow | 28.8 | 193704 | Red | 75 | 243 | 168 | 115 | 17 | 157 | 121 | 207 | 116 |
| | | | | | | | Green | 58 | 227 | 169 | 104 | 16 | 156 | 111 | 59 | 105 |
| | | | | | | | Blue | 39 | 212 | 173 | 100 | 16 | 162 | 104 | 39 | 101 |
| | | | | red | 0.0 | 4 | Red | 76 | 109 | 33 | 90 | 13 | 4 | 76 | 76 | 81 |
| | | | | | | | Green | 52 | 82 | 30 | 65 | 12 | 4 | 52 | 52 | 57 |
| | | | | | | | Blue | 42 | 73 | 31 | 54 | 12 | 4 | 42 | 42 | 45 |
| | | | | black | 2.5 | 16965 | Red | 0 | 74 | 74 | 55 | 17 | 75 | 74 | 2 | 61 |
| | | | | | | | Green | 0 | 74 | 74 | 48 | 17 | 75 | 63 | 73 | 53 |
| | | | | | | | Blue | 0 | 77 | 77 | 42 | 17 | 78 | 54 | 77 | 47 |

| Profile | Form | Horizon | Depth (mm) | Colour | Quantity (%) | Count (cells) | RGB | RGB colour statistics | | | | | | | | |
|---|---|---|---|---|---|---|---|---|---|---|---|---|---|---|---|---|
| | | | | | | | | Min | Max | Range | Mean | Std | Variety | Majority | Minority | Median |
| P210 | Bd | re | 810 | grey | 0.2 | 1648 | Red | 84 | 255 | 171 | 158 | 33 | 155 | 255 | 84 | 154 |
| | | | | | | | Green | 78 | 254 | 176 | 149 | 32 | 164 | 151 | 78 | 144 |
| | | | | | | | Blue | 70 | 255 | 185 | 141 | 32 | 171 | 143 | 70 | 138 |
| | | | | yellow | 67.6 | 451742 | Red | 75 | 255 | 180 | 152 | 20 | 181 | 159 | 247 | 154 |
| | | | | | | | Green | 55 | 238 | 183 | 127 | 18 | 183 | 133 | 227 | 128 |
| | | | | | | | Blue | 28 | 230 | 202 | 109 | 18 | 201 | 109 | 28 | 109 |
| | | | | red | 31.6 | 210856 | Red | 75 | 232 | 157 | 139 | 22 | 148 | 144 | 224 | 141 |
| | | | | | | | Green | 31 | 185 | 154 | 105 | 20 | 149 | 107 | 31 | 106 |
| | | | | | | | Blue | 0 | 159 | 159 | 81 | 19 | 150 | 82 | 0 | 82 |
| | | | | black | 0.6 | 3752 | Red | 14 | 74 | 60 | 62 | 11 | 61 | 74 | 14 | 65 |
| | | | | | | | Green | 0 | 66 | 66 | 36 | 11 | 62 | 39 | 66 | 38 |
| | | | | | | | Blue | 0 | 56 | 56 | 20 | 13 | 56 | 0 | 52 | 20 |
| P210 | Bd | re | 1200 | grey | 0.0 | 258 | Red | 76 | 255 | 179 | 181 | 50 | 122 | 255 | 76 | 180 |
| | | | | | | | Green | 70 | 252 | 182 | 171 | 49 | 126 | 242 | 70 | 170 |
| | | | | | | | Blue | 48 | 246 | 198 | 158 | 50 | 137 | 121 | 48 | 156 |
| | | | | yellow | 36.4 | 342312 | Red | 75 | 255 | 180 | 158 | 18 | 181 | 159 | 250 | 158 |
| | | | | | | | Green | 55 | 238 | 183 | 129 | 16 | 184 | 126 | 55 | 128 |
| | | | | | | | Blue | 20 | 229 | 209 | 100 | 15 | 206 | 97 | 20 | 100 |
| | | | | red | 62.2 | 585247 | Red | 75 | 232 | 157 | 146 | 21 | 150 | 158 | 227 | 149 |
| | | | | | | | Green | 26 | 187 | 161 | 110 | 20 | 157 | 119 | 26 | 113 |
| | | | | | | | Blue | 0 | 163 | 163 | 79 | 19 | 157 | 84 | 149 | 82 |
| | | | | black | 1.4 | 13367 | Red | 8 | 74 | 66 | 54 | 15 | 66 | 74 | 8 | 57 |
| | | | | | | | Green | 0 | 64 | 64 | 24 | 14 | 63 | 0 | 60 | 25 |
| | | | | | | | Blue | 0 | 52 | 52 | 6 | 8 | 48 | 0 | 44 | 0 |
| P210 | Bd | on | 1580 | grey | 0.0 | 75 | Red | 135 | 255 | 120 | 245 | 24 | 19 | 255 | 135 | 255 |
| | | | | | | | Green | 125 | 253 | 128 | 235 | 25 | 32 | 239 | 125 | 243 |
| | | | | | | | Blue | 100 | 243 | 143 | 211 | 25 | 39 | 223 | 100 | 218 |
| | | | | yellow | 44.3 | 357267 | Red | 75 | 255 | 180 | 169 | 16 | 181 | 172 | 75 | 170 |
| | | | | | | | Green | 55 | 238 | 183 | 139 | 15 | 182 | 137 | 55 | 139 |
| | | | | | | | Blue | 22 | 230 | 208 | 104 | 15 | 199 | 101 | 22 | 104 |
| | | | | red | 54.8 | 441347 | Red | 75 | 234 | 159 | 153 | 22 | 157 | 165 | 227 | 157 |
| | | | | | | | Green | 27 | 189 | 162 | 116 | 20 | 160 | 125 | 185 | 120 |
| | | | | | | | Blue | 0 | 157 | 157 | 78 | 20 | 154 | 84 | 146 | 81 |
| | | | | black | 0.9 | 6887 | Red | 13 | 74 | 61 | 56 | 14 | 60 | 70 | 13 | 58 |
| | | | | | | | Green | 0 | 58 | 58 | 23 | 13 | 58 | 0 | 56 | 25 |
| | | | | | | | Blue | 0 | 38 | 38 | 3 | 5 | 36 | 0 | 34 | 0 |

# APPENDIX C

Average RGB and Munsell colour per horizon

Table 1 Average corrected RGB colour determined from digital photographs taken per diagnostic horizon and Munsell colour as described in the field

| Profile | Form | Hor | Depth (mm) | RGB (dry) | | | Dry | | | | | | Wet | | | | | |
|---|---|---|---|---|---|---|---|---|---|---|---|---|---|---|---|---|---|---|
| | | | | Red | Green | Blue | Dominant | | Sub dominant | | Least | | Dominant | | Sub dominant | | Least | |
| | | | | | | | Munsell | Occ | Munsell | Occ | Munsell | Occ | Munsell | Occ | Munsell | Occ | Munsell | Occ |
| P201 | Lo | ot | 430 | 133 | 118 | 97 | 10YR4/4 | 80 | 10YR4/2 | 20 | | 0 | 10YR3/3 | 80 | 10YR3/2 | 20 | | 0 |
| | | gs | 730 | 153 | 126 | 84 | 7.5YR6/4 | 95 | 10YR4/4 | 5 | | 0 | 10YR4/4 | 95 | 10YR4/4 | 5 | | 0 |
| | | sp | 980 | 133 | 125 | 121 | 7.5YR6/4 | 100 | | 0 | | 0 | 10YR4/4 | 100 | | 0 | | 0 |
| | | so | 1210 | 138 | 136 | 141 | 7.5YR7/2 | 40 | 10YR4/8 | 10 | 10YR8/4 | 50 | 7.5YR4/4 | 40 | 10R4/6 | 10 | 7.5YR6/8 | 50 |
| P202 | Pn | ot | 400 | 120 | 121 | 120 | 10YR4/3 | 100 | | 0 | | 0 | 10YR3/3 | 100 | | 0 | | 0 |
| | | ye | 820 | 62 | 62 | 48 | 7.5YR5/6 | 95 | 7.5YR6/8 | 5 | | 0 | 7.5YR4/6 | 95 | 7.5YR4/4 | 5 | | 0 |
| | | on | 990 | 134 | 127 | 119 | 10YR8/2 | 90 | 7.5YR5/8 | 5 | 7.5YR6/8 | 5 | 7.5YR6/6 | 85 | 7.5YR5/6 | 5 | 7.5YR7/4 | 10 |
| | | on | 1500 | 132 | 127 | 114 | 2.5Y8/2 | 70 | 7.5YR5/8 | 20 | 10YR4/8 | 10 | 2.5Y6/2 | 70 | 10YR5/8 | 20 | 10R4/6 | 10 |
| P203 | Tu | ot | 380 | 123 | 119 | 117 | 10YR5/3 | 100 | | 0 | | 0 | 7.5YR3/2 | 100 | | 0 | | 0 |
| | | ne | 960 | 40 | 42 | 27 | 7.5YR7/4 | 90 | 7.5YR5/6 | 10 | | 0 | 7.5YR6/6 | 90 | 2.5YR5/8 | 10 | | 0 |
| | | on | 1300 | 140 | 120 | 93 | 7.5YR7/4 | 90 | 7.5YR6/6 | 10 | | 0 | 5YR5/6 | 90 | 2.5YR4/8 | 10 | | 0 |
| | | on | 1500 | – | – | – | 7.5YR8/2 | 40 | 7.5YR5/6 | 40 | 7.5YR6/8 | 20 | 5YR7/2 | 40 | 5YR5/6 | 40 | 2.5YR4/8 | 20 |
| P204 | Lo | ot | 140 | 127 | 122 | 111 | 7.5YR6/2 | 50 | 7.5YR7/2 | 50 | | 0 | 10YR3/3 | 50 | 10YR6/6 | 50 | | 0 |
| | | gs | 300 | 136 | 126 | 107 | 7.5YR7/5 | 60 | 7.5YR7/2 | 40 | | 0 | 2.5YR6/6 | 60 | 10YR2/4 | 40 | | 0 |
| | | sp | 470 | 154 | 126 | 97 | 10YR8/2 | 40 | 2.5YR5/8 | 40 | 2.5YR6/4 | 20 | 10YR6/4 | 40 | 2.5YR4/8 | 40 | 2.5YR5/4 | 20 |
| | | gh | 1000 | 159 | 126 | 112 | 10YR8/2 | 90 | 2.5YR5/8 | 10 | | 0 | 10YR7/2 | 90 | 2.5YR4/8 | 10 | | 0 |
| P205 | Kd | ot | 220 | 134 | 119 | 99 | 2.5Y5/2 | 100 | | 0 | | 0 | 2.5Y3/2 | 100 | | 0 | | 0 |
| | | gs | 460 | 122 | 120 | 112 | 2.5Y6/1 | 70 | 10YR6/6 | 30 | | 0 | 10YR3/3 | 70 | 10YR4/6 | 30 | | 0 |
| | | gs | 660 | 136 | 129 | 112 | 10YR6/2 | 80 | 10YR5/8 | 10 | 10YR5/2 | 10 | 10YR5/2 | 80 | 7.5YR5/8 | 10 | 10YR4/3 | 10 |
| | | gh | 1400 | 163 | 129 | 99 | 2.5Y7/1 | 70 | 10YR4/8 | 30 | | 0 | 2.5Y6/2 | 70 | 10YR4/8 | 30 | | 0 |
| P206 | Kd | ot | 550 | 110 | 115 | 120 | 10YR5/1 | 100 | | 0 | | 0 | 10YR3/1 | 100 | | 0 | | 0 |
| | | gs | 800 | 142 | 141 | 139 | 10YR5/1 | 95 | 7.5YR5/8 | 5 | | 0 | 10YR2/1 | 95 | 10YR4/6 | 5 | | 0 |
| | | gh | 1100 | 157 | 153 | 132 | 10YR6/1 | 90 | 7.5YR5/8 | 10 | | 0 | 10YR4/1 | 90 | 10YR5/8 | 10 | | 0 |
| P207 | We | ot | 300 | 128 | 124 | 119 | 10YR6/2 | 100 | | 0 | | 0 | 7.5YR4/3 | 100 | | 0 | | 0 |
| | | sp | 560 | 138 | 126 | 103 | 10YR6/3 | 90 | 10YR5/7 | 10 | | 0 | 7.5YR5/2 | 90 | 10YR4/6 | 10 | | 0 |
| | | sp | 670 | 142 | 132 | 116 | 10YR8/1 | 80 | 10YR5/6 | 20 | | 0 | 10YR6/2 | 80 | 10YR4/6 | 20 | | 0 |
| | | on | 1300 | 137 | 128 | 106 | 10YR8/2 | 60 | 10YR6/8 | 40 | | 0 | 10YR7/2 | 60 | 10YR4/6 | 40 | | 0 |
| P208 | Kd | ot | 350 | 111 | 114 | 116 | 10YR6/1 | 100 | | 0 | | 0 | 10YR4/1 | 100 | | 0 | | 0 |
| | | gs | 530 | 133 | 133 | 136 | 10YR6/2 | 90 | 10YR5/8 | 10 | | 0 | 10YR4/1 | 90 | 10YR4/6 | 10 | | 0 |
| | | gh | 800 | 136 | 131 | 124 | 10YR7/1 | 80 | 10YR6/6 | 20 | | 0 | 10YR5/2 | 80 | 10YR4/6 | 20 | | 0 |

| Profile | Form | Hor | Depth (mm) | RGB (dry) | | | Dry | | | | | | Wet | | | | | |
|---|---|---|---|---|---|---|---|---|---|---|---|---|---|---|---|---|---|---|
| | | | | Red | Green | Blue | Dominant | | Sub dominant | | Least | | Dominant | | Sub dominant | | Least | |
| | | | | | | | Munsell | Occ | Munsell | Occ | Munsell | Occ | Munsell | Occ | Munsell | Occ | Munsell | Occ |
| | | gh | 1700 | 131 | 131 | 128 | 10YR6/2 | 70 | 10YR5/8 | 20 | 10YR8/1 | 10 | 10YR5/2 | 70 | 10YR4/6 | 20 | 10YR7/1 | 10 |
| P209 | Kd | ot | 450 | 119 | 111 | 100 | 10YR5/2 | 90 | 7.5YR4/6 | 10 | | 0 | 10YR3/2 | 90 | 7.5YR3/4 | 10 | | 0 |
| | | gh | 1100 | 139 | 127 | 110 | 10YR6/1 | 90 | 7.5YR6/8 | 10 | | 0 | 10YR5/1 | 90 | 7.5YR5/8 | 10 | | 0 |
| | | so | 1400 | 157 | 158 | 146 | 10YR6/1 | 90 | 7.5YR5/8 | 10 | | 0 | 10YR5/1 | 90 | 7.5YR4/6 | 10 | | 0 |
| P210 | Bd | ot | 260 | 120 | 114 | 111 | 10YR4/2 | 100 | | 0 | | 0 | 10YR3/2 | 100 | | 0 | | 0 |
| | | ot | 530 | 120 | 113 | 106 | 10YR4/3 | 100 | | 0 | | 0 | 7.5YR3/2 | 100 | | 0 | | 0 |
| | | re | 810 | 151 | 121 | 98 | 7.5YR4/6 | 90 | 7.5YR4/2 | 10 | | 0 | 5YR4/6 | 90 | 7.5YR3/2 | 10 | | 0 |
| | | re | 1200 | 153 | 117 | 84 | 7.5YR6/6 | 90 | 5YR4/6 | 10 | | 0 | 5YR4/4 | 90 | 5YR4/4 | 10 | | 0 |
| | | on | 1580 | 165 | 128 | 87 | 10YR6/4 | 100 | | 0 | | 0 | 7.5YR3/4 | 100 | | 0 | | 0 |
| | | on | 1750 | – | – | – | 2.5YR3/6 | 100 | | 0 | | 0 | 5YR6/2 | 100 | | 0 | | 0 |

# APPENDIX D

Correlation coefficients ($R^2$) of selected properties

| | Red | Green | Blue | Hue | Chroma | Value | CvH | RR | MC | Gravel | coSa | meSa | fiSa | vfSa | Si | fiSi | Cl | Ca | Mg | K | Na | S |
|---|---|---|---|---|---|---|---|---|---|---|---|---|---|---|---|---|---|---|---|---|---|---|
| Red | 1.00 | | | | | | | | | | | | | | | | | | | | | |
| Green | **0.82** | 1.00 | | | | | | | | | | | | | | | | | | | | |
| Blue | 0.40 | **0.78** | 1.00 | | | | | | | | | | | | | | | | | | | |
| Hue | 0.12 | 0.20 | 0.23 | 1.00 | | | | | | | | | | | | | | | | | | |
| Chroma | 0.09 | 0.27 | 0.44 | **0.50** | 1.00 | | | | | | | | | | | | | | | | | |
| Value | 0.04 | 0.01 | 0.00 | 0.04 | 0.05 | 1.00 | | | | | | | | | | | | | | | | |
| CvH | 0.12 | 0.28 | 0.39 | **0.68** | **0.95** | 0.12 | 1.00 | | | | | | | | | | | | | | | |
| RR | 0.11 | 0.26 | 0.35 | **0.72** | **0.73** | 0.04 | **0.81** | 1.00 | | | | | | | | | | | | | | |
| MC | 0.10 | 0.15 | 0.14 | **0.95** | 0.29 | 0.03 | 0.47 | **0.56** | 1.00 | | | | | | | | | | | | | |
| Gravel | 0.00 | 0.02 | 0.03 | 0.00 | 0.01 | 0.01 | 0.01 | 0.04 | 0.00 | 1.00 | | | | | | | | | | | | |
| coSa | 0.01 | 0.01 | 0.07 | 0.01 | 0.17 | 0.12 | 0.14 | 0.04 | 0.00 | 0.00 | 1.00 | | | | | | | | | | | |
| meSa | 0.07 | 0.17 | 0.26 | 0.20 | 0.28 | 0.02 | 0.29 | 0.18 | 0.14 | 0.01 | 0.21 | 1.00 | | | | | | | | | | |
| fiSa | 0.08 | 0.09 | 0.10 | 0.01 | 0.04 | 0.18 | 0.01 | 0.01 | 0.00 | 0.03 | 0.01 | 0.24 | 1.00 | | | | | | | | | |
| vfSa | 0.06 | 0.01 | 0.00 | 0.00 | 0.03 | 0.10 | 0.04 | 0.01 | 0.00 | 0.10 | 0.36 | 0.02 | 0.34 | 1.00 | | | | | | | | |
| Si | 0.00 | 0.05 | 0.15 | 0.01 | 0.10 | 0.02 | 0.06 | 0.04 | 0.00 | 0.03 | 0.21 | **0.51** | 0.44 | 0.00 | 1.00 | | | | | | | |
| fiSi | 0.03 | 0.13 | 0.27 | 0.11 | 0.30 | 0.04 | 0.23 | 0.15 | 0.06 | 0.00 | 0.14 | **0.56** | 0.52 | 0.00 | **0.53** | 1.00 | | | | | | |
| Cl | 0.14 | 0.15 | 0.11 | 0.13 | 0.15 | 0.10 | 0.18 | 0.06 | 0.09 | 0.14 | 0.16 | 0.45 | 0.14 | 0.03 | 0.08 | 0.18 | 1.00 | | | | | |
| Ca | 0.03 | 0.13 | 0.25 | 0.15 | 0.41 | 0.01 | 0.37 | 0.21 | 0.07 | 0.03 | 0.29 | 0.37 | 0.10 | 0.00 | 0.09 | 0.46 | 0.49 | 1.00 | | | | |
| Mg | 0.08 | 0.14 | 0.19 | 0.22 | 0.34 | 0.17 | 0.38 | 0.22 | 0.15 | 0.10 | 0.29 | 0.39 | 0.03 | 0.01 | 0.04 | 0.21 | **0.70** | **0.72** | 1.00 | | | |
| K | 0.03 | 0.09 | 0.10 | 0.23 | 0.13 | 0.07 | 0.19 | 0.13 | 0.21 | 0.01 | 0.21 | 0.36 | 0.02 | 0.00 | 0.04 | 0.12 | **0.65** | 0.47 | **0.64** | 1.00 | | |
| Na | 0.03 | 0.14 | 0.25 | 0.06 | 0.31 | 0.00 | 0.25 | 0.13 | 0.01 | 0.01 | 0.33 | 0.54 | 0.26 | 0.00 | 0.34 | 0.57 | 0.48 | **0.77** | **0.61** | 0.39 | 1.00 | |
| S | 0.05 | 0.14 | 0.25 | 0.19 | 0.41 | 0.05 | 0.40 | 0.23 | 0.11 | 0.05 | 0.32 | 0.42 | 0.08 | 0.01 | 0.08 | 0.38 | **0.61** | **0.96** | **0.88** | **0.59** | **0.77** | 1.00 |
| $CEC_{soil}$ | 0.07 | 0.09 | 0.13 | 0.29 | **0.51** | 0.08 | **0.52** | 0.26 | 0.18 | 0.03 | 0.10 | 0.20 | 0.04 | 0.00 | 0.01 | 0.24 | 0.30 | **0.55** | 0.41 | 0.19 | 0.28 | **0.52** |
| $CEC_{clay}$ | 0.01 | 0.01 | 0.01 | 0.10 | 0.19 | 0.10 | 0.20 | 0.10 | 0.06 | 0.01 | 0.00 | 0.00 | 0.05 | 0.05 | 0.05 | 0.00 | 0.02 | 0.01 | 0.00 | 0.01 | 0.00 | 0.00 |
| BS | 0.02 | 0.13 | 0.24 | 0.14 | 0.24 | 0.02 | 0.24 | 0.17 | 0.09 | 0.01 | 0.36 | 0.40 | 0.05 | 0.04 | 0.13 | 0.29 | 0.43 | **0.65** | **0.72** | **0.59** | **0.71** | **0.73** |
| $pH_{Water}$ | 0.12 | 0.22 | 0.29 | 0.11 | 0.35 | 0.00 | 0.28 | 0.17 | 0.05 | 0.04 | 0.12 | 0.43 | 0.33 | 0.00 | 0.27 | **0.55** | 0.28 | **0.52** | 0.39 | 0.17 | **0.73** | **0.51** |
| $pH_{KCl}$ | 0.01 | 0.06 | 0.16 | 0.08 | 0.36 | 0.03 | 0.26 | 0.19 | 0.03 | 0.03 | 0.11 | 0.17 | 0.12 | 0.00 | 0.05 | 0.49 | 0.11 | **0.58** | 0.32 | 0.09 | **0.51** | **0.51** |
| OC | 0.04 | 0.00 | 0.03 | 0.01 | 0.08 | 0.19 | 0.04 | 0.04 | 0.00 | 0.07 | 0.01 | 0.03 | 0.07 | 0.00 | 0.04 | 0.28 | 0.01 | 0.14 | 0.00 | 0.00 | 0.03 | 0.05 |
| N | 0.02 | 0.00 | 0.04 | 0.03 | 0.12 | 0.13 | 0.07 | 0.06 | 0.01 | 0.04 | 0.02 | 0.08 | 0.10 | 0.00 | 0.07 | 0.38 | 0.00 | 0.22 | 0.01 | 0.00 | 0.07 | 0.11 |
| C:N | 0.18 | 0.11 | 0.03 | 0.05 | 0.01 | 0.38 | 0.05 | 0.01 | 0.06 | 0.13 | 0.08 | 0.18 | 0.00 | 0.01 | 0.00 | 0.00 | 0.44 | 0.11 | 0.40 | 0.31 | 0.14 | 0.22 |
| $Fe_d$ | 0.00 | 0.04 | 0.13 | 0.01 | 0.13 | 0.01 | 0.08 | 0.07 | 0.00 | 0.00 | 0.00 | 0.00 | 0.02 | 0.01 | 0.01 | 0.00 | 0.00 | 0.06 | 0.01 | 0.00 | 0.02 | 0.04 |
| $Fe_p$ | 0.02 | 0.00 | 0.00 | 0.01 | 0.00 | 0.37 | 0.01 | 0.00 | 0.01 | 0.05 | 0.04 | 0.00 | 0.10 | 0.07 | 0.01 | 0.13 | 0.05 | 0.02 | 0.07 | 0.05 | 0.00 | 0.00 |
| $Fe_o$ | 0.00 | 0.02 | 0.08 | 0.01 | 0.12 | 0.01 | 0.08 | 0.02 | 0.00 | 0.01 | 0.04 | 0.18 | 0.10 | 0.00 | 0.08 | 0.41 | 0.05 | 0.31 | 0.05 | 0.04 | 0.21 | 0.20 |
| $Fe_{o-p}$ | 0.00 | 0.03 | 0.09 | 0.03 | 0.15 | 0.01 | 0.12 | 0.03 | 0.01 | 0.00 | 0.09 | 0.24 | 0.06 | 0.00 | 0.08 | 0.35 | 0.11 | 0.34 | 0.13 | 0.09 | 0.29 | 0.27 |
| $Fe_{d-o}$ | 0.00 | 0.06 | 0.21 | 0.02 | 0.24 | 0.02 | 0.16 | 0.09 | 0.00 | 0.00 | 0.02 | 0.04 | 0.08 | 0.01 | 0.06 | 0.19 | 0.01 | 0.29 | 0.04 | 0.01 | 0.14 | 0.18 |
| $Mn_d$ | 0.05 | 0.08 | 0.05 | 0.00 | 0.00 | 0.00 | 0.00 | 0.00 | 0.00 | 0.01 | 0.02 | 0.18 | 0.20 | 0.05 | 0.13 | 0.11 | 0.24 | 0.15 | 0.13 | 0.27 | 0.37 | 0.16 |
| $Mn_p$ | 0.01 | 0.00 | 0.00 | 0.02 | 0.02 | 0.01 | 0.02 | 0.03 | 0.02 | 0.05 | 0.06 | 0.06 | 0.02 | 0.03 | 0.07 | 0.09 | 0.00 | 0.03 | 0.00 | 0.04 | 0.01 | 0.01 |
| $Mn_o$ | 0.01 | 0.01 | 0.02 | 0.02 | 0.01 | 0.00 | 0.01 | 0.02 | 0.01 | 0.02 | 0.03 | 0.20 | 0.08 | 0.09 | 0.31 | 0.12 | 0.00 | 0.00 | 0.00 | 0.02 | 0.02 | 0.00 |
| $Mn_{o-p}$ | 0.01 | 0.01 | 0.01 | 0.01 | 0.00 | 0.00 | 0.00 | 0.01 | 0.01 | 0.01 | 0.02 | 0.17 | 0.07 | 0.08 | 0.26 | 0.09 | 0.00 | 0.00 | 0.00 | 0.02 | 0.01 | 0.00 |
| $Mn_{d-o}$ | 0.01 | 0.02 | 0.01 | 0.01 | 0.01 | 0.00 | 0.01 | 0.01 | 0.01 | 0.02 | 0.00 | 0.00 | 0.03 | 0.13 | 0.01 | 0.00 | 0.16 | 0.10 | 0.09 | 0.23 | 0.15 | 0.11 |
| Fe:Cl | 0.05 | 0.14 | 0.24 | 0.09 | 0.22 | 0.01 | 0.20 | 0.09 | 0.04 | 0.06 | 0.11 | 0.32 | 0.20 | 0.03 | 0.18 | 0.23 | 0.45 | 0.41 | 0.39 | 0.29 | 0.36 | 0.43 |
| Total | 0.10 | 0.17 | 0.19 | 0.19 | 0.29 | 0.17 | 0.33 | 0.16 | 0.13 | 0.04 | 0.34 | 0.49 | 0.04 | 0.04 | 0.10 | 0.31 | **0.55** | **0.60** | **0.63** | 0.45 | **0.52** | **0.66** |
| Avg | 0.08 | 0.16 | 0.20 | 0.21 | 0.31 | 0.14 | 0.35 | 0.17 | 0.14 | 0.04 | 0.36 | 0.49 | 0.03 | 0.04 | 0.10 | 0.31 | **0.57** | **0.65** | **0.68** | **0.50** | **0.55** | **0.72** |
| Freq | 0.06 | 0.01 | 0.01 | 0.03 | 0.04 | 0.03 | 0.03 | 0.01 | 0.02 | 0.01 | 0.08 | 0.01 | 0.05 | 0.00 | 0.02 | 0.00 | 0.03 | 0.12 | 0.07 | 0.06 | 0.03 | 0.10 |

Table 1 Continued ...

| | $CEC_{soil}$ | $CEC_{clay}$ | BS | $pH_{Water}$ | $pH_{KCl}$ | OC | N | C:N | $Fe_d$ | $Fe_p$ | $Fe_o$ | $Fe_{o-p}$ | $Fe_{d-o}$ | $Mn_d$ | $Mn_p$ | $Mn_o$ | $Mn_{o-p}$ | $Mn_{d-o}$ | Fe:Cl | Water saturation | | |
|---|---|---|---|---|---|---|---|---|---|---|---|---|---|---|---|---|---|---|---|---|---|---|
| | | | | | | | | | | | | | | | | | | | | Total | Avg | Freq |
| $CEC_{soil}$ | 1.00 | | | | | | | | | | | | | | | | | | | | | |
| $CEC_{clay}$ | 0.32 | 1.00 | | | | | | | | | | | | | | | | | | | | |
| BS | 0.10 | 0.04 | 1.00 | | | | | | | | | | | | | | | | | | | |
| $pH_{Water}$ | 0.34 | 0.06 | 0.38 | 1.00 | | | | | | | | | | | | | | | | | | |
| $pH_{KCl}$ | 0.38 | 0.05 | 0.30 | **0.63** | 1.00 | | | | | | | | | | | | | | | | | |
| OC | 0.19 | 0.00 | 0.00 | 0.02 | 0.21 | 1.00 | | | | | | | | | | | | | | | | |
| N | 0.29 | 0.01 | 0.00 | 0.05 | 0.25 | **0.96** | 1.00 | | | | | | | | | | | | | | | |
| C:N | 0.08 | 0.00 | 0.21 | 0.13 | 0.01 | 0.30 | 0.17 | 1.00 | | | | | | | | | | | | | | |
| $Fe_d$ | 0.02 | 0.00 | 0.01 | 0.01 | 0.00 | 0.02 | 0.01 | 0.04 | 1.00 | | | | | | | | | | | | | |
| $Fe_p$ | 0.03 | 0.01 | 0.05 | 0.00 | 0.10 | **0.69** | **0.64** | 0.29 | 0.00 | 1.00 | | | | | | | | | | | | |
| $Fe_o$ | 0.24 | 0.01 | 0.06 | 0.12 | 0.20 | 0.48 | **0.53** | 0.01 | 0.00 | 0.25 | 1.00 | | | | | | | | | | | |
| $Fe_{o-p}$ | 0.24 | 0.01 | 0.14 | 0.15 | 0.15 | 0.23 | 0.28 | 0.01 | 0.00 | 0.04 | **0.90** | 1.00 | | | | | | | | | | |
| $Fe_{d-o}$ | 0.17 | 0.01 | 0.06 | 0.09 | 0.09 | 0.28 | 0.27 | 0.05 | **0.65** | 0.10 | 0.32 | 0.28 | 1.00 | | | | | | | | | |
| $Mn_d$ | 0.01 | 0.04 | 0.22 | 0.30 | 0.07 | 0.04 | 0.03 | 0.16 | 0.00 | 0.04 | 0.00 | 0.02 | 0.00 | 1.00 | | | | | | | | |
| $Mn_p$ | 0.10 | 0.01 | 0.00 | 0.00 | 0.01 | 0.30 | 0.33 | 0.06 | 0.02 | 0.08 | 0.10 | 0.07 | 0.01 | 0.01 | 1.00 | | | | | | | |
| $Mn_o$ | 0.01 | 0.02 | 0.01 | 0.05 | 0.00 | 0.00 | 0.01 | 0.00 | 0.00 | 0.00 | 0.00 | 0.00 | 0.00 | 0.00 | 0.00 | 1.00 | | | | | | |
| $Mn_{o-p}$ | 0.02 | 0.02 | 0.01 | 0.05 | 0.00 | 0.00 | 0.00 | 0.00 | 0.00 | 0.00 | 0.01 | 0.01 | 0.00 | 0.00 | 0.01 | **0.98** | 1.00 | | | | | |
| $Mn_{d-o}$ | 0.02 | 0.00 | 0.09 | 0.08 | 0.04 | 0.04 | 0.03 | 0.08 | 0.00 | 0.02 | 0.00 | 0.02 | 0.00 | **0.58** | 0.00 | 0.42 | 0.42 | 1.00 | | | | |
| Fe:Cl | 0.17 | 0.03 | 0.33 | 0.21 | 0.07 | 0.01 | 0.02 | 0.10 | 0.41 | 0.01 | 0.04 | 0.07 | 0.42 | 0.08 | 0.01 | 0.01 | 0.01 | 0.02 | 1.00 | | | |
| Total | 0.34 | 0.00 | **0.54** | 0.36 | 0.21 | 0.00 | 0.02 | 0.39 | 0.03 | 0.05 | 0.10 | 0.20 | 0.11 | 0.13 | 0.00 | 0.02 | 0.02 | 0.03 | 0.47 | 1.00 | | |
| Avg | 0.36 | 0.00 | **0.60** | 0.37 | 0.24 | 0.00 | 0.03 | 0.37 | 0.02 | 0.04 | 0.10 | 0.19 | 0.10 | 0.13 | 0.01 | 0.02 | 0.01 | 0.04 | 0.46 | **0.99** | 1.00 | |
| Freq | 0.04 | 0.00 | 0.09 | 0.01 | 0.07 | 0.01 | 0.02 | 0.00 | 0.05 | 0.01 | 0.00 | 0.01 | 0.02 | 0.00 | 0.01 | 0.12 | 0.11 | 0.03 | 0.04 | 0.01 | 0.04 | 1.00 |





Symbols used:

| | |
|---|---|
| Red | RGB Red |
| Green | RGB Green |
| Blue | RGB Blue |
| Hue | numeric Munsell Hue |
| Chroma | Munsell Chroma |
| Value | Munsell Value |
| CvH | colour index (Van Huyssteen, 1995) |
| RR | Redness rating (Torrent *et al.*, 1980) |
| MC | colour index (Mokma & Cremeens, 1991) |
| S | sum of basic cations |
| BS | base saturation |
| OC | organic carbon |
| $Fe_d$ | CBD extractable Fe |
| $Fe_p$ | pyrophosphate extractable Fe |
| $Fe_o$ | oxalate extractable Fe |
| $Fe_{o-p}$ | $Fe_o - Fe_p$ |
| $Fe_{d-o}$ | $Fe_d - Fe_o$ |
| $Mn_d$ | CBD extractable Mn |
| $Mn_p$ | pyrophosphate extractable Mn |
| $Mn_o$ | oxalate extractable Mn |
| $Mn_{o-p}$ | $Mn_o - Mn_p$ |
| $Mn_{d-o}$ | $Mn_d - Mn_o$ |
| Total | duration of water saturation above 0.7 of porosity |
| Avg | average duration of water saturation events above 0.7 of porosity |
| Freq | frequency of water saturation events above 0.7 of porosity |